Biochemical analysis of the factors controlling the process of membrane tubule formation from the Golgi complex

Thesis

UNRESTRICTED

Biochemical analysis of the factors controlling the process of membrane tubule formation from the Golgi complex

Alberto
R. Weigert

Discipline: Life sciences

Sponsoring establishment: Consorzio Mario Negri Sud

AUTHOR'S No: PA278953

DATE of AWARD: 2 MAY 2000

Thesis submitted in accordance with the requirements of the Open University for the degree of Doctor of Philosophy

November 1999

ABSTRACT

Membranous tubules are very abundant structures in living cells and form or are part of most intracellular organelles. The Golgi apparatus is mainly formed by tubules, which adopt different geometries and conformations. However, their physiological role has not yet been established and this is mainly due to the almost absolute lack of knowledge about the biochemical mechanisms regulating their formation, maintenance and disruption.

The aim of this thesis was to investigate in a systematic way these mechanisms. The first step has been to set up an *in vitro* morphological assay suitable for the visualisation of Golgi-associated tubules in isolated Golgi stacks. This assay was based on electron microscopy and specifically on negative staining of whole-mount preparations. It allowed both qualitative and quantitative analysis of the morphological changes of Golgi-associated tubules after *in vitro* incubations.

This assay was then used for screening several molecules or experimental conditions for their effect on tubular homeostasis. Among them, the most significant was BARS (BFA-dependent ADP-Ribosylation Substrate), a protein previously implicated in the maintenance of Golgi architecture. BARS has been found to cause the selective breakdown of the tubular part of the Golgi complex promoting fission events which convert the tubular structures into clusters of vesicles. This effect correlated with the enzymatic activity of BARS, which acts as an acyl-CoA dependent lysophosphatidic acid acyl transferase (LPAAT), increasing phosphatidic acid (PA) levels in Golgi membranes. This suggests that local modifications of the composition of the lipid bilayer is a possible mechanism for the fission of membranous tubules.

TABLE OF CONTENTS

ABSTRACT 1

TABLE OF CONTENTS 2

LIST OF FIGURES 9

CHAPTER 1 INTRODUCTION

1.1 Tubular structures in living cells 16

1.1.1 Basic features 16

1.1.2 Tubular structures in intracellular organelles. 16

1.1.3 Putative role for membranous tubules. 19

1.1.4 Curvature of membranous tubules 20

1.1.5 The Golgi apparatus as an experimental model for studying the mechanisms regulating tubular homeostasis 24

1.2 The Golgi apparatus 26

1.2.1 Basic features 26

1.2.2 Three dimensional structure 28

1.2.3 Golgi resident enzymes. 29

1.2.4 Mechanisms for the localization of the Golgi resident enzymes. 32

1.2.5 Lipid composition of the Golgi apparatus. 32

1.2.6 Dynamic analysis of Golgi tubules. 34

1.3 Protein transport and Golgi tubules 36

1.3.1 Classical models for protein transport 36

1.3.2 ER to Golgi transport. 38

1.3.3 Intra-Golgi transport 39

1.3.4 Transport from the Golgi to post-Golgi compartments 41

1.3.5 Retrograde transport from Golgi to the ER 42

1.4 Molecules implicated in the regulation of tubular structures 43

1.4.1 Introduction. 43

1.4.2 Molecules implicated in the formation of tubules 43

1.4.2.1 Brefeldin A (BFA) 43

1.4.2.2 The small GTP-binding protein ARF 45

1.4.2.3 The coatomer complex 47

1.4.2.4 BFA-dependent ADP-ribosylation substrate (BARS) 48

1.4.2.5 Calmodulin 51

1.4.2.6 Phospholipase A2 51

1.4.2.7 Lipidic composition 52

1.4.2.8 Microtubules 53

1.4.2.9 ATP levels 54

1.4.2.10 The tubulating factor p40 54

1.4.3 Molecules implicated in the fission of tubules. 55

1.4.3.1 Phosphoinositol transfer protein (PITP) 55

1.4.3.2 Dynamin 56

1.4.3.2 Acyl-coenzyme As 57

1.4.3.4 Mitotically -activated factors 58

1.4.3.5 βγ subunit of heterotrimeric G proteins 59

1.4..4 General conclusions 59

1.5 Techniques employed to visualise Golgi tubules 61

1.5.1 Introduction 61

1.5.2 EM conventional sectioning 61

1.5.3 Freeze-etch electron microcopy 62

1.5.4 Negative staining on whole-mount preparations 62

CHAPTER 2 MATERIAL AND METHODS

2.1 Materials 64

2.2 Protein determination 64

2.3 Cell Culture 65

2.3.1 Materials

2.3.2 Propagation of cell lines 65

2.3.2.1. Growth media **65**

2.3.2.2. Growth conditions **66**

2.4 Isolation of Golgi membranes **66**

2.4.1 Materials 66

2.4.2 Isolation of Golgi membranes from cell cultures 66

2.4.3 Isolation of Golgi membranes from animal tissues. 68

2.4.3.1 Golgi from rat testis or epidydimus **68**

2.4.3.2 Golgi from rat liver as described in Leelavathi et al., 1970 **69**

2.4.3.3 Golgi from rat liver as described in Slusarewicz et al., 1994 **69**

2.4.3.4 Golgi from rat liver by a modification of Cluett and Brown, 1992 **70**

2.4.3.5 Golgi from rat liver by a modification of Taylor et al., 1998 **71**

2.5 SDS page and immunoblotting **73**

2.5.1 Materials 73

2.5.2 Buffer for electrophoresis and blotting 73

2.5.3 Assembling polyacrylamide gels 74

2.5.4 SDS page 74

2.5.5 Blotting on nitrocellulose 74

2.5.6 Immunodetection of antigens 75

2.5.7 Silver staining 76

2.6 Electron Microscopy **77**

2.6.1 Materials 77

2.6.2 Preparation of formvar-coated grids for electron microscopy 77

2.6.3 Thin sections of isolated Golgi membranes (perpendicular) 77

2.6.4 Thin sections of isolated Golgi membranes (longitudinal) 78

2.6.5 Thin sections of permeabilized cells 78

2.6.6 Stereology in thin sections 80

2.6.7 Contrasters for negative staining 80

2.6.8 Standard protocols for negative staining 81

2.6.9 Quantitative analysis of the morphology of Golgi membranes 81

2.6.10 Determination of the frequency distribution of vesicular structures 82

2.7 Preparation of cytosolic extracts and recombinant GST-BARS **85**

2.7.1 Materials 85

2.7.2 Preparation of control cytosols from rat brain 85

2.7.3 Preparation of coatomer-defective cytosol 86

2.7.4 Expression in *E.Coli* and purification of recombinant GST-BARS and GST 86

2.8 ADP-ribosylation of BARS **89**

2.8.1 Materials 89

2.8.2 ADP-ribosylation and purification of ADP-ribosylated BARS 89

2.9 Cell permeabilization **91**

2.9.1 Materials

2.9.2 Protocol for cell permeabilisation and incubation 91

2.10 Assay for acyltransferase activity **91**

2.10.1 Materials 91

2.10.2 Incubations and lipid extraction 91

2.11 Analysis of lipids by TLC **92**

2.11.1 Materials 92

2.11.2 TLC preparation and elution 92

2.12 Preparation of Golgi-derived liposomes 93

CHAPTER 3 AN *IN VITRO* ASSAY FOR VISUALISING GOLGI TUBULES

3.1 Introduction 95

3.2 Characterization of Golgi preparations 96

3.1.1 Golgi membranes from cultured cells 96

3.1.2 Golgi membranes from animal tissues 99

3.3 Negative staining on whole-mount preparations 108

3.3.1 General description 108

3.3.2 Contrasters 108

3.3.3 Grids and support film 110

3.3.4 Time of incubation and volume of deposition 114

3.3.5 Visualization of Golgi membranes in non-fixed samples 118

3.3.6 Fixation protocol 122

3.3.7 Visualization of the Golgi membranes in fixed samples 123

3.3.8 Immunogold labeling of Golgi membranes 125

3.4 Validation of the assay 128

3.4.1 Response to known biological stimuli 128

3.4.2 Incubations with BFA 128

3.4.3 Incubations with GTP-γS 132

3.5 Discussion 136

CHAPTER 4 SCREENING FOR CONDITIONS AFFECTING TUBULAR HOMEOSTASIS

4.1 Introduction 137

4.1 Effect of cytosolic extracts 138

4.1.1 Rat brain cytosol 138

4.1.2 ARF-depleted cytosol 140

4.1.3 Coatomer-defective cytosol 143

4.1.4 NADase-pretreated cytosol 146

4.1.5 BARS-depleted cytosol 150

4.2 Modulators of lipidic metabolism 154

4.2.1 Effect of phospholipases A2, C and D 154

4.2.2 Acyl Coenzyme As 156

4.3 Calcium and the βγ subunits of heterotrimeric G-proteins 161

4.4 Discussion 164

CHAPTER 5 THE EFFECT OF BARS ON TUBULAR HOMEOSTASIS

5.1 Introduction 165

5.2 Characterization of BARS effect on Golgi tubules 166

5.2.1 Addition of BARS-enriched cytosol 166

5.2.2 Blocking antibody α–PEP9 170

5.2.3 ADP-ribosylated BARS 174

5.2.4 Cytosolic requirement for BARS 174

5.2.5 Effect of BARS in permeabilized cells 174

5.2.6 Analysis of fragments released from stacks 179

5.3 Characterization of the BARS-induced fission intermediates 182

5.3.1 Fisssion intermediates visualised by negative staining 182

5.3.2 Fisssion intermediates visualised by thin sections 184

5.4 Molecular mechanism of BARS effect 185

5.4.1 Acyl-CoenzymeAs as cofactors: characterization 185

5.4.2 BARS is a LPA-specific acyltransferase 191

5.4.3 Enzymatic characterization of BARS-specific LPAAT activity 198

5.4.4 Acyl-CoenzymeAs as cofactors for LPAAT activity 200

5.4.5 ADP-ribosylation and α-PEP9 abolish LPAAT activity 200

5.4.6 PA formation in Golgi membranes 203

5.4.7 LPA requirement for pCoA and BARS-dependent fission 206

5.4.8 PA induces fragmentation 206

5.4.9 Discussion 210

CHAPTER 6 FINAL DISCUSSION 211

ABBREVIATIONS 216

ACKNOWLEDGEMENTS 219

REFERENCES 220

PUBLICATIONS Cover Pocket

LIST OF FIGURES

CHAPTER 1

Fig. 1.1 Different arrangments for tubular structures in living cells 17

Fig. 1.2 Forces generating a bending moment (M) in a lipidic bilayer 21

Fig. 1.3 Shapes and phase behaviour of common lipid molecules 23

Fig. 1.4 Possible arrangements of lipids in tubular structures 25

Fig. 1.5 Schematic view of the ribbon-like structures of the Golgi apparatus in mammalian cells 27

Fig 1.6 Schematic drawing of the three-dimensional architecture of the Golgi apparatus 30

Fig. 1.7. Intracellular transport according to the vesicular theory 37

Fig. 1.8 Alternative models for intra-Golgi transport 40

Fig. 1.9 Effect of brefeldin A on the architecture of the Golgi apparatus 44

Fig. 1.10 Mechanism of ARF/coatomer binding to Golgi membranes 46

Fig. 1.11 Possible involvement of the BFA-dependent mono ADP-ribosylation of BARS in controlling the formation of BFA-dependent tubules from the Golgi apparatus 50

CHAPTER 2

Fig. 2.1 Scheme for the isolation of Golgi membranes from cell cultures and rat liver according to Slusarewicz et al. 1994 67

Fig. 2.2 Scheme for the isolation of Golgi membranes from rat liver 72

Fig. 2.3 Scheme for sectioning of the resin-embedded pellets 79

Fig. 2.4 Scheme for the stereological analysis using the negative staining technique 84

Fig. 2.5 Purity of recombinant GST and recombinant GST-BARS by SDS page and silver staining 88

Fig. 2.6 BFA-dependent ADP-ribosylation of recombinant GST-BARS 90

CHAPTER 3

Fig. 3.1 Immunoblot analysis of specific markers of intracellular organelles in the fractionation procedure used to purify Golgi membranes from cell cultures 97

Fig. 3.2 Morphological analysis by thin sectioning and electron microscopy of Golgi-enriched fractions prepared from cell cultures 98

Fig. 3.3 Biochemical and morphological characterization of Golgi-enriched fractions purified from rat testis and epididymus 101

Fig. 3.4 Biochemical and morphological characterization of Golgi-enriched fractions purified from rat liver according to the "Leelavathi" procedure 102

Fig. 3.5 Biochemical and morphological characterization of

Golgi-enriched fractions purified from rat liver according to the "Slusarewicz" procedure 103

Fig. 3.6 Golgi membranes isolated according to the "Slusarewicz" procedure as visualised by the negative staining technique 105

Fig. 3.7 Immunoblot analysis of specific markers of intracellular organelles in the fractionation procedure used to purify Golgi membranes from rat liver using the "Cluett" and the "Taylor" procedure 106

Fig. 3.8 Morphological analysis by electron microscopy of the Golgi-enriched fractions prepared from rat liver using the "Cluett" and the "Taylor" procedure 107

Fig. 3.9 Golgi membranes as visualised by the negative staining technique using 2% PTA as contraster 109

Fig. 3.10 Golgi membranes as visualised by the negative staining technique using UA as contraster 111

Fig. 3.11 Golgi membranes as visualised by the negative staining technique using the NanoW 2018 as contraster 112

Fig. 3.12 Effect of long exposure of Golgi membranes to the contraster 113

Fig. 3.13 Characterization of the negative staining technique 115

Fig. 3.14 Comparison between the morphology of the Golgi membranes as visualised by the negative staining or by the freeze-etch technique 117

Fig. 3.15 Golgi membranes are classified in 6 categories according to their morphological features 120

Fig. 3.16 Characterization of tubular and vesicular structures associated with the Golgi membranes as visualised by the negative staining technique 121

Fig. 3.17 Characterization of isolated Golgi membranes by using the negative staining technique after fixation with glutharaldehyde 124

Fig. 3.18 Immunogold labelling of the Golgi stacks 127

Fig 3.19 Effect of BFA on the morphology of the isolated Golgi membranes as visualised by the negative staining technique 129

Fig. 3.20 Effect of BFA on the morphology of isolated Golgi membranes as visualised by thin sections 131

Fig. 3.21 Effect of BFA on the morphology of isolated Golgi membranes as visualised by the negative staining technique without chemical fixation 133

Fig. 3.22 Effect of GTP-γS on the morphology of isolated Golgi membranes as visualised by the negative staining technique 135

CHAPTER 4

Fig. 4.1 Effect of rat brain cytosol on the morphology of isolated Golgi membranes 139

Fig. 4.2 Time course of the cytosol effects 141

Fig. 4.3 Effect of ARF-depleted cytosol on the morphology of the Golgi apparatus 142

Fig. 4.4 Time course of the effects of ARF-depleted cytosol 144

Fig. 4.5 Effect of the coatomer defective cytosol on the morphology of the isolated Golgi membranes 145

Fig. 4.6 Effect of NAD^+ on the morphology of isolated Golgi membranes 148

Fig. 4.7 Effect of NAD^+ depletion on the morphology of the isolated Golgi membranes 149

Fig. 4.8 Effect of BARS-depleted cytosol on the morphology of isolated Golgi membranes 151

Fig. 4.9 Comparison between the activity of chromatographically purified BARS and recombinant GST-BARS in reconstituting the cytosol fragmenting activity 153

Fig. 4.10 Effect of exogenous addition of PLA_2 and PLD on the morphology of isolated Golgi membranes 155

Fig. 4.11 Effect of stearoyl-CoA on the morphology of isolated Golgi membranes 157

Fig. 4.12 Characterization of the effect of acyl-CoAs on the morphology of isolated Golgi membranes 159

Fig. 4.13 Effect of calcium and the $\beta\gamma$ subunit of heterotrimeric G proteins on the morphology of isolated Golgi membranes 162

CHAPTER 5

Fig. 5.1 Effect of BARS-enriched cytosol on the morphology of the isolated Golgi membranes as visualised by negative staining 167

Fig. 5.2 Frequency distribution of diameters of the vesicular structures 168

Fig. 5.3 Comparison between the activity of chromatographically purified BARS and recombinant GST-BARS 169

Fig. 5.4 Effects of BARS on the Golgi tubular network in

conventional EM thin sections 171

Fig. 5.5 Characterization of the effect of BARS-enriched cytosol on the morphology of isolated Golgi membranes in conventional EM 172

Fig. 5.6 Effect of the blocking anti-BARS antibody, α-PEP9 on the fragmenting activity of rat brain cytosol 173

Fig. 5.7 Effect of BFA-dependent mono-ADP-ribosylation on the BARS-induced fragmentation of Golgi associated tubules 175

Fig. 5.8 Cytosolic requirement for the BARS-induced fragmentation of Golgi-associated tubules 176

Fig. 5.9 Effect of BARS on the morphology of the Golgi apparatus in permeabilized cells 178

Fig. 5.10 Visualisation of the BARS induced release of vesicular fragments from isolated Golgi stacks 181

Figure 5.11 Structure of BARS-induced fission intermediates in Golgi tubules 183

Fig. 5.12 Palmitoyl-CoA is an essential cofactor for the BARS-induced fragmentation of Golgi tubular networks 187

Fig. 5.13 Quantitative analysis of the pCoA and BARS-dependent fragmenting activity 188

Fig. 5.14 Time course of the acyl-CoA and BARS-dependent fragmenting activity 189

Fig. 5.15 Fragmenting activity of partially purified and recombinant BARS in the presence of pCoA 190

Fig. 5.16 Activity of different acyl-CoAs in supporting the BARS-

dependent fragmentation of Golgi tubules 192

Fig. 5.17 Effect of ATP-depletion in the acyl-CoA and BARS fragmenting activity of Golgi associated tubules 193

Fig. 5.18 Palmitoylation assay 194

Fig. 5.19 Synthesis of PA measured by TLC 196

Fig. 5.20 Synthesis of PA measured by HPLC 197

Fig. 5.21 Characterization of the BARS-dependent LPA-acyltransferase activity by TLC 199

Fig. 5.22 Selectivity of the BARS LPA-acyltransferase activity with respect to type of acyl chain in acyl-CoAs 201

Fig. 5.23 Effect of ADP-ribosylation and of the anti-PEP9 antibody on BARS-dependent LPA-acyltransferase activity 202

Fig. 5.24 BARS-dependent formation of PA in Golgi membranes 204

Fig. 5.25 Endogenous acyltransferase activity of Golgi membranes 205

Fig. 5.26 Requirement for LPA in the BARS-induced fragmentation of isolated Golgi membranes 207

Fig. 5.27 PA synthesis in Golgi membranes is associated with membrane fragmentation 209

CHAPTER 1
INTRODUCTION

1.1 Tubular structures in living cells

1.1.1 Basic features

The most widely accepted definition of a membranous tubule is a biomembrane, cylindrical in shape and with a length at least twice its diameter (Banta et al., 1995, Cluett et al., 1993). The diameter of a tubule varies from 20-30 nm up to 100-200 nm, while the maximal length can reach several microns (Mollenhauer and Morre', 1998, Rambourg and Clermont, 1997, Sciaky et al., 1997, van Deurs et al., 1996, Banta et al., 1995, Ladinsky et al., 1994, Cluett et al., 1993). In the last decade, several authors, using different techniques, have shown that tubules are highly abundant structures in living cells. They are arranged in several different ways: i) single discrete units of different length, that can be straight or convoluted; ii) reticuli, extending both bi or tri-dimensionally, and iii) arrays of perforations (called fenestrae) (fig. 1.1).

1.1.2 Tubular structures in intracellular organelles

Tubular structures occur frequently in most sub-cellular compartments. The endoplasmic reticulum (ER), is the largest intracellular membranous compartment. It has a great number of different functions which include the synthesis, folding, assembly, and degradation of proteins, the biosynthesis and metabolism of lipids, detoxification, compartmentalisation of the nucleus, regulation of ion gradients, and membrane transport (Lippincott-Schwartz, 1993). This organelle is physically divided in two different domains: i) the rough ER (RER), mainly involved in protein synthesis and composed of cisternae on which ribosomes are studded and ii) the smooth ER (SER), mainly involved in lipid metabolism and including some specialised subdomains, the so called ER exit sites (or exosomes), involved in the export of newly-synthesised proteins (Bannykh et al., 1998,

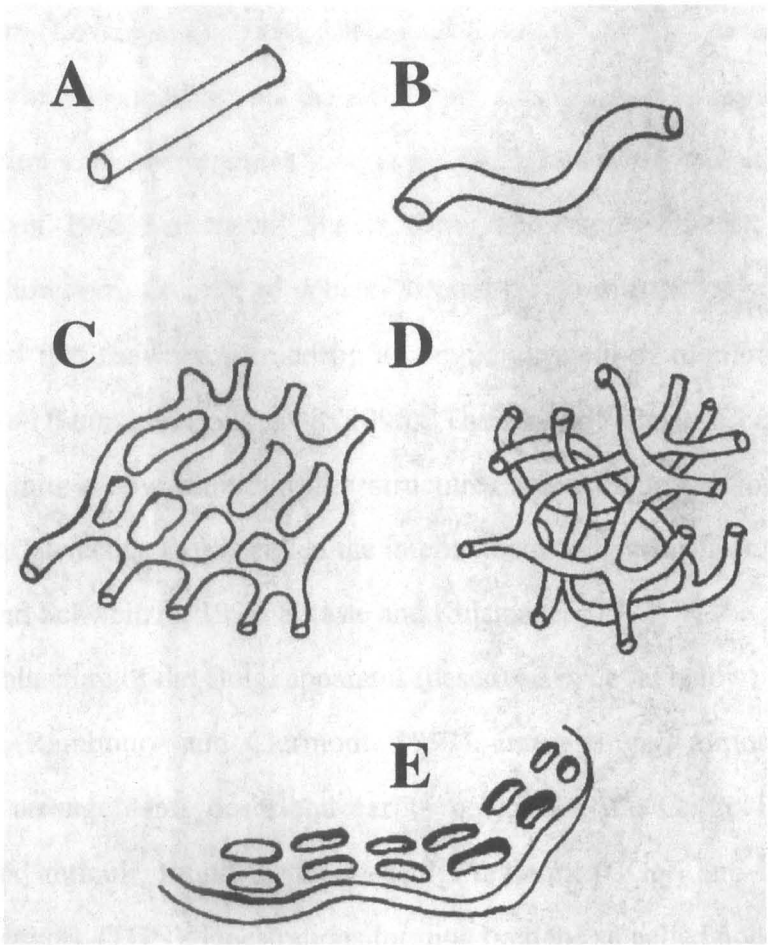

Fig. 1.1 Different arrangements for tubular structures in living cells

Single straight tubule (A). Single convoluted tubule (B). Bi-dimensional tubular reticulum (C). Tri-dimensional tubular anastomosed reticulum (D). Arrays of fenestrae (E).

Bannykh and Balch, 1997). SER is partially formed by an extensive reticulum (Lavoie et al., 1996, Lippincott-Schwartz, 1993, Lee and Chen, 1998) which depending on the cell type, extends and is regulated by association with microtubules (Lee et al., 1989, Lee and Chen, 1988, Vale and Hotani, 1988, Dabora and Sheetz, 1988). The nature of the ER exit sites is still, however, a matter of debate. Several recent morphological studies indicated that they are formed by a complex system of tubulo-vesicular elements (Bannykh et al., 1998, 1996). The ER exit sites are believed to mature into a new pleiomorphic structure, again composed of tubulo-vesicular elements, that is called the intermediate compartment (or ERGIC, Hauri and Schweitzer, 1992, Saraste and Kuismanen, 1992).

The architecture of the Golgi apparatus (described in detail below) is mainly tubular (Rambourg and Clermont, 1997). Interestingly, almost all the tubular arrangements described earlier coexist in the Golgi, including organised reticuli, found in the cis-Golgi network (CGN) and the trans-Golgi network (TGN), fenestrations forming both the so called non-compact zones and the rims of saccular (the compact zone) and single tubules. Finally, the endosomal compartment, which includes a series of pleiomorphic organelles involved in both the endocytic and the exocytic processes, consists of intricated tubular networks which have been implicated in both the transport and the recycling of different enzymes (Hemery et al., 1996, Stoorvogel et al., 1996, Gruenberg and Maxfield, 1995, Wood and Brown, 1992, Wood et al., 1991, Hopkins et al., 1990). The lysosomal compartments, that are devoted to the degradation of proteins or nutrients, are mainly formed by tubular structures (Swanson et al., 1987). Other organelles with a tubular component include peroxisomes, whose morphology is under the control of growth factors (Schrader et al., 1998, Yamamoto and Fahimi, 1987), mitochondria, traditionally considered as static structures but capable of forming tubules by fission-based mechanisms (Bereiter-Hahn, 1989, Johnson et al., 1980), and the plasma membrane (PM) that has been shown to be competent to generate tubules

under both physiological and pathological conditions (van Deurs et al., 1996, Sanan and Anderson, 1991).

1.1.3 Putative role for membranous tubules

In spite of the fact that the first morphological descriptions of tubular structures were provided in the sixties, their physiological role has only recently become clearer. These structures were neglected for many years and biochemical and morphological studies in the field of the intracellular transport were focused around the so called "vesicular theory" (Rothman and Orci, 1992, Rothman, 1994, 1992). This theory postulates that molecules are transported exclusively in vesicular carriers which form from donor compartments and fuse with acceptor compartments. For this reason, the biochemical mechanisms regulating the formation, maintenance and disruption of the membranous tubules were neglected.

The role of tubules has been re-evaluated during the last few years, though the approaches used to study them have so far been almost exclusively morphological.

Some cargo molecules (lipids, or enzymes) recycling between different compartments of the secretory pathway have been visualised in tubular structures using both light and electron microscopy (see below) prompting several authors to speculate that they may play a role as transport intermediates (Lippincott-Schwartz et al., 1998, Mironov et al., 1998, Mironov et al., 1997a, Stichcombe et al., 1995, Weidmann, 1995, Ajala, 1994). This view is consistent with observations that tubular structures are mainly present in those domains of the various organelles that are involved specifically in transport steps, suggesting that these processes may be linked to or favoured by a tubular conformation. In the ER for example the tubular shape is restricted to an area specialised in lipid metabolism and protein export (Lippincott-Schwartz, 1993, Bannykh et al., 1996). The intermediate and the early cis-Golgi compartments, which receive material from the ER, have a tubular structure (Rambourg and Clermont, 1997, Lindsey and Ellisman, 1985), while the middle compartments of the Golgi apparatus, that

are very active in processing both proteins and lipids, are mainly saccular (Ladinsky et al., 1999, Rambourg and Clermont, 1997). The TGN, the more distal compartment of the Golgi where cargo is sorted, is again tubular, as are the endosomal-lysosomal compartments (Rambourg and Clermont, 1997, Wood and Brown, 1991, Swanson et al., 1987). In principle, therefore, tubules could serve as transport intermediates between different compartments but also other functions might be speculated. To define their precise role, the mechanisms regulating their homeostasis, need to be addressed.

1.1.4 Curvature of membranous tubules

Membranous tubules are formed by a lipid bilayer forming a curved surface. They are different from other extremely flat structures such as the cell wall, the outer membrane of mitochondria, and the cisternae of both the Golgi and the ER. The curvature of a lipid bilayer is the result of a balance between two opposing forces: the surface pressure (π), which takes into account all the repulsive forces existing between the lipids forming the bilayer, and the surface tension (τ), which takes in account the aggregating forces at the interface between the lipid bilayer and the aqueous environment (Oster et al., 1989). When these two forces are balanced, the bilayer tends to be flat, but when one overcomes the other a bending moment is generated and the bilayer is curved (Sackman, 1994, Oster et al., 1989; fig. 1.2). The curvature is termed positive or negative if "convex" or "concave" surfaces are generated. This ultimately depends on several factors, among which the most important is probably the "shape" of the lipids forming the bilayer (Cullis et al., 1996, Cullis and de Kruijff, 1979).

Lipids are amphipathic molecules formed by a hydrophilic (polar head) and a hydrophobic moiety (tail) whose relative sizes determine the way in which lipids are packed together in the bilayer (Lichtenberg, 1993, Marsh, 1993). In this way lipids are divided into two main groups: the bilayer lipids and the non-bilayer lipids. The first group is formed mainly by lipids in which the lateral extension of the polar head does not exceed that of the tail; these

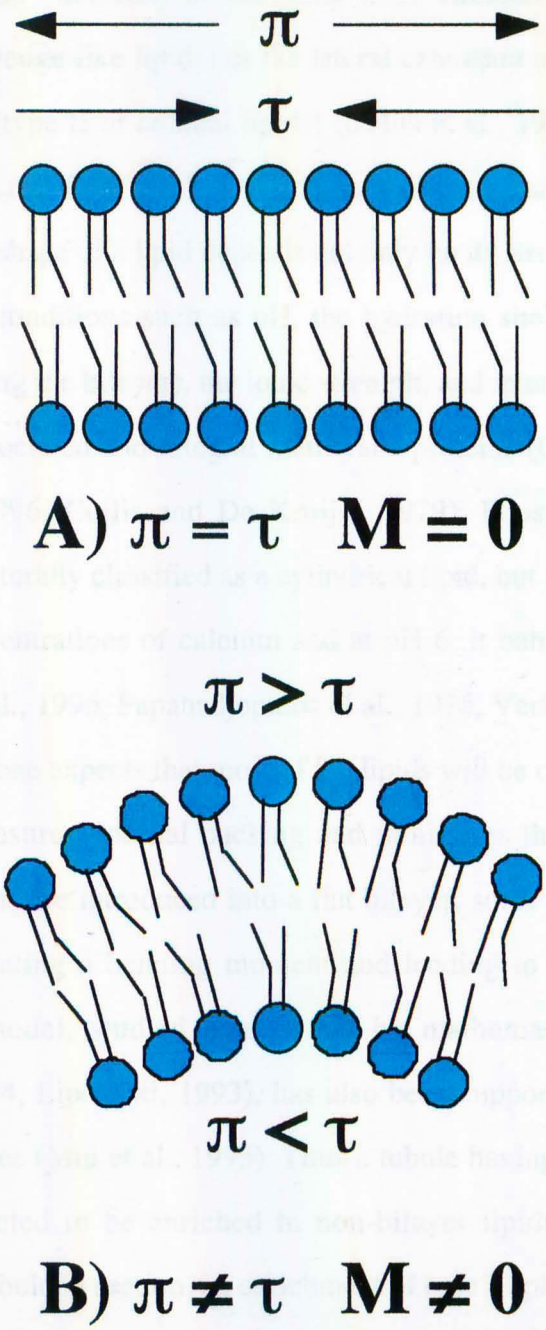

Fig. 1.2 Forces generating a bending moment (M) in a lipidic bilayer

A. Flat bilayer. The surface pressure (π) is equivalent to the surface tension (τ) and the bending moment (M) is null. B. Curved bilayer. $\pi<\tau$ in the concave surface while $\pi>\tau$ in the convex.

lipids are called "cylindrical". The second group is formed by lipids in which the lateral extension of the polar head exceeds the tail (type I, anticonical or wedge-like lipids) or the lateral extension of the tail exceeds the polar head (type II or conical lipids) (Cullis et al., 1996, Epand, 1988, Cullis and De Kruijff, 1979). In fig. 1.3. several examples of these classes are shown. The shape of a lipid depends not only on its structure, but also on environmental conditions such as pH, the hydration shell (the amount of water surrounding the bilayer), the ionic strength, and interactions with both peripherally associated and integral membrane proteins (Oster et al., 1989, Cullis et al., 1996, Cullis and De Kruijff, 1979). Phosphatidic acid for example is structurally classified as a cylindrical lipid, but in the presence of millimolar concentrations of calcium and at pH 6, it behaves as a conical lipid (Cullis et al., 1996, Papahadjopulos et al., 1976, Verkleij et al., 1982). In a flat bilayer one expects that most of the lipids will be cylindrical, as this conformation ensures optimal packing and minimises the free energy. If non-bilayer lipids are introduced into a flat bilayer, some deformations are expected, generating a bending moment and leading to curvature of the bilayer. This model, studied extensively by mathematical approaches (Sackmann, 1994, Lipowski, 1993), has also been supported by studies in model membranes (Mui et al., 1995). Thus a tubule having a highly curved surface is expected to be enriched in non-bilayer lipids. Analysing the geometry of a tubule in section, an enrichment of type I lipids in the external leaflet is expected whereas an enrichment of type II lipids is expected in the internal (see fig 1.4). This suggests that some of the factors regulating the dynamics of tubules are likely to be enzymes involved in lipid metabolism such as phospholipases or acyltransferases (see below). Flat lipid bilayers could be forced to adopt highly curved geometries by mechanical deformations induced by peripheral-associated proteins, even if the lipids do not have the correct structural requisites (Welti and Glaser, 1994, Mui et al., 1995).

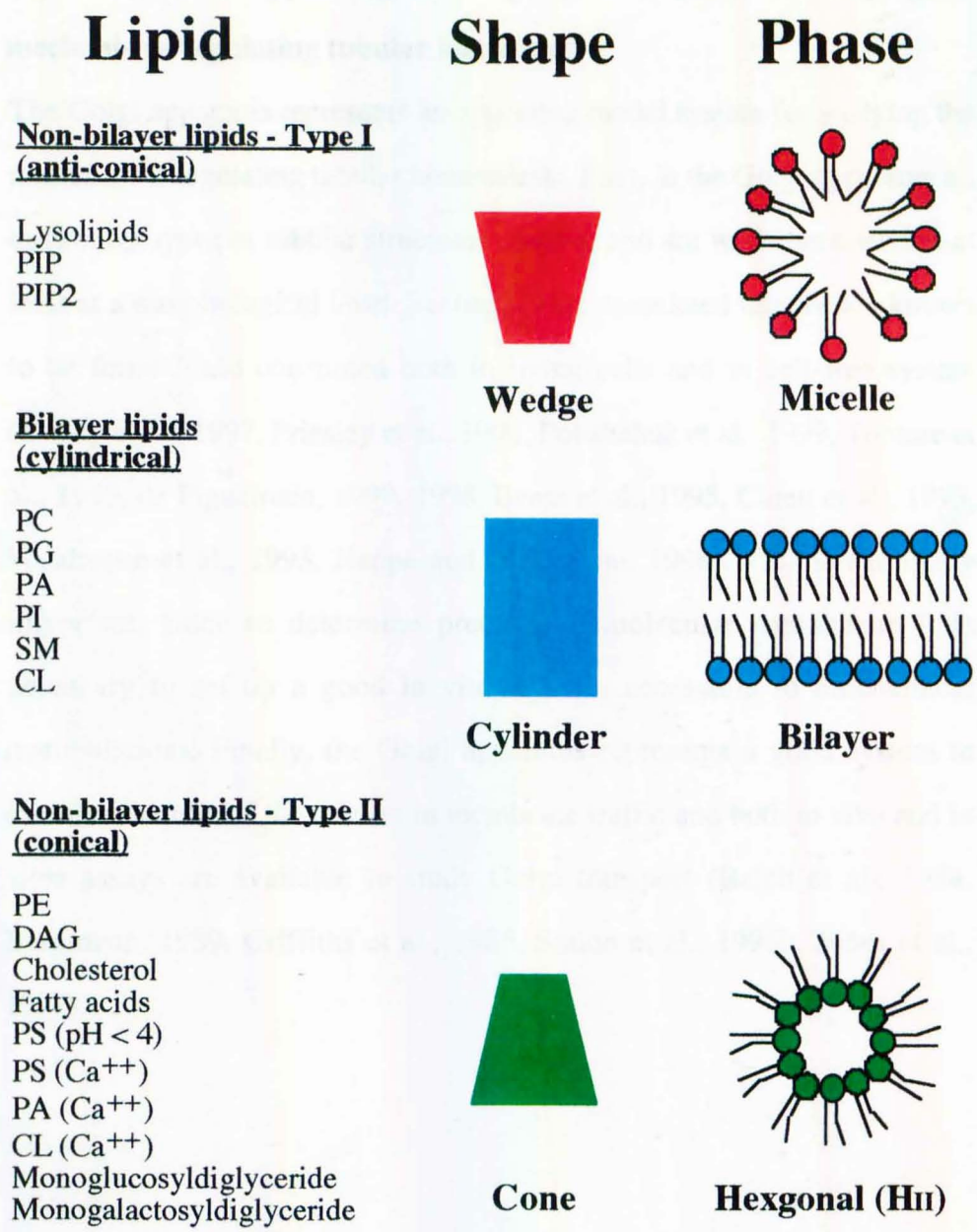

Fig. 1.3 Shapes and phase behaviour of common lipid molecules

Lipids form different structures according to their structural properties. Cylindrical lipids form bilayers, wedge-like lipids form micelles and conical lipids form hexagonal tubes.

1.1.5 The Golgi apparatus as an experimental model for studying the mechanisms regulating tubular homeostasis

The Golgi apparatus represents an appealing model system for studying the mechanisms regulating tubular homeostasis. First, in the Golgi apparatus all the known types of tubular structures co-exist and are well characterized at least at a morphological level. Second, Golgi associated tubules are known to be formed and consumed both in living cells and in cell-free system (Sciaky et al., 1997, Priesley et al., 1998, Polishchuk et al., 1999, Toomre et al., 1999, de Figueiredo, 1999, 1998, Banta et al., 1995, Cluett et al., 1993, Weidmann et al., 1993, Happe and Weidmann, 1998). This is extremely important, since to determine precisely a molecular mechanism it is necessary to set up a good in vitro system accessible to biochemical manipulations. Finally, the Golgi apparatus represents a good system to examine the role of the tubules in membrane traffic and both in vivo and in vitro assays are available to study Golgi transport (Balch et al., 1984, Bergmann, 1989, Griffiths et al., 1985, Simon et al., 1996b, Jones et al., 1997).

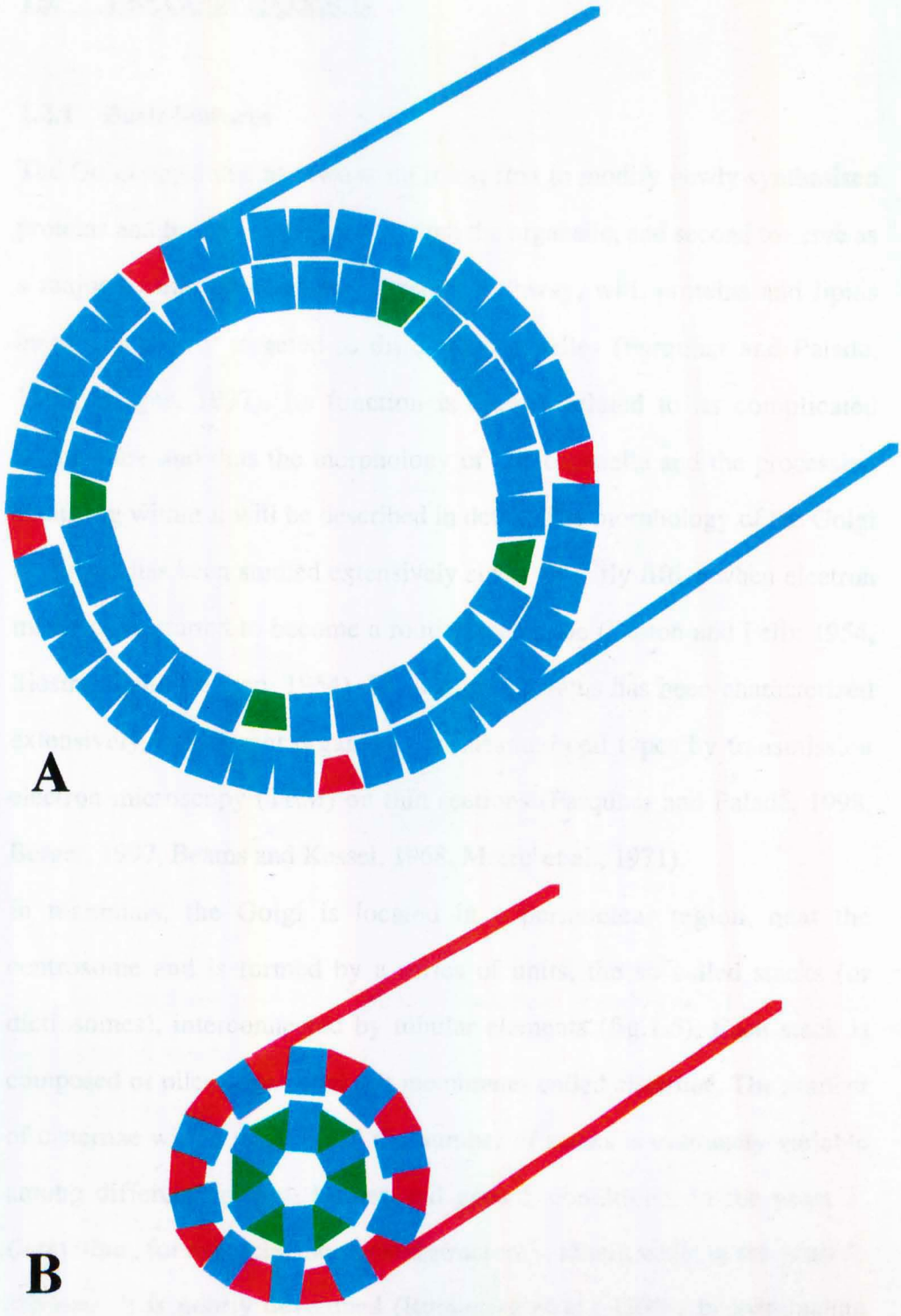

Fig. 1.4 Possible arrangements of lipids in tubular structures

A) Tubule with a low curvature. B) Tubule with a high curvature. In B the external leaflet is enriched in type I lipids while the internal leaflet is enriched in type II lipids.

1.2.1 Basic features

The Golgi apparatus has two main roles; first to modify newly synthesised proteins and lipids as they pass through the organelle, and second to serve as a major sorting point in the secretory pathway, with proteins and lipids being selectively targeted to different organelles (Farquhar and Palade, 1998, Berger, 1997). Its function is closely related to its complicated architecture and thus the morphology of this organelle and the processing occurring within it will be described in detail. The morphology of the Golgi apparatus has been studied extensively since the early fifties when electron microscopy started to become a routine technique (Dalton and Felix 1954, Sjostrand and Hanzon, 1954). The Golgi apparatus has been characterized extensively in different organisms, tissues and cell types by transmission electron microscopy (TEM) on thin sections (Farquhar and Palade, 1998, Berger, 1997, Beams and Kessel, 1968, Morre' et al., 1971).

In mammals, the Golgi is located in a perinuclear region, near the centrosome and is formed by a series of units, the so called stacks (or dictiosomes), interconnected by tubular elements (fig.1.5). Each stack is composed of piles of saccular flat membranes called cisternae. The number of cisternae within a stack and the number of stacks is extremely variable among different species, tissues and growth conditions. In the yeast *S. Cerevisiae* , for example, the stacked structure is absent while in the yeast *P. Pastoris* it is poorly developed (Rossanese et al., 1999). In mammalian cells, an average of 3 to 11 cisternae per stack can be observed, while in plants and lower organisms up to 30 cisternae per stack have been observed (Beams and Kessel, 1968, Morre' et al., 1971). These stacked structures are thought to be maintained by a so called "intercisternal matrix" composed of a series of proteins forming interconnecting bridges that can be observed at the EM level (Cluett and Brown, 1992, Mollenhauer and Morre', 1968). The real nature of this matrix is still unclear: the stacked

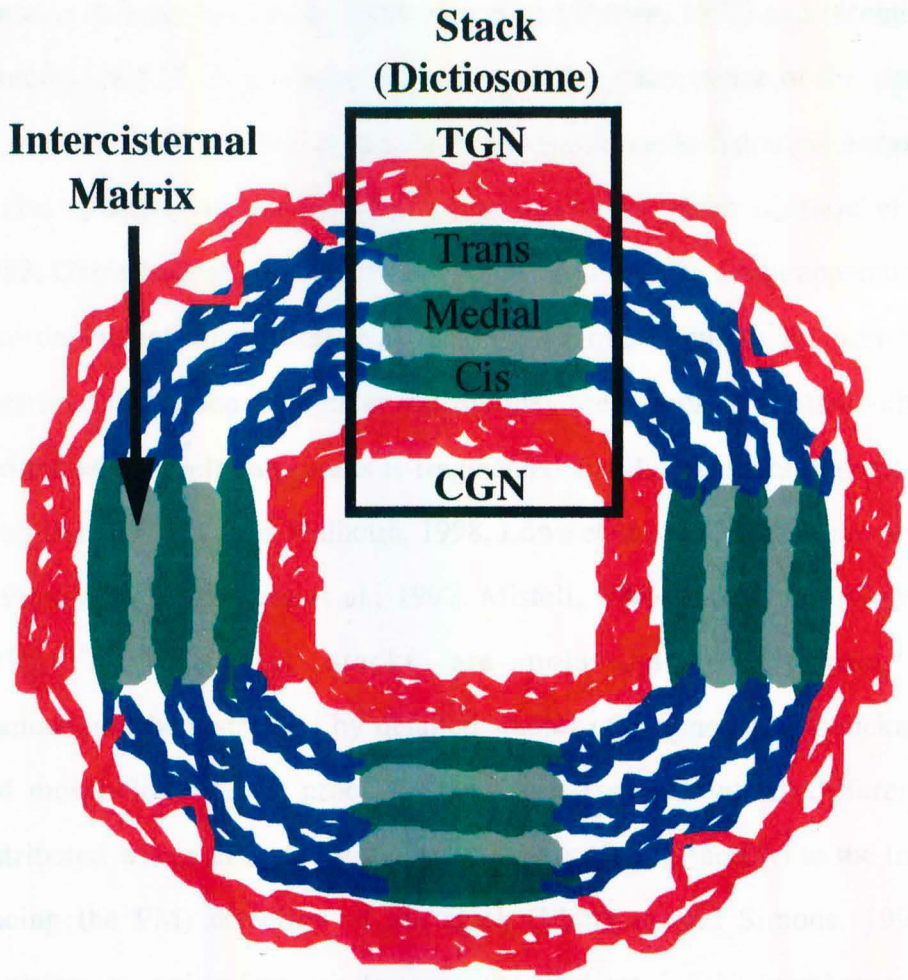

Fig. 1.5 Schematic view of the ribbon-like structures of the Golgi apparatus in mammalian cells

The Golgi apparatus is formed by single stacks composed of various saccular and reticular elements (dictiosomes, in green) bridged by tubular interconnections (red and blue).

structure is sensitive to different proteases, suggesting the involvement of proteins (Slusarewicz et al., 1994, Cluett and Brown, 1992) and recently a protein, GRASP65, has been implicated in the maintenance of the stacks (Barr et al., 1997). However, amylase, a polysaccharide degrading enzyme, is also effective in promoting unstacking in in vitro systems (Morre' et al., 1983, Ovtracht et al., 1973). The stacked structure of the Golgi apparatus is also dependent on the cell cycle; during interphase stacks are normally organised, but when cells enter mitosis they are completely disassembled and the whole Golgi apparatus is fragmented and dispersed throughout the cytoplasm (Warren and Malhotra, 1998, Lowe et al., 1998, Rabouille et al., 1997, 1995b, Nakamura et al., 1997, Misteli, 1996, Misteli and Warren, 1995, 1994). Golgi stacks are polarised as assessed by immunocytochemistry and by detailed studies of the membrane thickness and morphology. Golgi processing enzymes (see below) are differently distributed within cisternae going from the cis (facing the ER) to the trans (facing the PM) direction of the stack (Mellman and Simons, 1992). Furthermore, going from cis to trans, the thickness of the membrane, its cholesterol content and the lumenal calcium levels all increase, while the pH decreases (Bretscher and Munro, 1993, Orci et al., 1981, Taylor et al., 1998).

1.2.2 Three dimensional structure

In the last decade three-dimensional reconstructions of the Golgi apparatus in living cells have been carried out, using different techniques such as high voltage electron microscopy (HVEM) and computer axial tomography (Ladinsky et al., 1999, 1994), scanning electron microscopy (Inoue', 1992, Inoue' and Osatake, 1988, Tanaka et al., 1986), or stereoscopic techniques combined with immunocytochemistry (Rambourg and Clermont, 1997, 1990, Rambourg et al., 1995, 1994, 1993). From these studies, tubular structures are seen as a predominant feature of the Golgi apparatus. Rambourg and colleagues, in particurar, have clearly shown that the Golgi apparatus appears as a single organelle consisting of a branching and

anastomosing ribbon forming a juxta- or perinuclear network (fig.1.6). Along the Golgi ribbon, compact regions made up of stacked saccules alternate with non-compact, highly fenestrated or tubular regions that bridge saccules of either the same or adjacent compact zones (Thorne-Tjomsland et al., 1998, Rambourg and Clermont, 1990). On its cis-trans axis, the compact region of the Golgi ribbon may be subdivided into three main compartments: (i) the cis-compartment, made up exclusively of anastomosed membranous tubules, forming a network referred to as the cis-Golgi network (CGN, Ladinsky et al., 1999, Rambourg and Clermont, 1997, Lindsay and Ellisman, 1985), (ii) the mid-compartment comprising poorly fenestrated, more or less dilated saccules depending on the presence of secretory material within their lumen (Rambourg and Clermont, 1997, Hermo and Smith, 1998) and (iii) the trans-compartment composed of three or more sacculo-tubular elements which are not continuous along the Golgi ribbon but instead display a "peeling off" configuration (Rambourg and Clermont, 1997, 1990). In cells not engaged in the production of secretory granules, the tubular portions of the trans-elements are well developed and form extensive trans-tubular polygonal networks referred to as TGN (Roth and Taatjes, 1998, Rambourg and Clermont, 1997). In contrast, in glandular cells, the formation of secretory granules mobilises most of the membrane of the trans-Golgi elements, and the tubular portions or TGN are small or even absent (Rambourg and Clermont, 1997).

1.2.3 Golgi -resident enzymes

The Golgi apparatus is the central organelle along the secretory pathway where proteins and lipids are processed and sorted to their final destination. The most abundant processing enzymes of the Golgi apparatus include the glycosidases and glycosyltranferases responsible for synthesising the huge diversity of complex oligosaccharides that are attached to both glycoproteins, on N-linked and O-linked glycan branches, and glycolipids (Varki, 1998, Rabouille et al., 1995a, Mellman and Simons,

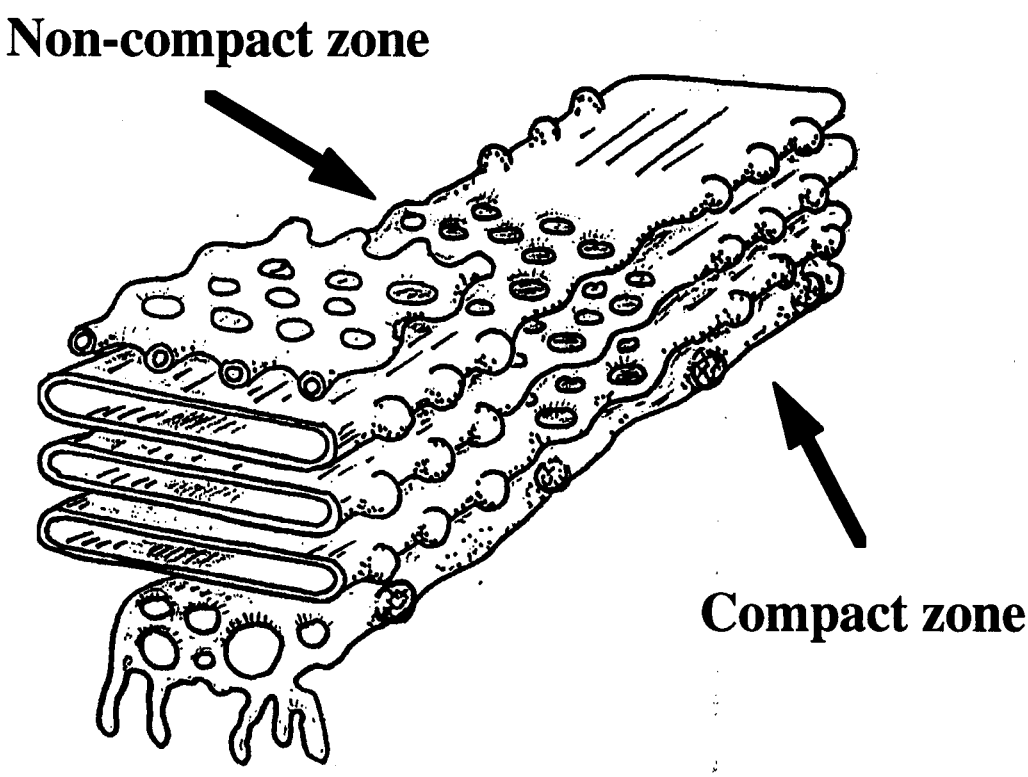

Fig. 1.6 Schematic drawing of the three-dimensional architecture of the Golgi apparatus

The arrows indicate the saccular part (compact zone) formed by cisternal elements and the tubular-reticular part (non-compact zone) formed by tubules and highly fenestrated elements.

1992). Indeed the Golgi is the site of synthesis of many sphingolipids, and glucosylceramide, the precursor of many other glycolipids (van Meer, 1998).

Most of the processing enzymes of the Golgi are type II integral membrane proteins with a small cytosolic domain and a large luminal domain harbouring the catalytic activity. Their distribution is compartmentalised in order to ensure the correct sequential processing of proteins. Most catalyse the transfer of different sugars (mannose, glucose, galactose, fucose or sialic acid) to the NH_2 group of the amino-acid asparagine on processed proteins. They are commonly used as markers for the different compartments, for example mannosidase II and NAGTI are found mainly in the cis-medial Golgi, galactosyl transferase and sialyltransferases in the medial and trans-Golgi. Several others are listed in table I.I (Farquhar and Hauri, 1997 and references therein).

Golgi compartment	Protein
cis and CGN	GalNAC-transferase
	GlCNAC Phosphotransferase
	KDEL-
medial	α-mannosidase I
	GlcNAC-transferase I
	α-mannosidase II
	Giantin
	GPP130/GIMPc
	MG160
trans	β-1,4-galactosyltransferase
	α-2,6-sialyltransferase
TGN	TGN-38
	Furin
	Mannose 6-phosphate receptor
	Tyrosylprotein/sulfotransferase

Table I.I. Localisation of membrane proteins to Golgi compartments in mammalian cells

1.2.4 Mechanisms for the localisation of Golgi enzymes

In spite of the continuous flow of both lipids and proteins across the Golgi apparatus, this organelle maintains a degree of compartmentalisation. The mechanism by which resident proteins are retained within the Golgi complex and specifically within certain cisternae is of great interest. So far four main mechanisms have been proposed. (i) An interaction between the transmembrane domain (TMD) of Golgi resident proteins and the lipid bilayer. According to this model, the length of the TMD is a sufficient signal for retention such that there is a match between the length of the TMD and the thickness of the lipid bilayer (Munro, 1998, Bretscher and Munro, 1993, Mouritsen and Bloom, 1993, Machamer, 1993, 1991). In this way the TMD that is formed by hydrophobic aminoacids would be totally buried in the lipid bilayer thus minimising the free energy of the system. (ii) The oligomerization of resident enzymes (kin-kin recognition) to form very large aggregates that are retained due to their inaccessibility to transport carriers (Nilsson et al., 1994). (iii) A specific signal located either in the luminal or in the cytoplasmic portion of the protein is responsible for localisation (Munro, 1998). These signals would be recognised by specific receptors localised in the Golgi, thus provide an anchoring site for the protein or could be used as retrieval signals by receptors localised in the next compartments allowing recycling back to the Golgi. (iv) Finally, some proteins could interact via specialised domains with cytoskeletal elements such as microtubules, the actin cytoskeleton or the intercisternal matrix (Munro, 1998, Nilsson et al., 1994)

1.2.5 Lipid composition of the Golgi apparatus

In mammalian cells, the existence of a continuous gradient along the secretory pathway has been proposed to occur for some lipid species (see table I.II, van Meer, 1998, Bretscher and Munro, 1993, Allan and Kallan, 1994). This model predicts that the Golgi apparatus should have a lipid composition intermediate between the ER and PM. While for phosphatidylserine (PS) and sphingomyelin (SM) this gradient has been

observed, for other lipids such as phospahtidylcholine (PC) and phospahtidylethanolamine (PE) the composition reflects more or less the general average composition of the Golgi for other intracellular organelles (van Meer, 1998).

Organelle	PC	PE	PS	PIs	SM	Chol*
ER	58	22	3	10	3	0.08
Golgi	50	20	6	12	8	0,16
PM	39	23	9	8	16	0,35

Table I.II. Lipid composition of intracellular organelles.

Values are expressed as mole percentage of total phospholipids. * Values represent the ratio between cholesterol and total phospholipids.

An exception is represented by phosphoinositides (PIs) which are highly enriched in the Golgi apparatus (van Meer, 1998, Howell and Palade, 1982). An exact determination of the lipid composition of the Golgi apparatus and an estimation of the fatty acid composition of lipids such as diacyglycerol (DAG), ceramide (CM), free fatty acids and lysophospholipids is still missing and for two main reasons. First, the techniques for purifying this organelle are not satisfactory and in the best conditions of purification, there is still some 30 % contamination from other membranes (Allan and Kallan, 1994). Second, since some lipids can be produced during membrane purification and they do not necessarily reflect the real composition of this organelle in living cells. The first problem has been partially solved recently by the introduction of a new technique based on the analysis of the lipid composition of the membranes surrounding specific viruses known to bud from specific organelles (Cluett and Machamer, 1996). This technique has confirmed the previous estimates of the lipid composition of the Golgi apparatus, at least for the major lipids (see table I.II). Furthermore it has led

to the identification of a special lipid, semilysobisphosphatidic acid (SLBPA), which is highly enriched in the tubular part of the Golgi apparatus (Cluett et al., 1997, Cluett and Machamer, 1996, van Blitterswijk and Hilkmann, 1993). This lipid, being a non-bilayer lipid, is compatible with the high curvature of a membranous tubule. Cholesterol is another interesting lipid for which a concentration gradient has been seen going from the endoplasmic reticulum towards the plasma membranes (van Meer, 1998). However, the existence of this gradient within Golgi stacks is still controversial (Bretscher and Munro, 1993, Allan and Kallan, 1994, Orci et al., 1981). The conclusion was based on morphological criteria, specifically on membrane thickness which is known to be dependent on cholesterol levels and which was found to increase from the CGN to the TGN. In parallel, the amount of cholesterol was measured by using gold-labeled filipin, a compound known to bind cholesterol with a high affinity (Orci et al., 1981). Furthermore, lipid domains enriched in cholesterol and sphingolipids (rafts) and present in the TGN have recently been proposed to have a specific role in sorting cargo destined towards apical membranes in polarised cells (Verkade and Simons, 1997, Scheiffele et al., 1996).

1.2.6 Dynamic analysis of Golgi tubules

The Golgi apparatus has recently been studied dynamically, taking advantage of modern technologies of molecular biology and the use of green fluorescent protein (GFP) technology. GFP is a 27-kDa protein derived from the jellyfish Aequorea victoria (Chalfie et al., 1994). It absorbs blue light and emits green light in the absence of added cofactors. Time-lapse imaging of Golgi membranes labelled with GFP fusion proteins has provided insights into the dynamic properties of Golgi tubules, including how they arise and their lifetime and fate in vivo (Toomre et al., 1999, Lippincott-Schwartz et al., 1998, Presley et al., 1998, Hirschberg et al., 1998, Sciaki et al., 1997). Using GFP-tagged KDEL-R (a protein recycling from Golgi to ER, Lewis and Pelham, 1992) and GalTase to label Golgi membranes, it has been shown that membrane tubules extend continuously from the Golgi and

break off and move at rates of 0.6 μm s-1 along microtubules (Sciaky et al., 1997). Similar findings were obtained using GFP-tagged VSVg and studying its fate during its transport from the TGN to the plasma membrane (Polishchuk et al., 1999, Toomre et al., 1999) or using the fluorescent lipid analogue NBD-ceramide, specific for the trans-TGN compartments (Cooper et al., 1990).

1.3.1 Classical models for protein transport

A long held view has been that proteins are concentrated, assembled and transported exclusively in vesicular carriers, the "vesicular theory" between different compartments in the secretory pathway (fig. 1.7, Rothman and Orci, 1992, Rothman, 1994, 1992, Pryer et al., 1992). Alternative models were largely neglected since a large amount of biochemical data appeared to support this model. In the last few years, however, these models have been re-evaluated especially with the growing body of evidence that the vesicular theory alone can not account for all the transport steps (Mironov et al., 1997). Furthermore, at least for some special cases such as intra-Golgi transport, cargo molecules have never been found to be concentrated in vesicular carriers, as might have been expected. Alternative models that have been considered are the maturation model (Allan and Balch, 1999, Bonfanti et al., 1998, Mironov et al., 1997) and the tubular model (Mironov et al., 1997, Weidmann, 1995, Ajala, 1994).

In the maturation model, molecules are not transported from one compartment to another, but it is the compartment itself which is transformed into a new one, undergoing both biochemical and morphological transformation (Mironov et al., 1997). In this model, the enzymes/lipids forming the different compartments are transported in a retrograde direction, thus leaving still pending the problem of defining how they are transported. In the tubular model, cargo is transported from one compartment to another, but the transport intermediates are tubules (Mironov et al., 1997, Weidmann, 1995). These tubules can form, detach and then fuse with the target compartment, or can form continuities that could be transient or permanent (Mironov et al., 1997).

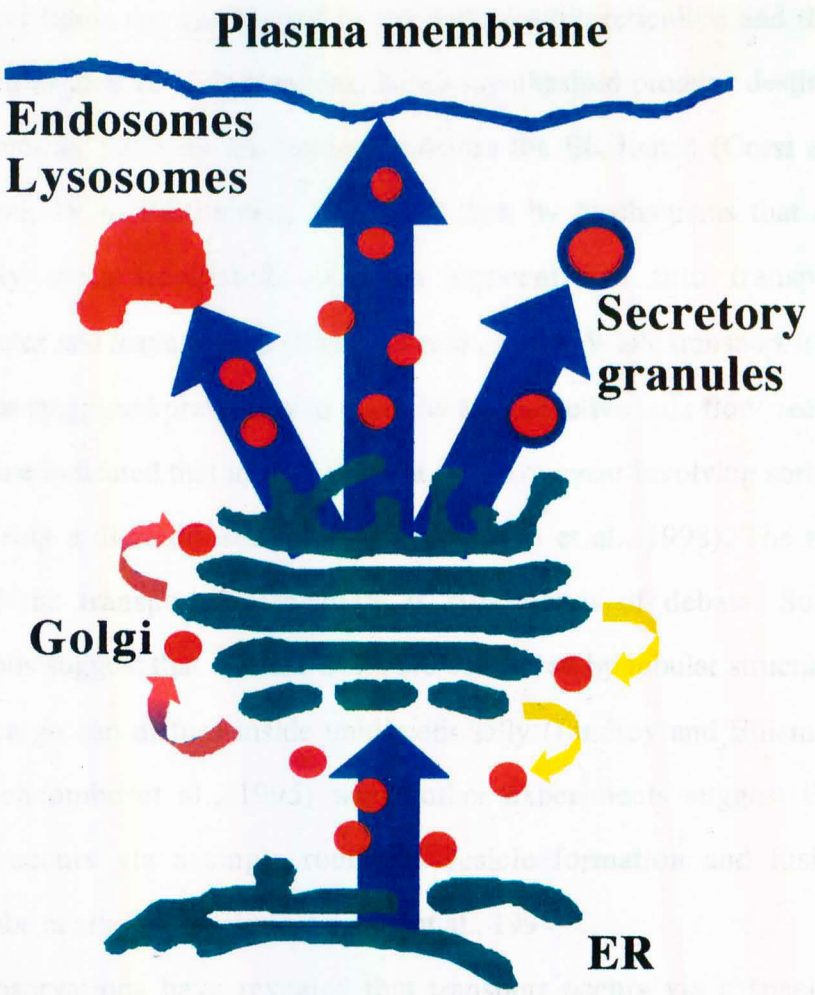

Fig. 1.7. Intracellular transport according the vesicular theory

Molecules are transported in vesicular carriers budding from a compartment and fusing with the next in the secretory pathway.

1.3.2 ER to Golgi transport

Protein and lipids are synthesised in the endoplasmic reticulum and then transported to their final destinations. Newly-synthesised proteins destined to the secretory pathway are translocated into the ER lumen (Corsi and Schekmann, 1996, Reithmeier, 1996) and then by mechanisms that are reasonably well elucidated, they are concentrated into transport intermediates and leave the ER (Bannykh et al., 1998). While transport from the ER was suggested previously to occur by a constitutive bulk flow, recent studies have indicated that instead this is a selective event involving sorting and requiring a di-acidic sorting signal (Bannykh et al., 1998). The real nature of the transport intermediate is still matter of debate. Some observations suggest that ER and Golgi are connected by tubular structures and that cargo can diffuse inside unidirectionally (Lindsey and Ellisman, 1985, Stichcombe et al., 1995) while other experiments suggest that transport occurs via a single round of vesicle formation and fusion (Stinchombe et al., 1995, Krijnse-Locker, et al., 1994).

Recent observations have revealed that transport occurs via a specific transport machinery referred to as COPII (Schekman and Orci, 1996, Barlowe et al., 1994). This complex has been extensively characterized both in yeast and in mammals and suggested to be necessary to bud 50-80 nm vesicular structures in which cargo is concentrated. The mature vesicles are then released and travel towards Golgi membranes where they either fuse releasing their contents, as happens in yeast (Aridor et al., 1998, Schekman and Orci, 1996, Barlowe et al., 1994) or, in mammals, they fuse together forming an intermediate compartment (ERGIC) which, with the help of the COPI machinery, can mature and then fuse with the cis-Golgi apparatus (Shima et al., 1999). Recent observations using electron microscopy has shown that these COPII-dependent transport intermediates are pleiomorphic structures, tubulovesicular in nature, and are transported towards the Golgi apparatus in a microtubule dependent fashion (Bannykh et al., 1998).

1.3.3 Intra-Golgi transport

In spite of the clear abundance of tubular interconnections between Golgi stacks, anterograde and retrograde intra-Golgi transport are thought to occur only via COPI-dependent transport vesicles budding from a cisterna and fusing with another. In the last decade this model has been supported by a huge body of biochemical data obtained from in vitro assays that were supposed to reconstitute intra-Golgi transport (referred as "Rothman transport assay", Balch et al., 1984). While this assay has undoubtedly led to the discovery of new molecules important for transport (for example the NSF, the SNAREs, the coatomer complex (COPI) and many others; see Rothman and Orci, 1992), it has recently been shown by different authors that the assay does not measure anterograde vesicular-based intra-Golgi transport, but rather a series of retrograde fusion events between cisternae (Happe and Weidmann, 1998, Dominguez et al., 1999). The role of the vesicles in intra-Golgi transport has, therefore, become less clear.

For the maturation model (fig. 1.8), that has been shown to be valid at least for the transport of supramolecular cargo, vesicles could be retrogradelly directed to relocate Golgi processing enzymes and lipids and allow maturation of the incoming cisterna (Bonfanti et al., 1998). Alternatively, vesicles could serve as carriers only for specific cargo. In the tubulation model, it has been proposed that transport occurs via tubular structures (fig. 1.8). However, so far tubules interconnecting adjacent stacks exclusively join homologous cisternae (i.e. cis with cis, medial with medial, etc.) and thus they could in principle serve as fast lanes for maintaining and regulating a homogenous composition between them (fig. 1.8, Ladinsky et al., 1999). Heterologous interconnections have not been seen, but they may be very transient (fig. 1.8). Another possible role for tubules is raised by the observation that vesicular structures often bud from them (Weidmann et al., 1993, Orci et al., 1986). This implies that tubules could serve as sites specialised for budding, and possibly fission, due to their peculiar geometry.

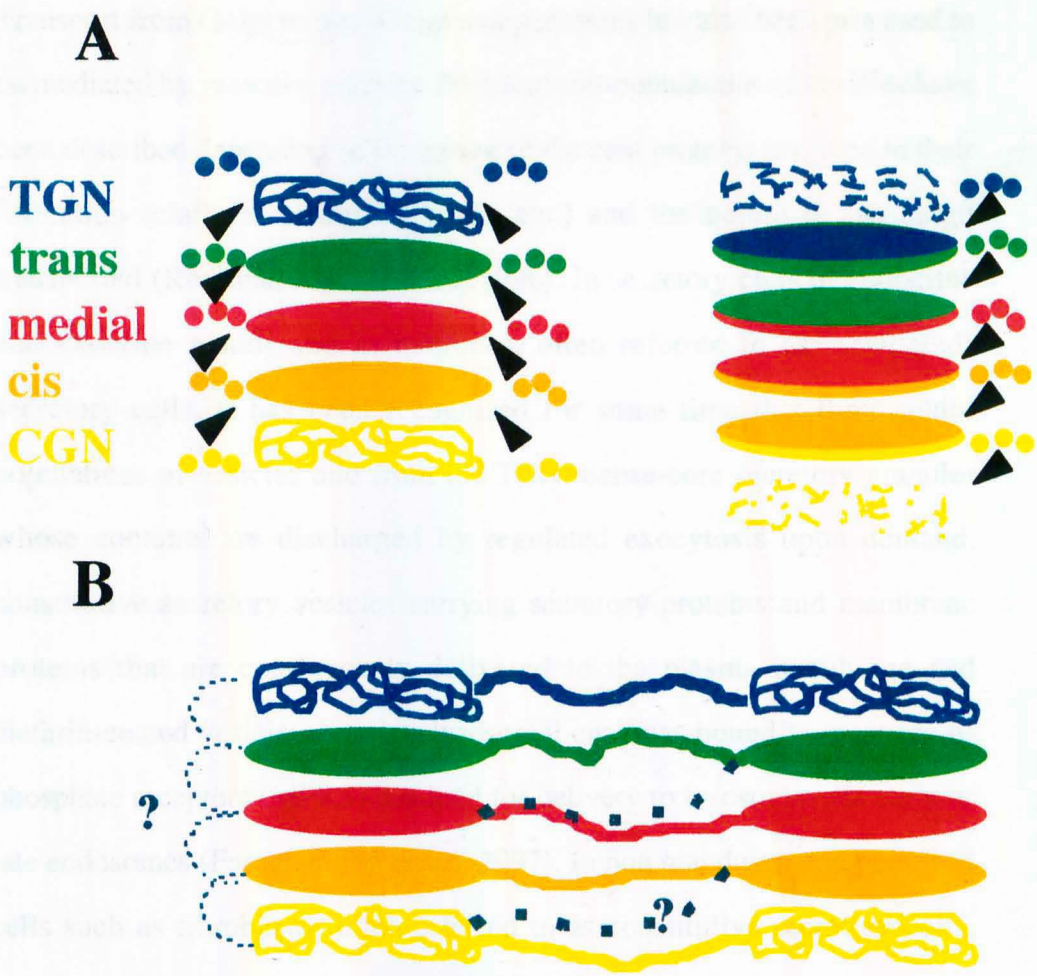

Fig. 1.8 Alternative models for intra-Golgi transport

A. Maturation model. Cargo molecules are not transported through the Golgi apparatus in vesicular carriers, but instead Golgi processing enzymes are relocated retrogradelly. B. Tubular model. Cargo molecules are transported in tubular structures which stably interconnect homologous cisternae (same colours) or via transient tubular continuities which interconnect heterologous cisternae (dashed tubules).

1.3.4 Transport from the Golgi to post-Golgi compartments

Transport from Golgi to post-Golgi compartments has also been proposed to be mediated by vesicular carriers. Different sub-populations of vesicles have been described depending of the nature of the coat proteins involved in their formation (clathrin, coatomer, p200, etc.) and the nature of the cargo transported (Rothman and Wieland, 1996). In secretory cells of endocrine and exocrine glands and in neurones, often referred to as "regulated" secretory cells, it has been recognised for some time that three major populations of vesicles bud from the TGN: dense-core secretory granules whose contents are discharged by regulated exocytosis upon demand, constitutive secretory vesicles carrying secretory proteins and membrane proteins that are continuously delivered to the plasma membrane and clathrin-coated vesicles carrying lysosomal enzymes bound to mannose 6-phosphate receptors (MPRS) destined for delivery to lysosomes via early or late endosomes (Farquhar and Hauri, 1997). In non glandular, non polarised cells such as fibroblasts, often referred to as constitutive secretory cells, only two TGN-derived vesicle populations have already been recognised, one carrying lysosomal enzymes destined for lysosomes and the other assumed to carry both constitutively secreted membrane and secretory proteins. With GFP-technology, however, it has been shown that other cargos, like the VSVg, are transported in non-vesicular carriers. At the light microscopy level, these carriers appear mostly as tubules which form, detach and are transported to the plasma membrane where they fuse (Toomre et al., 1999, Hirschberg et al., 1998, Nakata et al., 1998). A further characterization by electron microscopy of these structures has revealed that these structures are indeed sacculo-tubular in nature (Polishchuk et al., 1999). This finding further confirms the existence of multiple carriers and mechanisms for protein transport.

1.3.5 Retrograde transport from Golgi to the ER

Proteins and lipids are retrogradelly transported from the Golgi apparatus to the ER (Cole et al., 1998). This kind of transport appears to be dependent on the COPI machinery (Cosson and Letourner, 1997). Among the proteins that are transported retrogradely are those escaping the ER quality control system. These proteins bear a specific motif in their sequence (KKXX, KDEL) that binds to a cis-Golgi localised receptor (KDELR) and are then retrieved (Lewis and Pelham, 1992). Studies carried out with a GFP-KDELR chimera have clearly shown that this protein is localised in tubular structures which form from the Golgi apparatus, move towards the cell periphery, and then curl up and disappear from view (Sciaky et al., 1997). These characteristics suggest that they might represent retrograde transport intermediates.

1.4 Molecules implicated in the regulation of tubular structures

1.4.1 Introduction

The tubular structures associated with the Golgi apparatus or implicated in the transport events have been extensively characterized morphologically but their physiological role is still unclear.

1.4.2 Molecules implicated in the formation of tubules

1.4.2.1 Brefeldin A (BFA)

BFA is a metabolite synthesised in the fungus *Pennicillum Brefeldianum* as a metabolic product of palmitic acid (fig. 1.9 Harri et al., 1963). This toxin is a very popular tool in cell biology to study intracellular transport. BFA blocks, in a reversible manner, both intracellular trafficking and protein secretion and this is a consequence of the dramatic structural changes that BFA induces on the architecture of the Golgi apparatus (Klausner et al., 1992). Its main effect is to promote the redistribution of Golgi enzymes and lipids back to the ER. This process is very complex and involves several steps. First, a series of peripheral Golgi-associated proteins, including the ADP-ribosylation factor (ARF) and the coatomer complex detach from the Golgi apparatus and redistribute into the cytoplasm (see below and Donaldson et al., 1992,1991,1990, Helms and Rothman, 1992). Second, the Golgi undergoes a massive tubular reticular transformation (fig. 1.9 and Pavelka and Ellinger, 1993, Cluett et al., 1993, Orci et al., 1991) followed by a microtubule-dependent sprouting of very long tubules towards the cell periphery (Klausner et al., 1992, Lippicott-Schwartz et al., 1991, 1990). Finally, these tubules fuse with the ER thereby mediating the fast redistribution of Golgi proteins and lipids into the ER (Sciaki et al., 1997). When BFA is washed out from the cells, Golgi enzymes are exported out from the ER, and the Golgi apparatus is built up again, with a complete restoration of both intracellular transport and secretion (Lippincott-Schwartz

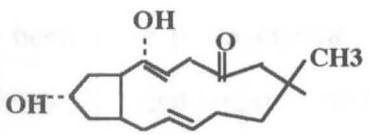

Brefeldin A

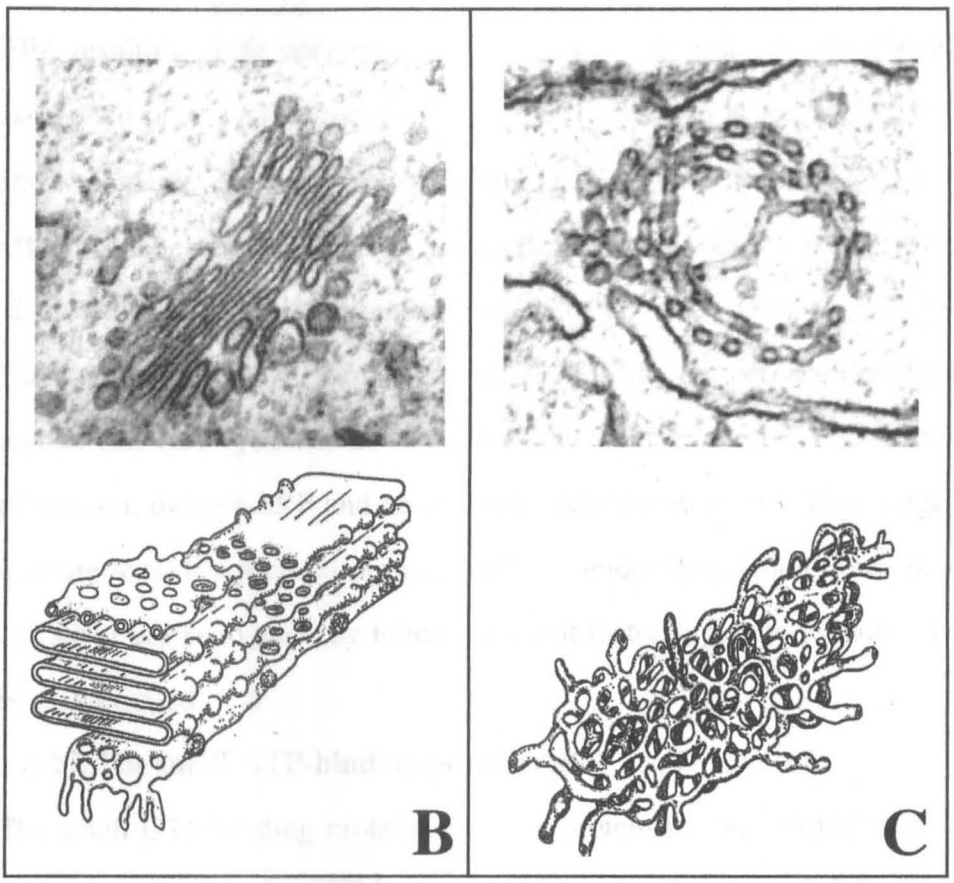

Fig. 1.9 Effect of brefeldin A on the architecture of the Golgi apparatus

A. Structure of BFA. B. Golgi apparatus in control conditions. C. Golgi apparatus in BFA-treated cells . Upper part, electron micrographs of Golgi complex from RBL cells (reproduced from Mironov et al., 1997). Lower part, schematic drawing of the three-dimensional rearrangements of the Golgi apparatus upon BFA treatment.

et al., 1989).

Several attempts have been made to understand the mechanism of BFA action at a molecular level. The first target of BFA to be identified was a guanosine exchange factor (GEF) specific for the small GTP-binding protein ARF (see below). ARF binding to Golgi membranes is inhibited by BFA resulting in the concomitant detachment of several other peripherally associated proteins (Peyroche et al., 1996, Donaldson et al., 1992, Helms and Rothman et al., 1992). BFA is also effective in*in vitro* systems and full effect can be reconstituted in permeabilized cells and a partial effect observed on Golgi membranes (Cluett et al., 1993, Orci et al., 1991, Donaldson et al., 1991, Mironov et al., 1997b). In both permeabilized cells and in cell-free systems, BFA requires cytosolic proteins for promoting tubulation, though ARF and coatomer detachment does not. This suggests that the loss of structural proteins, at least under these conditions, is not sufficient *per se* to generate tubules and that factor(s) promoting tubulation is(are) required.

1.4.2.2 The small GTP-binding protein ARF

The small GTP-binding protein ARF is a protein known to bind to Golgi membranes when in its GTP-bound form (fig. 1.10, Boman and Kahn, 1995, Donaldson and Klausner, 1994). In this state, ARF exposes a myristoylated tail which promotes insertion of the protein into the Golgi membranes. GTP binding is catalyzed by an exchange factor (GEF) that is one of the targets of BFA (Donaldson et al., 1992, Helms and Rothman, 1992).ARF-binding to Golgi membranes is well known to promote the binding of several other proteins including the coatomer complex, spectrin, actin, phospholipid kinases and many others (Orci et al., 1993, Godi et al., 1999, 1997). Furthermore it is known that ARF stimulates phospholipase D activity and the production of the phosphoinositide, PI(4,5)P_2 (Kahn et al., 1993, Godi et al., 1999). The release of ARF from the membrane is triggered by an ARF-specific GAP protein, which stimulates GTP hydrolysis to GDP(Boman and Kahn, 1995, Donaldson and Klausner, 1994)

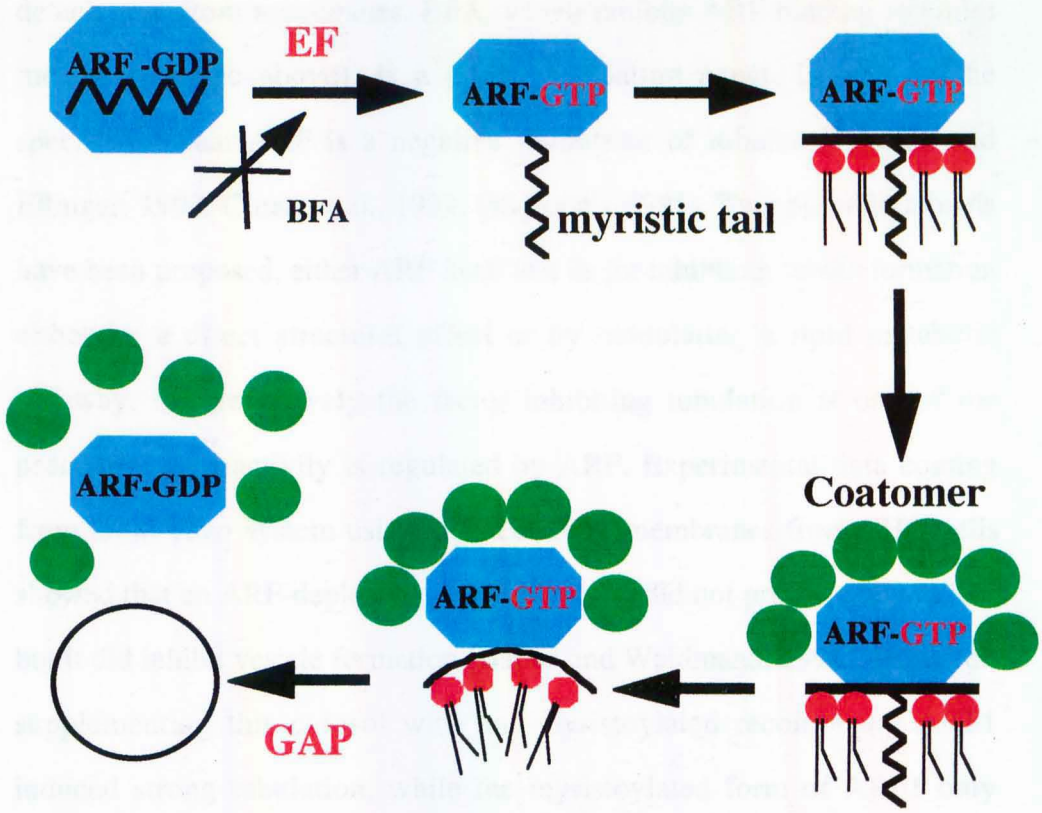

Fig. 1.10 Mechanism of ARF/coatomer binding to Golgi membranes

ARF inserts in the lipidic bilayer by a fatty acyl moiety that is exposed when the protein is in the GTP-bound form. This process is catalyzed by a BFA-sensitive exchange factor (GEF). The coatomer complex then binds to the membranes and budding starts to occur. When the fully-formed vesicle is released from the Golgi membranes, a GAP protein triggers GTP hydrolysis and ARF switches to the GDP-bound form and is released together with the coatomer complex.

causing a conformational change and retraction of the myristic tail and detachment from membranes. BFA, which inhibits ARF binding to Golgi membranes (see above), is a potent tubulating agent, leading to the speculation that ARF is a negative modulator of tubules (Pavelka and Ellinger, 1993, Cluett et al., 1993, Orci et al., 1991). Two possible models have been proposed, either ARF itself is a factor inhibiting tubule formation either by a direct structural effect or by modulating a lipid metabolic pathway, or alternatively the factor inhibiting tubulation is one of the proteins whose activity is regulated by ARF. Experimental data coming from an *in vitro* system using isolated Golgi membranes from CHO cells showed that an ARF-depleted cytosolic fraction did not promote tubulation, but it did inhibit vesicle formation (Happe and Weidmann, 1998). However, supplementing this cytosol with non-myristoylated recombinant ARF1 induced strong tubulation, while the myristoylated form of ARF1 only restored vesiculating activity. Non-myristoylated ARF is not competent to bind to Golgi membranes and this suggests that when ARF is in the cytosolic form it is directly able to stimulate tubule formation (Happe and Weidmann, 1998).

1.4.2.3 The coatomer complex

This complex is formed by seven subunits (α, β, β', γ, δ, ε, ζ) which assemble in the cytoplasm and bind to Golgi membranes in an ARF-dependent manner (fig. 1.10). Coatomer has been shown to be essential for the generation of coated buds from Golgi membranes which then mature in vesicles. When vesicles detach from the parental membranes, coatomer is released and redistributed to the cytoplasm ready for the next round of vesiculation (Zhao et al., 1997, Sheckman and Melmann, 1997, Orci et al., 1993, Palmer et al., 1993, Tanigawa et al., 1993). It has been suggested that the coatomer complex is one of the factors inhibiting the formation of Golgi tubules and this is based on different lines of evidence: (i) the drug BFA which prevents coatomer binding (Donaldson et al., 1991, 1990 and see above), induces in parallel the tubular reticular transformation of the Golgi

apparatus (Pavelka and Ellinger, 1993), (ii) when Golgi membranes were induced to tubulate using BFA or ATP-depletion and then isolated and re-incubated with coatomer, tubules were selectively broken (Cluett et al., 1993), (iii) in CHO mutants cells that are defective in the ε subunit of the coatomer (ldlf mutants), the Golgi complex is abnormally tubulated (Guo et al., 1994), (iv) cytosol derived from HeLa cells and immunodepleted of the β subunit of the coatomer complex induced tubular reticular transformation of isolated Golgi membranes (Misteli and Warren, 1995, 1994). However, another group found that depleting a rat liver cytosolic extract of the same subunit had no effect on the Golgi apparatus (Orci et al., 1993). Thus, the way in which coatomer influences tubules is far from clear. Several possibilities exist: (i) coatomer detachment eliminates some physical constraints impeding the tubulation of membranes, (ii) coatomer allows the binding of tubulating factor(s) residing either in the cytosol or on the membranes, (iii) coatomer-dependent vesicle formation could be the mechanism by which tubules are normally consumed and thus the inhibition of this pathway would allow the generation of tubules.

1.4.2.4 BFA-dependent ADP-ribosylation substrate (BARS)

Other targets of BFA have been recently discovered. BFA has been shown to induce the mono-ADP ribosylation of two cytosolic proteins (Di Girolamo et al., 1995, De Matteis et al., 1994). ADP-ribosylation is a post-translational modification in which the ADP-ribose moiety of the nucleotide NAD^+ is covalently bound to an aminoacidic residue of target proteins (Moss and Vaughan, 1988, Ueda, 1985). The targets of the BFA-dependent mono-ADP-ribosylation are the glycolytic enzyme glyceraldehyde 3-phosphate dehydrogenase (GAPDH), and a 50 kDa protein termed BARS (BFA dependent ADP-Ribosylating Substrates). BARS has been recently cloned (Spano' et al., 1999) and found to be an isoform of CtBPs (C-terminal binding proteins), a family of proteins involved in the regulation of transcriptional events (Schaeper et al., 1998, 1995, Kastanis et al., 1998, Boyd et al., 1993).

ADP-ribosylation of BARS facilitates BFA-dependent tubulation independently of the impairment of the ARF cycle (Mironov et al., 1997). This was shown by inhibiting the ADP-ribosylation of these proteins both in permeabilized and in living cells (Mironov et al., 1997, Weigert et al., 1997). Permeabilisation induces a rapid loss of cytoplasm and this was used as a way of depleting endogenous NAD^+, the essential substrate for the ADP-ribosylation reaction. Cytoplasm was replaced with cytosolic extracts extensively dialysed and with NAD^+ levels in the nanomolar range. Under these conditions BFA was not active in promoting the tubular reticular transformation of the Golgi apparatus, activity that was restored upon the addition of exogenous NAD^+ (Mironov et al., 1997). In living cells the effect of BFA was antagonized by a series of drugs that potently inhibited the BFA-dependent ADP-ribosylation (Weigert et al., 1997). Among them dicumarol and ilimaquinone (Achraya et al., 1995, Takizawa et al., 1995, Ma et al., 1992) were found to be the most potent and specific. However, neither NAD^+ depletion nor the inhibitors affect the BFA-dependent inhibition of the ARF-cycle. These data could be interpreted in two ways: i) one or both substrates in the ADP-ribosylated form possess a tubulogenic activity, or ii) one or both the substrates normally inhibit the formation of the tubules and the ADP-ribosylation abolishes this activity allowing the tubules to grow (fig. 1.11).

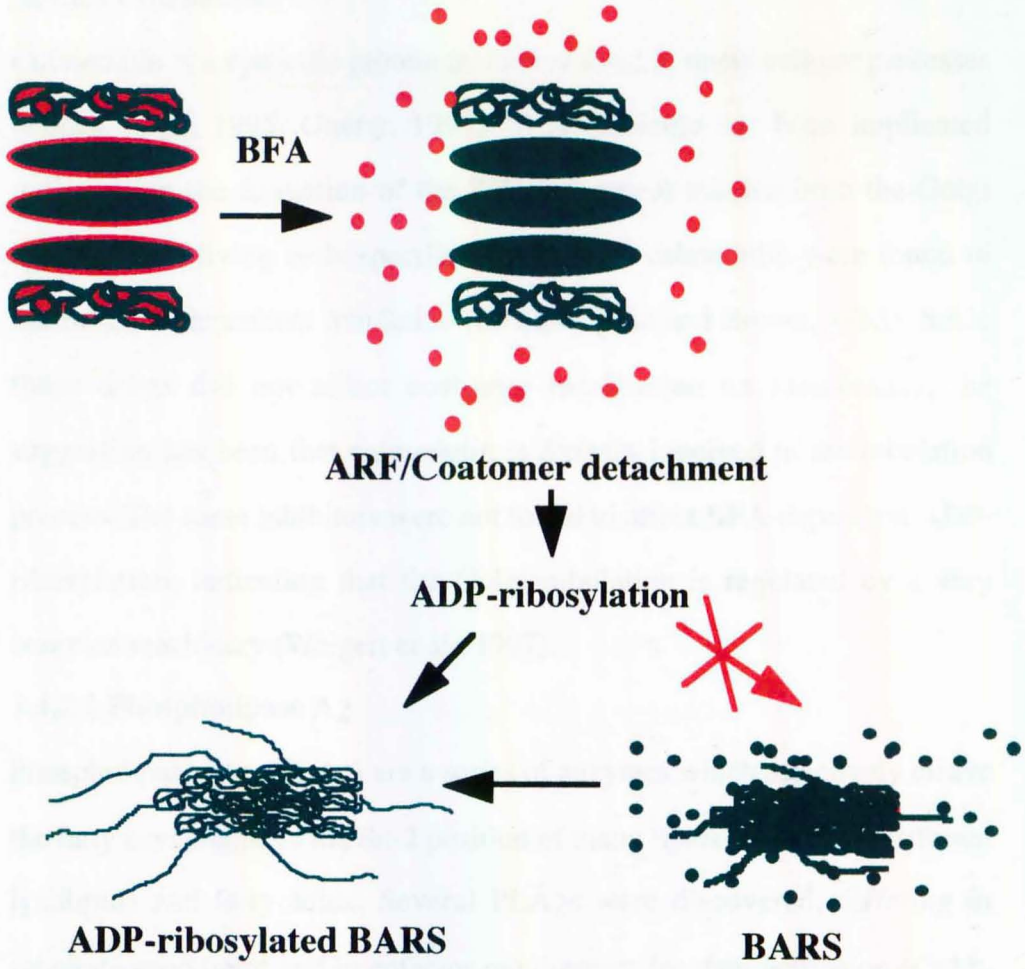

Fig. 1.11 Possible involvement of the BFA-dependent mono ADP-ribosylation of BARS in controlling the formation of BFA-dependent tubules from the Golgi apparatus

BFA triggers the release of the ARF/coatomer complex (red circles) from the Golgi membranes which undergo a tubular reticular transformation. When the ADP-ribosylation of BARS is allowed, long tubular structures are formed, when it is inhibited tubules are not formed or alternatively they are formed but rapidly destroyed (green circles).

1.4.2.5 Calmodulin

Calmodulin is a cytosolic protein that is involved in many cellular processes (James et al., 1995, Gneny, 1993). This molecule has been implicated indirectly in the formation of the BFA-dependent tubules from the Golgi apparatus. In living cells specific inhibitors of calmodulin were found to inhibit BFA-dependent tubulation (de Figueiredo and Brown, 1995). Since these drugs did not affect coatomer localisation on membranes, the suggestion has been that calmodulin is directly involved in the tubulation process. The same inhibitors were not found to affect BFA-dependent ADP-ribosylation, indicating that the Golgi tubulation is regulated by a very complex machinery (Weigert et al., 1997).

1.4.2.6 Phospholipase A_2

Phospholipases A_2 (PLA_2) are a series of enzymes which selectively cleave the fatty acyl chains in the Sn-2 position of many lipids to generate different lysolipids and fatty acids. Several PLA_2s were discovered, differing in substrate specificity and in cofactor requirement for their activation (Ca^{++}, ATP, reducing agents, see Leslie, 1997, Dennis, 1994, Mayer and Marshall, 1993). Using a pharmacological approach, it has been shown that a series of inhibitors of PLA_2 block BFA-dependent tubulation, yet have no effect on the ARF/coatomer cycle (de Figueiredo et al., 1999, 1998). Based on the specificity of these drugs it has been suggested that the PLA_2 involved in tubulation is a calcium-independent form which is activated and regulated by calmodulin (de Figueiredo, 1998). A possible model compatible with this finding is that PLA_2 activation leads to the formation of both lysolipids and fatty acids on the cytoplasmic side of the Golgi apparatus; the former are anticonical lipids which can induce a positive curvature in the membranes; the latter are conical lipids which can easily flip-flop and be accommodated in the luminal side of the membranes favouring a negative curvature (see fig. 1.4 and Cullis et al., 1996, Cullis and de Kruijff, 1979). The increase of the curvature could result in the formation of a tubular structure. However, none of the PLA_2 enzymes characterized so far has been localised in the

Golgi (Leslie, 1997, Dennis, 1994, Mayer and Marshall, 1993). The only exception is a PC-specific PLA2 that is active in the lumen of membranes enriched in cis-Golgi elements (Moreau and Morre', 1991). This finding does not fit with the proposed model, since cis-Golgi membranes are almost completely tubular and the formation of lysolipids in the internal leaflet (and lysolipids cannot flip-flop) is not compatible with their shape.

1.4.2.7 Lipid composition

From the previous data it emerges that the formation of tubules could be the direct consequence of changes in the composition of the lipid bilayer possibly coupled to the formation of particular lipid domains. But could lipids alone form tubules in the absence of any cytosolic proteins ? Or in other words are proteins required just for regulating the lipidic metabolism or do they play a structural role? The scenario appears a little bit confusing. First, pure lipids as a single compound or in a mixture spontaneously convert into tubules under physiological conditions (Mui et al., 1995, Chirovolu et al., 1994, Schoen et al., 1993). This indicates that in principle, a tubular conformation could be adopted even in the absence of any protein. In other studies pure lipid mixtures were competent to generate tubules only after the insertion of the TMD of certain proteins (Fuchs et al., 1995). This effect was found to be dependent on the composition of the lipids used (and specifically from the length of the acyl-chain), and from the length of the TMD. The model proposed is that the formation of tubules is driven by the mismatch generated between the TMD length and the membrane thickness of the liposomes. In other recent studies using liposomes with different lipidic composition and enriched in acidic phospholipids such as PA, it has been found that a series of cytosolic proteins including dynamin, amphiphysin (see below) and ribonuclease were capable of binding to liposomes and inducing massive tubulation (Takei et al., 1999, 1998, Sweitzer and Hinshaw, 1998). These findings have suggested that these proteins can interact directly with acidic lipids determining the formation of

domains which could spontaneously minimise their energy by arranging into a tubular conformation that could be stabilised by the same proteins.

1.4.2.8 Microtubules

Several findings both in vivo and in vitro indicate that microtubules play a role in the regulation of tubular homeostasis. For example microtubule depolymerisation by nocodazole or colchicine, slows down the formation of tubules after BFA treatment (Klausner et al., 1992). Further, in *in vitro* systems BFA can cause only a tubular transformation of the Golgi apparatus and only when purified microtubules are present, can long tubules be formed (Orci et al., 1991, Robertson and Allan, 1998). In other in vitro systems the elongation of tubules has been achieved in the presence of microtubules in a BFA-independent way. Strikingly tubules were found to associate with microtubules through their tips, which were enlarged with respect to the average diameter of the tubules, and to contain some kind of cargo molecules (Fullerton et al., 1998, Allan and Vale, 1994, 1991). This implies that microtubules are at least involved in the elongation process through binding to specialised areas of the tubules; possibly the site of attachments are determined by the presence of a cargo molecule (Allan and Vale, 1994, 1991). The elongation process is also dependent on microtubule-associated proteins which include the motor proteins kinesin and dynein. Blocking antibodies directed against kinesin were found to inhibit the growth of TGN-derived tubules (Kreitzer and Rodriguez-Boulan, 1999). Further several other examples are known from the literature in which microtubules are associated with the formation and the maintenance of tubular reticular networks. The most striking example is the microsomal membranes which, in the presence of polymerised microtubules, form a complex network of membranes morphologically is similar to those observed in the ER of intact cells (Lee et al., 1989, Lee and Chen, 1988, Vale and Hotani, 1988, Dabora and Sheetz, 1988).

1.4.2.9 ATP levels

Tubulation from isolated rat liver Golgi membranes is stimulated by rat brain cytosolic extracts in which the ATP levels have been reduced to the low micromolar range (Cluett et al., 1993). Increasing the concentration of ATP to the millimolar range inhibits tubulation and the formation of vesicles (Cluett et al., 1993). ATP is however an essential requisite since complete elimination from the system totally blocks activity. This finding has also been confirmed in living cells where a partial reduction of ATP levels, using pharmacological tools, leads to an extensive tubulation of the Golgi apparatus (Cluett et al., 1993, Donaldson et al., 1990). One likely explanation for this finding is that high ATP levels inhibit a tubulating factor present in the cytosol or alternatively stimulate a factor that inhibits tubule formation. Thus ATP may control two antagonistic mechanisms, one promoting and the other inhibiting tubulation. A discrepancy with this finding has emerged in a study in which μM ATP was reported to be required for tubulation but only in the absence of cytosolic proteins (Weidmann et al., 1993). In these experiments ATP could be replaced by other triphosphate nucleotides and addition of exogenous cytosol inhibited the formation of tubules (or destroyed newly formed tubules, Weidmann et al., 1993). The discrepancy regarding the requirement for cytosolic proteins could be due to the different kind of Golgi preparations, one from liver, the other from CHO cells, the latter may have a higher cytosolic contamination sufficient to induce nucleotide-dependent tubulation.

1.4.2.10 The tubulating factor p40

A cytosolic factor inducing tubulation in an ATP dependent fashion has been partially purified from bovine brain cytosolic extracts. The highly purified fraction contained a major protein migrating at 40 kDa in SDS-page and was found to promote tubulation in an ATP-specific dependent manner (Banta et al., 1995, Cluett et al., 1993). This highly purified fraction (p40) showed an activity that was saturable with ATP, but not inhibited even at mM concentrations, supporting the idea that another cytosolic factor, able to

antagonise tubulation, is present in cells (Banta et al., 1995). p40 has not yet been cloned and its biochemical role it is not clear. Recently, this enriched preparation was shown to possess a PLA_2 activity and the tubulating activity of p40 is inhibited by classical PLA_2 inhibitors and stimulated by PLA_2-activators. This strongly suggests that the two activities are related (see below, and de Figueiredo et al., 1999).

1.4.3 Molecules implicated in the fission of tubules

1.4.3.1 Phosphatidylinositol transfer protein (PITP)

A recent *in vitro* study (Simon et al., 1998) has suggested that the formation and the maintenance of Golgi tubules are regulated by the levels of phosphatidylinositol (PI). Specifically, a cytosolic activity was found which induces the scission of TGN-derived vesicles and this activity could be replaced by purified yeast PITP (see McGee et al., 1994) and inhibited by specific blocking antibodies directed against the mammalian PITP. PITP is active in promoting fission when pre-loaded with PI, but not with PC or phosphatidylglycerol (PG, the other ligands of this transporter). Furthermore, when PITP is added in the absence of cytosol, it has a dual effect. At 20°C it induces Golgi membranes to tubulate, while at 37°C tubules undergo fission and are converted into a series of small vesicles. Thus, a likely interpretation of these data is that PI accumulation in specific places can lead to the generation of tubules; at 20°C PI is efficiently delivered to target membranes and is capable of generating the proper curvature, while at 37°C PI is metabolised by a phospholipase to generate a metabolite that can induce fission. In this study products derived from PI phosphorylation (such as PIP or PIP2) were ruled out since fission also occurred in the presence of an ATP-depleting system .

1.4.3.2 Dynamin

Dynamin is a GTPase extensively characterized for its essential role in endocytosis (Kelly, 1999, McNiven, 1998, Roos and Kelly, 1997, Urrutia et al., 1997, Cremona and De Camilli, 1997). This protein has been suggested to assemble into rings around the neck of a nascent endocytic vesicle causing fission (Takei et al., 1995, Hinshaw and Schmid, 1995). This step is thought to be due to a conformational change induced upon GTP hydrolysis and dynamin, therefore, has been classified as mechanochemical scissors (McNiven, 1998). When dynamin's function is impaired using blocking antibodies or the non-hydrolyzable analogue of GTP (GTP-γS), long tubules wrapped with dynamin spirals are formed at membranes (Takei et al., 1995). This suggests that dynamin might physiologically modulate the growth of tubules. These phenomena do not occur exclusively on the plasma membrane and dynamin isoforms (dynamin II and its splicing variants) have been localised on the Golgi apparatus and implicated in the release of post-Golgi vesicles from the TGN (Cao et al., 1998, Jones et al., 1998, Altschuler et al., 1998).

The mechanism of action of dynamin has been extensively studied using pure lipids. Liposomes with different lipid composition and enriched in acidic phospholipids such as PA or PS have been used as model membranes. Strikingly it has been found that either in the absence of any nucleotides or in the presence of GTP-γS, both dynamin and its interacting protein amphiphysin are capable of binding to liposomes forming the characteristic rings and inducing massive tubulation. The addition of GTP, on the other hand, causes massive fragmentation of these tubules consistent with observations in living cells (Takei et al., 1999, 1998, Sweitzer and Hinshaw, 1998). Furthermore, dynamin is part of a huge complex including a series of accessory molecules which are thought to help this protein in promoting fission. Among them, the endophilins and synaptophysin are lipid modulating enzymes (Schmidt et al., 1999, McPherson et al., 1996).

1.4.3.3 Acyl-coenzyme A

Acyl-coenzyme As (AcCoAs) are small amphipathic molecules with a hydrophilic portion, the CoA, bound via a thioester bond to a fatty acyl residue. These molecules are key factors in regulating several cellular processes and they have also been implicated in the fission of Golgi-derived vesicles (Ostermann et al., 1993, Pfanner et al., 1990, 1989, Glick and Rothman, 1987). Specifically, AcCoAs are essential co-factors in the intra-Golgi transport as measured by the Rothman transport assay. Given the uncertainties in this assay (Happe and Weidmann, 1998, Dominguez et al., 1999) and the results that will be presented in this thesis work, AcCoAs may infact be involved in controlling Golgi tubule formation. Previously, it has been shown that long-chain AcCoAs are capable of affecting transport in an ATP-dependent manner (Glick and Rothman, 1987). More recent work has focused on palmitoyl-CoA (pCoA) which has been found to promote the detachment of COPI coated vesicles from parental Golgi membranes (Ostermann et al., 1993). This effect was claimed to be independent of cytosolic factors, even though the Golgi preparations used in that study were highly contaminated with cytosolic proteins. The hypothesis proposed was that pCoA is used as substrate for the covalent modification of Golgi proteins. Palmitoyl- and myristoyl-CoA are indeed used by some specific transferases to covalently attach fatty acyl moieties to a residue in the substrate (cysteine or glycine respectively, see Resh, 1996). But this hypothesis has not been confirmed. However, since other long-chain AcCoAs are active in promoting the same events, the most likely explanation is that acyl-CoAs are used for the modification of some lipids. AcCoAs are known to be essential cofactors in many reactions of lipid synthesis and remodelling. Several enzymes use acyl-CoA in these reactions, the type I acyltransferases, which reacylate polar headgroups to the corresponding lysolipids (Heath and Rock, 1998, Kent, 1995), the type II acyltransferases, which catalyse the reacylation of lysolipids to the corresponding lipids (Aguado and Campbell, 1998, Lawrence et al., 1994),

the transacylases which catalyse the transfer of an acyl chain from a lipid to another lipid or to a lysolipid (Hollenback and Glomset, 1998, Sugimoto and Yamashita, 1994, Sugiura et al., 1988). Type I acyltransferases are integral membrane proteins, primarily located in the ER, mitochondria and peroxisomes, and having no specific preferences for different AcCoAs (Kent, 1995), type II acyltransferases located in the ER, Golgi and plasma membrane, show a marked preference for the unsaturated AcCoAs (Kent, 1995). Transacylases are less well characterized enzymes exhibiting very complex regulation and substrate specificities.

1.4.3.4 Mitotically -activated factors

The Golgi apparatus undergoes dramatic modifications during the cell cycle and specifically during the mitotic state, the tubular interconnections between adjacent stacks are broken, the stacked structure is almost completely lost and Golgi fragments are scattered throughout the cytoplasm (Warren and Malhotra, 1998, Lowe et al., 1998, 1995a, Nakamura et al., 1997, Misteli, 1996, Misteli and Warren, 1995, 1994, Warren et al., 1995). When cells exit from mitosis Golgi stacks are re-built and the tubular interconnections are re-formed (Rabouille et al., 1997, 1995b). The mechanism by which these processes occur has been extensively investigated in vitro in cell-free systems.

It has been found that Golgi fragmentation occurs by two independent pathways, one COPI-dependent, the other COPI-independent (Misteli and Warren, 1995, 1994). Both the Golgi tubular elements and the cisternae are rapidly converted into a series of vesicles 50-100 nm in diameter. A biochemical characterization of this process reveals that mitotically-activated cdc2 kinase and possibly some of its downstream targets are involved (Misteli and Warren, 1995, 1994). Several Golgi structural proteins are hyperphosphorylated during mitosis, such as GM130 and GRASP65, leading to inhibition of the docking and fusion of COPI-vesicles and to destacking (Lowe et al., 1998, Nakamura et al., 1997, 1995). Others have studied the mitotic-Golgi fragmentation in permeabilized cells at the

light microscopy level. In these studies the fragmentation is independent of cdc2 kinase, but dependent on another mitotically-activated kinase, MEK, and its substrate, ERK2 (Achraya et al., 1998).

1.4.3.5 βγ subunit of heterotrimeric G proteins

Heterotrimeric G proteins are a broad class of proteins implicated in many cellular processes and originally discovered and localised at the plasma membrane (Gilman, 1987). They are formed from an α subunit and a βγ heterodimer which associate and dissociate with each other in a GTP-dependent manner. When the α subunit is in the GDP-bound state it is associated with the βγ subunits and inactive. When the complex dissociates (upon GTP binding), the subunits interact with multiple targets activating several processes (Clapham and Neer, 1997). Recently α subunits have been localised to Golgi membranes, though βγ have not (Denker et al., 1996). However βγ has been found to induce the breakdown of the Golgi apparatus via a vesicle mediated process whose mechanism is not known (Jamora et al., 1997). Intriguingly some lipid modifying enzymes such as PLA_2 or a PI-specific phospholipase C (PI-PLC) are the targets of the βγ subunit (see above and Di Girolamo et al., 1995, Clapham and Neer, 1997).

1.4.4 General conclusions

This overview of Golgi function and morphology paints a still confusing picture. It is clear that in the Golgi there are at least two complex mechanisms regulating the formation and the disruption of tubules. The fine balance between these two mechanisms determines the fate and the architecture of this organelle. Formation of tubules could be the result of: (i) an inherent property of the Golgi membranes, (ii) their complex architecture and arrangement of lipids providing a high energy state and requiring a constant influx of energy for its maintenance (for example high levels of ATP). Tubulation could then be seen as a way of minimising the energy of the system; lipids would tend to segregate into specific domains which would adopt a tubular geometry corresponding to a lower energy level. For the maintenance of the Golgi architecture this process would have to be

constantly counteracted, for example by cytosolic factors which could physically induce some constraint (the cytoskeleton or coat proteins), or activate specific alterations in the lipid composition. Blocking these activities would lead to the consumption of tubules and the formation of coated vesicles. Alternatively tubulation could be an active process, with cytosolic factors triggering modifications leading to tubulation. There is much evidence linking the formation of tubules to lipid metabolism and the formation of both general lysolipids and special molecules like SLBPA is very intriguing.

1.5 Techniques employed to visualise Golgi tubules

1.5.1 Introduction

Tubules are very small structures often with a length and diameter in the range of nanometers. For their study it is necessary to use a technique that has enough resolution to catch even small variations in their morphology and that offers the possibility to screen for molecules and conditions that affect their behaviour in a cell free-system and in reasonable times. Immunofluorescence light microscopy has been used extensively for looking at tubules, but it is limited to intact and permeabilised cells and it does not have high resolution. Video-enhanced light microscopy has been used for in vitro studies, particularly the role of microtubules, but again many structural details are lost at this resolution (Fullerton et al., 1998). Only electron microscopy has the resolution required (the order of few nanometers) to address the problem.

1.5.2 EM conventional sectioning

In conventional thin sections, membranes are concentrated in a pellet which, after different treatments of staining and dehydration (see material and methods), is embedded in a resin. After a polymerisation step to allow the hardening of the resin, the pellet is cut into sections with a microtome. The thickness of the sections can vary from 25 nm (ultra thin), to 60 nm (thin), to 100-200 nm (thick). Routinely thin sections are used. The main disadvantage with this approach is that the images obtained represent a projection in only one plane of a three-dimensional structure. Tubular structures, which are perpendicular to the plane of section are seen only as circular profiles. However, since the orientation of membranes in the pellet is random and the number of membranes is normally very high, there is a high probability of visualising tubules, even if some detail is lost. To overcome this problem there are two possibilities, one is to use serial thin sections and then reconstruct the three-dimensional organisation of the organelle of interest and the other is to use thick sections with a high voltage

electron microscope coupled to a goniometer to apply the stereopair technique (Rambourg and Clermont, 1997). Unfortunately these two alternatives are extremely time consuming and they could not be applied for screening purposes.

1.5.4 Freeze-etch electron microscopy

Another very interesting technique having a very high degree of resolution is the freeze-etch technique (Weidmann et al., 1993). With this technique membranes are immobilised on a glass surface and are stabilised using chemical fixatives. Samples are fast-frozen in liquid helium, covered by evaporation-sputtering using a thin layer of platinum, recovered and observed by a transmission electron microscope. The organelles are visualised in three-dimensions and with a very high degree of resolution. However, again, this technique is time consuming and not suitable for repetitive screening purposes.

1.5.5 Negative staining on whole-mount preparations

This technique is based on the deposition of the specimen on a grids. It is then covered with a support film, a contraster is applied to stain the membranes and then the sample is air-dried. The staining process, which depends largely on the contraster used, is not well understood. Some contrasters, such as those based on phosphotungstic acid (PTA), are thought to deposit uniformly on the grids and to accumulate at the borders of membranes, since they are not capable of crossing the hydration sphere surrounding proteins and lipids. Others, like uranyl acetate (UA) are thought to interact directly with lipids. Negative staining was originally introduced to visualise viruses (Hall et al. 1954) and was later developed to study bacteria. In the sixties it was used to qualitatively describe the morphology of some intracellular organelles (including the Golgi complex) in both animal and plant tissues (Cunningham et al., 1966; Mollenhauer et al., 1973; Morre' et al., 1970; Prezbindowsky et al., 1968). This technique has been used to follow purification during the isolation of intracellular organelles and more recently to follow the purification of a cytosolic tubulation factor

p40 (Banta et al., 1995). Compared to conventional techniques like TEM, negative staining on whole-mount preparations has the advantage that a direct visualisation in three dimensions of Golgi-associated tubules together and other details of Golgi morphology can be obtained. It allows a clear discrimination between tubules and vesicles and it is a very fast technique suitable for both screening purposes and for quantitative analysis (see below).

CHAPTER 2

MATERIAL AND METHODS

2.1 Materials

Chromatographically-purified BARS, BARS-depleted cytosol, an antibody against BARS (α-PEP9), PEP9 and purified βγ subunits were provided by the laboratory of Molecular and Cellular Endocrinology - Department of Cell Biology and Oncology - Mario Negri Sud (Giusy Silletta, Claudia Cericola, Stefania Spano', Rosita Lupi, Daniela Corda). These reagents were prepared as described in Spano' et al., 1999 and Mironov et al., 1997. Chromatographically-purified ARF from bovine brain, recombinant myristoylated ARF1, ARF-depleted and reconstituted cytosol were provided by the laboratory of Physiopathology of Secretion - Department of Cell Biology and Oncology - Mario Negri Sud (Antonella De Matteis, Giuseppe Di Tullio). These reagents were prepared as described in Weiss et al., 1989 and Godi et al., 1997. The GRK4 peptide was provided by the Laboratory of Molecular Biology and Pharmacology of the Receptors - Mario Negri Sud (Michele Sallese).

2.2 Protein determination

The protein content of various samples was determined by the Bio-Rad protein assay (Bio-Rad, Germany). To determine the proper range of dilution, samples were diluted 1:100, 1:500, and 1:1000 with phosphate saline buffer (PBS, Sigma) and 800 µl of each solution were mixed with 200 µl of the Bio-Rad reagent, vortexed vigorously and placed in a plastic couvette. As controls, sample buffers were treated in the same way. Measurements were then carried out in a dual beam spectrophotometer (Beckman) using controls as blanks. The absorbances at 595 nm were recorded. The appropriate dilution was chosen such that the absorbance fell between 0.4 and 0.8 (the range in which this assay is linear with respect to the protein concentration). The determination was then repeated in triplicate,

the absorbances were converted into concentration units by using the appropriate calibration curve (for each batch of the Bio-Rad reagent a curve is performed every month) and taking in account the dilution factors. The final protein concentration was calculated by averaging several determinations (2-4).

2.3 Cell Culture

2.3.1 Materials

Normal rat kidney (NRK), wild type Chinese hamster ovary (CHO) and rat basophilic leukaemia 2H-3 (RBL) cells were originally bought form American tissue type collection (ATTC). CHO(ldlf) cells were a gift of Dr. M. Krieger (MIT, Cambridge - USA). Proline and ethylendiaminetetraacetic acid (EDTA) were from Sigma. Dulbecco's Modified Eagle Medium (DMEM), fetal calf serum (FCS), penicillin, streptomycin, trypsin-EDTA, and L-glutamine were from Eurobio (France). Modified Eagles Medium (MEM), and HAM'S F12 were from GIBCO (Scotland). All these reagents were 10 x stock solutions. All plasticware was from Corning (USA). Filters (0.45 μm) were from Amicon.

2.3.2 Propagation of cell lines

2.3.21. Growth media

NRK cells were grown in DMEM with 10% FCS, 10 U/ml penicillin, 10 μg/ml streptomycin and 2 mM glutamine. CHO cells were grown in the same medium but with 5% FCS and 40 μg/ml proline. RBL cells were grown in MEM with 16% FCS, 10 U/ml penicillin, 10 μg/ml streptomycin and 2 mM glutamine. CHO(ldlf) were grown in HAM'S F12 with 5% FCS, 10 U/ml penicillin, 10 μg/ml streptomycin and 2 mM glutamine. All the complete media were prepared by mixing stock solutions in the proper amount, complementing them with sterile water and filtering the mixture through 0.45 μm filters.

2.3.2.2. Growth conditions

All cell lines were grown in a controlled atmosphere in the presence of 5% CO2 at 37°C with the exception of CHO(ldlf) which were grown at 34°C. Cells were grown on plastic untill they reached 90% confluency. They were then washed twice with sterile PBS. NRK and CHO cells (both wild type and the ldlf) were then incubated with commercial trypsin-EDTA (1x) for 1 min at room temperature, while RBL cells where incubated for 10 minutes with 0.7 mM EDTA in PBS. Cells were detached by adding fresh medium and pipetting up and down, collected in a plastic tube and centrifuged for 5 min at 1000 rpm. Pellets were resuspended in an appropriate volume of medium, and the suspensions were placed in plastic dishes for the further growth.

2.4 Isolation of Golgi membranes

2.4.1 Materials

Sucrose, sodium hydroxide (NaOH) and magnesium chloride ($MgCl_2$) were from Carlo Erba (Italy). Trizma-base (TRIS), maleic acid, and dextran were from Sigma. β-mercaptoethanol was from Fluka. Di-Potassium hydrogen phosphate (K_2HPO_4) and potassium di-hydrogen phosphate (KH_2PO_4) were from Merck. Both the centrifuges and the tubes were from Beckman. Sucrose concentrations were checked by a refractometer (PBI international).

2.4.2 Isolation of Golgi membranes from cell cultures

Tris-HCl was prepared as follows: 1.21 g of trizma-base were dissolved in 900 ml of deionized water, the pH was adjusted to 7.4 by adding dropwise 0.5 M HCl, and finally the volume was brought to 1 l. Cells were grown in 15 cm Petri dishes, detached (see above), and pelletted. From hereafter all the procedures were rigorously carried out at 0°C. The pellet was washed with ice-cold 0.25 M Sucrose in 10 mM Tris-HCl pH 7.4 (HB), and the cells repelletted (1500 rpm for 5 minutes) and resuspended in 4 volumes of HB. Cells were then homogenized with 10-12 passes inside a

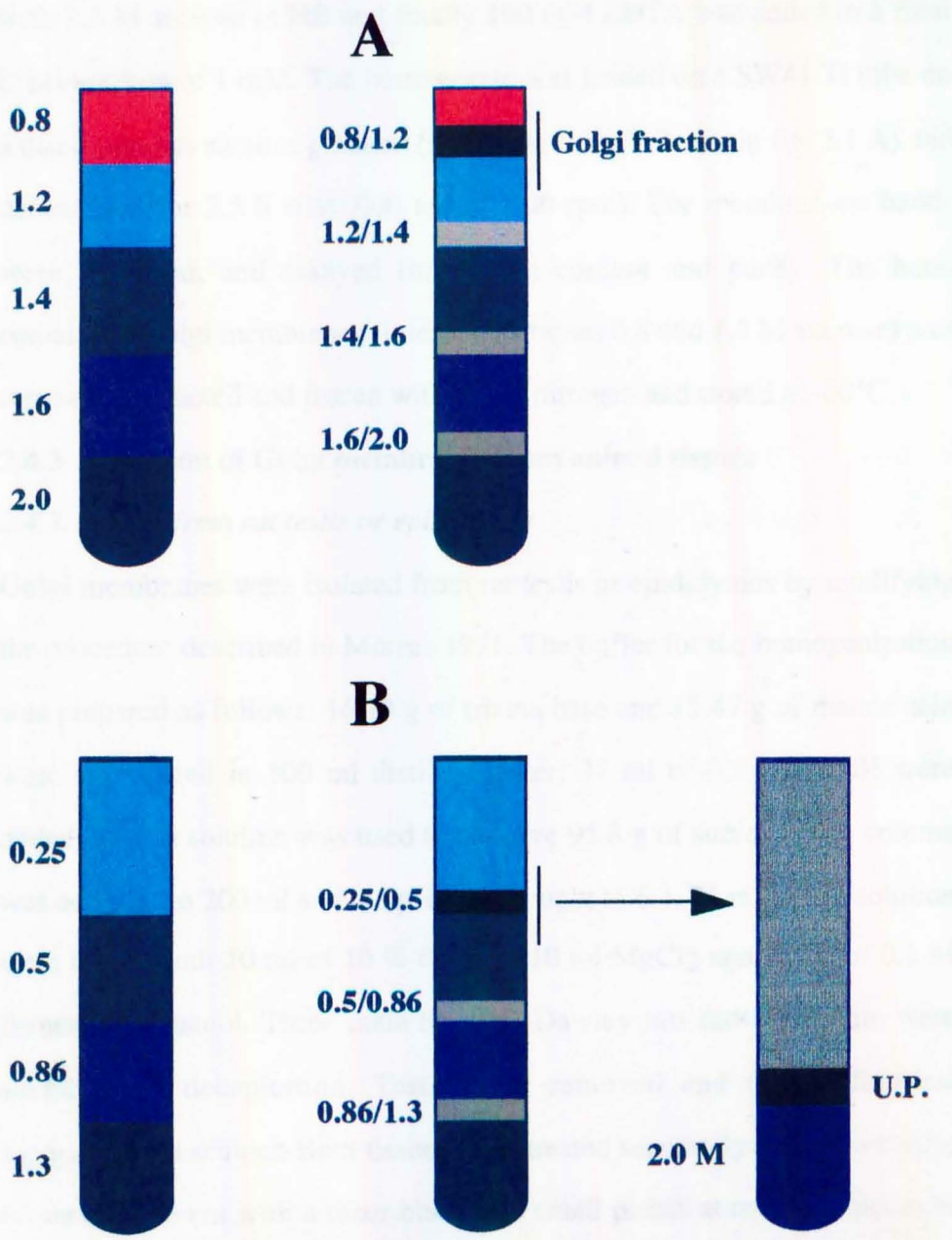

Fig. 2.1 Scheme for the isolation of Golgi membranes from cell cultures and rat liver according to Slusarewicz et al., 1994

Fractionation procedure for cell cultures as described in Balch et al., 1984 (A) and for rat liver as described in Slusarewicz et al., 1994 (B).The molarity of the sucrose solutions is shown on the left of each tube.

Balch and Rothman chamber (EMBL, Heidelberg - Germany) checking cell integrity under a light microscope. A ball with a diameter of 8,002 mm was used. The sucrose concentration of the homogenate was adjusted to 1.4 M with 2.3 M sucrose in HB and finally 100 mM EDTA was added to a final concentration of 1 mM. The homogenate was loaded on a SW41 Ti tube on a discontinuous sucrose gradient (according to the scheme in fig. 2.1 A) and centrifuged for 2.5 h at 90.000 x g (26500 rpm). The membranous bands were collected, and assayed for protein content and purity. The band containing Golgi membranes (interface between 0.8 and 1.2 M sucrose) was removed, aliquoted and frozen with liquid nitrogen and stored at -80°C.

2.4.3 Isolation of Golgi membranes from animal tissues

2.4.3.1 Golgi from rat testis or epididymus

Golgi membranes were isolated from rat testis or epididymus by modifying the procedure described in Morre', 1971. The buffer for the homogenisation was prepared as follows: 16.13 g of trizma base and 15.47 g of maleic acid were solubilized in 100 ml distilled water; 37 ml of 0.2 M NaOH were added and the solution was used to dissolve 95.8 g of sucrose. The volume was adjusted to 200 ml and the pH was brought to 6.4. 75 ml of this solution were mixed with 10 ml of 10 % dextran, 10 ml $MgCl_2$ and 10 ml of 0.1 M β-mercaptoethanol. Three male Sprague-Dawley rats fed ad libitum were sacrified by decapitation. Testis were removed and the epididymus separated by a scalpel. Both tissues were treated separately as follows. 10 g of tissue were cut with a razor blade into small pieces at room temperature and placed in 20 ml of the ice-cold homogenisation buffer. From here, all the procedures were carried out on ice. The tissue was homogenised for 40-80 sec at 8000-9500 rpm with the Ultraturrax (T25, Janke and Kunkell). The homogenate was squeezed through a single layer of gauze, placed in a SW28 tube for ultracentrifugation, and covered with 1.5 volumes of both 1.25 M and 0.25 M sucrose. The tube was centrifuged for 30 minutes at 27000 rpm (100000 x g) and the Golgi-enriched fraction was recovered at the 0.25/1.25 M interface using a Pasteur pipette. All the fractions were

assayed for the protein content, aliquoted, frozen in liquid nitrogen and stored at -80°C.

2.4.3.2 Golgi from rat liver as described in Leelavathi et al., 1970

Phosphate buffer (0.5 M) was prepared as follows: 43.6 g of K_2HPO_4 and 34 g of KH_2PO_4 were each dissolved each in 500 ml of distilled water. To 400 ml of the latter solution, the former was gradually added until the pH reached 6.65. This buffer was diluted to 0.1 M to prepare the sucrose solutions. $MgCl_2$ (2M in water) was added to a final concentration of 5 mM. Six male Sprague-Dawley rats (100-200 g) were fed ad libitum. Animals were sacrified by decapitation and livers quickly removed, chilled in the homogenisation buffer (0.5 M sucrose). 4 g of tissue were minced by cleaned scissors in 20 ml of homogenisation buffer and homogenised for 30 sec using the Ultraturrax at medium speed. The homogenate was centrifuged for 10 minutes (600 x g), the supernatant (termed post-nuclear) layered on a sucrose cushion (5 ml of 1.3 M sucrose) and centrifuged for 60 minutes (105000 x g). The interface between 0.5/1.3 M sucrose was collected, the sucrose concentration adjusted to 1.1 M by adding 2.3 M sucrose and the volume brought to 8 ml with 1.1 M sucrose. The suspension was then layered on a sucrose gradient (6 ml of 1.4 M, 6 ml of 1.3 M and 6 ml of 1.25 M sucrose) and covered with 6 ml of the homogenisation buffer The gradient was centrifuged for 90 minutes (105000 x g), the Golgi-enriched fraction collected at the 1.1 / 1.25 M sucrose interface, assayed for protein content, aliquoted, frozen in liquid nitrogen and stored at - 80°C.

2.4.3.3 Golgi from rat liver as described in Slusarewicz et al., 1994

Six female Sprague-Dawley rats were starved for 24 hours. Sucrose solutions were prepared as described in the previous sections and six discontinuous gradients consisting of 13 ml of 0.86 M sucrose layered on 7.5 ml of 1.3 M sucrose were placed in SW28 rotor tubes on ice. Rats were killed by decapitation, the livers were excised, placed in 200 ml of ice-cold 0.5 M sucrose (homogenisation buffer), and squeezed to expel blood. The livers (48 g) were then minced with scissors to obtain 0.5 cm pieces. Buffer

was added to 100 ml, and the suspension was passed through a 150 μm steel mesh sieve (Endecott Ltd. UK) by gentle pressure with the bottom of a conical flask. The homogenate was collected in an ice-cooled steel tray, the volume adjusted to 80 ml with the homogenisation buffer, and finally layered with 0.25 M sucrose (fig 2.1 B). The gradient was centrifuged for 60 minutes (28000 rpm), the 0.5 M / 0.86 M sucrose interfaces were collected using a Pasteur pipette (2-3 ml per tube), pooled and diluted with 0.1 M phosphate buffer, 2.5 mM $MgCl_2$ till the sucrose concentration reached 0.25 M. The pooled fraction was centrifuged on a 2 M sucrose cushion for 30 minutes (SW28, 7000 rpm), the membranous band was collected, assayed for protein content, aliquoted, frozen in liquid nitrogen and stored at - 80°C.

2.4.3.4 Golgi from rat liver by a modification of Cluett and Brown, 1992

The Golgi membranes used routinely in the experiments in this thesis work were prepared by modifying the protocol described in Cluett and Brown, 1992. Male Sprague Dawley rats (3 x 200-250 g) fed ad libitum were killed by decapitation, and their livers were excised, placed in an ice-cold homogenization buffer (10 mM Tris-HCl pH 7.4, 0.25 M sucrose) and squeezed to expel blood. The livers (30 g) were then minced with scissors to obtain 0.5 cm pieces. Buffer was added to 100 ml, and the suspension was passed through a 150 μm steel mesh sieve (Endecott Ltd. UK) by gentle pressure with the bottom of a conical flask. The homogenate was collected in an ice-cooled steel tray, adjusting the sucrose concentration to 1.4 M with 2.3 M sucrose in 10 mM Tris-HCl pH 7.4 and placed in the bottom of six SW28 tube for ultracentrifugation (15 ml each). A small fraction of the homogenate was left to assay the protein content (typically 70-75 mg/ml). The homogenate was then layered with 1.2 M (10 ml), 1.0 M (10 ml), 0.9 M (5 ml), 0.8 M (5 ml) sucrose in 10 mM Tris-HCl pH 7.4 (fig. 2.2 A). Tubes were then ultracentrifuged at 26000 rpm for 2.5 hours. The 0.9/1.0 M interface (low-purity Golgi) was collected, and processed again as for the homogenate while the other interfaces (0.8/0.9 M, 1.0/1.2 M and 1.2/1.4 M) were collected and assayed for their protein content and purity. The Golgi-

enriched fraction (0.9/1.0 M interface - ultra pure, U.P.) was collected, assayed for protein content, aliquoted, frozen in liquid nitrogen, and stored at -80°C for no longer than one month.

2.4.3.5 Golgi from rat liver by a modification of Taylor et al., 1998

Rats and excised livers were treated as for the "Slusarewicz" procedure with the difference that the sucrose concentration of the pooled Golgi fraction from the first centrifugation was brought to 1.2 M, placed on the bottom of a SW28 rotor tube and layered with equal volumes of 1.0 M, 0.86 M, and 0.25 M sucrose, respectively. The gradient was centrifuged for 3 hours (76000 x g) and the Golgi-enriched fraction collected at the 0.25/0.5 M sucrose interface (fig. 2.2 B) was assayed for protein content, aliquoted, frozen in liquid nitrogen, and stored at -80°C for no longer than one month.

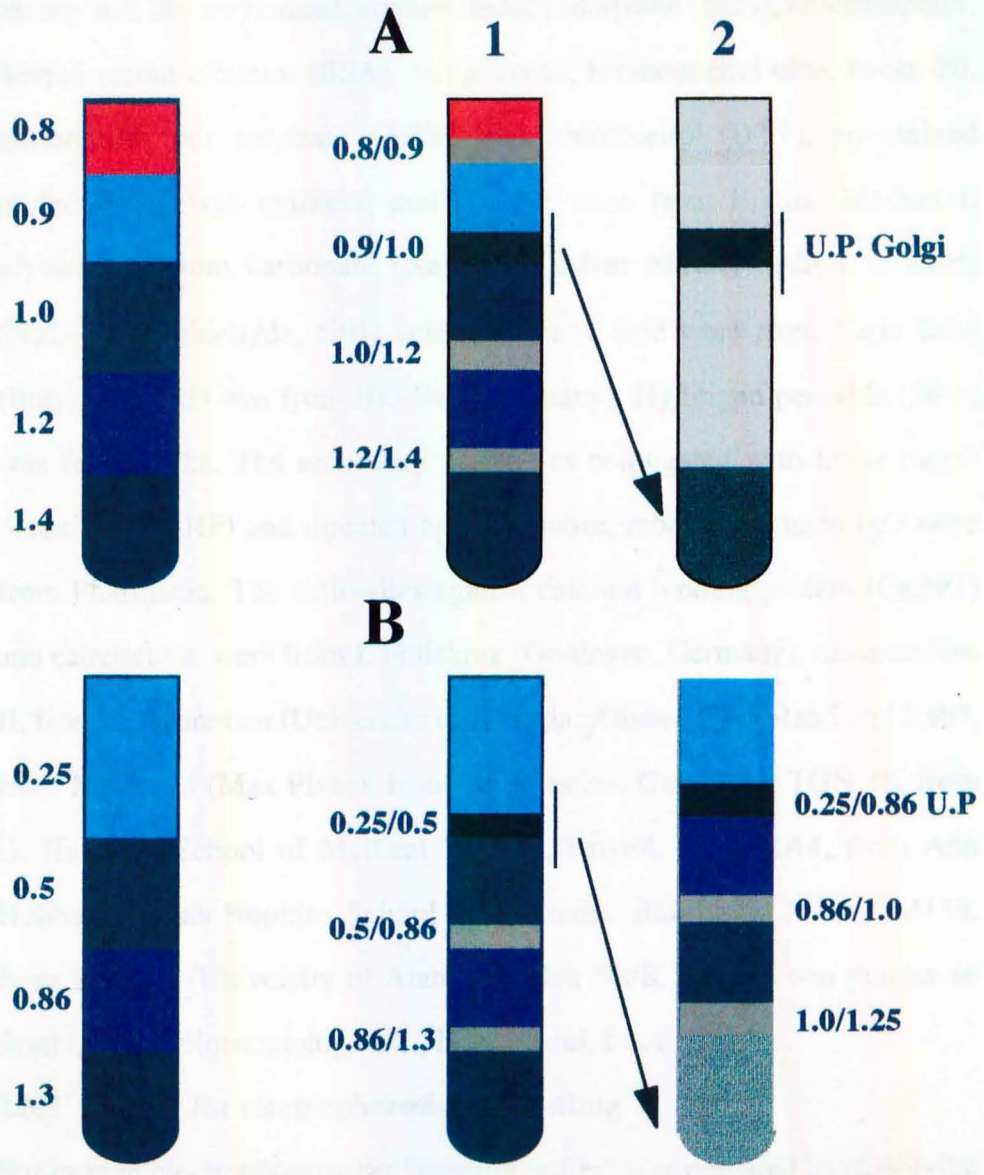

Fig. 2.2 Schemes for the isolation of Golgi membranes from rat liver

Fractionation procedure for rat liver as described in Cluett and Brown, 1992 (A) and in Taylor et al., 1998 (B). The molarity of the sucrose solutions is shown.

2.5 SDS page and immunoblotting

2.5.1 Materials

Mono- and bis-acrylamide, sodium dodecyl sulphate (SDS), chloronaphtol, bovine serum albumin (BSA), red ponceau, bromophenol blue, tween-20, ammonium per sulphate (APS), DL-dithiothreitol (DTT), pre-stained molecular weight markers, and glycine were from Sigma. Methanol, glycerol, sodium carbonate (Na_2CO_3), silver nitrate, sodium chloride (NaCl), formaldehyde, citric acid and acetic acid were from Carlo Erba (Italy). TEMED was from Bio-Rad (Germany). Hydrogen peroxide (30%) was from Fluka. The secondary antibodies conjugated with horse radish peroxidase (HRP) and directed against mouse, rabbit and sheep IgG were from Pharmacia. The antibodies against calcium binding protein (CaBP1) and calreticulin, were from J. Füllekrug (Göttingen, Germany); mannosidase II, from K. Moremen (University of Georgia, Athens, GA); Rab5 and Rab7, from M. Zerial (Max Planck Institute, Dresden, Germany); TGN 38, from G. Banting (School of Medical Science, Bristol, UK); HA4, from Ann Hubbard (Johns Hopkins School of Medicine, Baltimore, MD); GM130, from E. Sztul (University of Alabama, AL); Na/K ATPase was purchased from Upstate Biotechnology inc., Lake Placid, USA.

2.5.2 Buffer for electrophoresis and blotting

For protein electrophoresis the "running buffer" was prepared by dissolving 72 g of glycine, 15 g of trizma base and 5 g of SDS in 5 l of deionized water. The "sample buffer 2X" was prepared by mixing 0.5 M Tris-HCl pH 6.8 (10 ml), 10 % SDS (20 ml), glycerol (10 ml), 0,5 % bromophenol blue (2.5 ml), deionized water (5 ml) and β-mercaptoethanol (2.5 ml). For protein blotting on nitrocellulose the "transfer buffer" was prepared by dissolving 72 g of glycine, 15 g of trizma base in 5 l of deionized water.

2.5.3 Assembling of polyacrylamide gels

Two 16 cm x 15 cm square glasses were assembled to form a chamber using two 1.5 mm plastic spacers lined on the lateral edges of the glasses. This chamber was fixed by using two clamps and mounted on a plastic base which sealed the bottom (Hoefer Scientific Instruments). The polyacrylamide gel was then prepared. For 12% polyacrylamide gels, 10 ml of a mixture of 30% mono-acrylamide and 0.8% bis-acrylamide in water were placed under stirring and sequentially mixed with the following reagents: 1.5 M Tris-HCl pH 8.8 (7.5 ml), deionized water (12.5 ml), 10% SDS (300 µl), 10% (APS, 160 µl), TEMED (16 µl). This mixture (running mixture) was immediately percolated into the glass chamber and covered with 1 ml of deionized water. After 2 hours, when the mixture was completely polymerised, the water was removed and replaced with the "stacking mixture" (6 ml of deionized water , 1.5 ml of the acrylamide mixture, 2.5 ml of 0.5 M Tris-HCl pH 6.8, 100 µl of 10% SDS, 100 µl of 10% APS, and 7 µl of TEMED). A 15 tooth plastic comb (Hoefer Scientific Instruments) was embedded in the stacking mixture untill the polymerisation was complete (ca. 1 hours). The comb was then removed and the wells formed were washed with the running buffer.

2.5.4 SDS page

Samples for the SDS page were treated with an equal volume of sample buffer 2X, boiled for 10 minutes and loaded in the wells. The lateral wells were loaded with 10 µl of a mixture of pre-stained molecular weight standards. The polymerised chambers were then assembled into the apparatus for electrophoresis (Hoefer Scientific Instruments) and electrophoresis carried out with the power supply set to maximal voltage and with a constant current of 8 mA (for overnight runs) or 30-40 mA (for 4 hours runs).

2.5.5 Blotting on nitrocellulose

At the end of the run the chamber was disassembled and the polyacrylamide gel was soaked for 15 minutes in the transfer buffer, together with 2 pieces

of filter paper (Whathman n° 3) and one of nitrocellulose (Schleicher & Schuell) previously cut into 16 cm x 15 cm rectangles. The gel was assembled into a sandwich as follows: first, a sheet of filter paper was covered with the nitrocellulose, the gel was then placed on the nitrocellulose (eliminating all the air bubbles by applying a gentle pressure), finally, a second sheet of filter paper was layered on the gel. This sandwich was assembled in the blotting apparatus (Hoefer Scientific Instruments) and the transfer started setting the power supply to 500 mA. At the end of the run (typically 4-5 hours) the sandwich was disassembled and the nitrocellulose was soaked in 0.2 % red ponceau in 5% acetic acid for 5 minutes to visualise the protein bands and rinsed with 5% acetic acid untill the excess of unbound dye was eliminated.

2.5.6 Immunodetection of antigens

Nitrocellulose blots were cut with a razor blade into strips at the level of the protein of interest (determined by the molecular weight standards). The strips were incubated, for 10 minutes in TTBS-BSA (1 % BSA, 0.05 % tween-20, 150 mM NaCl, 50 mM Tris-HCl pH 7.5) and then with the antibody directed against the protein of interest, diluted at the appropriate concentration in TTBS-BSA. A list of the antibodies used in this thesis and their working dilution is provided in table II.I. The incubations with the antibodies were carried out at room temperature (2-4 hours) or at 4°C (overnight) under continuos agitation. At the end of the incubations the antibodies were removed and the strips were washed 3 x 3 minutes with T-TBS (0.05 % tween-20, 150 mM NaCl, 50 mM Tris-HCl pH 7.5). Then the strips were incubated for 1 hour with the appropriate HRP-conjugated secondary antibody (1:500 in TTBS-BSA) and washed sequentially with TTBS (2 x 2 minutes) and TBS (150 mM NaCl, 50 mM Tris-HCl pH 7.5, 2 x 2 minutes). The strips were then incubated with the developing solution (10 mg chloronaphtol, 3 ml methanol, 17 ml TBS, 10 µl of 30 % hydrogen peroxide) untill the bands started to appear. The reaction was stopped with deionized water.

Antibody	Dilution	Source
Mannosidase II	1:1500	Rabbit
GM130	1:1000	Mouse
TGN38	1:500	Mouse
Rab5	1:2500	Mouse
Rab7	1:1000	Rabbit
Ha4	1:1000	Mouse
Na/K ATPase	1:250	Rabbit
CaBP	1:500	Rabbit
Calreticulin	1:1000	Sheep

Table II.I List of the antibodies for immunoblotting used in this study

2.5.7 Silver staining

Polyacrylamide gels were soaked in 50 % methanol (2 x 15 minutes) with stirring, then in 5% methanol (1 x10 min) and finally washed with water (3 times rapidly). Gels were soaked for 20 min in 10 μM DTT, 0.1% silver nitrate and were developed in the dark with 250 ml of 0.28 M sodium carbonate plus 250 μl of 37% formaldehyde (2 rapid washes and exposure untill bands become visible). The reaction was stopped by adding 12 g citric acid and gels were dried with a gel dryer (Hoefer Scientific Instruments).

2.6 Electron Microscopy

2.6.1 Materials

Formvar, potassium ferrocyanide, potassium cacodilate, phosphotungstic acid - sodium salt (PTA) were from Sigma. Glutharaldehyde (50%) was from Fluka. Osmium tetroxide (OsO_4), EPON, lead citrate and uranyl acetate (UA) were from Electron Microscopy Sciences (USA). Acetone and ethanol were from Carlo Erba (Italy). NanoW 2018 and Nanovan 2011 were from Nanoprobes (Stony Brook, NY)

2.6.2 Preparation of formvar-coated grids for electron microscopy

Coated grids for electron microscopy were prepared as follows: formvar was solubilized in chloroform (0.5%, 1% and 1.5% final concentration) and filtered through a filter paper (Whathman paper n°3). Glass slides (76 x 26 mm), cleaned with paper towels to remove dust, were soaked for 20 sec in the formvar solution, removed, allowed to touch with one edge a sheet of filter paper and left to dry in air. The slides covered with formvar film were exposed to a lamplight for 20 min and then the films were cut in rectangles (50 x 15 mm), removed and floated on deionized water. Ten grids (3 mm in diameter, 200 or 400 mesh, in nickel or copper) were placed on each film, recovered with a parafilm strip and allowed to dry. Grids were stored in a Petri dishes to avoid dust contamination and cleaned under a gentle nitrogen flow prior to usage. Formvar coated grids were occasionally covered with a carbon film that was deposited through a carbon coater (CED 020, Balzer). A single carbon thread was mounted between the two electrodes of the carbon coater, the chamber was sealed and vacuum was set to 10^{-3} bar. To get a 20 nm carbon film, grids were placed at 30 mm from the electrodes and a brief electric discharge was given at the maximum voltage (as recommended by the manufacturer).

2.6.3 Thin sections of isolated Golgi membranes (perpendicular)

Isolated Golgi membranes (untreated or after any incubation) were fixed with an equal volume of 4 % glutharaldehyde in PBS for 30 min at room

temperature, incubated with an equal volume of 2 % BSA for an additional 30 min, then pelletted in a refrigerated microcentrifuge (13000 rpm x 30 min). The supernatant was discarded and the pellet washed 3 times with 500 µl PBS, and stained for 1.5 hour with 100 µl 1% OsO_4 and 1.5 % potassium ferrocyanide in 0.1 M potassium cacodilate. The pellet was then washed with 500 µl PBS and dehydrated by the following treatment: 500 µl of 50 %, 70% and 90% ethanol (10 minutes each) and finally 500 ml of absolute ethanol (3 x 10 minutes). After this step the pellet was first incubated 2-4 hours with EPON-ethanol 1:1 (300 µl), then with EPON (200 µl) for another 2-4 hours and finally placed for 10 hours in an oven at 60°C to allow polymerisation. The embedded pellet was removed from the test tube and cut perpendicularly (fig. 2.3) with an ultra-microtome (Nova) set for a section thickness of 60 nm. Sections (silver colour) were picked up on a copper grid and contrasted with 2% lead citrate (2 x 1 min) and finally washed with degassed water (6 times rapidly).

2.6.4 Thin sections of isolated Golgi membranes (longitudinal)

Isolated Golgi membranes were fixed and blocked as described above and ultracentrifuged at 150000 x g for 1h in a TLA100.3 rotor (4°C). The pellet was treated as described above, with the difference that sectioning was performed on the longitudinal axis parallel to main axis of the test tube (see fig. 2.3).

2.6.5 Thin sections of permeabilized cells

Cells placed in adjacent wells located across the major axis of the chamber slides were incubated under the same experimental conditions. After permeabilisation and incubation they were fixed with 2% glutharaldehyde in PBS (200 µl per well) for 15 minutes and then washed with 500 µl PBS. The staining with osmium, dehydration and embedding were performed as described for isolated Golgi membranes. After the polymerisation, the plastic scaffold was removed and the resin-embedded blocks of equivalent samples were glued with EPON and polymerised overnight in the oven. Samples were then cut as described above.

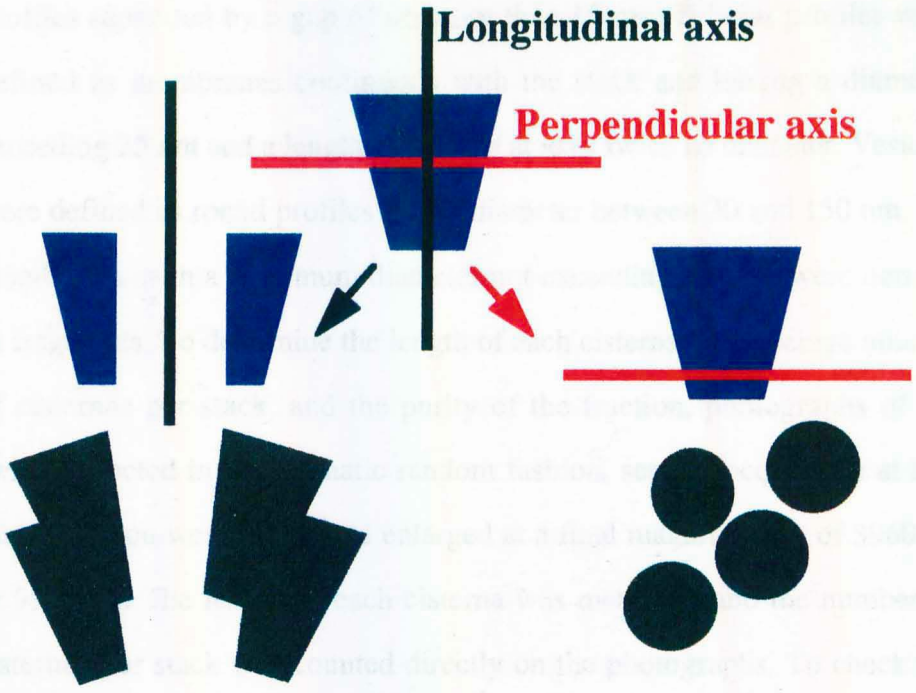

Fig. 2.3 Scheme for sectioning of the resin-embedded pellets

The resin-embedded pellet (blue) was fractured in the center with a razor blade along the longitudinal axis (green line) and then sections were cut parallel to the fractured face. Alternatively, sections were cut from the bottom of the pellet along the perpendicular axis (red line).

2.6.6 Stereology

Golgi cisternae were defined as membrane profiles having a length more than four times their width. Stacks were identified as two or more cisternal profiles separated by a gap of no more than 15 nm. Tubular profiles were defined as membranes continuous with the stack and having a diameter exceeding 25 nm and a length exceeding at least twice its diameter. Vesicles were defined as round profiles with a diameter between 30 and 150 nm. All membranes with a maximum diameter not exceeding 200 nm were defined as fragments. To determine the length of each cisterna , the average number of cisternae per stack, and the purity of the fraction, photographs of the fields (selected in a systematic random fashion, see Lucocq, 1993) at low magnification were taken, and enlarged at a final magnification of 39600 x or 99000 x. The length of each cisterna was measured and the number of cisternae per stack was counted directly on the photographs. To check the purity, a 1 cm point grid was applied on a photograph and the number of intersections of each Golgi structure with the points was scored and divided for the total number of intersections of all membranes. This ratio further multiplied by 100 gave the percentage of Golgi membranes in one sample. This procedure was repeated for at least 8 photographs, the single results were averaged, and the final result expressed as average ± S.E.M. A similar procedure was applied to the sections cut along the longitudinal axis.

2.6.7 Contrasters for negative staining

2 % PTA was prepared by dissolving 20 mg of the powder in 500 µl deionized water. The pH was adjusted to 6.8 by adding dropwise 0.5 M KOH and the volume was brought to 1 ml by deionized water. The same procedure was used for the other concentrations tested (see section 3.3.2). 2 % UA was prepared by dissolving 20 mg of the powder in 1 ml of distilled water. The solution was wrapped with aluminium foil and stored at 4°C. Prior to use, the uranyl acetate is centrifuged for 5 minutes at 10000 rpm to remove contaminations and precipitates. Most of the experiments in this

thesis were carried out using commercially available contrasters NanoW 2018 and Nanovan 2011.

2.6.8 Standard protocols for negative staining

Golgi membranes were initially visualised by the "standard" negative staining technique as described in Cluett et al., 1993. The procedures and all the modifications introduced are described in detail in section 3.3.2, since they were developed as an essential part of this thesis work.

2.6.9 Quantitative analysis of the morphology of the Golgi membranes

One of the main expectations from setting up this morphological assay was to get not only qualitative but also quantitative data about the way in which Golgi-associated tubules are regulated. To generate unbiased and reliable results, samples were evaluated in a single blind fashion using a systematic random procedure (Lucocq, 1993). First, samples were analyzed from a qualitative point of view to give a general judgement about the morphology of the Golgi membranes. During this step 200-300 Golgi membranes were scored for each sample. Then, samples were re-introduced under the microscope in a random orientation and the observations were started from a point determined by setting to the zero position both the micrometric screws which regulate the position of the sample. This ensured a randomly chosen starting point. The fields (magnification 12000 x) were then selected moving always as described in fig. 2.4, and each Golgi membrane encountered was evaluated for its morphological feature. 30-100 Golgi membranes were evaluated for each sample, 2-4 measurements were performed per experimental condition and the results were pooled together. The main morphological transformations observed in this thesis were: the tubular reticular transformation, vesiculation, tubulation and fragmentation of the Golgi stacks. Golgi stacks were considered: i) tubulo reticular when they were formed completely by tubules and no cisternal elements were clearly visible; ii) vesiculated when the number of vesicles associated with the stack (within 1 μm from the centre of the stack) exceeded 40; iii) tubulated when even a single tubule was seen to protrude from the stack for

a length more than 400 nm. Further Golgi stacks were scored for the presence or the absence of the tubular reticular networks. The percentage of the stacks exhibiting one of these phenotypes or the percentage of Golgi stacks bearing tubular reticular networks were calculated and reported in most of the experiments performed. The process of fragmentation of the tubular part of the Golgi stacks was much more complicated and to quantitatively analyse it an "index of fragmentation" was evaluated for each stack using four criteria: 1) disappearance of tubular-reticular structures and fenestrations; 2) number of vesicular structures (20 vesicles per stack was the control value in untreated membranes); 3) number of fission intermediates; and 4) fraction of naked over tubule-decorated cisternae. Parameter 4 was replaced by: - disappearance of recognisable cisternae - in the case of experiments in which not only tubules, but also cisternae, became fragmented. These parameters varied with identical time courses under all conditions, except that the increase in number of constriction sites usually slightly preceded the other 3 events scored. This discrepancy is minor and does not affect the results significantly. Each criterion was given a score from 0 to 5 (for a total of 20).

2.6.10 Determination of the frequency distribution of vesicular structures

For samples processed for negative staining, 30 stacks were selected for each condition (according to the systematic random procedure described in section 2.6.7), pictures were taken and enlarged at a final magnification of 80000 x. The diameters of the vesicles associated with the stacks were measured and grouped into the following categories: 20-30 nm, 30-70 nm, 70-100 nm, 100-150 nm, 150-200 nm. The total number of vesicles scored was calculated, the percentage of the vesicles falling in one of the above mentioned categories and the frequency distribution was calculated. For the samples processed for thin sectioning, eight fields at low magnification (4400 x) were chosen for each experimental condition by using systematic random sampling. Pictures were taken, enlarged up to 47000 x, and a cross

grid was superimposed on them. The diameter of the vesicles intersecting the crosses were measured and the frequency distribution was calculated as described above.

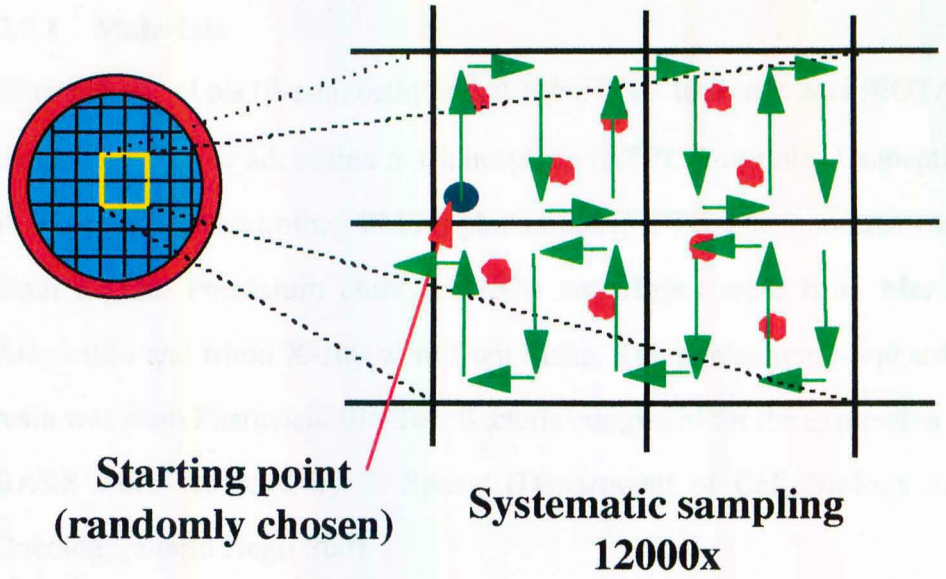

Fig. 2.4 Scheme for stereological analysis using the negative staining technique

Golgi membranes were processed for negative staining and placed in the electron microscope with a random orientation. The micrometric screws used to move the sample laterally were set to the 0 position. The electron beam was switched on and the magnification set to 12000 x. The analysis was started from the left-lower corner of the mesh appearing in the field and the screws were moved positioning the beam along the pathway delineated in the figure by the arrows. Each structure encountered was analysed on the screen, or, alternatively, pictures at the same magnification were taken

2.7 Preparation of cytosolic extracts and recombinant proteins

2.7.1 Materials

Ethylene glycol bis (β-aminoethylether)-N,N,N',N' - tetracetic acid (EGTA), the sodium salt of adenosine 5' triphosphate (ATP), Aprotinin, Leupeptin, Pepstatin, o-Phenantroline, PMSF, gluthathione, IPTG, and lysozime were from Sigma. Potassium chloride (KCl) and Hepes were from Merck. Ampicillin and triton X-100 were from Fluka. The gluthathione-sepharose resin was from Pharmacia Bio-Tec. Bacteria competent for the expression of BARS were provided by S. Spano' (Department of Cell Biology and Oncology, Mario Negri Sud).

2.7.2 Preparation of control cytosols from rat brain

Rat brain cytosol was prepared using a modification of the protocol described by Malhotra et al., 1989. All the procedures were carried out on ice. Sprague Dawley male rats (6 x 250-400 g) fed ad libitum were killed by decapitation, and the brains were removed and placed in 25 mM Tris-HCl pH 7.4, 0.32 M sucrose and washed extensively. Brains were transferred to 6 ml of buffer A (25 mM Tris-HCl pH 8.0, 0.25 M sucrose, 0.05 M KCl, 1 mM DTT, 2 mM EGTA, 5 mM ATP, 2 mg/ml Aprotinin, 0.5 μg/ml Leupeptin, 2 μM Pepstatin, 0.5 mM o-Phenantroline, 1 mM PMSF), minced with clean scissors into small pieces and homogenised with 4-5 strokes (20 sec each, medium speed) of the Ultraturrax. The homogenate was centrifuged at 5000 x g (30 minutes) to eliminate debris and large fragments and the supernatant was collected and ultracentrifuged at 150000 x g for 90 minutes. Both the supernatant of the ultracentrifugation (termed "non dialysed cytosol") and the pellet (resuspended in PBS and termed "total rat brain membranes") were assayed for protein content (typically 15-20 mg/ml, and 5-10 mg/ml respectively), aliquoted, frozen with liquid nitrogen and stored at -80°C. Alternatively, the supernatant was dialysed overnight against 1000 volumes of the desired buffer using membranes for dialysis with a cut off of 3000 Da. Typically the buffer employed was a Tris buffer

(25 mM Tris-HCl pH 8.0, KCl 50 mM, 1 mM DTT). After dialysis, cytosol was centrifuged to remove precipitated materials (150000 x g, 90 minutes) and the supernatant termed "dialysed" cytosol was treated as for the non-dialysed.

2.7.3 Preparation of coatomer-defective cytosol

CHO(ldlf) were grown at the permissive temperature (34°C) or to induce the defect in the εCOP subunit the temperature was raised to 39°C for 12 hours. For standard preparations, 6 totally confluent Petri dishes (15 cm), were used. Cells were detached as previously described and the pellets were resuspended in 0.5 ml of buffer A. Cells were then broken with the Balch-Rothman chamber (8.01 mm ball) and the homogenate was ultracentrifuged for 1h in a TLA100.1 at 60000 rpm. The pellet was discarded while the supernatant was collected and concentrated with Microcon filters (3000 Da as cut-off, Amicon) down to 60-70 µl. The material recovered, termed crude cytosol, was assayed for protein content (8-10 mg/ml on average), aliquoted, frozen with liquid nitrogen and stored at -80°C.

2.7.4 Expression in *E.Coli* and purification of recombinant GST-BARS and GST

In this thesis work, recombinant gluthathione-S-transferase (GST) was used as a negative control for the recombinant GST-BARS. For this reason for every batch of GST-BARS, a batch of GST was expressed and purified in parallel. Bacteria competent for the expression of either recombinant GST or GST-BARS were transferred with a sterile plastic tip into 4 ml of LB containing 60 µg/ml ampicillin. The LB was diluted up to 100 ml with the same medium and left overnight with shaking (37 °C - 220 rpm). The suspension was diluted to 1 l and the bacteria were grown untill the O.D. (at 600 nm) reached the value of 0.4. Expression of the protein was induced by the addition of 0.1 mM IPTG and a further 2 hours shaking. The cell suspension was cooled on ice and centrifuged for 10 min (6000 rpm, JA10 rotor). The pellet was resuspended in 25 ml of 20 mM Tris-HCl pH 8.0, 100 mM NaCl, 1 mM EDTA, 1 mg/ml lysozyme in the presence of the same

cocktail of protease inhibitors described above. Finally, 1% triton X-100 was added, the suspension was stirred for 30 minutes, and sonicated (2 min) on ice. The lysed cells were centrifuged for 20 minutes (18000 rpm, JA20). Meanwhile, 2.5 ml of a gluthathione-sepharose resin was diluted up to 40 ml with PBS and centrifuged for 5 min (2000 x g). The supernatant was discarded and the resin was resuspended again in PBS and the procedure repeated twice. The supernatant from the bacterial lysis was added to the gluthathione-sepharose resin, stirred at 4°C for 30 minutes and then centrifuged (2000 x g for 5 minutes). The supernatant was removed (termed "flow through"), 1 ml of the resin was washed 3 times with PBS and percolated on a column. The resin was allowed to pack for 10 minutes and then elution was started by the addition of 1 ml of 100 mM Tris-HCl pH 8.0 , 20 mM gluthathione, 5 mM DTT (elution buffer). After 10 min, 1 ml of eluant was collected and termed fraction 1. This step was repeated 6 times. Fractions 1-3 were pooled together, assayed for protein content (typical concentrations are 0.6-1 mg/ml for GST-BARS and 1.5-2 mg/ml for GST) and 5 μg of protein were analyzed by SDS page as previously described. The purity of the GST and the GST-BARS was checked by the silver staining procedure (see fig. 2.5)

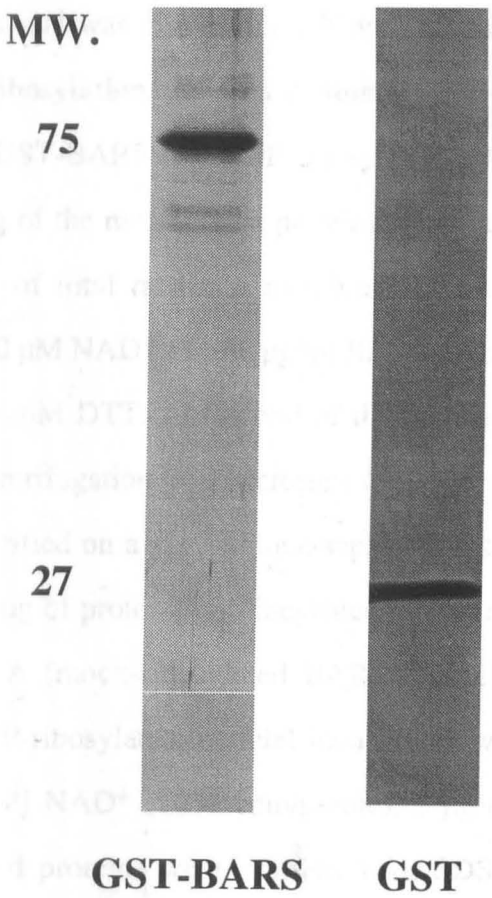

Fig. 2.5 Purity of the recombinant GST and the recombinant GST-BARS by SDS page and silver staining

5 µg of either recombinant GST-BARS (1) or recombinant GST (2) were processed for the SDS-page and silver staining as described. Both GST-BARS and GST are the major band visible. The few bands detected below BARS are degradation products (S. Spano' personal communication -Department of Cell Biology and Oncology - Mario Negri Sud).

2.8 ADP-ribosylation of BARS

2.8.1 Materials

Brefeldin A (BFA), nicotinamide adenine di-nucleotide (NAD+) were from Sigma. [^{32}P] NAD^{+} was from Du Pont New England Nuclear.

2.8.2 ADP-ribosylation and purification of ADP-ribosylated BARS

Recombinant GST-BARS was ADP-ribosylated as follows (Weigert et al., 1997). Fifty µg of the recombinant proteins were incubated for 20 minutes with 1 mg/ml of total rat brain membranes (see section 2.7.1), in the presence of 500 µM NAD^{+} and 60 µg/ml BFA. The reaction was carried out in PBS with 5 mM DTT. At the end of the incubation, membranes were removed by centrifugation in a microfuge (10000 rpm) and the ribosylated protein was purified on a gluthathione-sephadex resin as described above. As control, 50 µg of protein were incubated as described above, but in the absence of BFA (mock-ribosylated BARS). To check that BARS was effectively ADP-ribosylated, parallel incubations were carried out in the presence of [^{32}P] NAD^{+} (1000 cpm/pmole). 2 µg of the mock- and the ADP-ribosylated proteins were processed for SDS-page and blotted on nitrocellulose. The radiolabelled proteins were visualised and quantified by autoradiography (fig. 2.6).

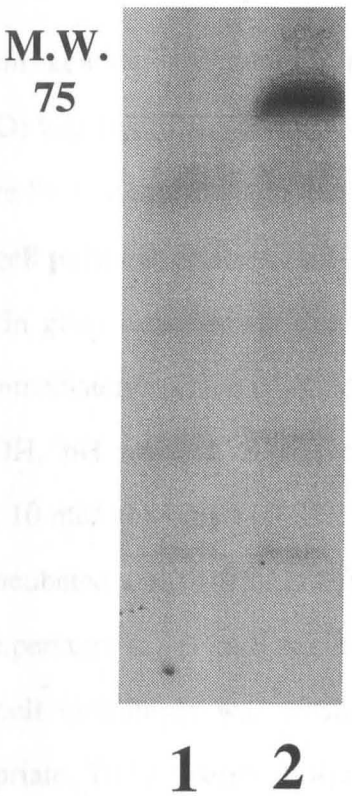

Fig. 2.6 BFA-dependent ADP-ribosylation of recombinant GST-BARS

Two μg of mock- (lane 1) or ADP-ribosylated (2) BARS were processed for SDS-page and blotted onto nitrocellulose. Blots were analyzed by autoradiography (Instant Imager - Canberra Packard)

2.9 Cell permeabilisation

2.9.1 Materials

Glucose, potassium acetate, magnesium acetate were from Merck. Streptolysin O (SLO) was from Biomerieux (Marcy l'Etoile, France). Taxol and trypan blue were from Sigma (Milano, Italy).

2.9.2 Protocol for cell permeabilisation and incubation

RBL cells (grown in glass chamber slides, 100.000 cells per well) were placed on ice and immediately washed with the permeabilisation buffer (PB: 25 mM Hepes-KOH, pH 6.95, 125 mM potassium acetate, 2.5 mM magnesium acetate, 10 mM glucose, 1 mM DTT, 1 mM EGTA, and 0.5 μM taxol). Cells were incubated with 3 U/ml of SLO, previously activated for 5 minutes at room temperature in PB for 8 minutes on ice. Unbound SLO was removed and the cell monolayer was washed with cold PB, and then incubated as appropriate. To test permeabilisation, cells were stained with trypan blue and propidium iodide and the leakage of the cytosolic enzyme lactic dehydrogenase was measured. With this method 95% of the cells were stained with trypan blue and > 80% of the lactic dehydrogenase activity was recovered in the supernatant of the permeabilized cell monolayer (A. Colanzi, personal communication, Department of Cell Biology and Oncology, Consorzio Mario Negri Sud).

2.10 Assay for acyltransferase activity

2.10.1 Materials

[^{14}C]-pCoA, [^{3}H]-LPA were from Du Pont New England Nuclears. Acyl-CoAs, creatin phosphate (CP), creatinphosphokinase (CPK), guanosine tri-phosphate (GTP) were from Sigma. Chloroform was from Carlo Erba

2.10.2 Incubations and lipid extraction

GST-BARS or His-BARS were incubated for different times with 5-40 μM [^{14}C]-pCoA (specific activity 60 μCi/μmol) in the presence or in the

absence of different concentrations of both lysolipids and polar headgroups. Alternatively in experiments assaying for the LPA-specific acyltransferase activity the incubations were carried out with 10 μM of unlabelled acyl-CoAs and 30 μM of [^{3}H]-LPA (specific activity 350 cpm/pmole). The reactions were carried out in a buffer containing 25 mM Hepes pH 7.4, 50 mM KCl, 1mM ATP, 1 mM GTP, 5 mM DTT, 10 mM CP, 10 U/ml CPK and 2.5 mM MgCl2 (final volumes 5 or 12.5 μl). The components of the reaction were mixed together on ice by vortexing and transferred to 37°C. When Golgi membranes were present, the reaction mixture was prepared with the exception of the Golgi membranes, which were placed gently in the bottom of a test tube. The reaction was started by gently mixing the mixture with the Golgi membranes and by pipetting up and down 5 times. Reactions were stopped by adding an equal volume of methanol/8M HCl 1500:1 (kept at -20°C) and lipids were extracted by the additions of 2-3 volumes of chloroform/methanol 2:1. Samples were vigorously vortexed and centrifuged in a microfuge for 5 min at room temperature to allow phase separation. The lower organic phase was collected, washed with one volume of distilled water, vortexed and loaded on a TLC plate.

2.11 Analysis of lipids by thin layer chromatography (TLC)

2.11.1 Materials

[^{14}C]-PA, was from Du Pont New England Nuclears. Potassium oxalate, PC, PI, PE, PA, lyso-PC (LPC), lyso-PE (LPE), lyso-PI (LPI) and Sn1 C18:1 LPA were from Sigma. Ammonia (32 %) was from Carlo Erba.

2.11.2 TLC preparation and elution

Solution for TLC plates pretreatment: 5 g of potassium oxalate were dissolved in 250 ml of distilled water, 146 mg of EDTA were added and the solution was stirred until the powder dissolved. 250 ml of ethanol were added and the solution used to soak TLC plates (Kieselgel G from Merck, 20 x 20 cm) for 80 seconds. Plates were allowed to dry overnight under a

hood, then wrapped in aluminium foil and stored. Prior to use, the silica was scraped from the lateral margins (1 cm) and the loading points were labeled with a pencil 1 cm from the bottom. Samples were loaded with a pipette and dried with a hair drier. As standards [^{14}C]-PA, [^{14}C]-pCoA, [^{3}H]-LPA were used or alternatively 1-5 µg of cold lipids (PC, PI, PE, LPC, LPI, LPE) that were revealed by iodination. Briefly, after the run, TLC plates were exposed in a sealed tank saturated with iodine vapours, and lipids containing double bonds were revealed. As elution buffer, a mixture of chloroform, methanol, 32 % ammonia and water (54:42:2.9:9.1) was prepared and left in a sealed tank for TLC for at least 2 hours. TLC plates were loaded with samples and placed in the tank, and allowed to develop for 2 hours. The TLC plates were removed and dried under a nitrogen stream. Radiolabelled spots were visualised by autoradiography (3-4 days exposure at -80°C) or alternatively revealed and quantified by electronic autoradiography (Instant Imager, Canberra Packard). For tritiated samples, TLC plates were evaluated by gas ionisation scanning using a linear analyser INB 384 (Inotech, Switzerland). Counting efficiency was ~2%. Counts were collected until a counting error <2 % was obtained.

2.12 Preparation of Golgi-derived liposomes

1 mg of Golgi membranes (approximately 200 µl) was mixed vigorously with one volume of cold methanol, and then with two volumes of chloroform. After centrifugation in a microfuge for 5 minutes, the organic lower phase was collected, washed with one volume of water and centrifuged again as described above. The organic phase was complemented with 10 µl of 1.5 mM LPA and dried under a stream of nitrogen. The extracted lipids were resuspended in 100 µl of 25 mM Hepes pH 7.4, vortexed and used immediately. Under these conditions, LPA was at a final concentration of 150 µM. The formation of liposomes was assessed by negative staining using uranyl acetate as described in section 2.6.7. As

controls 10 µl of 1.5 mM LPA were dried and resuspended in 100 µl of 25 mM Hepes pH 7.4.

CHAPTER 3

AN *IN VITRO* ASSAY FOR VISUALISING GOLGI TUBULES

3.1 Introduction

To set up a morphological assay suitable for the visualisation of Golgi-associated tubules and for studying their modifications in a cell-free system, three requirements must be met: i) to prepare highly purified Golgi membranes with the lowest level of contaminants from other organelles; ii) to preserve both the stacked organisation and the tubular part in the isolated Golgi membranes; iii) to maintain the responsiveness of Golgi membranes to known biological stimuli. To achieve this, Golgi membranes were prepared using a variety of protocols described in the literature and starting from different sources which included both different cell types and animal tissues. Each preparation was analyzed for purity and preservation, using both biochemical and morphological criteria. In parallel, the morphological assay was set up and the response of membranes to agents known to modify the Golgi was evaluated Specifically, the effect of the tubulating toxin BFA and the vesiculating nucleotide analogue GTP-γS were checked (see section 1.4.2.1 and Melançon et al., 1987). The same experiments were performed in parallel using a well-established technique (i.e. the resin-embedding and thin sectioning) to determine the reliability of the new assay.

3.2 Characterization of Golgi preparations

3.1.1 Golgi membranes from cultured cells

Different cell lines and specifically, NRK and CHO cells were used as sources for isolating Golgi membranes. The purifications were carried out as described in material and methods using a modified version of the protocol described in Balch et al., 1984 based around a special device for breaking and homogenising cells (the so called Balch-Rothman chamber). This device breaks cells in a gentler and more effective way than conventional methods such as osmotic stress, sonication or dounce homogenization. Membranous fractions purified with this method were assayed by immunoblotting using antibodies directed against various intracellular organelles (as described in material and methods).

Fig 3.1 shows a comparison between these preparations. For all cell types, fractions highly enriched in Golgi membranes, as assessed by the presence of the cis-medial Golgi enzyme mannosidase II (Velasco et al., 1993), were contaminated mainly by early and late endosomes (detected using Rab5 Rab7 as probes, Chavrier et al., 1990) and with traces of endoplasmic reticulum and plasma membrane (detected using calcium binding protein CaBP1 and Na^+/K^+ ATPase as probes; Füllekrug et al., 1995, Godi et al., 1997). The Golgi-enriched fractions were then analyzed by EM using conventional thin sectioning. The stacked structure of the Golgi apparatus was badly preserved (fig. 3.2 A,B) and single Golgi cisternae were mainly observed with no associated tubular profiles. Less than 5% of the structures recognisable as Golgi membranes were piled in stacks of 2-3 cisternae (see stereological definitions in material and methods). With the exception of the multivesicular bodies (MVB, Gruenberg and Maxfield, 1995) and the mitochondria that are easily recognisable (fig 3.2 C, D), the other membranes contaminating the Golgi-enriched fractions, had no distinctive morphology (fig 3.2). The other fractions were variably enriched in the other subcellular organelles and morphologically they appeared to contain

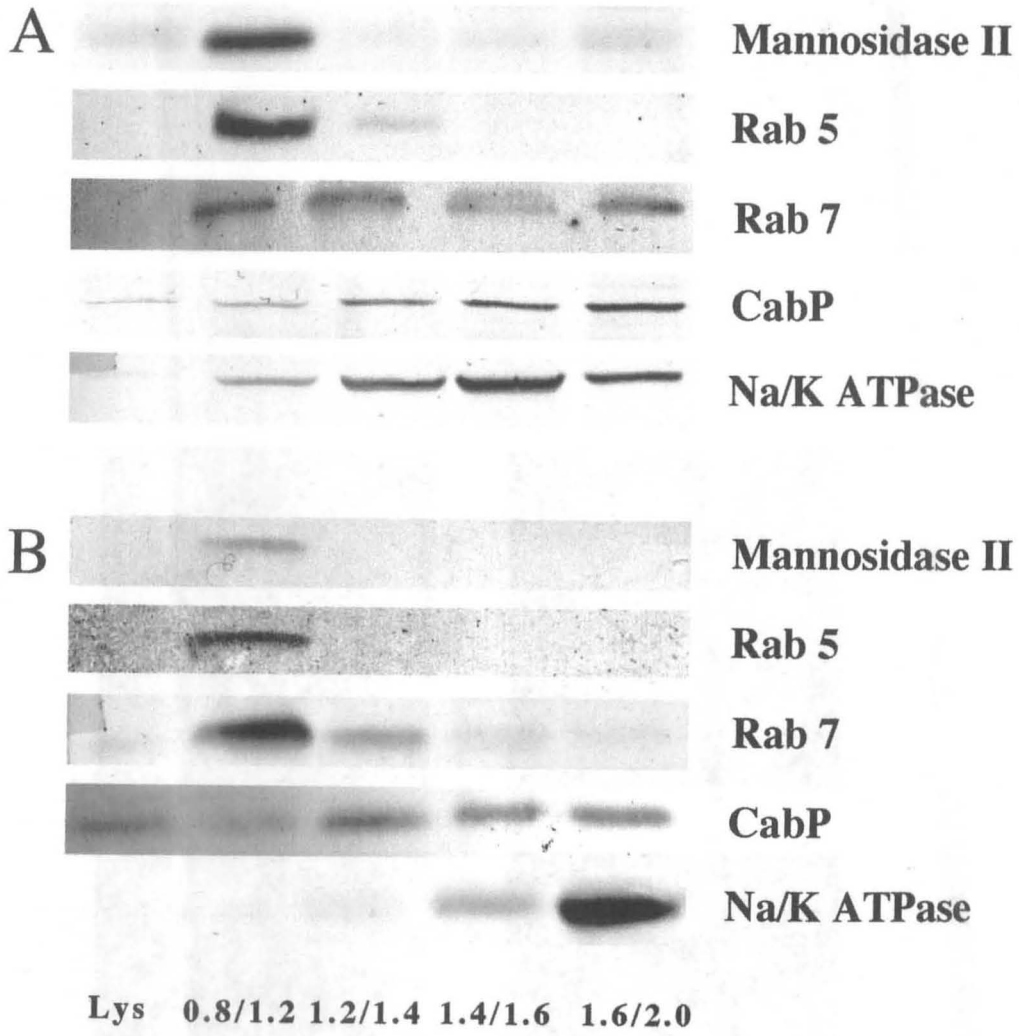

Fig. 3.1 Immunoblot analysis of specific markers for intracellular organelles in the fractionation procedure used to purify Golgi membranes from cell cultures

Seventy-five μg of each of the fractions collected during the purification of the Golgi membranes from either CHO (A) or NRK (B) cells were separated by SDS-PAGE, blotted onto nitrocellulose, and probed with antibodies against the various intracellular organelles shown in the figure(see material and methods). The interfaces collected are shown: Lys indicates the cell homogenate, while 0.8/1.2 represents the Golgi-enriched fraction. These blots are representative of two independent preparations for each cell line.

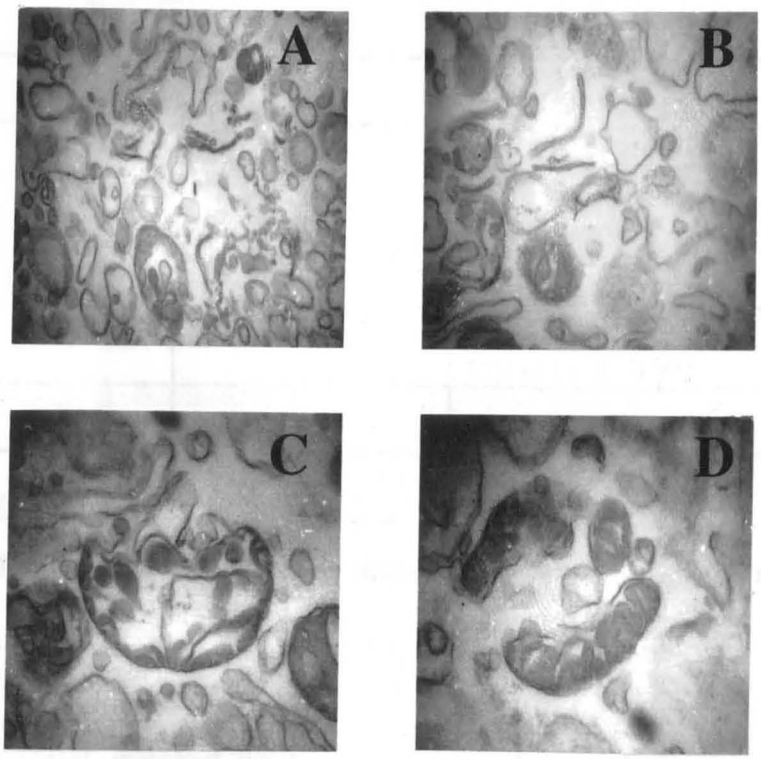

Fig. 3.2 Morphological analysis by thin sectioning and electron microscopy of the Golgi-enriched fractions prepared from cell cultures

Aliquotes (100 µl) of the freshly prepared Golgi-enriched fractions were fixed and processed for thin sections and electron microscopy as described in material and methods. A, C-D. Golgi-enriched fraction from CHO cells. A. Single cisterna and fragments. C. Multivesicular body (MVB). D. Mitochondria. B. Golgi enriched fraction from NRK cells. Single cisterna and fragments. These pictures are representative of two independent preparations for each cell line. Magnifications: 16600 x (A), 25000 x (B),. 70000 x (C) and 43000 x (D).

mainly fragmented structures or vacuoles of non-determined origin. Thus the Golgi-enriched fractions prepared from cell cultures by this protocol were not satisfactory, at least from a morphological point of view.

3.1.2 Golgi membranes from animal tissues

Golgi membranes were also isolated from different animal tissues and using different protocols (see material and methods). Again membranes were assayed both morphologically and biochemically. In table III.I a summary of the tissues and the protocol used is reported.

Tissue	Source	Protocol
Liver	Rat	Leelavathi et al., 1970 Cluett and Brown, 1992 Slusarewicz et al., 1994 Taylor et al., 1998
Testis	Rat	Morre', 1971
Epididymus	Rat	Morre', 1971

Table III.I Protocol used for isolating Golgi membranes from animal tissues

All the Golgi-enriched fractions were enriched in Golgi enzymes but various levels of contaminations were present. As shown in fig. 3.3 A,B membranes from testis and epididymus were largely contaminated by endosomes with some traces of endoplasmic reticulum and plasma membrane. From a morphological point of view they contained a small population (around 20%) of perfectly preserved stacks with associated tubules and a large population of single cisternae (fig 3.3 C). The best preparations in terms of purity were from rat liver. Those obtained by the protocols derived from Leelavathi et al., 1970 were less contaminated than those from the other tissues but their preservation was as not good. (fig. 3.4) The reason resides probably in the fact that the homogenisation step was performed using an Ultraturrax device as homogenizer (see material and

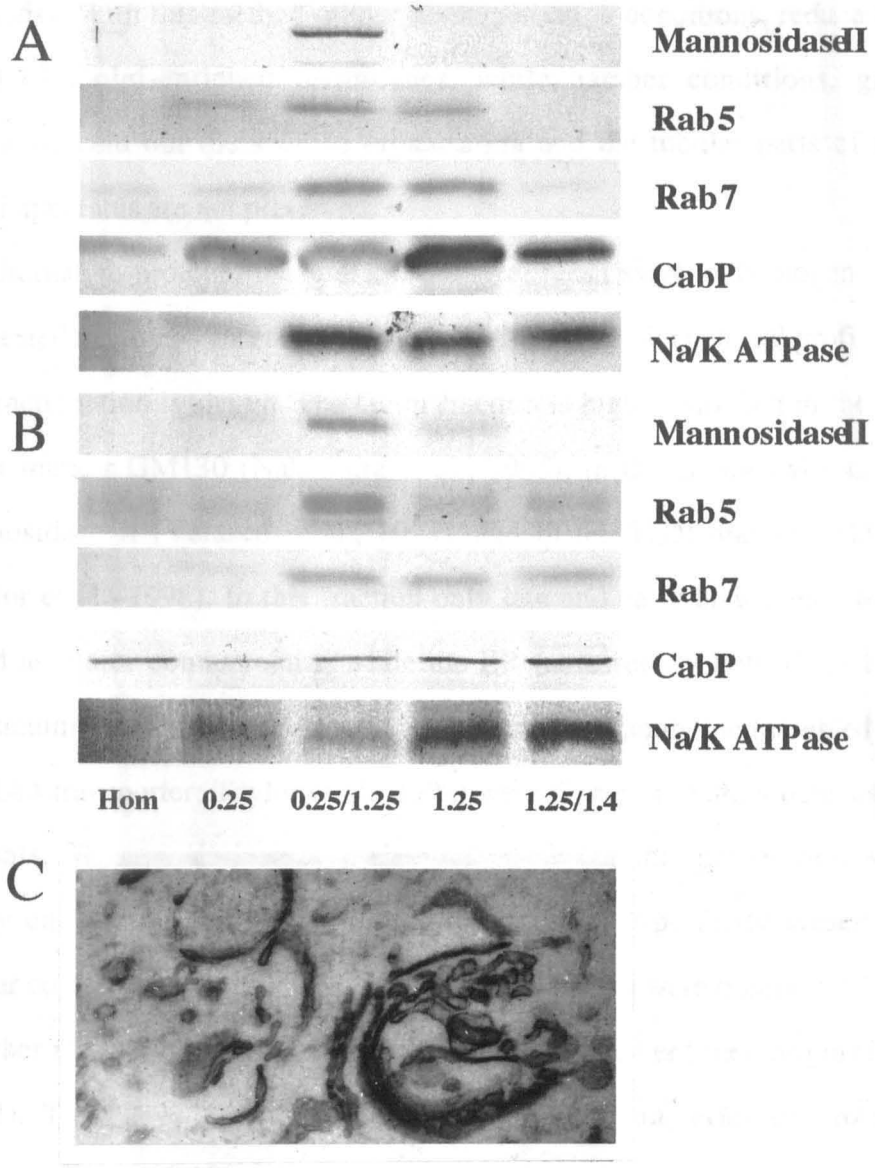

Fig. 3.3 Biochemical and morphological characterization of the Golgi-enriched fractions purified from rat testis and epididymus

A,B Seventy-five μg of each of the fractions collected during the purification of the Golgi membranes from either rat testis (A) or epididymus (B) were separated by SDS-PAGE, blotted onto nitrocellulose, and probed with antibodies against the various intracellular organelles shown in the figure. Hom represents the tissue homogenate, while 0.25/1.25 represents the Golgi-enriched fraction. C. 100 μl of the Golgi-enriched fraction derived from rat testis were processed for thin sections and electron microscopy as described in material and methods. Golgi membranes derived from epididymus had a very similar morphology. Final magnification 46000 x. Both the blot and the electron micrographs are representative of two independent preparations.

methods). With this method milder homogenisation conditions, reduce the yield of Golgi-enriched membranes, while harsher conditions, give increased yeld but the stacked organisation and the tubular parts of the Golgi apparatus are not preserved.

An alternative protocol using a 150 μm steel mesh sieve as homogeniser, was tested (Slusarewicz et al., 1994). In fig. 3.5 A the biochemical profile of the fractionation is shown. The Golgi fraction is highly enriched in the cis Golgi marker GM130 (Nakamura et al., 1995), in the cis-medial marker mannosidase II (Velasco et al., 1993), and in the TGN marker TGN38 (Taylor et al., 1998). In this fraction only late and early endosomes were found as major contaminants, while the ER (assessed by both CaBP1 or calreticulin; Füllekrug et al., 1995) and the plasma membrane (assessed by the HA4 transporter; Taylor et al., 1998) were present in barely detectable amounts. The morphological analysis showed that this preparation was highly enriched in stacked Golgi membranes with a perfectly preserved tubular component (fig. 3.5 B). Very few mitochondria were observed while the other membranes were mostly fragments of non-determined origin (fig. 3.5 B). These fractions were highly concentrated in terms of protein contents (around 6-10 mg/ml), at least 10 fold higher than other standard preparations (normally around 0.4-1 mg/ml). When these fractions were visualised using the negative staining technique (as described in section 3.3.2), Golgi membranes, recognised by the presence of typical fenestrations (Weidmann et al., 1993), appeared clustered, rendering their visualisation difficult (fig. 3.6 and see below). For this reason some modifications were introduced to the purification procedures.

Different buffers (as described in Cluett and Brown, 1992) or sucrose gradients (as described in Taylor et al., 1998) were tried along with the mesh sieve homogeneization protocol (see material and the methods). Fig 3.7 shows the Golgi-enriched fractions prepared using both the methods (shortly termed "Cluett" and "Taylor"), had a similar enrichment in terms of

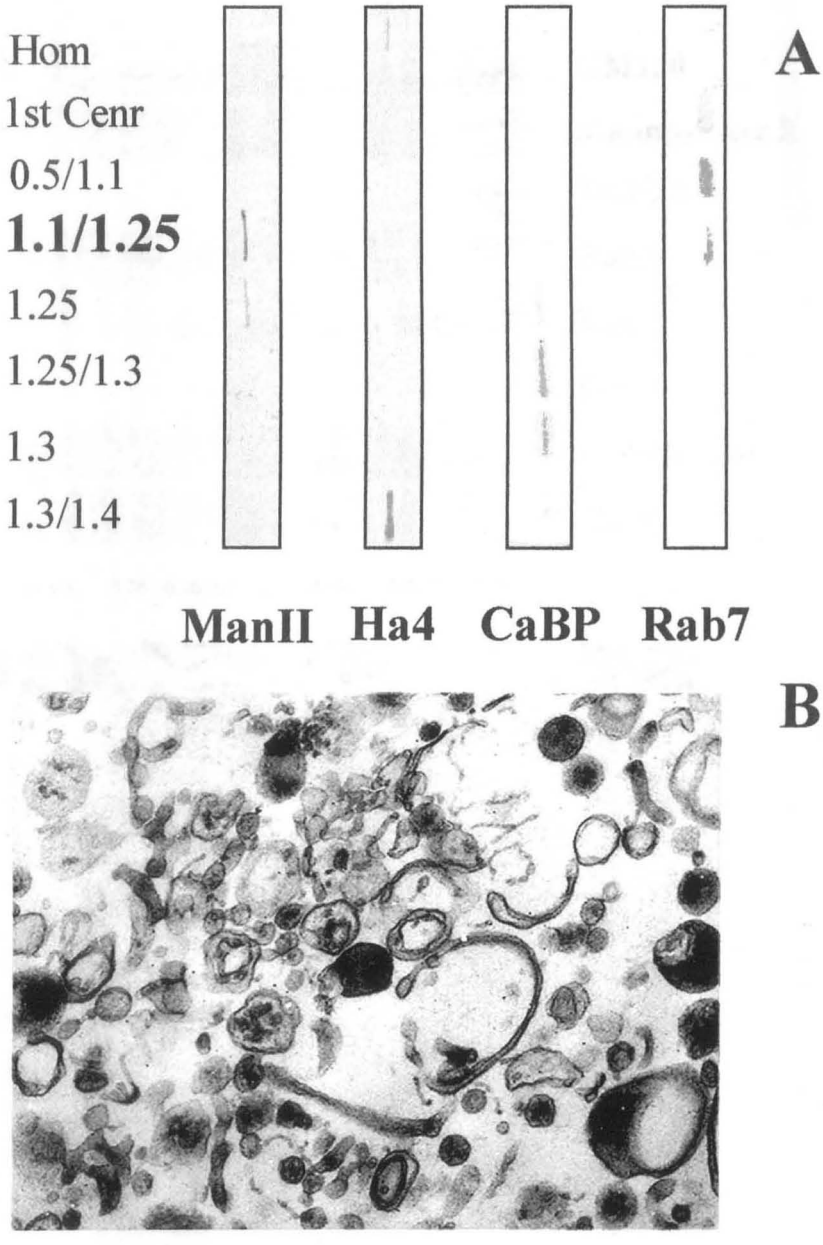

Fig. 3.4 Biochemical and morphological characterization of the Golgi-enriched fractions purified from rat liver according to the "Leelavathi" procedure

A. Seventy-five μg of each of the fractions collected during the purification of the Golgi membranes (according to Leelavathi et al., 1970, see material and methods) were separated by SDS-PAGE, blotted onto nitrocellulose, and probed with antibodies against the various intracellular organelles shown in the figure. B. 100 μl of the Golgi-enriched fraction were processed for thin sections and electron microscopy as described in material and methods. Final magnification 35000 x. Both the blots and the micrograph are representative of three independent preparations.

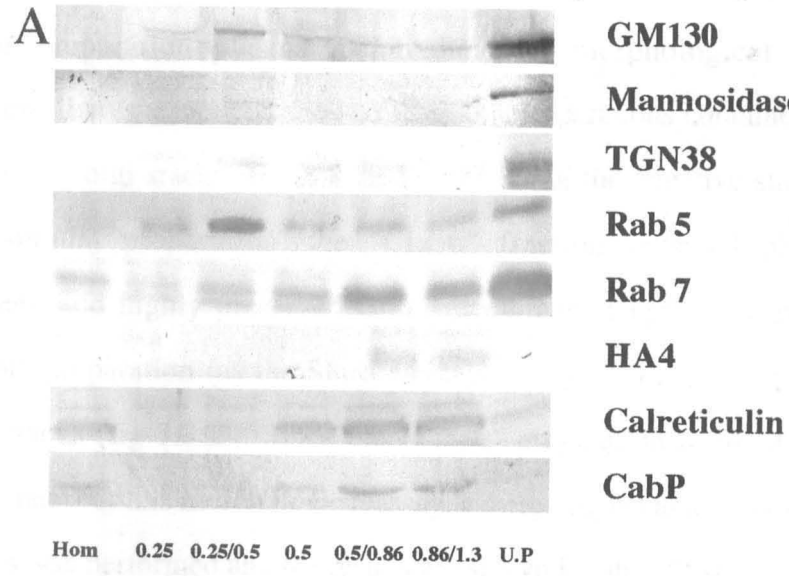

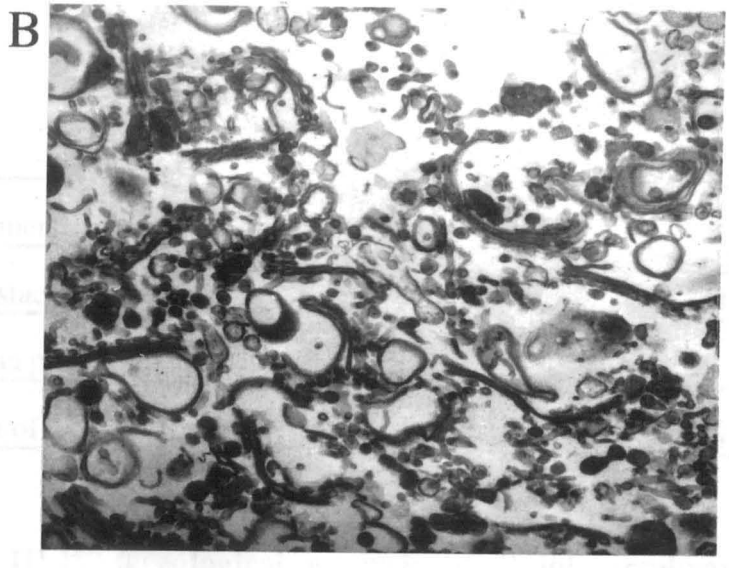

Fig. 3.5 Biochemical and morphological characterization of the Golgi-enriched fractions purified from rat liver according to the "Slusarewicz" procedure

A. Seventy-five μg of each of the fractions collected during the purification of the Golgi membranes (according to Slusarewicz et al.., 1994, see material and methods), were separated by SDS-PAGE, blotted onto nitrocellulose, and probed with antibodies against the various intracellular organelles shown in the figure. B. 100 μl of the Golgi-enriched fraction were processed for thin sections and electron microscopy as described in material and methods. Final magnification 35000 x. Both the blots and the micrograph are representative of four independent preparations.

Golgi markers, with the main contaminants being endosomes and, for the Taylor preparation plasma membrane. The morphological analysis performed by thin sections showed that both preparations contained highly preserved Golgi stacks (fig. 3.8 A, B), but using the negative staining on whole-mount preparation, the "Cluett" fraction revealed physically separated and highly preserved Golgi membranes (fig 3.8 C), while the "Taylor" preparation (as the Slusarewicz) contained clusters of preserved Golgi stacks (fig 3.8 D). Since the "Cluett" preparation fulfilled the first requirement for this morphological assay, a stereological analysis of the thin sections was performed and the results are shown in table III.II.

	Mean ± S.E.M. n=3
Golgi membranes (% of total membranes)	**42 ± 3**
Golgi stacks (% of the total Golgi membranes)	**69 ± 4**
Cisterna per stack	**2.36 ± 0.09**
Length of cisternae (nm)	**586 ± 35**

Table III.II Stereological analysis of Golgi membranes (Cluett preparation) analyzed by thin sectioning

100 µl of Golgi membranes were fixed, processed for the thin section and the electron microscopy, and analyzed by stereology as described in material and methods. Data are means ± S.E.M of three independent experiments.

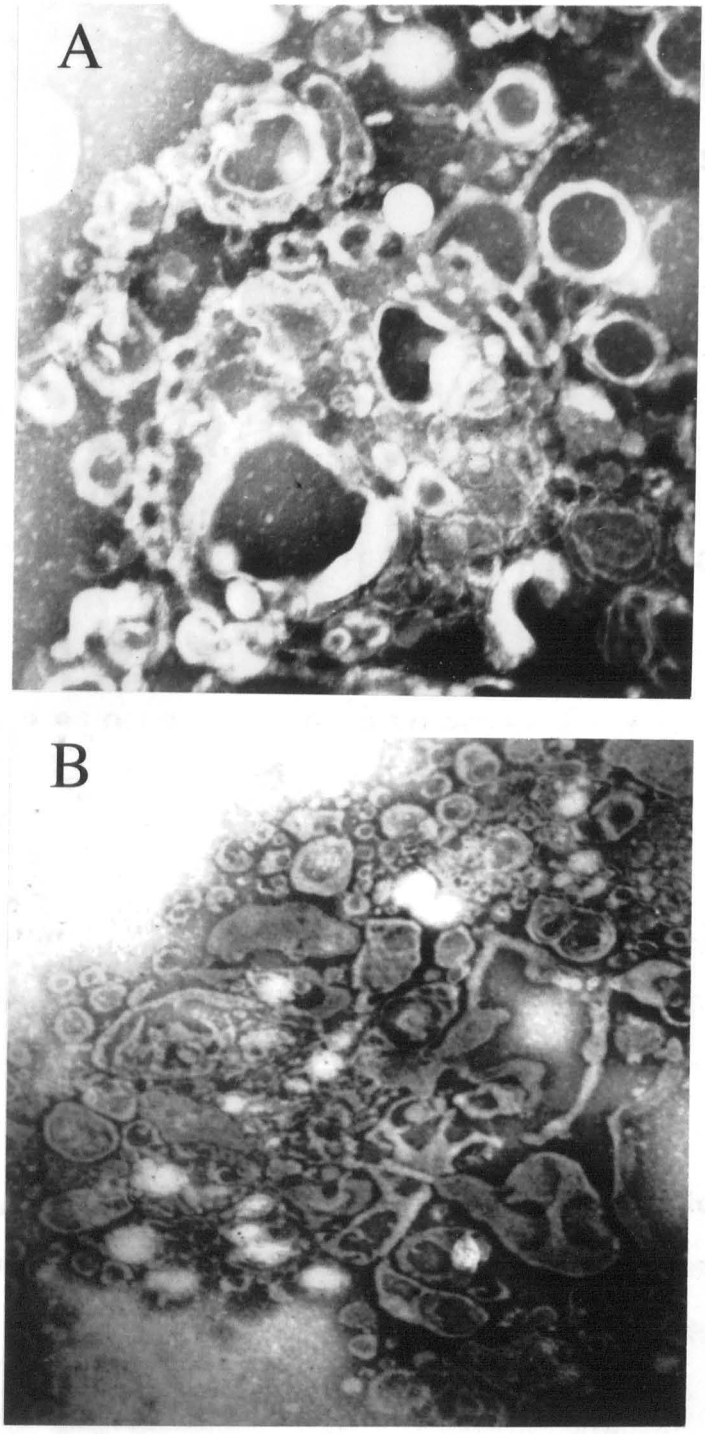

Fig. 3.6 Golgi membranes isolated according to the "Slusarewicz" procedure as visualised by the negative staining technique

A, B. 10 µl of freshly prepared Golgi membranes were processed for the negative staining and electron microscopy as descibed in section 3.3.2. Magnifications: 75000 x (A) and 25000 x (B). Micrographs are representative of three independent preparations.

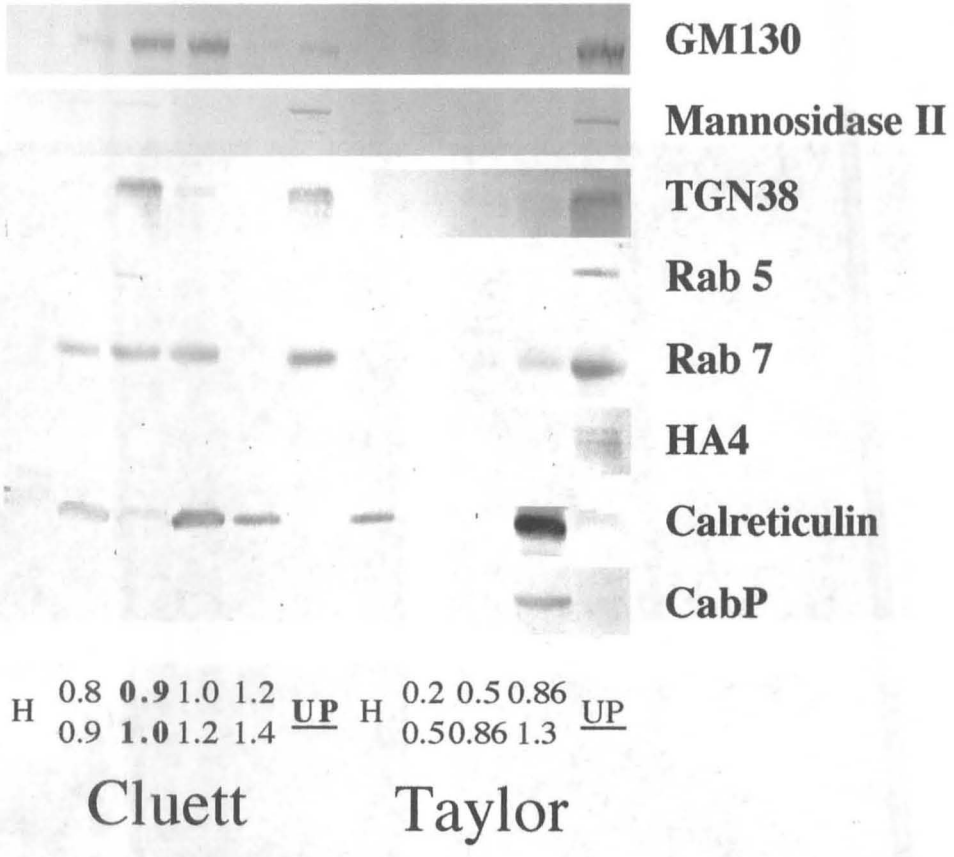

Fig. 3.7 Immunoblot analysis of specific markers of intracellular organelles in the fractionation procedure used to purify Golgi membranes from rat liver using the "Cluett" and the "Taylor" procedure

Seventy-five μg of each of the fraction collected during the purification of the Golgi membranes were separated by SDS-PAGE, blotted onto nitrocellulose, and probed with antibodies against the various intracellular organelles shown in the figure. These blots are representative of four ("Cluett) and two ("Taylor") independent preparations respectively.

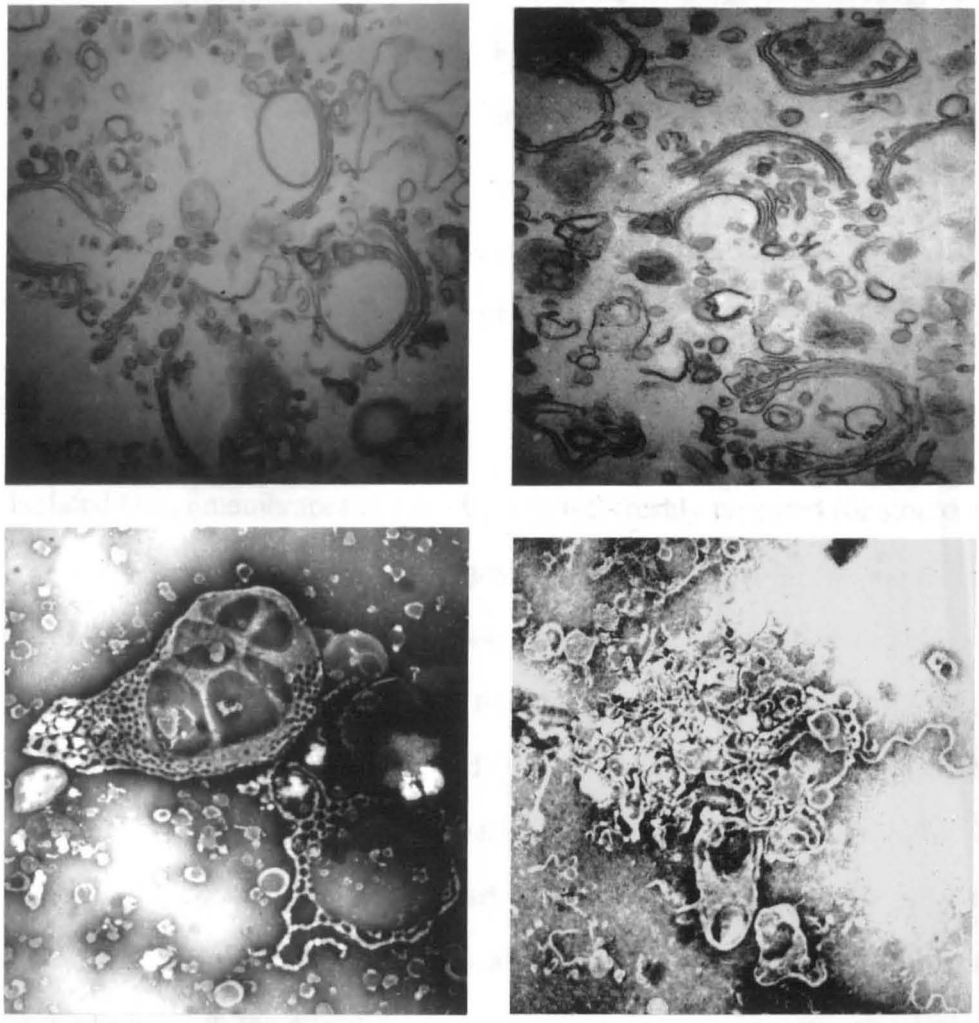

Fig. 3.8 Morphological analysis by electron microscopy of the Golgi-enriched fractions prepared from rat liver using the "Cluett" and the "Taylor" procedure

A,B. 100 µl of Golgi membranes were processed for thin sectioning and electron microscopy as described in material and methods. C, D. 10 µl of Golgi membranes were processed for the negative staining and electron microscopy as described in section 3.3.2. A, C Golgi-enriched fraction prepared using the "Cluett" procedure. B, D Golgi-enriched fraction prepared using the "Cluett" procedure. Magnifications: 30000 x (A), 32500 (B), 40000 x (C), and 20000 (D). These micrographs are representative of four ("Cluett) and two ("Taylor") independent preparations respectively.

3.3 Negative staining on whole-mount preparations

3.3.1 General description

As previously mentioned, the negative staining technique has already been used to visualise Golgi membranes before (Cunningham et al., 1966) and after in vitro incubations (Banta et al., 1995, Cluett et al., 1993). Several protocols were used using different concentrations of contraster, different application times and different ways of adhering membranes to the grid. As starting point for setting up a morphological assay, the protocol used in Cluett et al. 1993 was tried first.

3.3.2 The contrasters

Isolated Golgi membranes (10 µl - 0.5 mg/ml) freshly prepared (or stored at -80°C and rapidly thawed in a thermostatic bath at 37°C) were incubated for 20 minutes at room temperature on a commercially available copper grid for electron microscopy (3 mm, 400 mesh, Electron Microscopy Sciences, USA), covered with a carbon-coated / 0.25 % formvar support film. Excess fluid was drained by a filter paper strip (Whatmann n°3) and a drop (ca. 7 µl) of 2% PTA was applied 2 x 30 sec. The contraster was removed with a filter paper and the grid was slowly allowed to dry. When the membranes were observed in the electron microscope they appeared mostly as a series of flat structures circular or elliptical in shape, closely apposed and having one or more regular arrays of fenestrae associated with some tubules of very variable length (fig. 3.9). All the other membranes appeared as flat saccules with no special features. Very often structures or other areas of the grids were covered by black precipitates of contraster (fig. 3.9 D); further many areas of the grids were physically damaged or so weakened as to be rapidly burnt by the electron beam. In conclusion, using these conditions the quality of the staining (i.e. the contrast and the resolution) was not reproducible. By varying the experimental conditions, using different concentrations of PTA (1.5%, 1%, 0.5%, 0.1%), or buffering with different agents (NaOH or

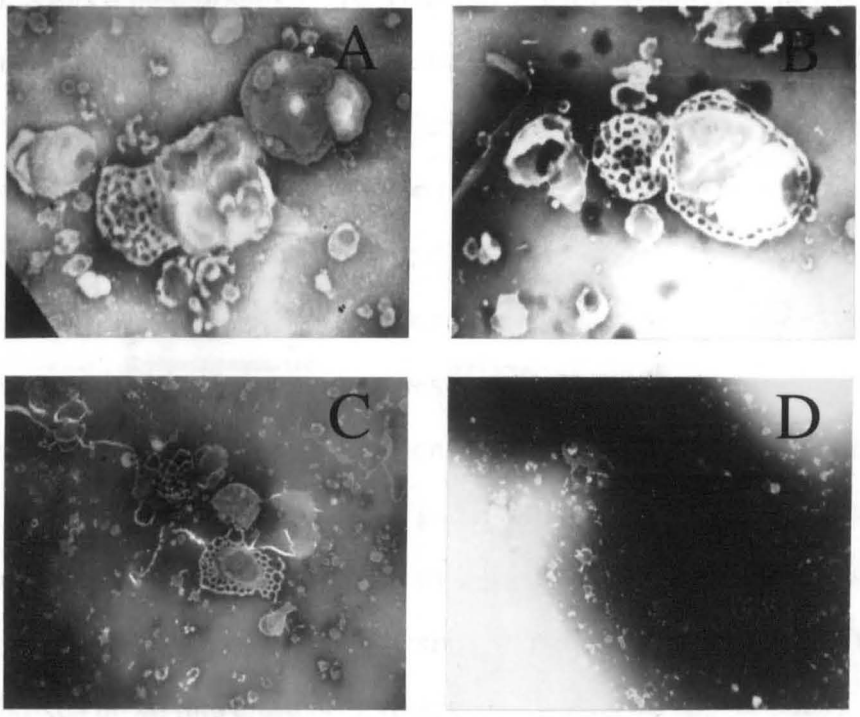

Fig. 3.9 Golgi membranes as visualised by the negative staining technique using 2% PTA as contraster

A-D, Golgi membranes were processed for the negative staining and electron microscopy as described in material and methods. A,B. Cisterna showing peripheral fenestrations and membranes with no particular features. C. Group of cisternae some of which are connected by tubules. D. Precipitates of contraster covering membranous structures. Magnifications: 50000 x (A, B), 20000 x (C, D).

NH_4OH) or at different pHs (7.0, 7.2, 7.4), no significant improvements were achieved. Another contraster, uranyl acetate (UA) was tested applying the same protocol described above. It gave a worse resolution than PTA, and changed completely the morphology of the membranes (see fig 3.10). Fenestrae and tubules were less evident and Golgi stacks appeared as masses of fused membranes. Finally, a commercially available PTA containing product (NanoW 2018 from Nanoprobes), but whose precise composition is covered by patent, was tested. This contraster was excellent giving a much higher reproducibility and quality in terms of staining (fig. 3.11). Golgi membranes were visualised with a better contrast and resolution and the amount of precipitate and the darkness of the samples were markedly reduced. From hereafter the NanoW 2018 has been used for the negative staining assay and will be referred simply as "contraster".

The optimal staining conditions were determined by applying the contraster twice for different times varying in a range between 5 sec and 10 minutes. Below 10 seconds Golgi membranes were very well preserved but the contrast was very low. The incubations between 20 seconds and 1 minute gave an optimal contrast and a fairly good preservation of the structures. By increasing the time, the contrast slightly improved but both Golgi stacks and the other unknown membranes extensively tubulated (fig 3.12 A) and were then broken down into clusters of vesicles and fragments (fig. 3.12 B).

3.3.3 Grids and support film

The grids initially used in this characterization were commercially available carbon coated 0.25 % formvar grids (Electron Microscopy Sciences). The support film was too thin and very often it was not resistant to the contraster itself. For this reason different support films and grids of different materials, with or without the carbon coating, were prepared and tested under the staining conditions described above. In terms of thermal and mechanical resistance 1% formvar grids were the best. Four hundred mesh copper or nickel grids provided a much more resistant frame.

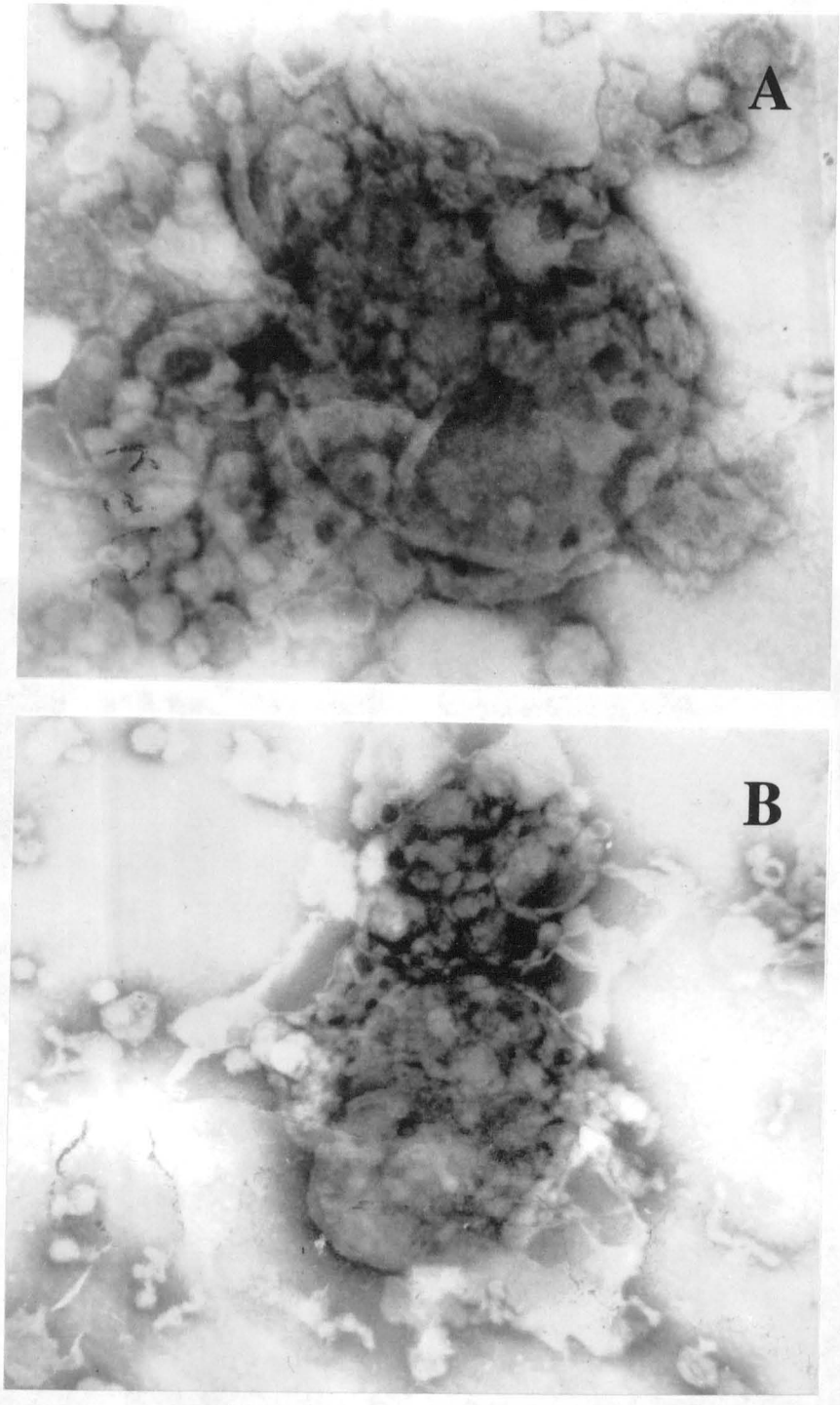

Fig. 3.10 Golgi membranes as visualised by the negative staining technique using UA as contraster

A,B Ten µl of Golgi membranes were processed for the negative staining and electron microscopy using UA as described in the material and methods . Magnifications: 75000 x (A) and 37500 x (B).

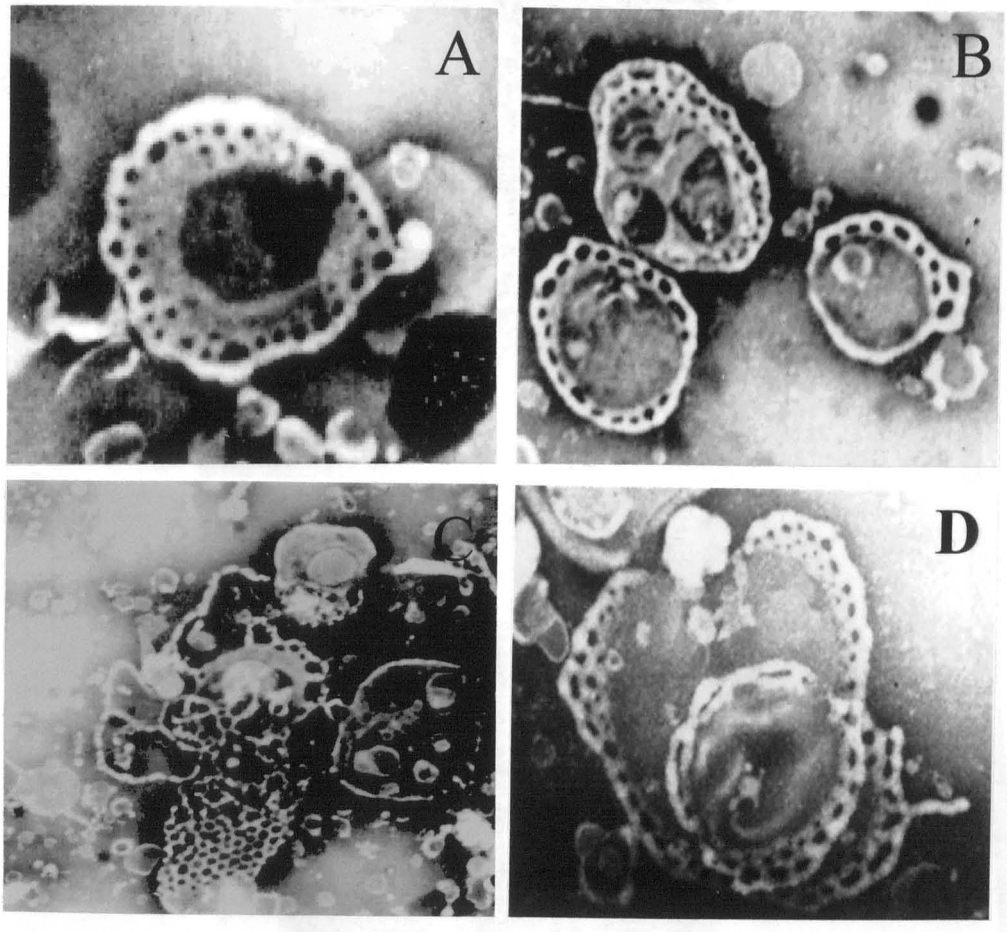

Fig. 3.11 Golgi membranes as visualised by the negative staining technique using the NanoW 2018 as contraster

A,B. Golgi membranes were processed for the negative staining as described in material and methods A. Isolated cisterna showing peripheral fenestrations. B. Group of disconnected cisternae. C. Group of cisternae interconnected by tubular structures. D Group of piled cisternae. Magnifications: 66000 x (A), 35000 x (B), 25000 x (C) and 66000 x (D).

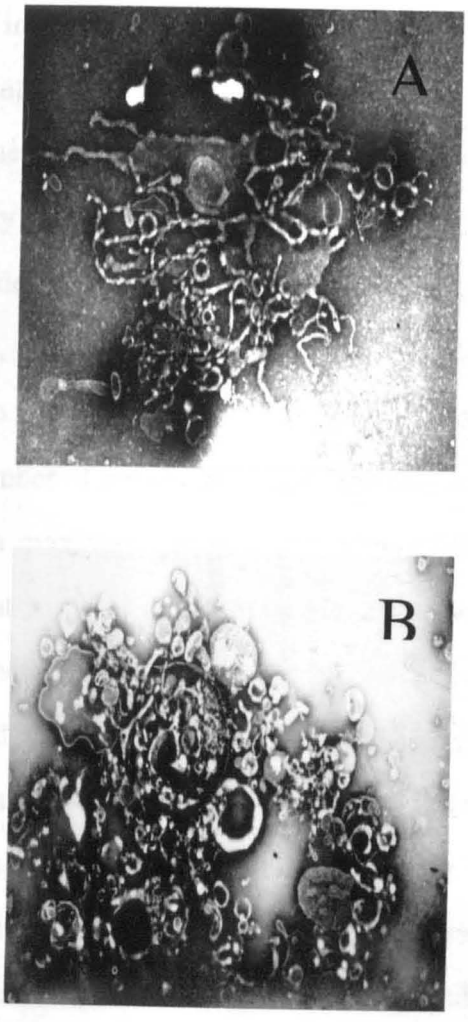

Fig. 3.12 Effect of the long exposure of Golgi membranes to the contraster

10 µl of Golgi membranes were processed for the negative staining as described in material and methods with the exception that they were exposed twice for 5 (A) and 10 (B) minutes to the contraster. Magnifications: 30000 x (A) and 20000 x (B).

Copper grids were used routinely, while nickel grids were employed only when the incubations lasted more than 4 hours (as in the case of the immunogold technique; see below) and to avoid oxidative phenomena. Carbon coats of different thickness were generated on the support film, as described in material and methods but neither the spreading of the contraster nor the quality of the staining were affected and thus the coating was not used.

3.3.4 Time of incubation and volume of deposition

The nature of the interactions between the membranes and the formvar support film covering the grids and the dependency of the incubation times on the amount of membranes deposited had not previously been described. Thus, the possibility that only a sub-population of Golgi membranes were being selectively deposited on the grids, and the rest floating in the overlaying medium, was tested. 10 µl of 0.5 mg/ml Golgi membranes were allowed to adhere to the grids for different times and from 10 seconds up to 40 minutes. The number of membranes deposited on the grids (regardless of their nature) with a maximal diameter exceeding 200 nm was scored as described in the material and methods (see also below) and expressed as number of membranes per mesh (fig 3.13). Below 1 minute the amount of membrane deposited was highly variable while at longer times the amount did not change. Thus 5 minutes were chosen as standard time for incubation. This finding suggests that membranes do not deposit via sedimentation-based process but probably via some interactions between the membranes and the surface of the formvar coat. To check the possibility of a selective deposition, membranes were incubated for 5 minutes on a grid, the drop was removed by a micropipette and deposited for 5 minutes on another grid. The procedure was repeated until the volume of the drop was too small to cover a new grid. On average seven samples were obtained and stained as described above. The samples observed at the electron microscope revealed an homogeneous population of membranes with almost no detectable differences.

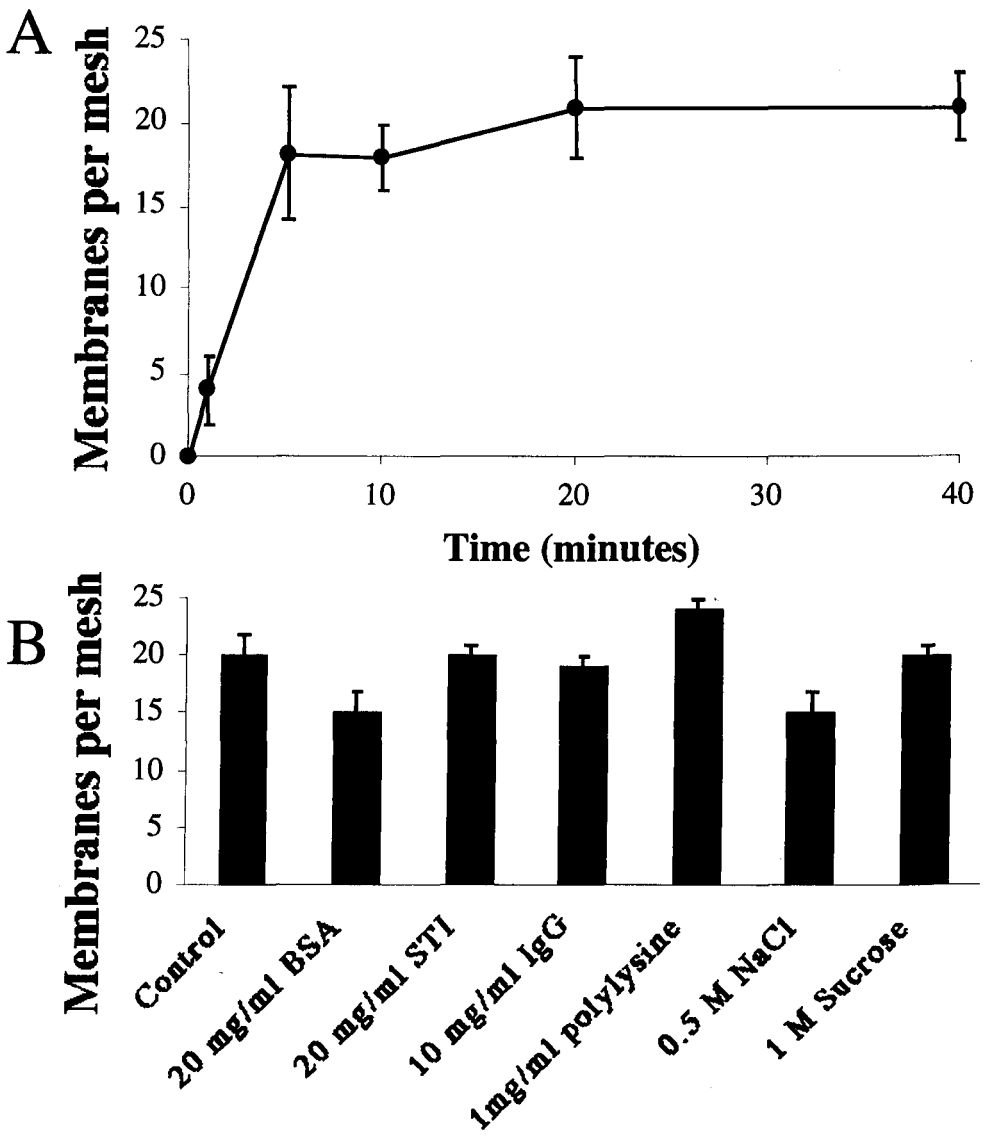

Fig. 3.13 Characterization of the negative staining technique

A,B Golgi membranes were allowed to deposit on formvar coated grids for different times (A) or for 5 minutes under the indicated experimental conditions (B). The number of membranes deposited per mesh was reported. Values are means of triplicates ± S.D. The experiments were repeated two times with similar results.

The volume of the membranes deposited on the grid was also optimised and set between 6 and 12 µl. Other factors such as the sucrose concentration and the ionic strength did not influence the quality of the staining, though the latter slightly reduced the amount of membrane deposited (fig. 3.13 B). Membranes were also deposited in the presence of different concentrations of various bulk proteins such as BSA, STI or human IgG (from 1 to 20 mg/ml) with no significant differences. The total amount of membrane deposited was increased only by pretreating the grids for 30 minutes with 1 mg/ml polylysine (fig. 3.13 B). Indeed, the number of the membranes adhering to the support film was increased while the staining and the resolution were reduced and became less reproducible.

3.3.5 Visualisation of Golgi membranes in non-fixed samples

The standard Golgi preparation used in this thesis was the Cluett and it will now be referred to simply as "Golgi membranes". They were characterized extensively by the negative staining technique and the results of this analysis were compared with the stereological analysis performed using the thin sectioning procedure. 10 µl of Golgi membranes were deposited under the standard conditions determined above and their morphology was analyzed. Almost all the membranes observed were circular or elliptical in shape. 31% ± 10 (average ± S.E.M. n=5) did not show any significant morphological features, the other 69% ± 22 (average ± S.E.M. n=5) showed one or more regular arrays of fenestrae (fig. 3.14 A). Based on their morphological features the fenestrated structures were likely to be Golgi membranes. Indeed these structures matched those previously identified and described as Golgi membranes both in vitro (Weidmann et al., 1993, Happe and Weidmann, 1998, see fig 3.14 B-C) and in living cells (Rambourg and Clermont, 1990). The putative cisternae displayed a central area darker than the peripheral area, very similar to the core described previously using the freeze-etch technique (Weidmann et al., 1993). These putative Golgi cisternae appeared isolated (32% ± 19) or in groups (68 % ± 19, the average number of cisternae per group being 2.3 ± 0.2).

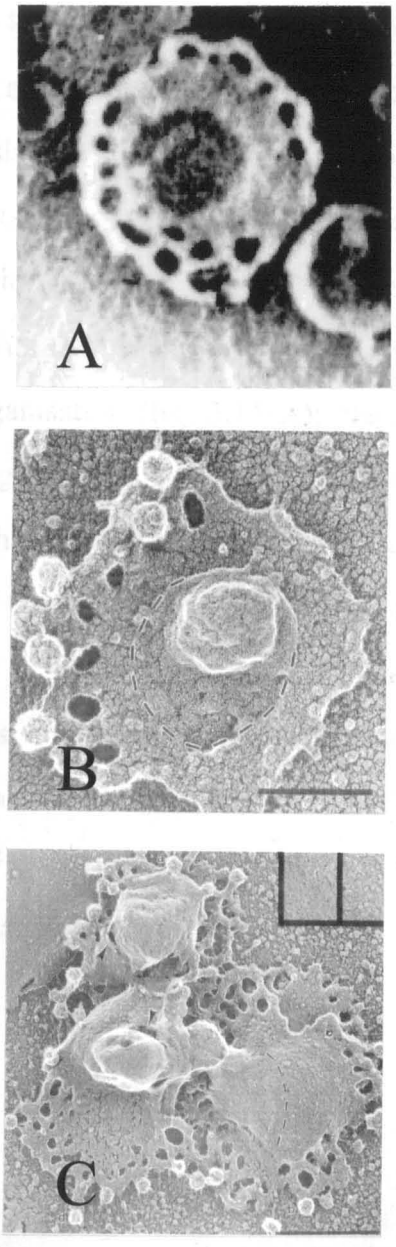

Fig. 3.14 Comparison between the morphology of the Golgi membranes as visualised by the negative staining or by the freeze-etch technique

A Isolated Golgi cisterna as visualised by the negative staining technique (magnification 50000 x). B-C Golgi cisternae as visualised by the freeze-etch technique (Weidmann et al., 1993; reproduced with the permission kindly provided of the author).

Such groups were composed of both fenestrated and non fenestrated membranes and disconnected or interconnected by tubular structure (see fig 3.11). The average maximal diameter for the cisternae was 667 nm ± 75 (average ± S.E.M. n=5), closely matching the length obtained with the conventional thin section technique (see table III.II) and the average number of fenestrae was 15 ± 4 (average ± S.E.M. n=5) with a diameter of 45 nm ± 10 (average ± S.E.M. n=5). According to the location and the morphology of the fenestrated/tubular area, which occupied 42 % ± 3 (average ± S.E.M. n=2) of the total area, these putative cisternae were classified into the following six categories which might possibly represent different Golgi compartments: class A, structures completely fenestrated and showing a three-dimensional organisation (fig. 3.15 A); class B, structures with a single array of very large fenestrae (diameter more than 50 nm) (fig 3.15 B); class C, structures with one or two arrays of small fenestrae (diameter less than 20 nm) (fig. 3.15 C); class D, structures with small fenestrae located only on one side of the structures and occupying more than 30% of the total area (fig. 3.15 D); Class E, structures completely fenestrated but having a two-dimensional organisation (fig. 3.15 E); Class F, completely saccular cisternae (fig. 3.15 F). The morphological features for each class of cisternae are shown in table III.III.

	% of structure	Max diameter (nm)	Fenestrated area (%)	Fenestrae	Fenestrae diameter (nm)
A	10 ± 4	661 ± 107	100 ± 0	11 ± 0	54 ±10
B	5 ± 4	816 ± 304	75 ± 0	2 ± 1	195 ± 35
C	31 ± 4	728 ± 9	67 ± 0	13 ± 0	38 ± 2
D	13 ± 1	499 ± 26	70 ± 7	9 ± 2	35 ± 3
E	10 ± 1	383 ± 31	100 ± 0	14 ± 0	40 ± 0
F	21 ± 3	544 ± 99	-	-	-

Table III.III Stereological analysis of the different classes of Golgi cisternae

Very few Golgi cisternae showed vesicular profiles (only 50 % ± 12 of the cisternae showed vesicles associated each of them having on average 2.9 ± 1.3 vesicles). This could be due to the fragility of the proteinaceous bridges which bind the vesicles to the stacks and which are not resistant to the contraster or to air drying. Two different populations of Golgi-associated vesicles were identified: contraster repelling (88 ± 15 %) with a diameter of 50 ± 5 nm and contraster absorbing (12 ± 15 %) with a diameter of 41 ± 5 nm (fig. 3.16 A). In this preparation 26 % ± 13 of the Golgi cisternae emanated tubules regardless of whether they were isolated or grouped. These tubules were contraster-repelling, sometimes convoluted with an average diameter of 47 nm ± 3 and variable lengths from 50 nm up to 2-3 μm. On average each tubulated cisternae bears 2.4 ± 0.9 tubules (fig. 3.16 B). These might represent tubules that were formed de novo during the preparation or might be the remnants of tubular continuities described as connecting different Golgi stacks (even if several fold less abundant) and partially destroyed during the ultracentrifugation step of the fractionation procedure.

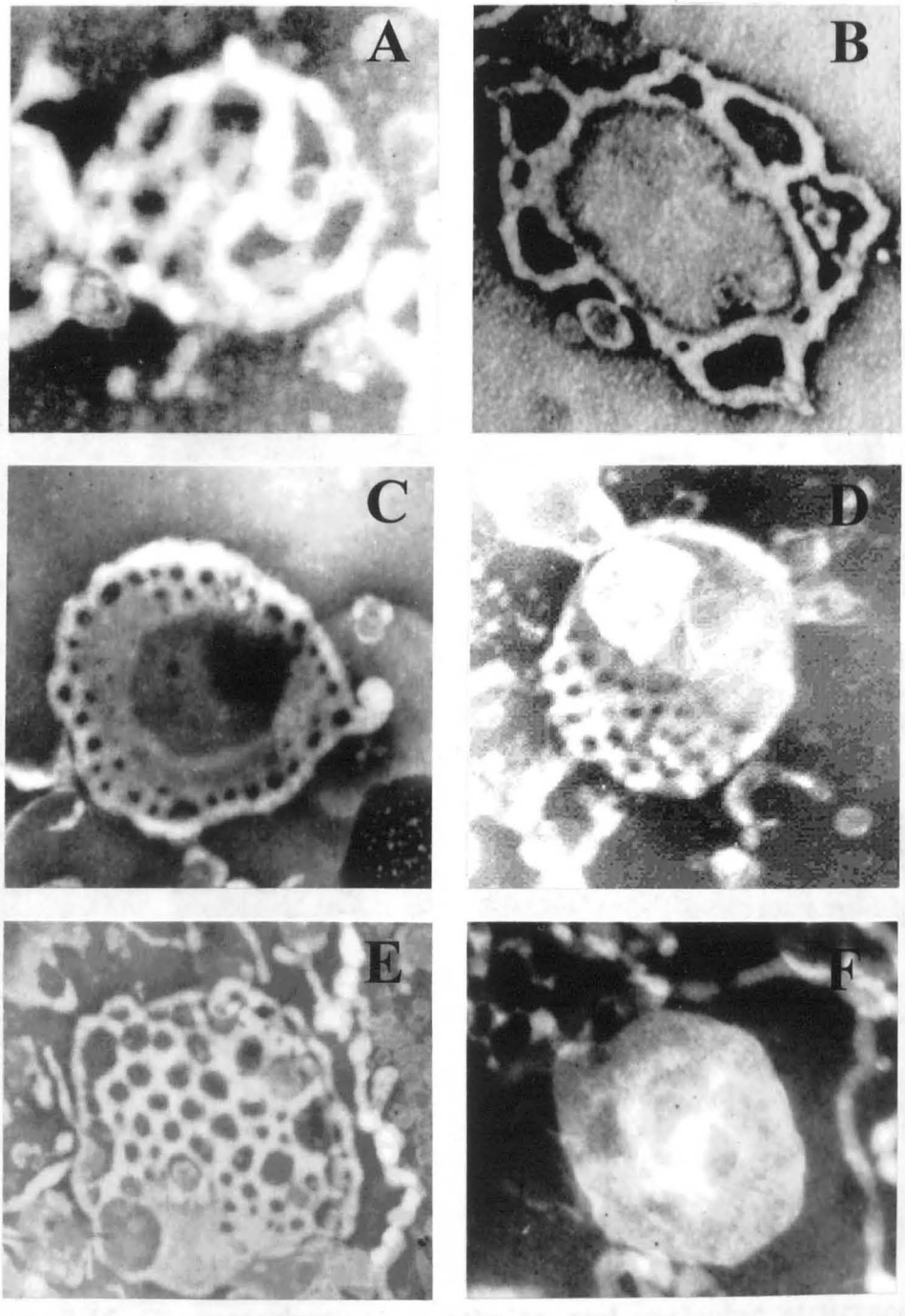

Fig. 3.15 Golgi membranes are classified in 6 categories according to their morphological features

A-F Golgi membranes were processed for the negative staining as described in material and methods. They were classified according the presence, the location and the size of the fenestrae (magnification 50000 x).

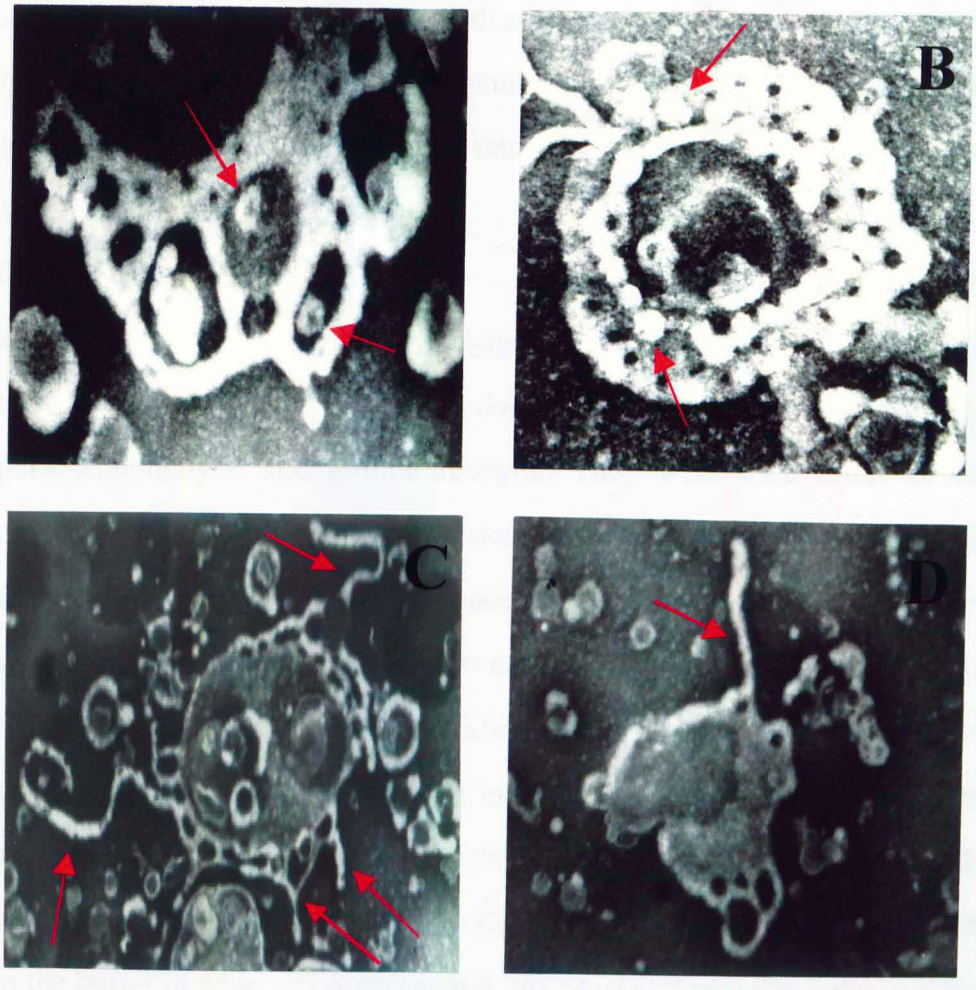

Fig. 3.16 Characterization of tubular and vesicular structures associated with the Golgi membranes as visualised by the negative staining technique

A-D Golgi membranes were processed for the negative staining as described in material and methods. The arrows show contraster-adsorbing vesicles (A), contraster-repelling vesicles (B), straight or convoluted tubules (C, D). Magnifications: 80000 x (A), 62500 x (B), 37500 x (C, D).

A comparison between the main morphological features of the Golgi membranes as visualised by negative staining or by thin sectioning analysis revealed that they are in very good agreement. However, the main difference observed is that in the thin sections, Golgi membranes are perfectly organised in stacks of 2-3 cisternae, while in the negative staining they appear to be unstacked and grouped. This destacking effect is likely due to the PTA-based contraster. Indeed PTA has been described to weaken the intercisternal matrix (see fig. 3.11) which then becomes sensitive to mechanical stress and is lost during the whole-mount technique (Cunningham et al., 1966). Golgi membranes that are chemically fixed are probably more resistant and, during thin sectioning, they are not exposed to such stress.

3.3.6 Fixation protocol

A protocol for the fixation of the isolated Golgi membranes was set up using the most common chemical fixatives used in electron microscopy, paraformaldehyde and glutharaldehyde. They were used alone or in combination, changing the concentrations and the times of incubation. The main problem was that in the presence of these compounds the contraster strongly deposited on the membranes causing a complete loss of resolution, furthermore the paraformaldehyde showed a strong propensity to induce vesiculation of the membranes and induced general damage to their fine architecture (as described by other authors; Griffith et al., 1993). The strong deposition of the contraster could be due to the presence of an amino group in the buffer in which PTA was stored (the exact composition is covered by patent). For this reason several blocking agents (BSA, human IgG, lysine, polylysine, ethanolamine) were used, the incubation times varied from 1 minute to 18 hours and different washing procedures were used. The final optimised procedure, ensuring the highest resolution and preservation of membranes and used hereafter, is the following: 10 µl of the sample were fixed by the addition of 2 µl of 2% glutharaldehyde in PBS pH 7.4 at room temperature and placed on a 1 % formvar-coated grid for 5 min. The excess

fluid was removed, and the grid was gently washed with 20 mM Hepes, pH 6.8. 10 mg/ml BSA was applied for 1 min, and 3 washing steps were performed with 20 mM Hepes, pH 6.8. Finally, the contraster (NanoW 2018 from Nanoprobes) was applied for 2 x 20 sec, the excess was removed by a strip of filter paper, and the grid was allowed to dry slowly.

3.3.7 Visualisation of the Golgi membranes in fixed samples

The Golgi apparatus was identified in these samples as piled (fig 3.17 A,B) or individual cisternae having a fenestrated area. These structures matched perfectly the three-dimensional reconstructions performed by serial sectioning (Rambourg and Clermont, 1990) or the images produced by freeze-etch electron microscopy (Weidmann et al., 1993, Happe and Weidmann, 1998) in non-fixed membranes. While the single cisternae showed a circular or elliptical shape (with a maximal diameter of 481 ± 29 nm), the stacks appeared with an irregular shape and were composed of a variable number of cisternae that were not piled along the same axis. Sometimes a single cisterna was found to be completely out of the stack but still in continuity with it through a tubular network. From the edges of the stack very often fenestrations were found to emerge and to project tubular profiles with a diameter of 49 ± 4 nm (average ± S.E.M. n=3) and an average length not exceeding 200 nm. Very often stacks were covered by a reticular network from which short tubules or fully formed vesicular profiles of 56 ± 3 nm (average ± S.E.M. n=3) in diameter were found to be closely associated (28 ± 5 vesicles per stack; average ± S.E.M. n=3). Micrographs at higher magnification revealed that these vesicular profiles were both buds and fully formed vesicles, the latter being always linked through a subtle membranous bridge to the parental reticular networks (fig. 3.17 C, D). Notably, all the buds or the fully formed vesicles were formed from the fenestrated area and the reticular network but never from the saccular part of the stacks. Thus after fixation, Golgi membranes appeared much more complicated in terms of morphology. However the stacked organisation, the vesicles and the tubular profiles were largely maintained.

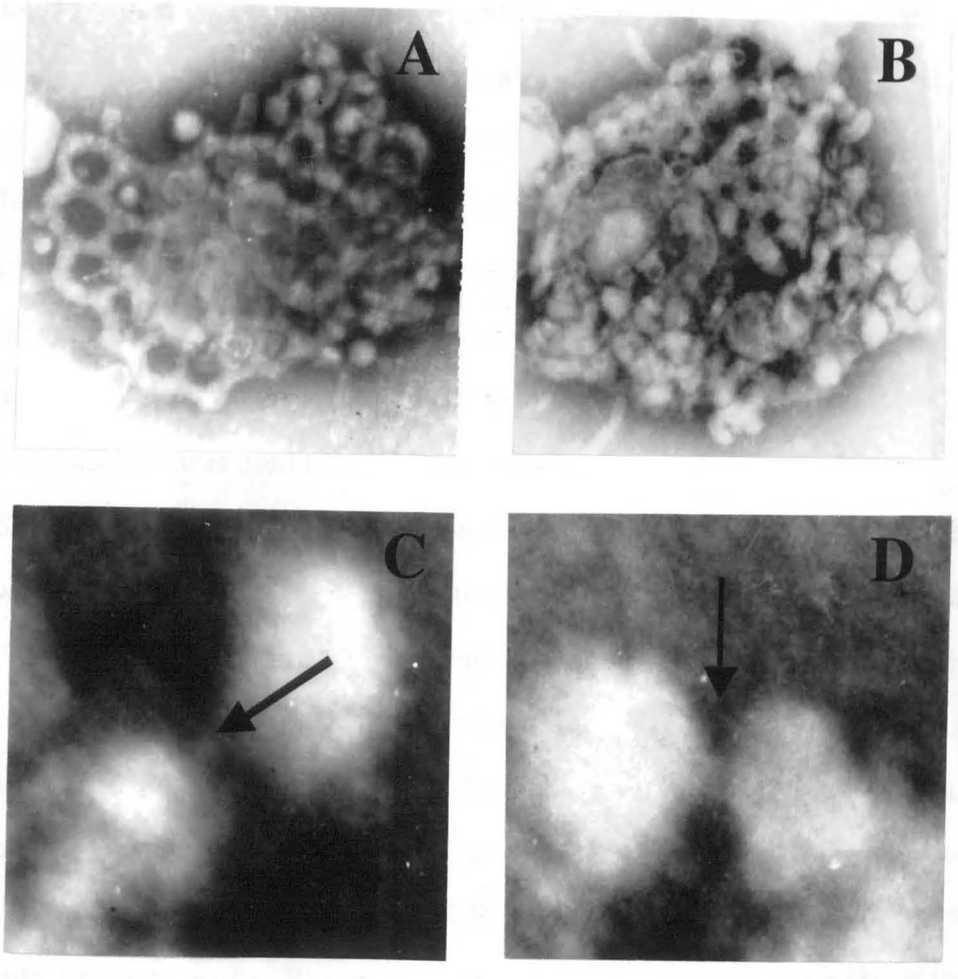

Fig. 3.17 Characterization of isolated Golgi membranes by using the negative staining technique after fixation with glutharaldehyde

Isolated Golgi membranes were fixed with glutharaldehyde and visualised by negative staining as described in material and methods. Note the fenestrated edges (A), and the tubular reticular network partially covering the topmost cisterna (B). C, D The arrows indicate the subtle bridges, probably of proteinaceous material, which link the vesicles to the cisternae. Magnifications: 60000 x (A, B), 300000 x (C, D).

3.3.8 Immunogold labelling of Golgi membranes

To confirm that the membranes visualised by the negative staining technique were really Golgi membranes, immunoelectron microscopy was used. Specifically a method based on the immunogold technique was set up. Golgi membranes were treated with 20 mg/ml BSA in PBS (final concentration) and immediately fixed with a mixture of 4% paraformaldehyde and 0.05 % glutharaldehyde in PBS. This fixative was used to combine the two main properties of the chemicals, glutaraldehyde was introduced to fix the membranes and to prevent the vesiculating effect of paraformaldehyde, and kept at a low level to avoid a loss of antigenicity. Indeed, isolated membranes are without their natural environment of cytosolic proteins (in living cells cytoplasm has an estimated concentration of 100-200 mg/ml) and a strong fixative could induce cross linking of Golgi proteins resulting in a dramatic loss of antigenicity. A high BSA concentration was used to block these effects.

Samples were allowed to deposit on 1 % formvar-coated grids, pre-treated with polylysine (1 mg/ml for 30 min), and the excess fluid was removed. Polylysine was necessary to cross link membranes strongly to the formvar, since for this procedure, membranes have to be left on the grids for at least 18 hours and during this period of time, membranes, in the absence of polylysine, slowly detach and are lost in the fluid. The grids were placed upside-down on a large drop of PBS-BC (PBS containing 0.5 % BSA, 0.1 % cold fish gelatin) for 30 min, and exposed to the primary antibody at the proper concentration overnight at 4 °C. Grids were washed with PBS-BC (2 x 5 min), incubated with secondary antibodies conjugated with 10 nm gold particles (Nanoprobes), washed with PBS-BC (2 x 5 min), fixed for 5 min with 1 % glutharaldehyde, and stained with Nanovan 2011 (a Vanadium-based contrast that is milder than the NanoW 2018 and strongly recommended for the immunogold labelling). As primary antibody, the monoclonal anti-giantin, an integral membrane protein localised in the Golgi complex (Linstedt and Hauri, 1993) and universally accepted as a

Golgi marker, was used. Different dilutions of the antibody (1:100, 1:200, 1:500, 1:1000), with the correspondent control dilutions of an unrelated antibody (the monoclonal antibody against protein G of the vesicular stomatitis virus) were used. Secondary antibodies were tried at different dilutions (1:20, 1:50, 1:100, 1:500) in the presence or in the absence of the primary antibodies. In term of ratio signal/noise, the best dilution for the giantin antibody was 1:1000 and 1:50 for the secondary. In these samples, the membranes that were considered as Golgi based on morphological criteria, were strongly labelled by 10 nm gold particles, while labelling was absent in the samples treated with the anti-VSVg antibody or in the absence of primary antibody. Interestingly giantin was localised in the tubular part of the Golgi complex (see fig. 3.18). Other markers were used for the identification of the Golgi complex and the results are shown in table III.IV

Antigen	Labelling of stacks
GM130	yes
p115	yes
Rab7	no
Rab5	no

Table III.IV Immunogold labelling of Golgi stacks

Antibodies directed against the antigens listed in the table were used at a 1:1000 dilution, while the secondary gold-conjugated antibodies at 1:50.

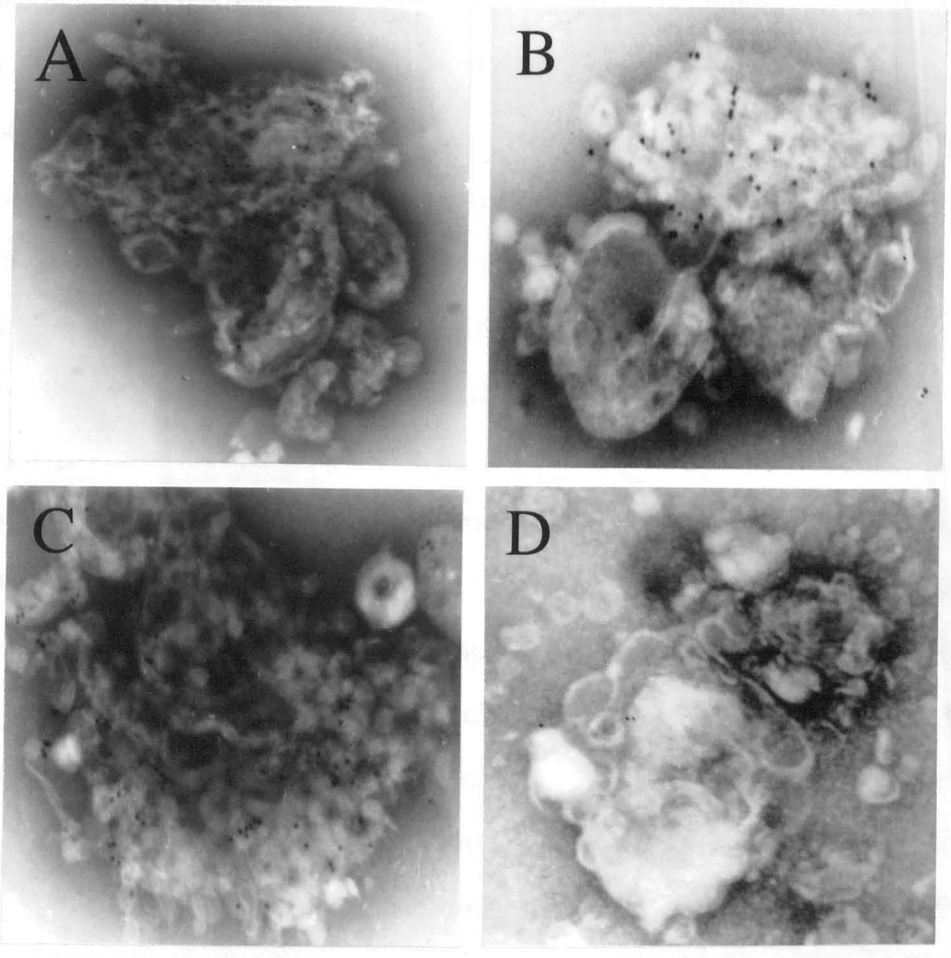

Fig. 3.18 Immunogold labelling of the Golgi stacks

Golgi membranes were labelled as described in the text by a monoclonal antibody against the Golgi marker giantin (A-C). Many gold particles are visible on the tubular membranes. Saccular-vacuolar membranes (possibly late endosomes) not labelled by the Golgi marker giantin (D). Magnifications: 30000 x (A, B, D), 50000 x (C).

3.4 Validation of the assay

3.4.1 Response to known biological stimuli

The third requirement for the assay is that Golgi membranes remain responsive to known stimuli. For this reason the effects of the fungal toxin BFA in inducing the tubular-reticular transformation of the Golgi apparatus (see introduction , 1.4.2.1), and of the non-hydrolizable GTP analogue GTP-γS (Melançon et al., 1987) known to induce the vesiculation of the Golgi apparatus, were tested. These experiments were essential not only to check the viability of the membranes but also to validate the reliability of the assay in detecting two different and oppositely directed processes.

3.4.2 Incubations with BFA

0.1 mg/ml of isolated Golgi membranes were incubated in the presence or in the absence of 30 µg/ml BFA as described in Cluett et al., 1993. The incubation mixture included 2 mg/ml of dialysed rat brain cytosol (prepared as described in the methods), 25 mM HEPES pH 7.4, 50 mM KCl, 2.5 mM $MgCl_2$, 1 mM ATP, 5 mM DTT, 10 mM CP and 10 U/ml CPK in a final volume of 10 µl. Incubations were carried out at 37°C for different times (5, 10, 20, 40, 60 minutes). At the end of the incubation, samples were processed for negative staining on whole-mount preparations and observed in the electron microscope. In the absence of BFA, Golgi membranes underwent slow but marked modification that will be described below. The addition of BFA, however, only slightly induced the appearance of tubular networks (fig. 3.19 A,B). To rule out the possibility that the negative staining technique, even if suitable for the visualisation of untreated membranes might not be appropriate for the observation after in vitro incubation, the experiment was repeated under the same conditions but processing the samples for the conventional electron microscopy using the thin sectioning procedure. Again, under these experimental conditions, BFA was not active in promoting the tubular reticular transformation of the isolated Golgi membranes (fig. 3.20 A).

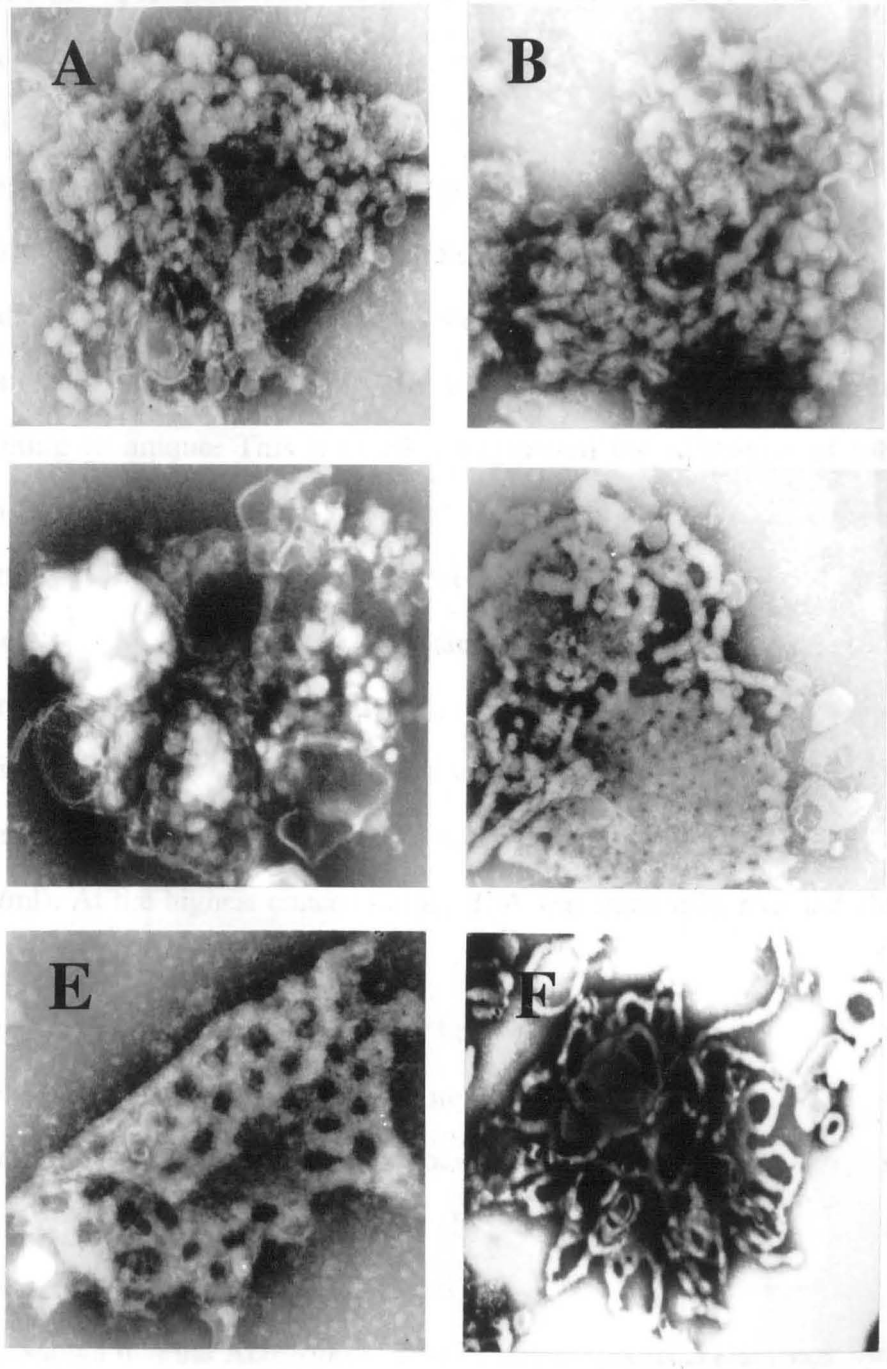

Fig 3.19 Effect of BFA on the morphology of the isolated Golgi membranes as visualised by the negative staining technique

Golgi membranes were incubated for 20 minutes with 2 mg/ml of dialysed (A,B) or non-dialysed rat brain cytosol (C-F) either in the absence (A, C) or in the presence of 30 μg/ml BFA (B, D-F). Samples were then fixed and processed for negative staining as described in the text (magnifications 50000 x).

The possibility that the toxin was inactive was ruled out by checking its activity in vivo.

Since the BFA effect is known to be strictly dependent on a cytosolic factor, a different protocol for preparing the rat brain cytosol was used. The rationale was that cytosol undergoes a step of dialysis which might result in the loss of an essential factor. Also there is some protein precipitation after this treatment, depending on the buffer used. For these reasons a crude non-dialysed cytosol was tested (see material and method). The experiment described above was repeated and the effect evaluated with the negative staining technique. This time BFA stimulated the formation of tubular reticular networks after 20 and 40 minutes. The percentage of stacks transformed into tubular reticular networks was quantified by systematic random sampling as described in material and method. 20 % of the stacks were almost completely tubular, with very clear fenestrations and a marked reduction in the number of associated vesicular profiles (fig. 3.19 C-E). This effect was maximised using higher concentrations of cytosol (4, 6, 8, and 10 mg/ml). At the highest concentration, BFA was more effective and almost 50 % of the stacks became tubular.

The lack of a full effect had already been described in vitro for BFA, most likely due to the dilution of some important factors. BFA had previously been shown to stimulate an endogenous mono-ADP-ribosyl-transferase with two cytosolic proteins as targets, the glycolytic enzyme GAPDH and the 50 kDa protein BARS (Di Girolamo et al., 1995, De Matteis et al., 1994). We have shown that the ADP-ribosylation of these proteins is necessary for the BFA effects. An essential cofactor for this reaction is the small molecule NAD^+. NAD^+ is known to be rapidly degraded in cytosolic extracts by several NAD^+-specific hydrolases and thus its concentration rapidly drops (A. Colanzi, Department of Cell Biology and Oncology, Consorzio Mario Negri Sud, unpublished observation). For this reason 500 μM NAD^+ was added to the reaction mixture. In the presence of NAD^+, BFA was much more active in promoting the tubular reticular transformation of 80% of the

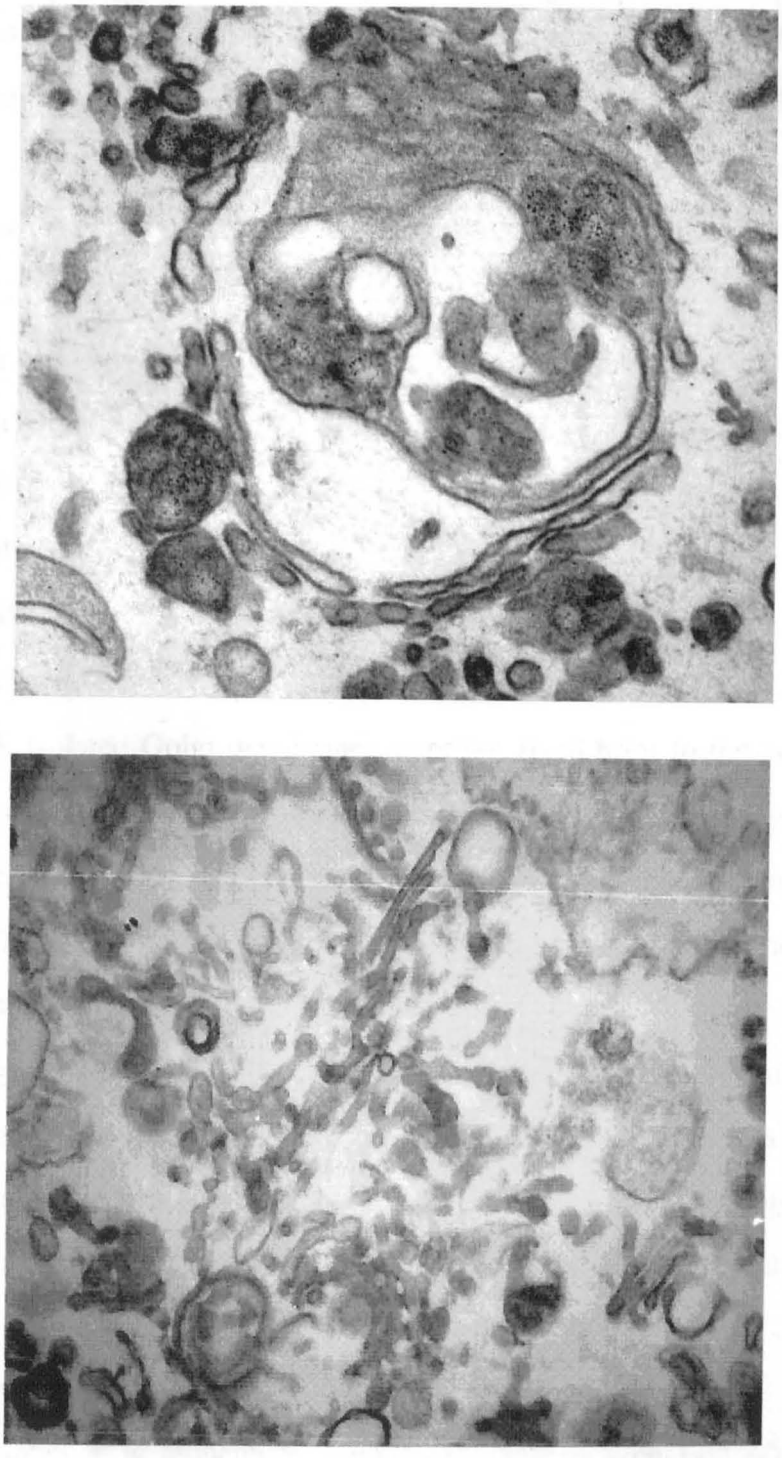

Fig. 3.20 Effect of BFA on the morphology of the isolated Golgi membranes as visualised by thin sections

Golgi membranes were incubated for 20 minutes with 2 mg/ml of dialysed (A) or non-dialysed (B) rat brain cytosol in the presence of 30 μg/ml BFA. Samples were then fixed and processed for the thin sectioning as described in material and methods. Magnifications: 100000 x (A), 75000 (B).

stacks. Similar pictures were obtained by using the conventional thin sectioning procedure (fig. 3.20 B). However while these data are in agreement with the general effect of BFA seen in Orci et al., 1991, a significant difference exists from the conclusions reached by Cluett et al., 1993. In this paper, Golgi membranes were incubated with BFA and both the thin sectioning procedure and the negative staining technique were used. In the thin sections the authors described a tubular reticular transformation, but with the negative staining technique they described the formation of long tubules reaching the surprising value of 7 μm. Under those conditions microtubules were not present and the discrepancy with the thin sections was explained as a technical limitation of the thin sectioning procedure. Indeed, this technique does not allow visualisation of long tubules, which have a high probability to be cut during sectioning. However, in Cluett et al., 1993, isolated Golgi membranes were not fixed prior to the negative staining and the mechanical stress generated during the air drying could easily deform the structures, pushing the membranes and generating long tubules. To test this possibility Golgi membranes were incubated under the conditions described above for 30 minutes, with or without the fixation step. Strikingly in the non-fixed samples treated with BFA, Golgi membranes protruded very long tubules up to 10 μm, but also in the absence of BFA the level of tubulation was high. These results show that the fixation step in the negative staining technique is essential for the reliability of the results (fig. 3.21).

3.4.3 Incubations with GTP-γS

Golgi membranes were incubated with the vesiculating agent GTP-γS in the presence of cytosol. Since high concentrations of cytosol were found to induce the vesiculation of the Golgi apparatus (Hidalgo et al., 1995 and see below), the isolated Golgi membranes were incubated in the absence or in the presence of 20-50 μM GTP-γS, for different times and with different concentrations of non-dialysed cytosol. Samples were fixed and processed for negative staining.

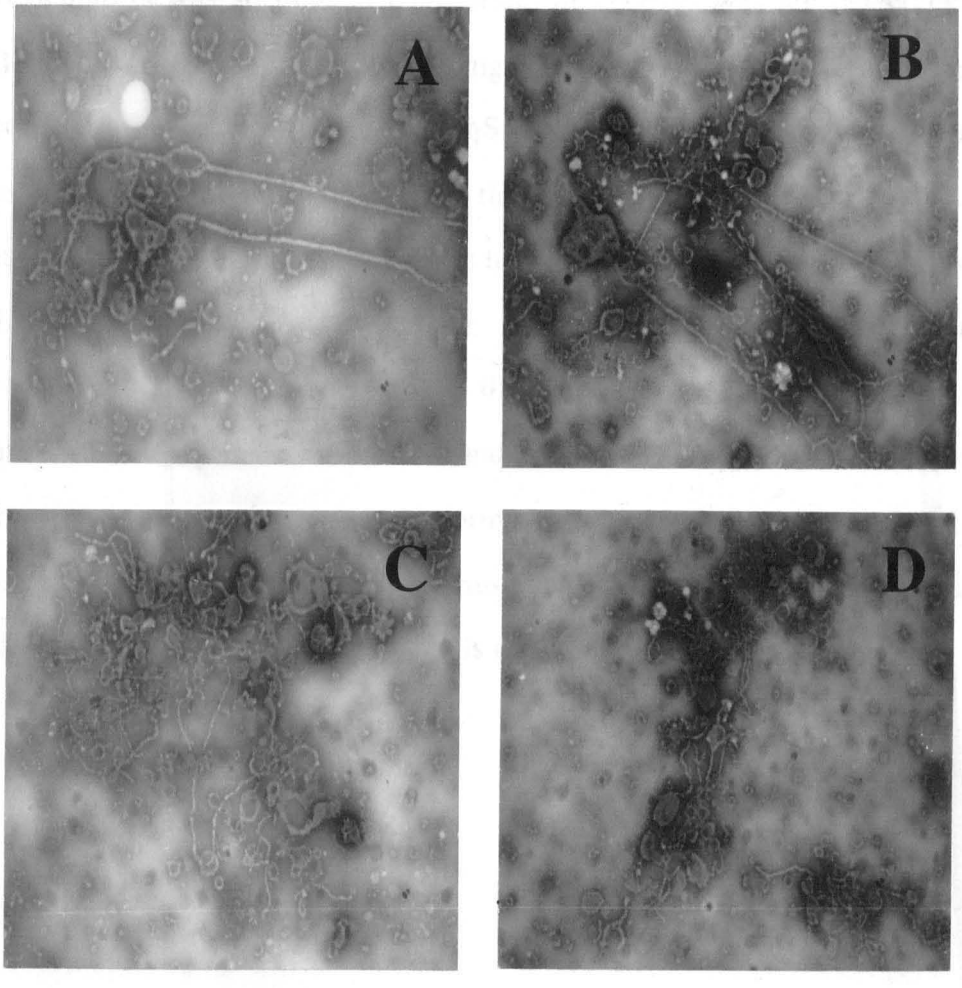

Fig. 3.21 Effect of BFA on the morphology of the isolated Golgi membranes as visualised by the negative staining technique without the chemical fixation

Isolated Golgi membranes were incubated for 30 minutes with 2 mg/ml of non-dialysed rat brain cytosol in the absence (C, D) or in the presence (A,B) of 30 μg/ml BFA. Samples were processed for the negative staining without the fixation step as described in material and method. Magnifications 12000 x.

Using the systematic random sampling procedure, Golgi stacks were scored for the presence of vesicles; Golgi stacks were considered "vesiculated" when the number of vesicles per stack was at least 2 fold higher than the number of vesicles associated with untreated membranes (at least 40 per stack). The % of vesiculated stacks was then calculated and is shown in fig. 3.22. When the concentration of cytosol was above 3-4 mg/ml, the level of vesiculation was so high that the effect of GTP-γS was not detectable. Below these concentrations (0.5 mg/ml of cytosol being the optimal concentration) the effect of GTP-γS was remarkable resulting in, as expected, a massive vesiculation of the Golgi stacks. As shown by other authors, vesicles bud mainly from the tubular-reticular part rather than from the cisternae. However, when the incubations were repeated under conditions in which GTP-γS induced the vesiculation but samples were not fixed and were processed for the negative staining, Golgi stacks were not found to vesiculate but rather the formation of tubules was observed (fig. 3.22). This observation further confirms that the negative staining technique carried out in the absence of fixation is not reliable.

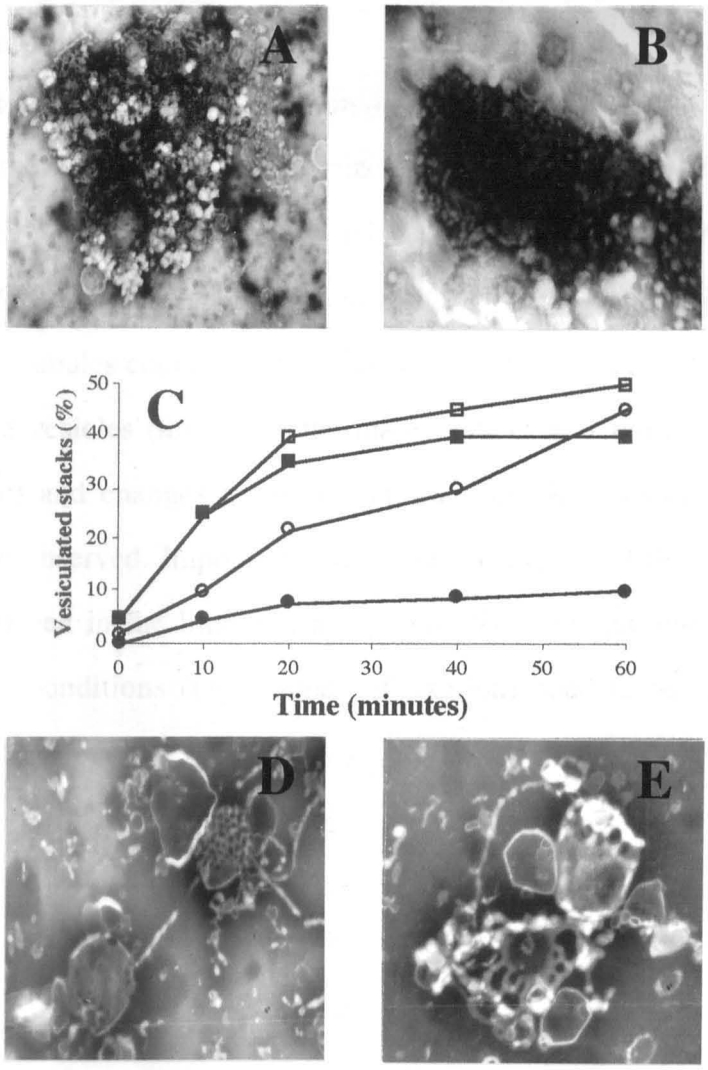

Fig. 3.22 Effect of GTP-γS on the morphology of isolated Golgi membranes as visualised by the negative staining technique

A,B. Golgi membranes treated for 20 minutes with 0.5 mg/ml non-dialysed rat brain cytosol in the presence of 20 μM GTP-γS (magnifications 30000 x) Samples were fixed and processed for negative staining as described in the text. C. Time course of the effect of GTP-γS. Golgi membranes were incubated with 3 mg/ml (squares) or 0.5 mg/ml (circles) either in the absence (filled symbols) or in the presence (empty symbols) of 20 μM GTP-γS. The percentage of vesiculated stacks was calculated as described in the text. This experiment was repeated three times with similar results. D, E Golgi membranes were incubated as described in A,B either in the absence (D) or in the presence (E) of 20 μM GTP-γS. Samples were processed for the negative staining without the fixation step as described in Cluett et al., 1993.

3.5 Discussion

A morphological assay based on negative staining of whole mount preparations was set up and optimized and could be applied for studying factors that control the formation and maintenance of the Golgi associated tubules. Golgi membranes could be visualised at high resolution, Golgi-associated tubules could easily be visualised and discriminated from Golgi-associated vesicles (this being the main limitation of the thin sectioning procedure) and changes in the morphology of Golgi membranes could readily be observed. Importantly, this work has revealed that some of the data described in the literature and using this technique under less well controlled conditions (i.e. absence of fixation) need to be carefully re-evaluated.

CHAPTER 4
SCREENING FOR CONDITIONS AFFECTING TUBULAR HOMEOSTASIS

4.1 Introduction

A key step in the determination of the physiological role of Golgi-associated tubules is the elucidation, at the molecular level, of the mechanisms which regulate their formation, maintenance and consumption. To get an insight into these mechanisms, different molecules (proteins, lipids, small molecules) were screened for their ability to modulate tubular homeostasis in isolated Golgi membranes. The assay that has been set up allows between 20 and 30 samples to be analyzed per day, giving a good chance to test several experimental conditions in a reasonable time. First, a preliminary screening was performed by checking molecules already described (more or less clearly in the literature) to have some influence on tubular structures (see introduction, section 1.4). Also general conditions were tested including the use of crude cytosolic extracts supplemented or depleted of some specific factors, and the stimulation of known metabolic pathways. At the end of this preliminary screening the most interesting molecules or conditions influencing the morphology of Golgi-associated tubules were investigated in a more detailed manner.

4.1 Effect of cytosolic extracts

4.1.1 Rat brain cytosol

Isolated Golgi membranes (0.1 mg/ml final concentration) were incubated at 37°C with non-dialysed rat brain cytosol prepared as described in the method. The reaction mixture included 25 mM Hepes pH 7.4, 50 mM KCl, 2.5 mM MgCl2, 1 mM ATP, 1mM GTP, 5 mM DTT, 10 mM CP and 10 U/ml CPK (incubation buffer) in a final volume of 10 µl. This condition will be referred to from now as "standard conditions". First a time course was carried out using different concentrations of cytosol (0.2, 2, 5, 10 mg/ml). As controls, Golgi membranes were incubated with the same concentrations of the bulk protein soybean trypsin inhibitor (STI, Calbiochem) solubilized in the buffer in which cytosol was stored (buffer A, see material and method). To take account of effects due to the different amounts of protein, Golgi membranes were also incubated with different concentrations of cytosol but adding STI to maintain the final concentration of the total protein at 10 mg/ml.

Samples incubated with STI were only slightly affected in their morphology at all the concentrations tested (fig. 4.1 D). However, in samples treated with 0.2 mg/ml cytosol, there was an initial increase in the surface occupied by the tubular networks (within 20-30 minutes), and later (40-60 min) vesicles were observed to bud from these tubules. Increasing the concentration of cytosol (both in the presence or in the absence of the complementing bulk protein) up to 2 mg/ml, caused Golgi membranes to undergo slow, yet evident, changes in morphology. Within 15 min, there was an increase (2-fold) in the number of vesicles and buds, most of which appeared to sprout from tubular domains (fig. 4.1 A and see fig. 3.17 A as control). The tubular networks on the other hand were slightly enlarged. Later (within 30 min), buds decreased markedly, and a profound breakdown of the tubular networks ensued, resulting in the formation of vesicular fragments of irregular sizes (50-90 nm), sometimes aligned in rows, and rare

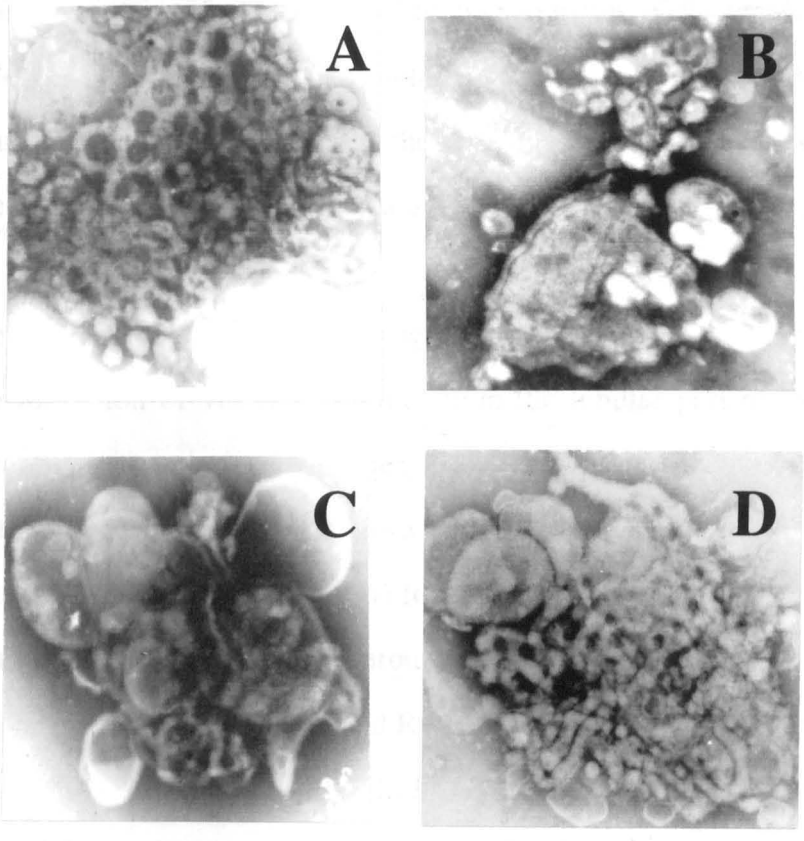

Fig. 4.1 Effect of rat brain cytosol on the morphology of the isolated Golgi membranes

Isolated Golgi membranes were incubated with 2 mg/ml non-dialysed rat brain cytosol for 15 (A), 30 (B) and 60 (C) min. A. Fenestrations and tubular networks are largely preserved, and several vesicles are visible. B. Tubular domains are markedly disrupted and a few vesicles, tubular fragments, and cisternal profiles are visible. C. Tubular domains are completely lost and only naked cisternae and fragments of saccular membranes are left. D. Isolated Golgi membranes incubated for 60 minutes with 10 mg/ml STI. Magnifications: 50000 x (A), 37500 x (B), 55000 x (C, D).

short tubules (fig. 4.1 B). At 60 min, only naked cisternae and partially fragmented saccular membranes were left (fig. 4.1 C). Increasing the amount of cytosol from 8 to 10 mg/ml accelerated fragmentation. The formation of vesicles occurred in 5 minutes and fragmentation was completed in 30-40 minutes (fig 4.2). Under these conditions the cytosol appears to contain a factor inducing the fragmentation of the tubular part of the Golgi apparatus and which is active at higher cytosolic concentrations and another factor that promotes the formation of tubules and which is active at the lower cytosolic concentrations.

4.1.2 ARF-depleted cytosol

One of the key events observed during the incubation with cytosolic extracts is the formation of vesicles budding from the tubular part of the Golgi apparatus. Golgi derived vesicles are formed by well characterized processes involving the binding to Golgi membranes of the small GTP-binding protein ARF (leading to the formation of the COPI-coated vesicles, Rothman, 1994), of the adaptor protein AP2 (leading to the formation of clathrin coated vesicles, Pearse and Robinson, 1990) or of p200 (leading to a new set of vesicles, Ladinski et al., 1994). The first two subpopulations of vesicles differ in their size, the former being 50-80 nm in diameter, the latter around 100 nm. The vesicles formed in the presence of cytosol mainly had a diameter compatible with the first class of vesicles, suggesting a possible role of ARF in the process of tubular fragmentation.

To address this point, isolated Golgi membranes were incubated with 2 or 10 mg/ml of ARF-depleted cytosol (see material and method) under standard conditions and for different times (20, 40 and 60 minutes). As expected the budding of vesicles was largely inhibited at both cytosolic concentrations and furthermore at earlier times (within 20 min) an increase in the surface area occupied by tubular networks and a tubular reticular transformation of some stacks (around 30%) was observed (fig 4.3 A,B). At longer times (40 minutes) fenestrations and tubules started to break down forming fragments of different sizes and shapes leading in the end to naked

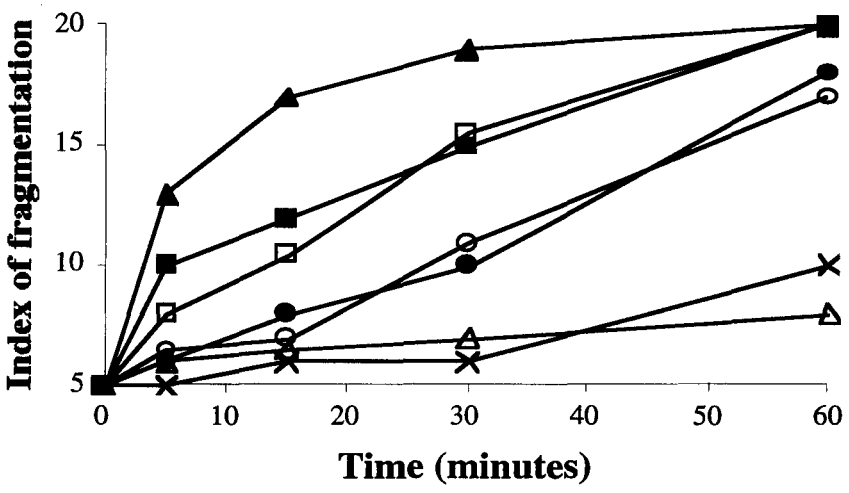

Fig. 4.2 Time course of the cytosol effects

Golgi membranes were incubated for the times indicated with: 2 mg/ml (crosses) or 10 mg/ml (empty triangle) STI, 0.2 mg/ml (plus), 2 mg/ml (filled circles), 5 mg/ml (filled squares), 10 mg/ml (filled triangle) non-dialysed rat brain cytosol, and the following combinations of non-dialysed rat brain cytosol and STI: 2/8 mg/ml (empty circles), 5/5 mg/ml (empty squares). The index of fragmentation was calculated as described in material and methods. This experiment was repeated three times with similar results.

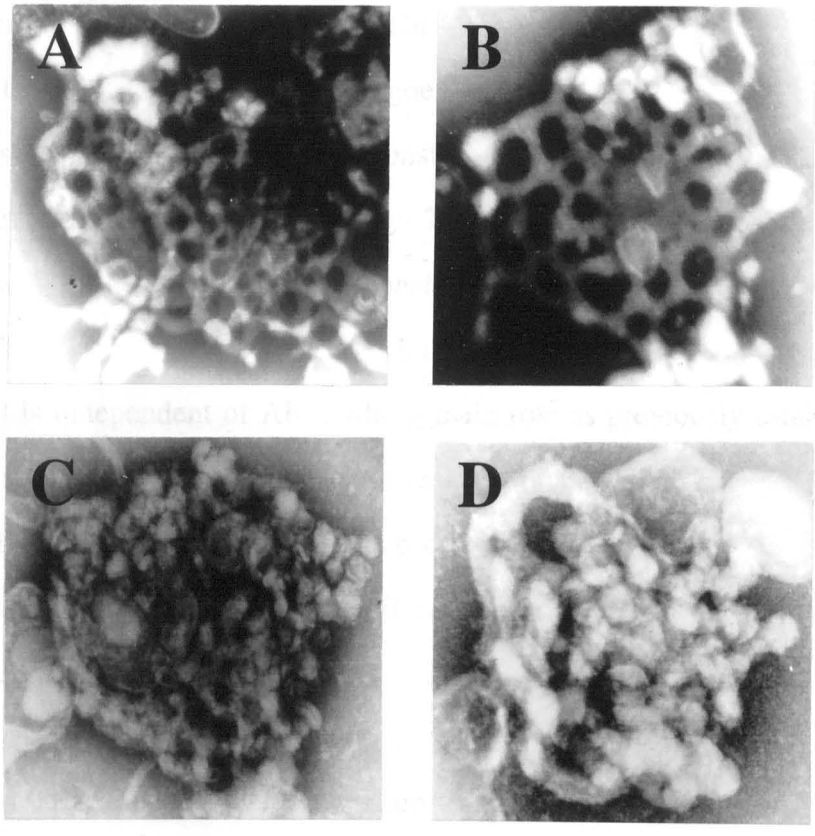

Fig. 4.3 Effect of ARF-depleted cytosol on the morphology of the Golgi apparatus

A-D Golgi membranes were incubated for 20 minutes in the presence of 10 mg/ml of ARF-depleted cytosol (A,B), ARF-depleted cytosol supplemented with the ARF containing fraction (C) or with 0.2 mg/ml of the chromatographically purified ARF (D). Samples were then processed for the negative staining and electron microscopy as described in material and methods. Magnifications 50000 x

cisternae as was the case with crude non-dialysed cytosol (fig. 4.1). As controls, Golgi membranes were incubated with control cytosol or with ARF-depleted cytosol supplemented with the ARF-containing fractions derived from the preparation of depleted cytosol, or with ARF that was chromatographically purified from bovine brain, or with the recombinant ARF1 (fig. 4.4). ARFs were added in amounts sufficient to restore their estimated endogenous levels (0.2 mg/ml see Happe and Weidmann, 1998). The recombinant myristoylated-ARF1 was added at a concentration 5 fold higher than the endogenous levels. This was done since in bacteria only 20 % of the expressed protein undergoes myristoylation and is functional (Weiss et al., 1989). All the reconstituted cytosols fragmented Golgi membranes as described previously. The vesiculation activity was fully restored, and the tubular reticular transformation was inhibited (fig. 4.3 and 4.4). These results suggest that the tubular fragmenting activity found in the cytosol is independent of ARF, whose main role as previously established seems to be limited to the budding of vesicles. However, ARF-depletion had a slight but significant effect in promoting the formation of tubular structures. This could be explained if vesicle formation was consuming the continuously forming tubules.

4.1.3 Coatomer-defective cytosol

Isolated Golgi membranes were incubated in standard conditions and for different times (20, 40, 60 minutes) with 2 mg/ml of cytosol (termed ldlf39-cytosol) prepared from CHO(ldlf) cells that were grown at the non-permissive temperature (39°C). Under these conditions the ε subunit of the coatomer complex is degraded and the whole complex is non-functional (Guo et al., 1994). As a control, cytosol derived from the same strain of cells but grown at the permissive temperature (ldlf34-cytosol) was used. Golgi stacks incubated with ldlf34-cytosol underwent the same changes in morphology observed with similar concentrations of the non-dialysed rat brain cytosol (fig 4.5 A). The formation of small vesicles, the

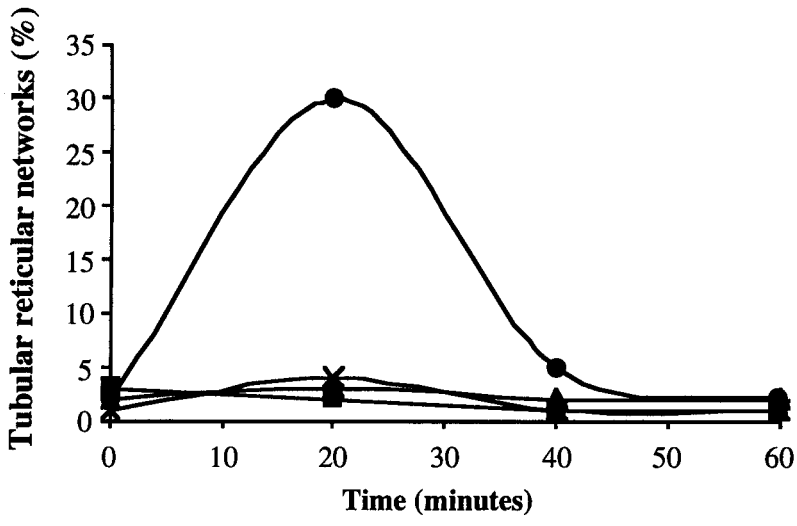

Fig. 4.4 Time course of the effects of ARF-depleted cytosol

Golgi membranes were incubated for the time indicated with 10 mg/ml of untreated cytosol (filled squares), ARF-depleted cytosol (filled circle), ARF-depleted cytosol supplemented with the ARF containing fraction (filled triangle) or with 0.2 mg/ml of the chromatographically purified ARF (crosses). The percentage of the Golgi stacks transformed into tubular reticular networks was evaluated as described in material and methods. The experiment was repeated three times with similar results.

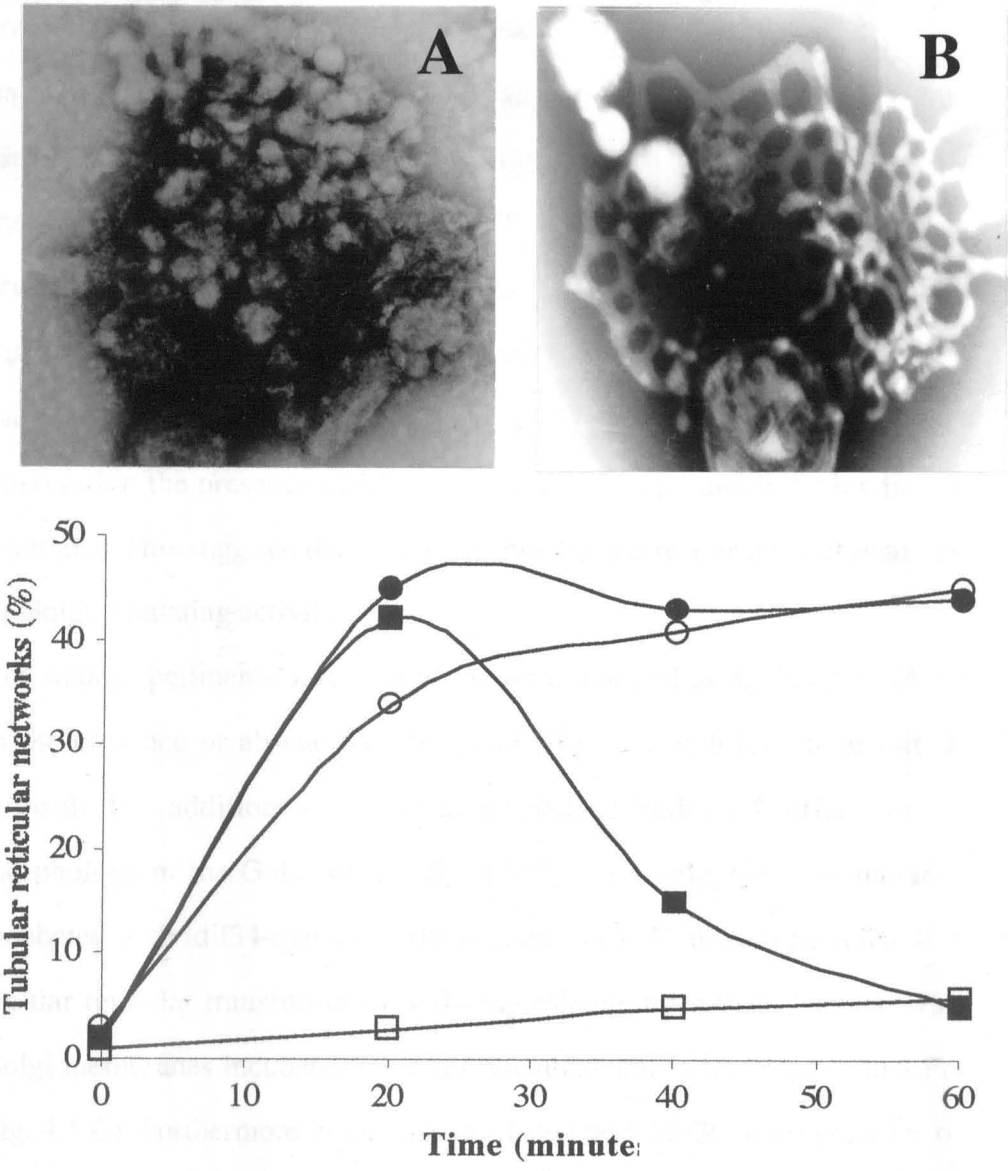

Fig. 4.5 Effect of the coatomer defective cytosol on the morphology of isolated Golgi membranes

Golgi membranes were incubated for 20 minutes in the presence of ldlf34- (A) or ldlf39-cytosol (B). Samples were processed for negative staining and electron microscopy. Magnifications: 60000 x. C. Time course of the effect of the coatomer defective cytosol. Golgi membranes were incubated for the time indicated in the presence of 500 μM NAD^+ with 2 mg/ml ldlf34 (empty symbols) or ldlf39 (closed symbols) cytosol either in the absence (squares) or in the presence (circles) of 30 μg/ml BFA. The percentage of Golgi stacks transformed into tubular reticular networks was evaluated as described in material and methods. The experiment was repeated two times with similar results.

fragmentation of the tubular structures and the concomitant appearance of naked cisternae followed the same kinetics described above. However, when Golgi membranes were incubated with the ldlf39-cytosol a tubular reticular transformation was observed within 20 minutes, with a parallel marked reduction in the formation of vesicular structures (fig 4.5.B). After 40 minutes, these tubular structures fragmented as previously described. The tubular reticular transformation of Golgi membranes was similar to that observed in the presence of BFA, which is known to inhibit the binding of coatomer. This suggests that coatomer could be a direct or indirect regulator of Golgi tubulating activity.

The same experiments described above were repeated using 500 μM NAD^+ in the presence or absence of 30 mg/ml BFA and with ldlf34- or ldlf39-cytosol. The addition of NAD^+ alone had no additional effect on the morphology of the Golgi stacks (fig. 4.5 C). Strikingly, Golgi membranes incubated with ldlf34-cytosol in the presence of BFA underwent a massive tubular reticular transformation indistinguishable from that observed with Golgi membranes incubated with ldlf39-cytosol but in the absence of BFA (fig. 4.5 C). Furthermore in samples incubated with ldlf39 in the presence of BFA the tubular networks were preserved for longer times and started to be fragmented only at 60 minutes. This finding suggests that: i) the fragmenting activity is independent of the COPI machinery; ii) the tubulating activity is greatly facilitated by the impairment of the COPI machinery, (this is in agreement with the data obtained with ARF-depleted cytosol as described above); iii) BFA inhibits the fragmenting activity present in the cytosolic extracts in a COPI independent way.

4.1.4 NADase-pretreated cytosol

The nucleotide NAD^+ is an essential component of the machinery regulating the formation of tubules, at least in the presence of BFA. It has been shown that NAD^+ is an important cofactor for BFA-dependent ADP-ribosylation and that the substrate of this reaction could be important in the regulation of tubular growth (Mironov et al., 1997). This raises an

interesting question as to what the role, if any, is of NAD^+ in the absence of BFA. The addition of 500 μM NAD^+ to the ldlf-34 cytosol was ineffective. Since this could be a peculiarity of that particular cytosolic extract, Golgi membranes were incubated for different times (20, 40, and 60 minutes) and under standard conditions with 2 mg/ml rat brain cytosol in the presence of increasing concentrations of NAD^+ (1, 10, 100, 500, 5000 μM). The kinetics of vesiculation and of fragmentation were only slightly accelerated by increasing the NAD^+ levels (fig. 4.6). Non-dialysed cytosol contains micromolar levels of NAD^+, enough to hide the effects of exogenous additions (M.G. Silletta, Department of Cell Biology and Oncology, Consorzio Mario Negri Sud, unpublished observation). For this reason NAD^+ was depleted from non-dialysed cytosol using a specific NADase. This enzyme was used since it removes NAD^+ much more effectively than dialysis (even after 24 h of dialysis NAD^+ is present at 100 nM concentration, M.G. Silletta, Department of Cell Biology and Oncology, Consorzio Mario Negri Sud, unpublished observation) and is more specific. Golgi membranes were incubated for different times (20, 40 and 60 minutes) and in standard conditions with 2 mg/ml cytosol that has been pretreated for 15 minutes at 37°C with 1 U/ml of a NADase from Neurospora Crassa. As controls, either a non-dialysed cytosol pretreated with the NADase storage buffer (PBS) or the NADase appropriately diluted in the buffer in which cytosol is stored (see material and methods) were used. NADase alone did not have any noticeable effect on the structure of the Golgi apparatus and the mock-pretreated cytosol behaved as previously described. Strikingly Golgi membranes incubated with the NADase-pretreated cytosol underwent a massive and extensive tubulation starting from 20 minutes (fig. 4.7 A, B). Only at longer times (60 minutes) did Golgi tubules start to be fragmented. To check if the effect of the NADase was specific, cytosol was pretreated with 1 U/ml NADase in the presence of 500 μM of cybacron blue, a well known inhibitor of NAD^+

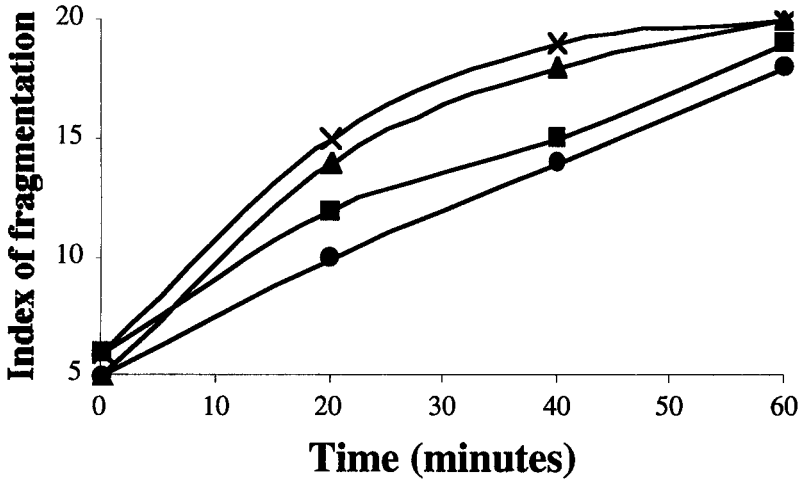

Fig. 4.6 Effect of NAD^+ on the morphology of isolated Golgi membranes

Time course of the effect of NAD^+. Golgi membranes were incubated for the time indicated with 2 mg/ml non-dialysed cytosol with no additions (filled circles), supplemented with 10 μM (filled squares), 500 μM (filled triangles), 5000 μM (crosses) of NAD^+. Samples were processed for negative staining and electron microscopy and the index of fragmentation was calculated as described in material and methods. The experiment was repeated two times with similar results.

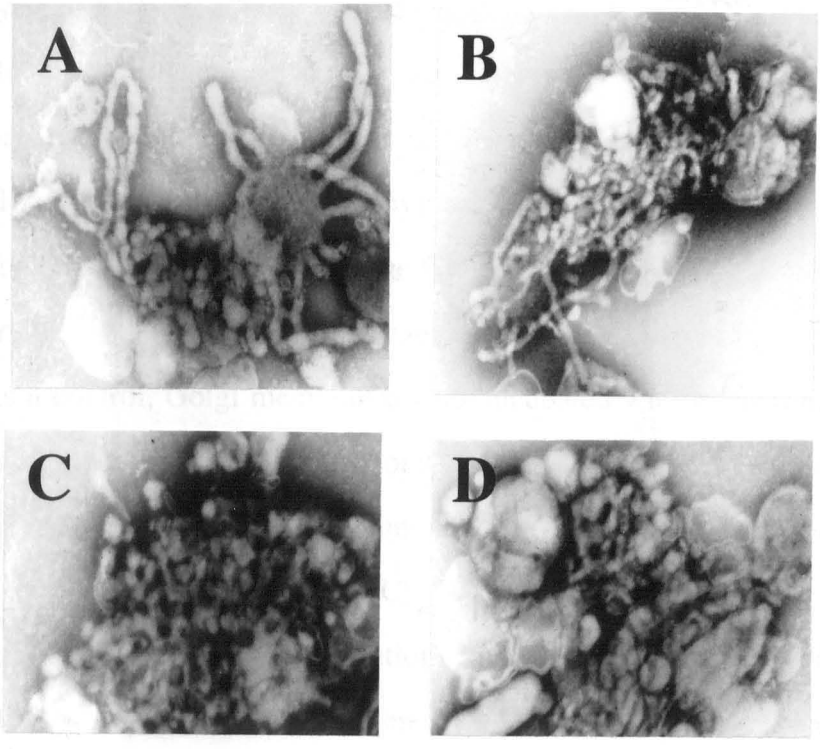

Fig. 4.7 Effect of NAD^+ depletion on the morphology of the isolated Golgi membranes

Golgi membranes were incubated for 20 minutes with 2 mg/ml rat brain cytosol pretreated with 1 U/ml of N.Crassa in the absence (A, B) or in the presence of 500 μM cybacron blue (D), or with the buffer in which cytosol is stored (buffer A, see material and methods) pretreated with 1 U/ml N. Crassa (C). Samples were then processed for the negative staining and electron microscopy as described in material and methods. Magnifications: 30000 x (A), 20000 x (B), 30000 x (C), 44000 (D).

glycohydrolases (Kim et al., 1993). This treatment strongly inhibited the tubulating activity (fig. 4.4, D). This result would be consistent with a model in which NAD^+ is an essential component of the tubulating machinery or alternatively a factor regulating the fragmenting machinery. However it is not possible to rule out at this stage whether NADase affects NAD^+ or another metabolite with a similar structure.

4.1.5 BARS-depleted cytosol

The observation that BFA inhibited the fragmentation of the tubular structure associated with the Golgi and the previous indication that ADP-ribosylation played a role, suggested that the substrates of ADP-ribosylation should be investigated. Isolated Golgi membranes (0.1 mg/ml) were incubated under standard conditions and for different times with 2 mg/ml of a BARS-immunodepleted cytosol. Within 20 minutes vesicles were seen to bud from the tubular domains of the Golgi stacks. Golgi tubules remained preserved and by 60 minutes they were only slightly damaged (fig 4.8 A, C). As a control, Golgi membranes were incubated with a mock-depleted cytosol exactly under the same conditions (fig. 4.8 B, C). This cytosol fragmented the Golgi tubular domains in a way indistinguishable from non-dialysed untreated cytosol (fig. 4.8 C).

To test if the lack of fragmentation activity might be due to BARS, membranes were incubated for different times with BARS-depleted cytosol supplemented with 0.3 (which corresponds to the endogeneous level), 1, and 3 μg/ml of the chromatographically purified BARS (Di Girolamo et al., 1995). BARS-depleted cytosol supplemented with 0.3 μg/ml of BARS regained its fragmenting activity, while the addition of further amounts of the protein accelerated the kinetics of fragmentation (fig 4.8 C). However, chromatographically-purified BARS is an enriched fraction that contains several other cytosolic proteins and the experiment was repeated, therefore, supplementing the BARS-depleted cytosol with recombinant GST-BARS expressed in bacteria. Recombinant GST purified using the same procedure as BARS, was used as control.

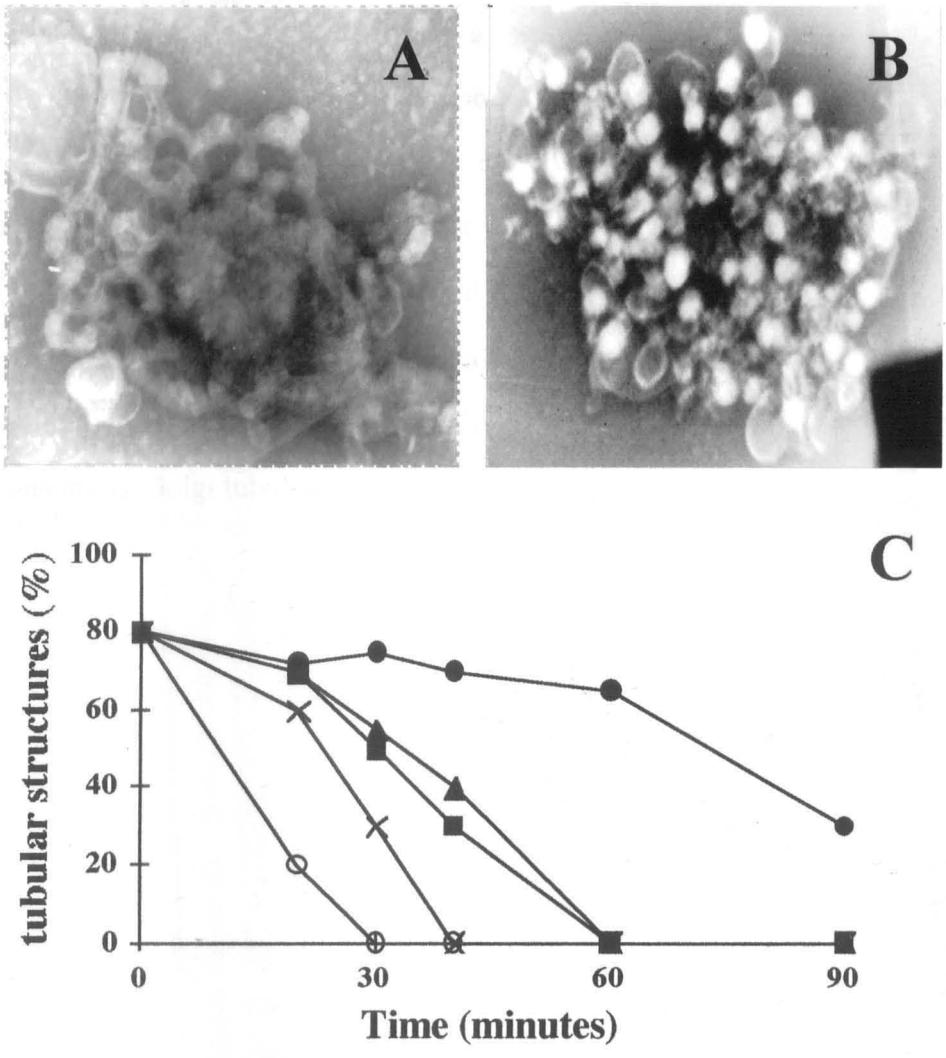

Fig. 4.8 Effect of BARS-depleted cytosol on the morphology of isolated Golgi membranes

Golgi membranes were incubated for 60 minutes with 2 mg/ml of either a BARS-depleted cytosol (A) or a mock-depleted cytosol (B). Samples were then processed for negative staining and electron microscopy. Magnifications 50000 x. C. Time course of the effect of BARS-depleted cytosol. Golgi membranes were incubated for the times indicated with 2 mg/ml BARS-depleted cytosol (filled circles), mock-depleted cytosol (filled triangles), BARS-depleted cytosol supplemented with 0.3 μg/ml (filled squares), 1 μg/ml (crosses), 3 μg/ml (empty circles) of chromatographically purified BARS. Samples were processed for negative staining and the percentage of the Golgi stacks with a preserved tubular network was calculated as described in the material and methods. The experiment was repeated three times with similar results.

This time the concentration of BARS required for recovering the fragmenting activity was 3 μg/ml, and just as with the purified protein, higher concentrations of recombinant GST-BARS accelerated fragmentation. GST even at higher concentrations was not active in this assay (fig. 4.9). The 10 fold less activity of the recombinant protein is not surprising since the protein expressed in bacteria lacks the post-translational modifications usually occurring in eukaryotes. Thus this experiments strongly indicates that BARS is a component of a cytosolic machinery consuming Golgi tubules.

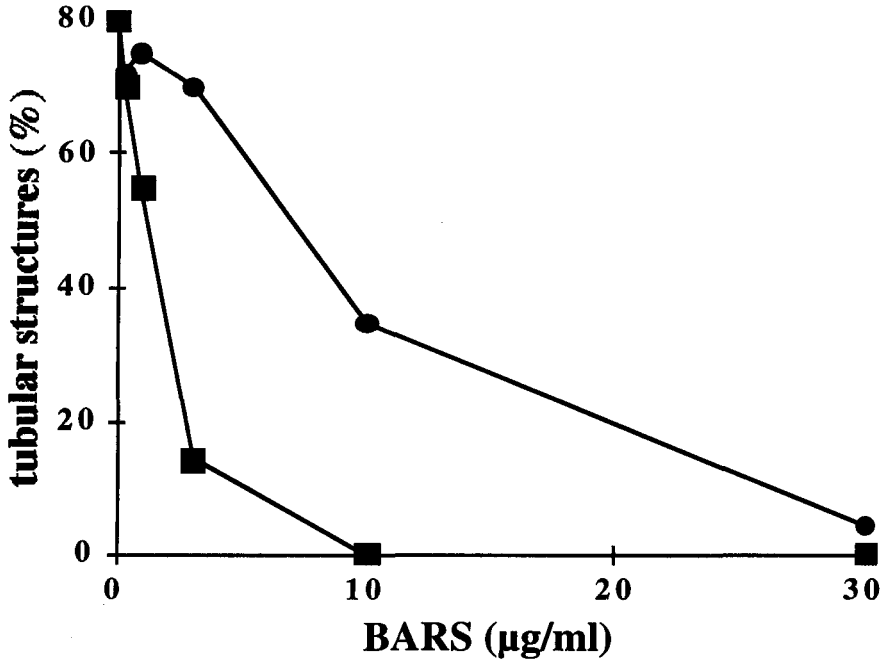

Fig. 4.9 Comparison between the activity of chromatographically purified BARS and recombinant GST-BARS in reconstituting the cytosol fragmenting activity

Golgi membranes were incubated for 30 minutes with 2 mg/ml of BARS-depleted rat brain cytosol supplemented with the indicated concentrations of either chromatographically purified BARS (squares) or recombinant GST-BARS (circles). Samples were processed for negative staining and electron microscopy as described in material and methods. The percentage of Golgi stacks having a preserved tubular network was calculated as described in material and methods. The experiment was repeated two times with similar results.

4.2 Modulators of lipidic metabolism

4.2.1 Effect of phospholipases A_2, C and D

Data in the literature suggest that lipid modifying enzymes are crucial components in the machinery regulating tubular homeostasis, though this is based mainly on the use of pharmacological inhibitors (see introduction; 1.4.2.6). Thus Golgi membranes were incubated under various conditions in the presence of commercially available phospholipases, specifically with a phospholipase A_2 (from bee venom, Apis Mellifera), a phospholipase D (PLD, from Streptomyces Chromofuscus) and a PI-specific phospholipase C (from Bacillus Cereus). Golgi membranes were incubated under standard conditions for 20 or 40 minutes with different concentrations (0.2, 2, 20, 200 U/ml) of PLA2. The experiment was carried out in the presence of 10 μM calcium (needed for the activity of the enzyme; Mayer and Marshall, 1993), and in the presence or in the absence of 2 mg/ml non-dialysed cytosol. In the absence of cytosol Golgi membranes were seen to be covered by blebs on both the tubular domains and the saccular part, but the structures were substantially preserved (fig. 4.10). Strikingly, in the presence of cytosol, PLA_2 strongly accelerated in a dose dependent manner the fragmentation of the Golgi associated tubules (below 2 U/ml) and further promoted the fragmentation of Golgi cisternae (above 2 U/ml) (fig. 4.10 A). This finding is in contrast to the data suggesting a role for PLA_2 in stimulating tubulation. The discrepancy could be due to the use of a non-physiological PLA_2.

Golgi membranes were then incubated with different concentrations of PLD (0.2, 2 and 20 U/ml) either in the presence or in the absence of 2 mg/ml of non-dialysed rat brain cytosol. Incubations were carried out for different times (20 and 40 minutes) under standard conditions in the presence of 1 mM free calcium (required for PLD activation). Golgi membranes both in the presence and in the absence of cytosol were observed to undergo a massive fragmentation in both tubular and saccular domains

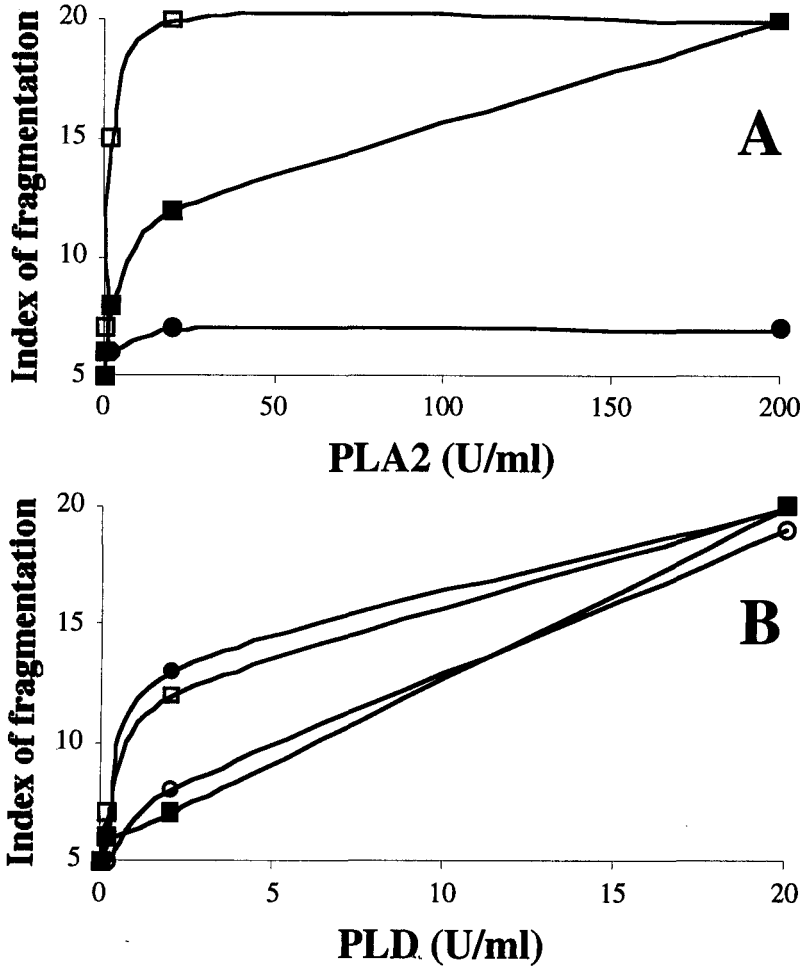

Fig. 4.10 Effect of exogenous addition of PLA_2 and PLD on the morphology of the isolated Golgi membranes

Golgi membranes were incubated with increasing concentrations of either a PLA_2 from Apis Mellifera (A) or a PLD from Streptomyces Chromofuscus (B) for 20 (filled symbols) or 40 (open symbols) minutes either in the presence (squares) or in the absence (circles) of rat brain cytosol (2 mg/ml). Samples were processed for negative staining and the index of fragmentation was calculated as described in material and methods. The experiment was repeated three times with similar results.

(fig. 4.10 B). Fragmentation was prominent at 40 minutes starting from 2 U/ml and at 20 minutes using 20 U/ml. Finally Golgi membranes were incubated with different concentrations of a PI-PLC (0.075, 0.75, 7.5 U/ml) for 20 or 40 minutes, both in the presence and in the absence of 2 mg/ml rat brain cytosol. This treatment had no effect in altering the normal morphological changes induced by the non-dialysed cytosol.

4.2.2 Acyl Coenzyme As

AcCoAs are some of the major substrates involved in lipid synthesis and remodelling as described in the introduction (1.4.3.3). Golgi membranes (0.1 mg/ml) were incubated in the absence of cytosol under standard conditions with a series of saturated AcCoAs (20 μM) having different chain lengths (C 0, C 2:0, C 6:0 , C14:0, C:16:0, C18:0, C20:0) or with the reaction mixture alone.

The incubations were carried out for different times (5, 10, 20, 30 minutes). While Golgi membranes incubated with the buffer alone or with the C 2:0, C 6:0 and C16:0 did not show any significant change in their morphology, the C 0, C14:0, C18:0 and C 20:0 species did have an effect. Fenestrations started to grow forming very large loops, some of which were broken leading to the generation of 2 long tubules reaching up to 1 μm in length (fig 4.11 A, B). Some tubules were seen to elongate from the cisternae with no clear indications that they were derived from the breaking down of pre-existing fenestrations. Some stacks were totally transformed into tubular reticular networks while others started to vesiculate. At longer times, tubules were converted into vesicles by a fission mediated mechanism. Several constrictions appeared along the tubules which sometimes acquired a necklace-like structure. In other cases rows of vesicles seemed to be linked by subtle bridges (fig. 4.11 C).These morphological changes were fast for stearoyl-CoA (C18:0) and arachidoyl-CoA (C 20:0) and slow for myristoyl-CoA (C14:0) and CoA (fig 4.12 A).

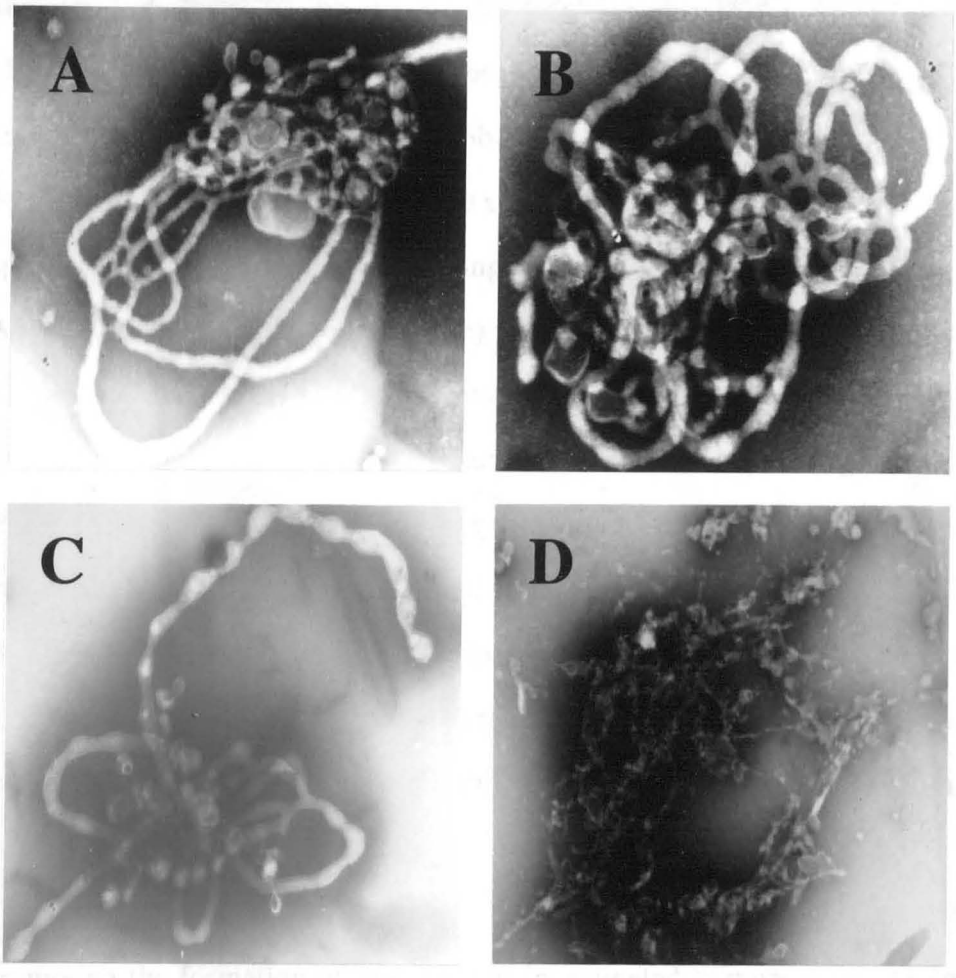

Fig. 4.11 Effect of stearoyl-CoA on the morphology of the isolated Golgi membranes

Golgi membranes were incubated for 10 (A, B) or 30 (C, D) minutes with 20 μM stearoyl-CoA (A, B, C) or with 500 μM SDS (D). Samples were processed for negative staining and electron microscopy as described in material and methods. Magnifications: 37500 x (A), 52000 x (B), 31000 x (C), 40000 x (D)

The possibility that the effects described above were due to a detergent-like action of the AcCoA or to an increase in the amount of total lipids, was ruled out by several approaches. First, Golgi membranes were incubated with 2 mM Triton X-100 or 500 μM SDS i.e. above their CMCs (1.7 mM and 230 μM, respectively; see Kragh-Hansen et al., 1998). Their major effect was to solubilize the membranes leading to thread-like structures or amorphous membranes, but not to tubulation or vesiculation (fig. 4.11 D). Furthermore some of the components of the reaction mixture were omitted: specifically, ATP and its regenerating system were not included, and an ATP scavenger (Hexokinase-glucose) was added (Cluett et al., 1993). The various active AcCoAs were not affected, with one exception of CoA which was no longer able to promote the tubulation/fission of the Golgi tubules (fig 4.12 B). Adding back ATP along with a regenerating system restored the effect of CoA but only when used at millimolar concentration (fig 4.12 B). This is compatible with the resynthesis of AcCoA by ATP-dependent ligases, which use the free fatty acids present in the lipidic bilayer as substrates and are known to be present in microsomal fractions (Bar-Tana and Shapiro, 1975).

The effect of stearoyl-CoA, being the most potent of the AcCoAs in promoting the formation of tubules, was investigated in more detail. Golgi membranes were incubated in standard conditions for 10 minutes in the presence of increasing concentrations of C 18:0 (2, 10, 20, 200 μM) and its activity in promoting Golgi tubulation was measured. Starting from the lowest concentration a tubulating activity was observed, becoming maximal at 10 μM. At the highest concentration, Golgi tubules were completely fragmented and the cisternae were covered in a series of vesicular structures. Golgi membranes were also incubated for different times (2.5, 5, 10, 20 minutes) as described above with 10 μM C18:0, both in the absence and in the presence of 1 mM GTP. While in the presence of GTP, the tubulating effect was visible at 2.5 minutes, being maximal at 5 minutes, in the absence of the nucleotide it was significantly inhibited (fig. 4.12 B). These finding.

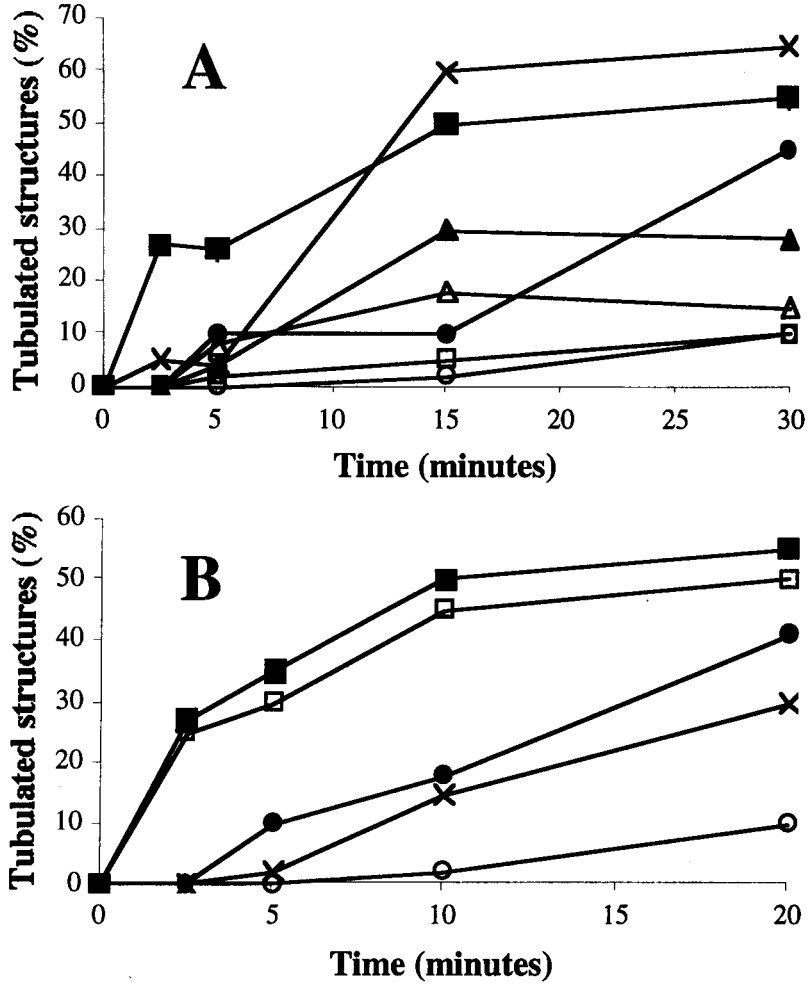

Fig. 4.12 Characterization of the effect of acyl-CoAs on the morphology of isolated Golgi membranes

A. Golgi membranes were incubated for the indicated times with the reaction buffer (empty squares) or with 20 μM of CoA (filled circles), acetyl-CoA (empty circles), myristoyl-CoA (filled triangles), palmitoyl-CoA (empty triangles), stearoyl-CoA (filled squares), arachidoyl-CoA (crosses). B. Golgi membranes were incubated for the indicated times with 10 μM stearoyl CoA (squares and crosses) or with 20 μM CoA (circles). in the presence (filled symbols) or in the absence (empty symbols) of ATP and a regenerating system, or in the absence of GTP (crosses). To efficiently scavange ATP, 20 U/ml of Hexokinase from baker's yeast (Sigma) and 10 mM Glucose were added. Samples were processed for negative staining and the percentage of tubulated stacks was calculated as described in material and methods. The experiments were repeated three times with similar results.

indicate that AcCoAs are very interesting molecules that play an important role in controlling the behaviour of Golgi associated tubules.

.

4.3 Calcium and the βγ subunits of heterotrimeric G-proteins

Calcium has been implicated in several key cellular processes and it is also known to activate enzymes such as phospholipases and calmodulin that have been implicated in the formation of Golgi associated tubules. To examine its effect on the morphology of the Golgi apparatus, isolated Golgi membranes were incubated in the presence or absence of 2 mg/ml non-dialysed cytosol for 20 minutes with increasing concentration of Ca^{++}, using an EGTA-buffering system. These buffers were calibrated at pH 7.4, with 1 mM ATP, 1 mM GTP, and 2.5 mM free Mg^{++} for having the following concentrations of free calcium: 0.01, 0.1, 1, 10, 100, 1000 μM. Calculations were performed using a specific computer program (Calcium, V. I.I from Chang, Hsieh and Dawson). In the absence of cytosol, the morphology of the Golgi membranes did not change at any of the calcium concentrations tested. In the presence of cytosol a concentration dependent increase in fragmentation of the tubular domain of the Golgi apparatus was observed (fig. 4.13 A), whereas in the absence of calcium, Golgi membranes were only vesiculated as previously described (fig. 4.13 A).

The possibility that the calcium- and cytosol- dependent fragmentation observed was due to a non specific effect, such as protease activity, was checked. Some cytosolic proteases are known to be activated in the presence of micromolar calcium levels and for this reason the same experiment described above was repeated in the presence of a cocktail of protease inhibitors (2 mg/ml Aprotinin, 0.5 μg/ml Leupeptin, 2 μM Pepstatin, 0.5 mM o-Phenantroline, 1 mM PMSF). Under these conditions the fragmentation still occurred and at the same calcium levels and in a way totally indistinguishable from the absence of the protease inhibitors (fig. 4.13 A).

Another factor recently implicated in the fragmentation of the Golgi tubular domain is the βγ complex of heterotrimeric G-proteins (Jamora et al., 1997). Golgi membranes were incubated for 20 minutes with 20 nM of the βγ

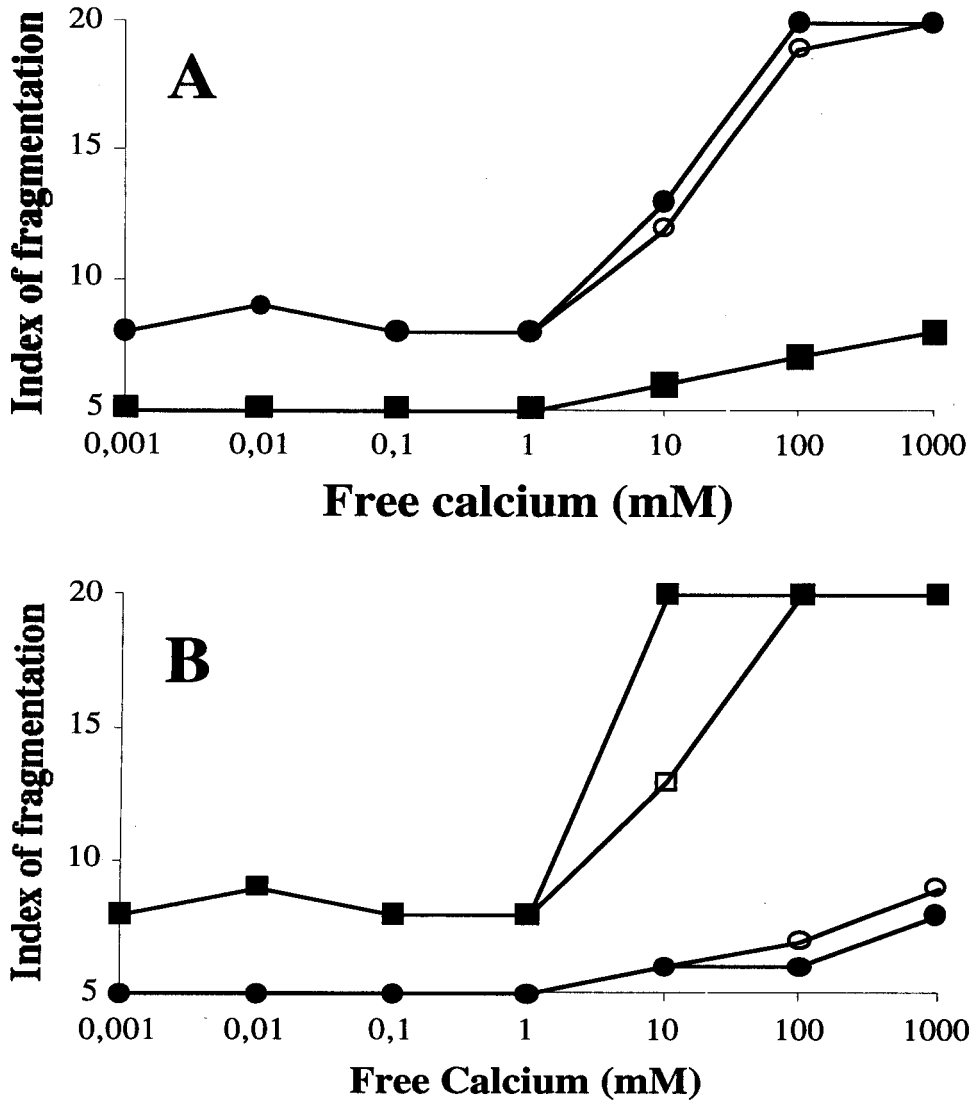

Fig. 4.13 Effect of calcium and the βγ subunits of heterotrimeric G proteins on the morphology of isolated Golgi membranes

A. Golgi membranes were incubated for 20 minutes with different concentration of free calcium in the absence (squares) or presence (circles) of 2 mg/ml rat brain cytosol in the absence (empty symbols) or presence (filled symbols) of a cocktail of protease inhibitors. B Golgi membranes were incubated for 20 minutes with different concentration of free calcium in the absence (circles) or presence (squares) of 2 mg/ml rat brain cytosol either in the presence (filled symbols) or absence (empty symbols) of 20 nM of chromatographically purified βγ subunits isoalted from trasducin. Samples were processed for negative staining and the index of fragmentation was calculated as described in material and methods. The experiments were repeated two times with similar results.

subunit , purified from bovine brain, in the presence or absence of cytosol. The addition of βγ did not affect the morphology of the Golgi membranes in the absence of cytosol nor did it affect the cytosol-dependent vesiculation (fig. 4.13 B). The βγ subunits are known to activate several enzymes including PLA2 and the PLC, the former has already been suggested to regulate Golgi-associated tubules. Since both enzymes require calcium for their activity Golgi membranes were incubated as described above in the absence or in the presence of increasing concentrations of calcium (0.01, 0.1, 1, 10, 100, 1000 μM). Above 10 μM calcium and in the presence of cytosol, βγ slightly but significantly enhanced the fragmentation of Golgi associated tubules (fig. 4.13 B). To determine if the βγ subunits play a role in this activity other approaches are required.

4.4 Discussion

The result of this initial screening was very useful for establishing the direction to follow. Each of the single findings are rather complex but the most promising condition is the effect of the protein BARS in fragmenting the tubular domain. This effect is very specific for Golgi associated tubules and molecular tools such as purified and recombinant protein, antibodies, and immuno-depleted cytosol are available.

CHAPTER 5
THE EFFECT OF BARS ON TUBULAR HOMEOSTASIS

5.1 Introduction

The effects of BARS on Golgi associated tubules was examined using BARS-immunodepleted cytosol, purified native or recombinant GST-BARS, and anti-BARS antibodies. An accurate morphological characterisation of the Golgi stacks and their associated tubules during and after the action of BARS was obtained and the released membranes were examined by EM. The effect of BARS was also analyzed in permeabilized cells. Finally, the cofactors and the molecular mechanism by which BARS exerts its fragmenting activity were analyzed in detail.

5.2 Characterization of BARS effect on Golgi tubules

5.2.1 Addition of BARS-enriched cytosol

Isolated Golgi membranes were incubated in standard conditions (see section 4.1) and for different times (5, 15, 20, 30, 40 minutes) with 2 mg/ml of non-dialysed cytosol in the presence or absence of 3 μg/ml of chromatographically purified BARS (10 times the endogenous levels). Samples were further processed for negative staining (fig. 5.1). After 5 minutes, vesicles were seen to bud from Golgi tubules both in the presence or absence of BARS. At 15 and 20 minutes and in the absence of BARS, tubules were still preserved and the number of vesicles only slightly increased. In the presence of BARS, tubules were almost totally fragmented and vesicles of different diameters were formed (fig 5.1 B, C). At 30 minutes the fragmentation of the tubules started to occur even in the absence of BARS and at 40 minutes, samples incubated either in the presence or in the absence of BARS were indistinguishable (fig. 5.1 C). At 20 minutes the diameters of the vesicles were compared by stereology in the presence and absence of BARS. In the absence of BARS vesicles were mainly 60-70 nm in diameter, while in the presence of the protein, the diameters were larger and also fragments exceeding 100 nm were formed (fig. 5.2).

Recombinant GST-BARS was also tested in incubations at 20 minutes. Golgi membranes were incubated with 2 mg/ml of non-dialysed cytosol in the presence of different concentrations of GST-BARS (3, 30, 100 μg/ml) or, as control, with equal concentrations (on a molar basis) of recombinant GST (1, 10, 30 μg/ml). Recombinant GST-BARS was at least 10 fold less effective than the chromatographically purified protein (fig. 5.3). This could be due to the absence in recombinant GST-BARS of post-translational modifications. The effects of BARS on Golgi stacks were also examined using conventional resin embedding and thin sectioning. Golgi membranes were incubated as described above for 15 or 40 minutes (using

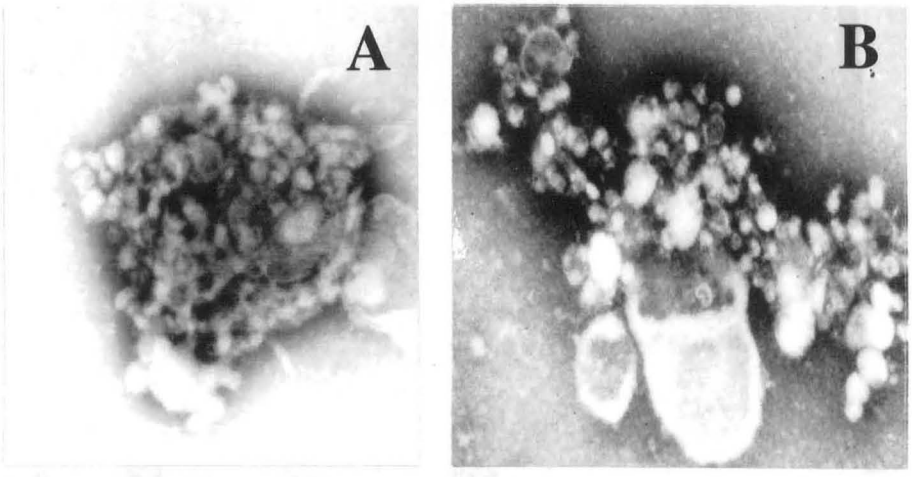

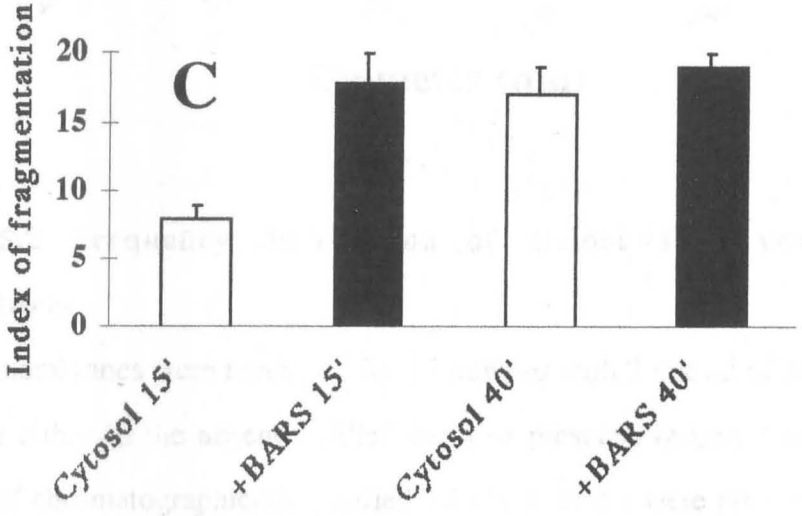

Fig. 5.1 Effect of BARS-enriched cytosol on the morphology of isolated Golgi membranes as visualised by negative staining

A, B Golgi membranes were incubated in standard conditions for 15 minutes with 2 mg/ml of rat brain cytosol either in the absence (A) or presence (B) of 3 μg/ml of chromatographically purified BARS. Samples were processed for negative staining and electron microscopy as described in material and methods. Magnifications: 50000 x (A) and 31000 x (B). C Golgi membranes were incubated in standard conditions as indicated, and processed for negative staining and electron microscopy. The index of fragmentation was calculated as described in material and methods. Values are means ± S.D.s of triplicates. The experiment was repeated four times with similar results.

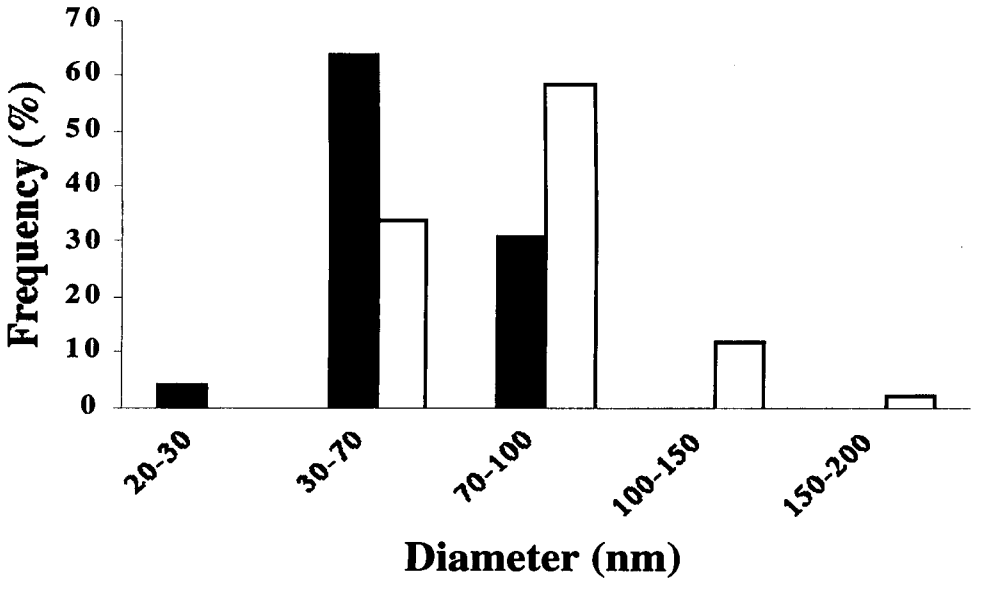

Fig. 5.2 Frequency distribution of diameters of vesicular structures

Golgi membranes were incubated for 15 minutes with 2 mg/ml of rat brain cytosol either in the absence (filled bars) or presence (empty bars) of 3 μg/ml of chromatographically purified BARS. Samples were processed for negative staining and electron microscopy and the frequency distribution of the diameter of the vesicles was calculated as described in material and methods. The experiment was repeated two times with similar results

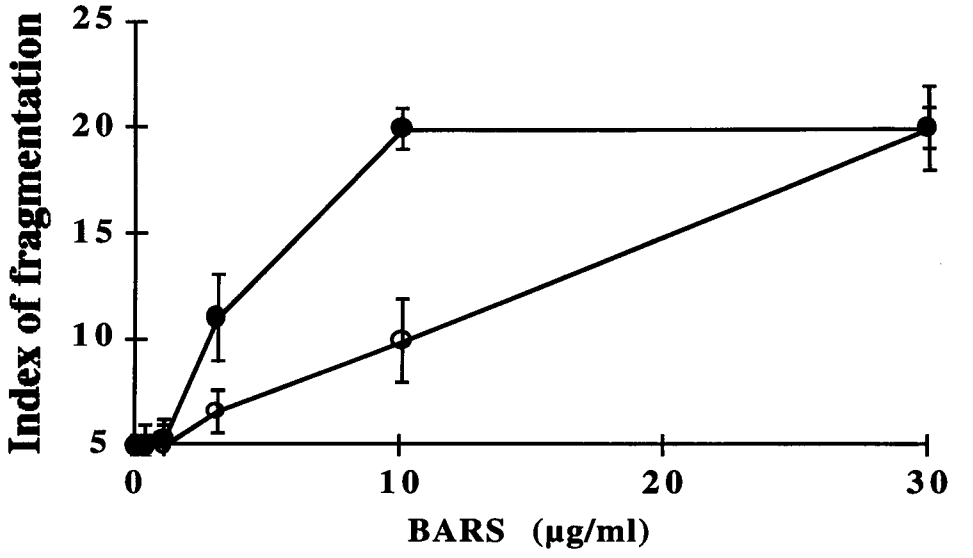

Fig. 5.3 Comparison between the activity of the chromatographically purified BARS and recombinant GST-BARS

Golgi membranes were incubated in standard conditions for 15 minutes with 2 mg/ml of rat brain cytosol in the presence of the indicated concentrations of either chromatographically purified (filled circles) or recombinant GST-BARS (empty circles). Samples were processed for negative staining and electron microscopy and the index of fragmentation was calculated as described in the material and methods; Values are means ± S.D.s of triplicates. The experiment was repeated two times with similar results.

chromatographically purified BARS and recombinant GST-BARS). At 15 minutes, the exposure to BARS induced fragmentation and vesiculation of the tubular-reticular domains. At 40 minutes tubules were fragmented even in the absence of BARS and the stacks appeared to be reduced in number and size (fig. 5.4 and 5.5 A). The fragments were either vesicular (50-100 nm in diameter), or ovoidal in agreement with the negative-staining data. Furthermore, the distribution of vesicle diameters was analyzed at 15 minutes. In the presence of BARS there was a higher frequency of vesicles having a diameter of 30-70 nm with respect to control conditions, while for the larger diameters no differences were seen (fig. 5.5 B). This discrepancy with the negative staining data could be due to the fact that an unknown fraction of vesicles is lost in the medium during the washing procedures and further in thin sectioning some of the circular profiles could easily represent sections of tubules.

5.2.2 The blocking antibody α–PEP9

As a further control that the cytosolic fragmenting activity acting on Golgi tubules was due to BARS, a blocking antibody directed against peptide 174-181 of BARS (PEP9) was used (Spano' et al., 1999). Non-dialysed cytosol was pre-incubated on ice for 1 hour with either 10 or 50 μg/ml of both the α-PEP9 antibody and an IgG fraction. Pre-treated cytosols were incubated (2 mg/ml) with Golgi membranes in standard conditions for 60 minutes. The cytosolic fragmenting activity was inhibited by the α-PEP9-pretreatment, totally (50 μg/ml) or partially (10 μg/ml) while IgG pretreatment was ineffective (fig. 5.6). As a further control, cytosol was pretreated for 1h on ice with 50 μg/ml of the α-PEP9 in the presence of 1 mM of either PEP9 or an unrelated peptide (GRK4-PEP). When Golgi membranes were incubated with this cytosol, the fragmenting activity was inhibited when GRK4-PEP was present. Neither the PEP9 nor the GRK4-PEP influenced the cytosol fragmenting activity (fig. 5.6).

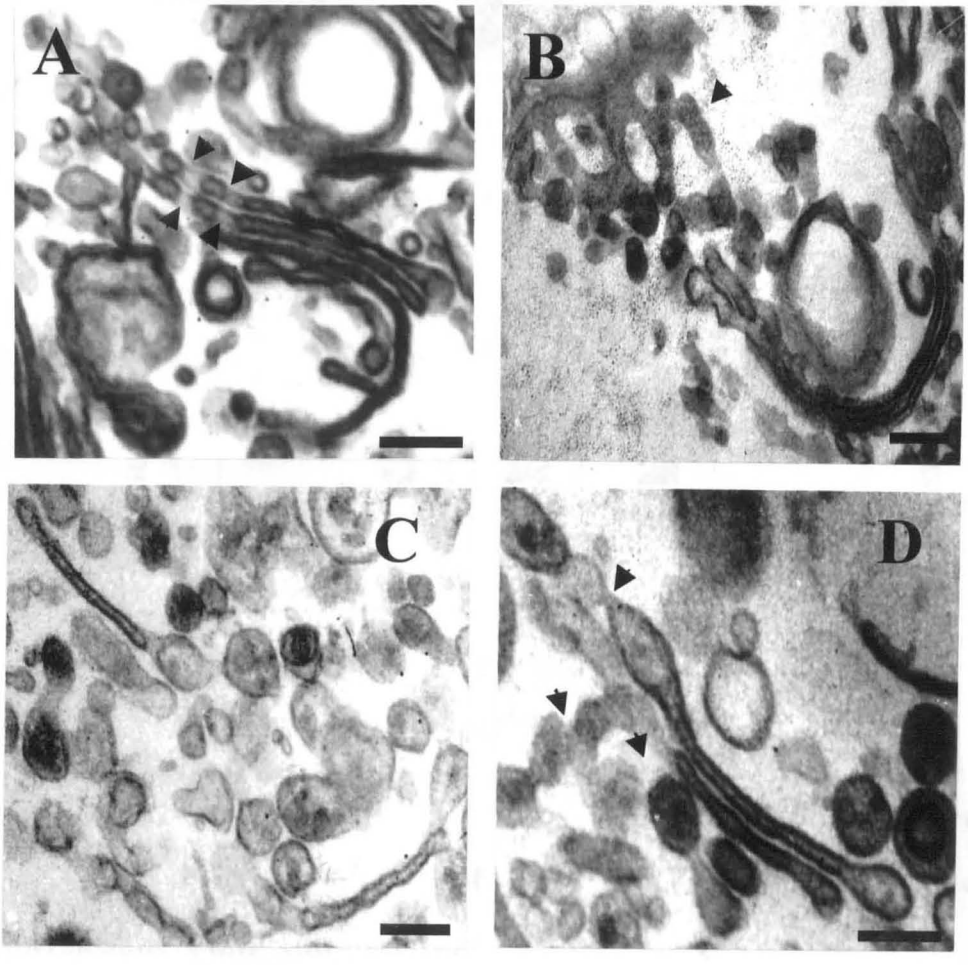

Fig. 5.4 Effects of BARS on the Golgi tubular network in conventional EM thin sections

A - Untreated Golgi membranes. The micrograph shows a stack formed by four cisternae with well preserved fenestrations (arrowheads). B - Golgi membranes were incubated with 2 mg/ml rat brain cytosol for 15 minutes. A stack with a preserved tubular reticular network (arrowhead) is visible. C, D - Golgi membranes were incubated for 15 minutes with 2 mg/ml of cytosol in the presence of 3 μg/ml chromatographically purified BARS. Tubular domains are absent and replaced by a series of round profiles of different diameters (C). Isolated cisternae are frequent (C). Constricted tubules are visible (D, arrowheads). Bar, 100 nm

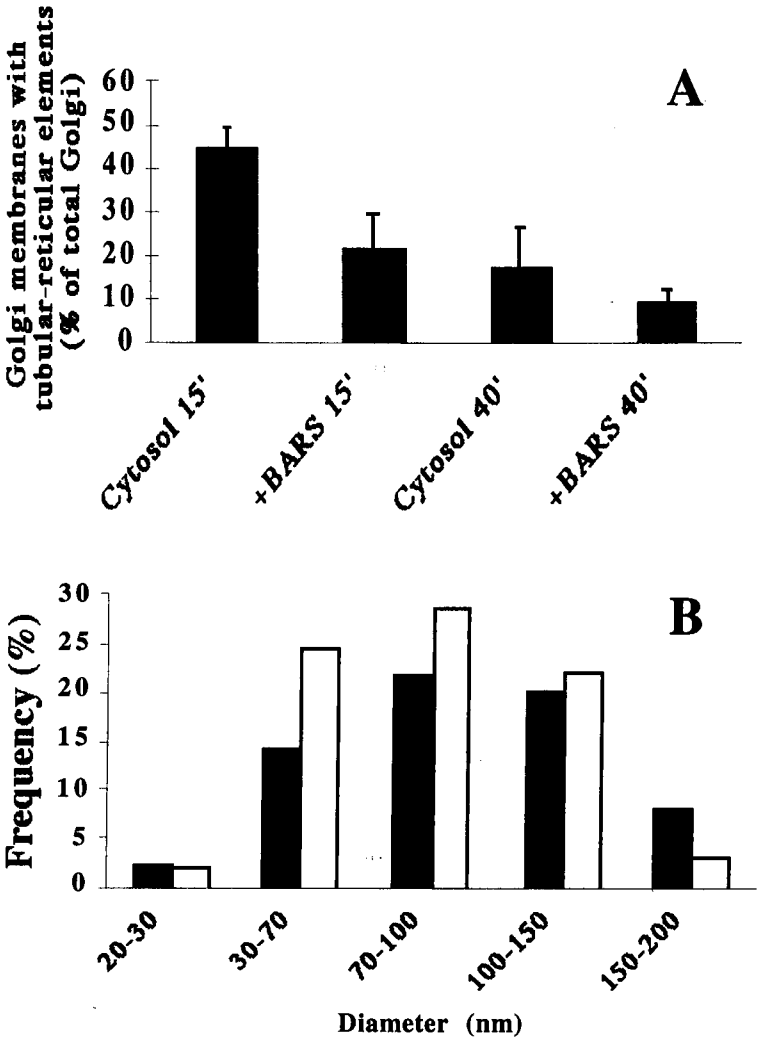

Fig. 5.5 Characterization of the effect of BARS-enriched cytosol on the morphology of isolated Golgi membranes in conventional EM thin sections

A. Quantification of the effect of BARS-enriched cytosol. Golgi membranes were incubated as described in the legend to fig. 5.1 C and processed for thin sectioning and electron microscopy. The percentage of Golgi stacks with preserved tubular reticular networks was calculated as described in material and methods. Values are means of duplicates ± S.D.s. The experiment was repeated two times with similar results. B. Frequency distribution of diameters of the vesicular structures. Golgi membranes were incubated in standard conditions for 15 minutes with 2 mg/ml of rat brain cytosol either in the absence (filled bars) or presence (empty bars) of 3 μg/ml of the chromatographically purified BARS. The diameters of the vesicles formed during the incubation were measured and frequency distribution was calculated as described in material and methods.

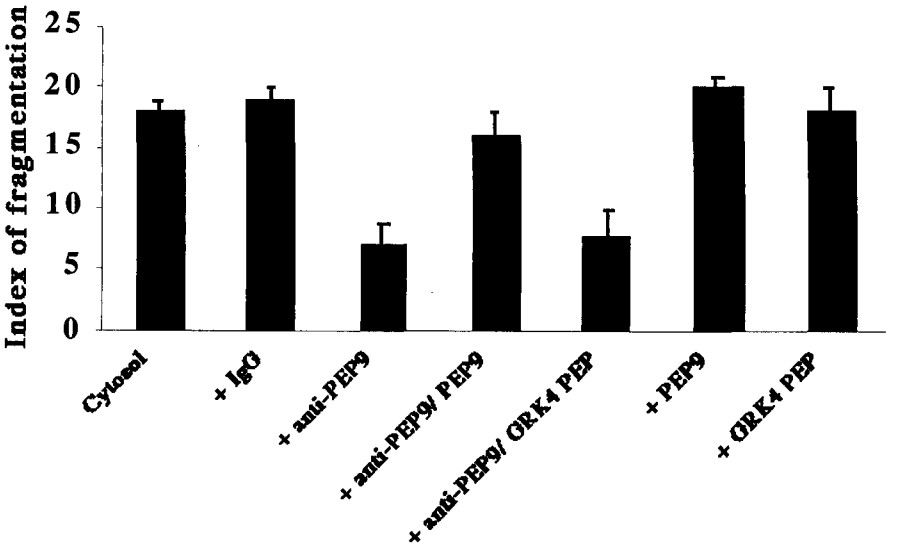

Fig. 5.6 Effect of the blocking anti-BARS antibody, α-PEP9 on the fragmenting activity of rat brain cytosol

Golgi membranes were incubated for 60 minutes with 2 mg/ml of rat brain cytosol either untreated or pretreated for 60 minutes at 0°C as follows: 10 μg/ml (+ IgG, empty bars) or 50 μg/ml (+IgG, filled bars) of a purified IgG fraction , 10 μg/ml (+anti-PEP9, empty bars) or 50 μg/ml (+anti-PEP9, filled bars) of the α-PEP9 antibody alone or in the presence of either 1 mM of the PEP9 (+anti-PEP9/PEP9) or 1 mM of the GRK4 peptide (+anti-PEP9/GRK4-PEP), with 1 mM of either the PEP9 (+PEP9) or the GRK4 peptide (+ GRK4 PEP). Samples were processed for negative staining and the index of fragmentation was calculated as described in material and methods. Values are means of duplicates ± S.D.s. The experiment was repeated three times with similar results.

5.2.3 ADP-ribosylated BARS

BARS was originally identified as the substrate of a BFA dependent mono-ADP-ribosyltransferase and its ADP-ribosylation was shown to facilitate the BFA-induced Golgi tubulation (Weigert et al., 1997, Mironov et al., 1997) For this reason the effect of ADP-ribosylation on the BARS fragmenting activity was checked. Recombinant GST-BARS was ribosylated as described in material and methods and mock ribosylated BARS was prepared as control. Thirty μg/ml of either the ribosylated or the mock-ribosylated GST-BARS were incubated for 20 minutes with Golgi membranes in the presence of 2 mg/ml of non-dialysed cytosol. The mock-ribosylated protein still fragmented the Golgi associated tubules but with a lower efficiency, when compared to a non-ribosylated BARS (fig. 5.7); this is probably due to the degradation of the protein which occurs during the procedure. Strikingly the ADP-ribosylated BARS completely lost its fragmenting activity. Golgi associated tubules appeared preserved and not increased in number, suggesting that the BFA-dependent ribosylation of BARS does not promote the formation of tubules, but inhibits their consumption (fig. 5.7).

5.2.4 Cytosolic requirement for BARS

Golgi membranes were incubated for different times (20, 40, and 60 minutes) and in the absence of cytosolic proteins, with different concentrations of either the chromatographically purified BARS (0.3, 1, 3 μg/ml) or the recombinant GST-BARS (1, 3, 10, 30 μg/ml). As controls, parallel incubations were carried out in the presence of equal amounts of recombinant GST. In the absence of cytosol, the Golgi associated tubules were highly preserved in all the conditions tested, indicating that BARS needs a cytosolic cofactor(s) for exerting its fragmenting activity (fig. 5.8).

5.2.5 Effect of BARS in permeabilized cells

To examine the effects of BARS on Golgi associated tubules in cells, we used a permeabilized cell system. RBL cells were permeabilized with SLO as described in material and methods and incubated for 20 minutes

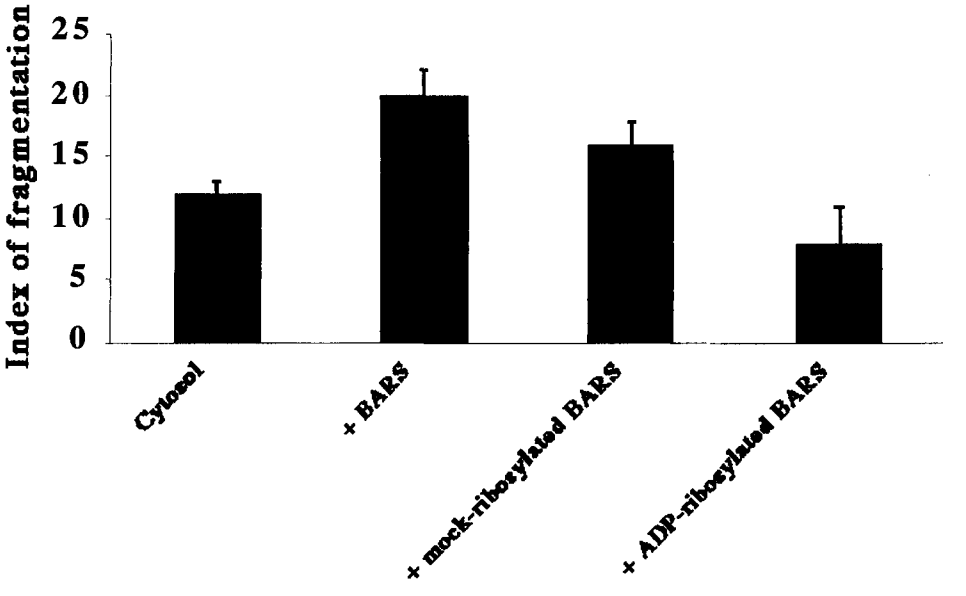

Fig. 5.7 Effect of BFA-dependent mono-ADP-ribosylation on the BARS-induced fragmentation of Golgi associated tubules

Golgi membranes were incubated for 20 minutes with 2 mg/ml of rat brain cytosol with no additions or with 30 μg/ml of recombinant GST-BARS, either in the native, the ADP-ribosylated, or the mock-ADP ribosylated form. Samples were processed for negative staining and the index of fragmentation was calculated as described in material and methods. Values are means of duplicates ± S.D.s. The experiment was repeated three times with similar results.

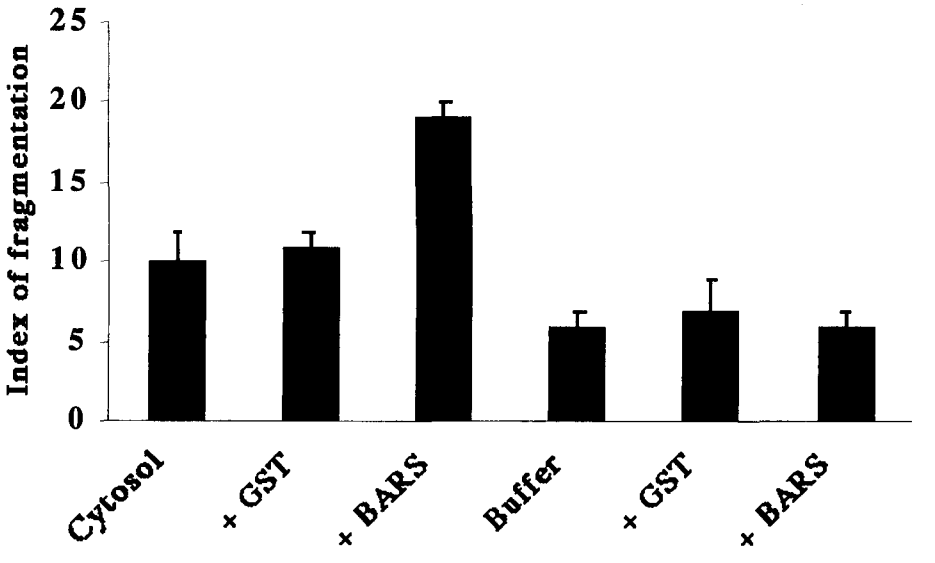

Fig. 5.8 Cytosolic requirement for the BARS-induced fragmentation of Golgi-associated tubules

Golgi membranes were incubated for 20 minutes in the presence of 2 mg/ml rat brain cytosol (filled bars) or in the presence of the buffer in which cytosol is stored (empty bars). 30 μg/ml of either recombinant GST or recombinant GST-BARS were added and samples without any additions were used as controls. Samples were processed for negative staining and the index of fragmentation was calculated as described in material and methods. Values are means of duplicates ± S.D. The experiment was repeated three times with similar results.

under the following conditions: (i) with the buffer in which the cytosol is stored in the absence or in the presence of 30 μg/ml recombinant GST ii) with 2 mg/ml of non-dialysed cytosol in the absence or presence of 30 ng/μl recombinant GST, iii) with 30 μg/ml of recombinant GST-BARS, iv) with 2 mg/ml of non-dialysed cytosol in the presence of 30 ng/μl GST-BARS. After the incubations, samples were fixed and processed for electron microscopy as described in material and methods. The Golgi apparatus in SLO-permeabilized RBL cells, was very well preserved and almost indistinguishable from that seen in intact cells. It retained its perinuclear location near the centrosome, its ribbon-like structure with a well preserved non-compact zone (Buccione et al., 1996). When cells were incubated without BARS , with BARS in the absence of cytosol or with cytosol for 20 minutes, the Golgi apparatus did not show any noticeable changes in its morphology (fig. 5.9 A, C). However, exposure to BARS-enriched cytosol, caused a reduction in the tubular-reticular zones of the Golgi, their partial replacement with fragments of variable sizes, and an overall disruption of the stacks (fig. 5.9 B). Cisternae were partially preserved, and other cellular compartments were not affected.

Similar experiments were performed by incubating the SLO-permeabilized RBL cells for 40 minutes in the presence of 5 mg/ml of BARS-depleted cytosol either alone (fig. 5.9 E) or supplemented with 7.5 μg/ml of recombinant GST-BARS (fig. 5.9 F). As controls, parallel incubations were carried out with 5 mg/ml of a mock-depleted cytosol or with 5 mg/ml of a BARS-depleted cytosol supplemented with 7.5 μg/ml of the recombinant GST. The Golgi tubular networks appeared fragmented as described above when treated with the mock-depleted cytosol (fig. 5 D), while they were preserved during treatment with BARS-depleted cytosol (fig. 5.9 E). The addition of the highest amount of GST-BARS restored the fragmenting activity (fig. 5.9 F), while GST was ineffective. This data shows that BARS fragmenting activity occurs not only in a cell-free system but also in a more physiological condition such as permeabilized cells.

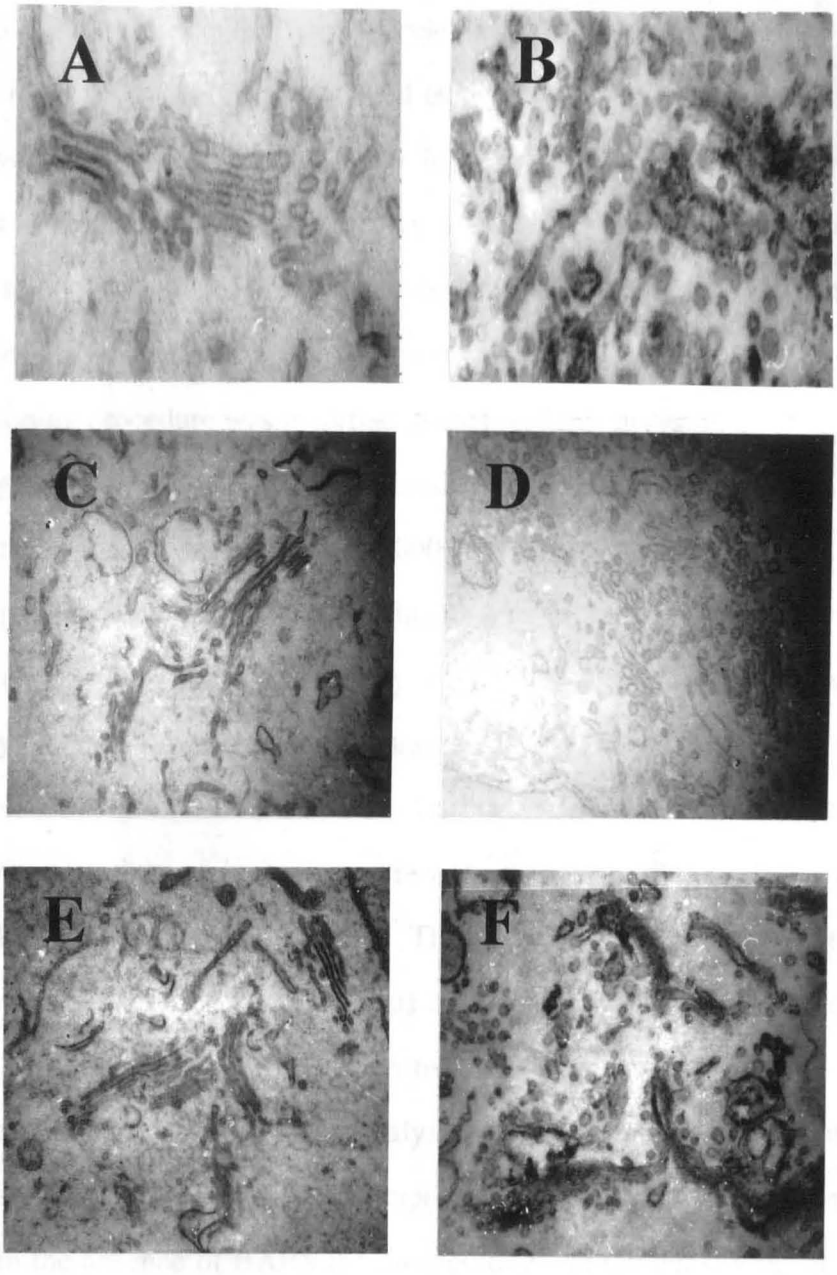

Fig. 5.9 Effect of BARS on the morphology of the Golgi apparatus in permeabilized cells

SLO-permeabilized RBL cells were incubated for 20 minutes with 2 mg/ml rat brain cytosol with no additions (A) or with 30 μg/ml of the recombinant GST-BARS (B), without cytosol in the presence of 30 μg/ml of the recombinant GST-BARS (C). Incubations were also carried out for 40 minutes in the presence of 5 mg/ml of mock-depleted rat brain cytosol (D) or with 5 mg/ml of BARS-depleted cytosol either with no additions (E) or with 7.5 μg/ml of recombinant GST-BARS. Samples were processed for electron microscopy as described in material and methods. The experiment was repeated three times with similar results.

5.2.6 Analysis of the fragments released from stacks

The morphological analysis carried out so far by negative staining and by conventional thin sectioning, gave information about the morphology of both the Golgi associated tubules and the stacks, without a detailed characterization of the membranes (both vesicles and fragments) that were released from the Golgi and lost to the medium. For this reason the thin sectioning procedure was modified to analyzed this material.

Golgi membranes were fixed, blocked with BSA as described, and centrifuged at very high speed (150000 x g for 1h) a condition in which all the membranes including the lightest were pelletted. Pellets were then processed for electron microscopy, embedded and cut as described. The analysis of the untreated samples showed that Golgi stacks were layered at the bottom of the pellet (in layers 1-2 μm thick); above the stacks a series of fragments mainly vesicular in nature were dispersed within a distance from the bottom of 5 μm (fig. 5.10). The density of these fragments was calculated by stereological methods and found to be 27 ± 3 fragment per μm^2 (average ± S.E.M. n=2). Golgi membranes were then incubated for 15 minutes with 2 mg/ml of non-dialysed cytosol either in the absence or presence of 3 μg/ml of chromatographically purified BARS. At 15 minutes and in the absence of BARS the morphology and the density of the Golgi stack did not change significantly, while in the adjacent area the density of vesicular fragments increased (53 ± 10 fragments per μm^2; average ± S.E.M. n=2) (fig. 5.10 B). The addition of BARS induced massive changes in the stacks (fig 5.10 lower panels), as previously described, and in the density of the released fragments. Stacks were reduced in number while a marked increase in the density of the vesicles was observed (141 ± 26 fragments per μm^2; average ± S.E.M. n=2) (fig. 5.10 C). Further the analysis of the diameters of the vesicular profiles released from the Golgi stacks were performed showing again that in the presence of BARS, more irregular fragments with a slightly larger diameter were formed. Thus, altogether, the effects of BARS on the release of vesicular fragments are

complementary to the effects of BARS on the morphology of the Golgi stacks

.

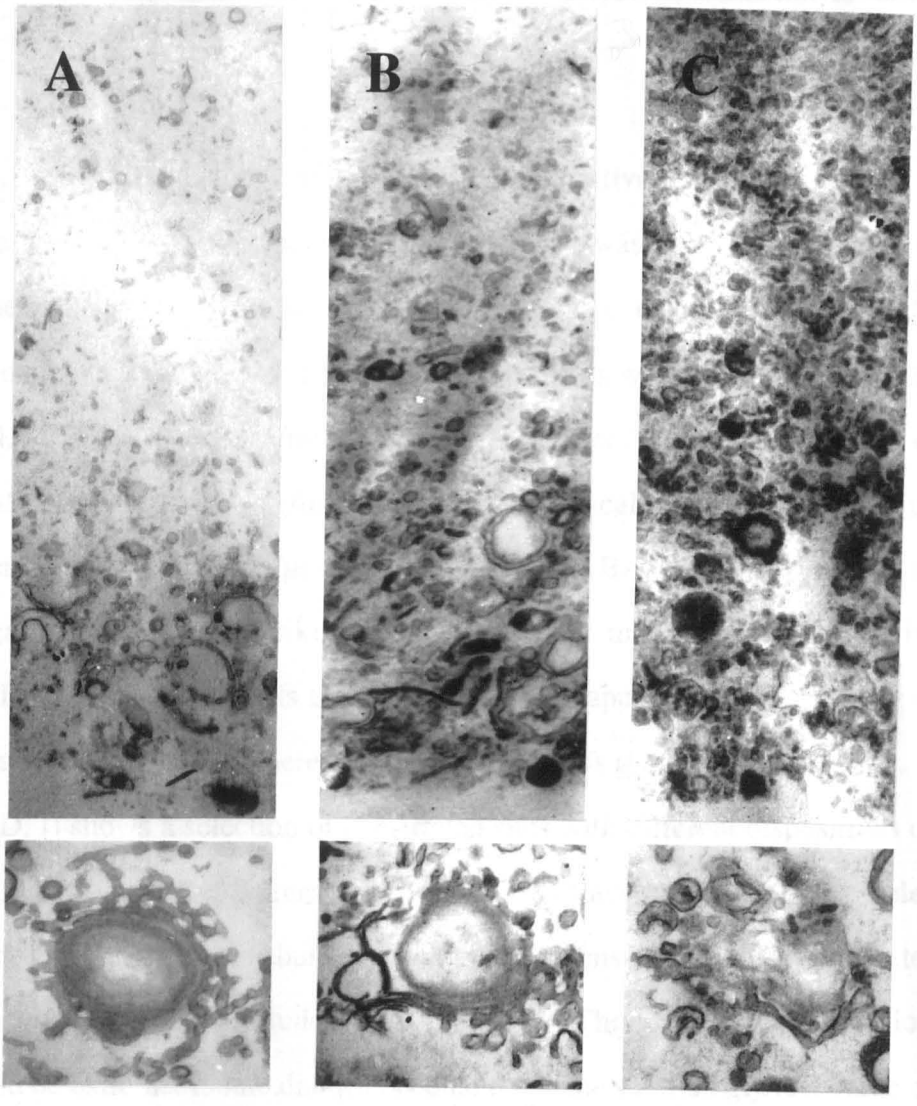

Fig. 5.10 Visualisation of the BARS induced release of vesicular fragments from the isolated Golgi stacks

Golgi membranes were incubated for 20 minutes with 2 mg/ml of rat brain cytosol in the absence (B) or in the presence (C) of 3 μg/ml of chromatographically purified BARS. Untreated membranes were taken as control (A). After ending the incubation, samples were ultracentrifuged and the pellets were processed for electron microscopy as described in material and methods, resin-embedded, and cut along the longitudinal axis of the test tube. Golgi stacks accumulated at the bottom of the pellets in layers 1.0-1.5 μm thick, while the lighter fragments were distributed above the stacks in a layer of 5 μm. In the lower panels Golgi stacks in en-face profiles are shown. Magnifications: 24000 x (upper panels), 50000 x (lower panels). The experiment was repeated twice with similar results.

5.3 Characterization of the BARS-induced fission intermediates

5.3.1 Fission intermediates visualised by negative staining

The effect of the exogenous addition of BARS was carefully evaluated in order to collect information about the possible mechanism of BARS-induced fragmentation activity. Golgi membranes were incubated for 5, 10 or 15 minutes with 2 mg/ml of non-dialysed cytosol either in the absence or in the presence of 3 μg/ml of chromatographically purified BARS (or alternatively with 30 μg/μl of recombinant GST-BARS) and visualised by negative staining. A striking feature of Golgi membranes treated with BARS-enriched cytosol is the early (at 10 min) appearance of a number of sites (9 ± 2 per stack) where the tubule diameter is greatly reduced. Fig 5.11 (A-D, I) shows a selection of constricted sites with different dispositions of tubules and varying degrees of constriction. To avoid ambiguities, tubules without clear margins, tubule bifurcations, and constrictions with a diameter above 25 nm were excluded from the study. The degree of constriction could be extreme: tubule diameters could reach the surprisingly low value of 11 ± 1 nm. The physical transition between normal and constricted segments was gradual, and the sites were symmetrical, with the narrowest point at the center. The constrictions were unevenly distributed along the length of tubules, apparently without a preferential localisation for specific zones (for instance, the junctions between tubules and cisternae, or between tubules, etc.). However, when several constrictions were present in a single tubule (fig. 5.11 I), they were spaced at regular intervals (85 ± 3 nm). These dimensions were compatible with those of the vesicles produced by fission. Moreover, images were found of what appeared to be stages of transition between series of constricted sites and the rows of aligned vesicles often observed at later times in the incubation. Based on these combined features, a likely explanation is that those are the sites where fragmentation

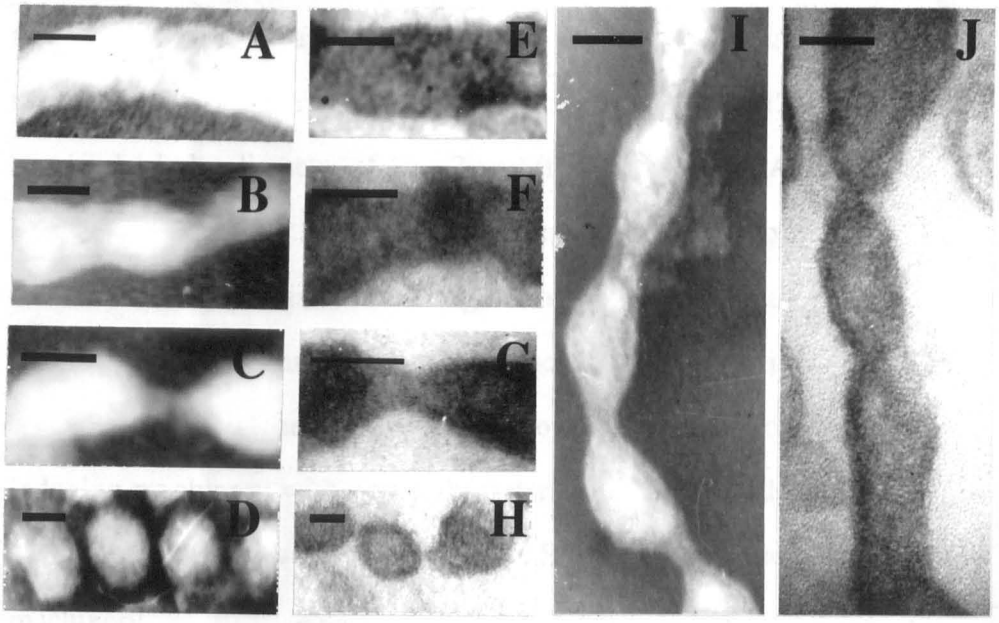

Figure 5.11 Structure of BARS-induced fission intermediates in Golgi tubules

A, B, C, D, I - Negative stains of whole-mount preparations. E, F, G, H, J - Thin sections of resin-embedded samples. A, E - Membranes were incubated for 15 min with control cytosol. Examples of unconstricted tubules. B-J - Golgi membranes were incubated for 15 min with 3 μg/ml purified rat brain BARS added to 2 mg/ml cytosol. Moderate constrictions (B, F). Extreme constrictions (C, G). Rows of aligned vesicles presumably resulting from clipping of a single tubule at regular intervals (D, H). Series of fission intermediates in single tubules (I, J). Bars 40 nm

occurs and so they will be referred to as fission intermediates. These observations prompted further analysis and a search for fission intermediates in samples treated with cytosol alone, in which tubule fission occurs at a slower rate. Structures with similar features could be found, albeit rarely (2 ± 1 per stack). Thus, BARS increases the frequency of a phenomenon also induced by normal cytosol.

5.3.2 Fission intermediates visualised by thin sections

To check if the fission intermediates visualised by the negative staining technique could be artefacts, for example, due to the air drying procedure, the same experiments were carried out as in the previous section but using thin sectioning. In resin-embedded, thin-sectioned samples, BARS-induced fission intermediates appeared as sites of variable thickness, very similar to those seen by negative stain, with a minimum diameter of 12 ± 1 nm (from a maximal tubular diameter of 48 ± 2 nm) (fig. 5.11 E-H, J). At these sites, the bilayer structure was visible, and measured at 4 nm as expected. When a series of sites were visible in a single tubule, the average distance between them was 92 ± 10 nm, again in excellent agreement with the negative-staining data. Together, these results show that cytosol contains a fission-inducing machinery with novel characteristics, inducing the fragmentation of Golgi tubular networks, and that BARS is an essential component of that machinery.

5.4 Molecular mechanism of BARS effect

5.4.1 Acyl-coenzymeAs as cofactors: characterization

BARS stimulated the fission of Golgi-associated tubules and this process required one or more unknown cytosolic co-factors. Since the cytosol used in these experiments was non-dialysed, this cofactor could either be a protein or a small molecule. Some studies have implicated the long chain AcCoAs (see section 1.4.3.3 and Ostermann et al., 1993) in the fission of COPI-coated vesicles and AcCoAs have been found in cytosolic extracts at micromolar concentrations both as free molecules and bound to acyl-carrier proteins (Jolly et al., 1998, Schroeder et al., 1998). Thus palmitoyl- and other acyl-CoAs were tested as cofactors for the BARS-induced fission.

Chromatographically-purified BARS from rat brain (10 μg/ml) was incubated for 15 minutes with isolated Golgi membranes in the presence or absence of 10 μM pCoA and as a control pCoA alone was used. BARS together with pCoA, exhibited full fissiogenic activity on Golgi tubules (fig. 5.12), whereas BARS or pCoA alone were without effect (fig. 5.12 D). The effects of BARS plus pCoA on isolated Golgi membranes were similar to those observed on exposure of membranes to BARS-enriched cytosol (fig. 5.12 B). Golgi tubular reticular networks were fragmented into heterogeneous vesicles and rare short tubules, while cisternae were much less affected. Numerous fission sites were also observed, though they were more numerous (3-4-fold) than in cytosol-dependent reactions (fig. 5.13). A possible explanation for this is that the cytosol contains additional fission factors which destabilise the fission intermediates to complete the fission process.

To test if the pCoA-dependent activity was due to BARS or to some other protein contaminating the BARS purified fraction, the experiment was repeated using recombinant GST-BARS. Golgi membranes were incubated for 15 minutes as indicated in the legend to fig. 5.13. Recombinant GST-BARS was effective in fragmenting the Golgi associated tubules either in

the presence of cytosol or in combination with 10 μM pCoA (fig. 5.13). Strikingly, the pCoA dependent activity of GST-BARS was inhibited by ADP-ribosylation (fig. 5.13). The time dependence of the pCoA and BARS-dependent fragmenting activity was analyzed. Golgi membranes were incubated for different times (10, 20, 30, 40 and 60 minutes) with 30 μg/ml GST-BARS either in the absence or presence of 10 μM pCoA. As a control 30 μg/ml GST was used. GST-BARS and pCoA were fully effective at 20 minutes, however, at longer times pCoA in the absence of BARS also induced fragmentation in Golgi-associated tubules (fig. 5.14).

Some kinetic aspects of the fission reaction were then characterised semi-quantitatively. The effects of BARS on Golgi tubular networks were time and concentration dependent with respect to both pCoA and BARS. A maximal fission/fragmentation effect was reached at 10 μg/ml of chromatographically purified BARS though again, this was less potent than recombinant GST-BARS (fig. 5.15). Using a standard incubation time of 20-30 min and 10 μg/ml protein, the threshold fissiogenic concentration of pCoA was 2 μM, and the full effect was observed at 10 μM, well below the CMC for this compound (Requero et al., 1995). Interestingly, the potency of BARS was lower (roughly 3-fold) than in the presence of cytosol even when a maximal concentration of pCoA (10 μM) was used, again consistent with the idea that the cytosol contains additional factors which facilitate fission.

Next, a series of different Ac-CoAs were tested to analyze the role of the length and degree of saturation of the acyl chain in the fission reaction. Golgi membranes were incubated for 5 minutes with different AcCoAs (all at 10 μM with the exception of CoA, which was tested at 50 μM) either in the absence or presence of 30 μg/ml of recombinant GST-BARS. Under these conditions, AcCoAs did not show any significant effect on the morphology of the Golgi associated tubules. In the presence of BARS, the shortest active molecule was myristoyl-CoA (C14:0), and the potency increased with chain length and unsaturation. Arachidonoyl-CoA (C20:4)

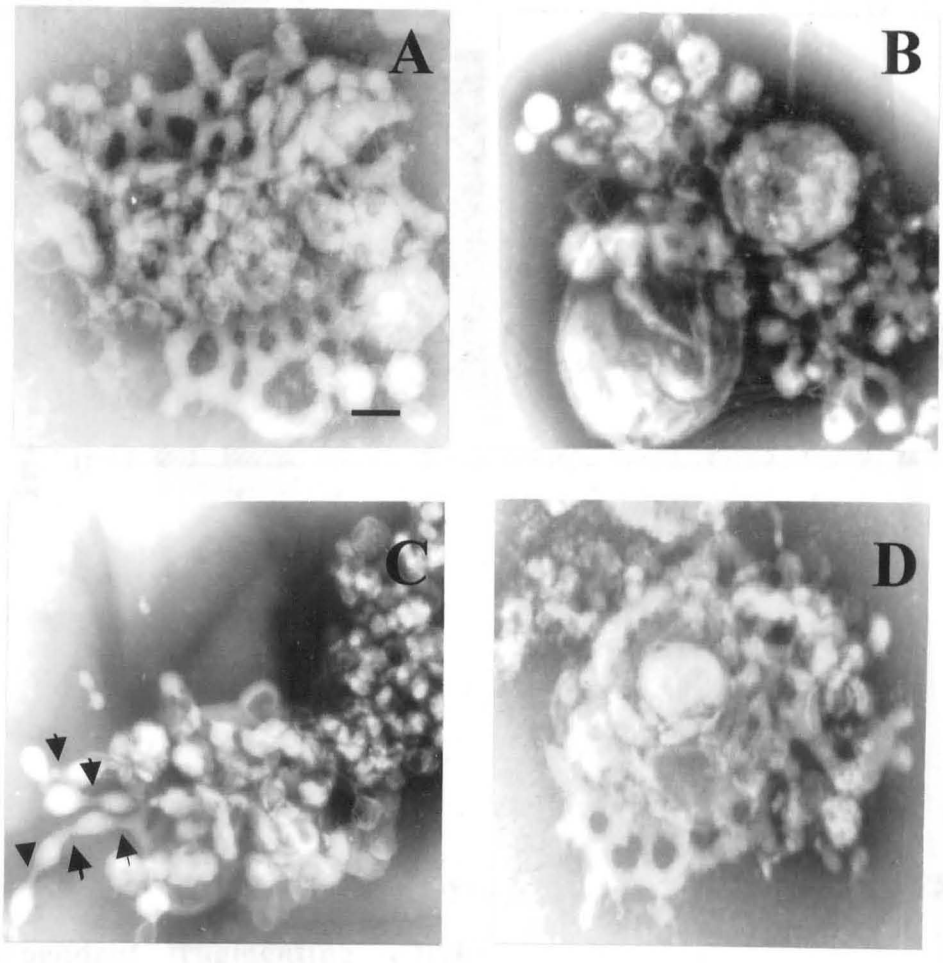

Fig. 5.12 Palmitoyl-CoA is an essential cofactors for the BARS-induced fragmentation of Golgi tubular networks

A-D, Isolated Golgi membranes visualised by the negative-staining of whole-mount preparations A. Untreated membranes. B. Isolated Golgi membranes incubated for 20 min with 2 mg/ml rat brain cytosol enriched with 3 μg/ml chromatographically purified rat brain BARS, the tubular/fenestrated area is fragmented and replaced by a series of heterogeneous vesicular structures. C. Golgi membranes incubated for 20 min with 10 μM pCoA and 10 μg/ml chromatographically purified rat brain BARS in the absence of cytosol. The tubular network is completely fragmented into vesicular structures which are very similar to those observed in the presence of cytosol, and numerous constriction sites are observed on the tubules (arrowheads). D. Golgi membranes incubated with rat brain BARS alone, in the absence of acyl-CoA and cytosolic proteins. The tubular network is preserved and no tubular constrictions are observed.

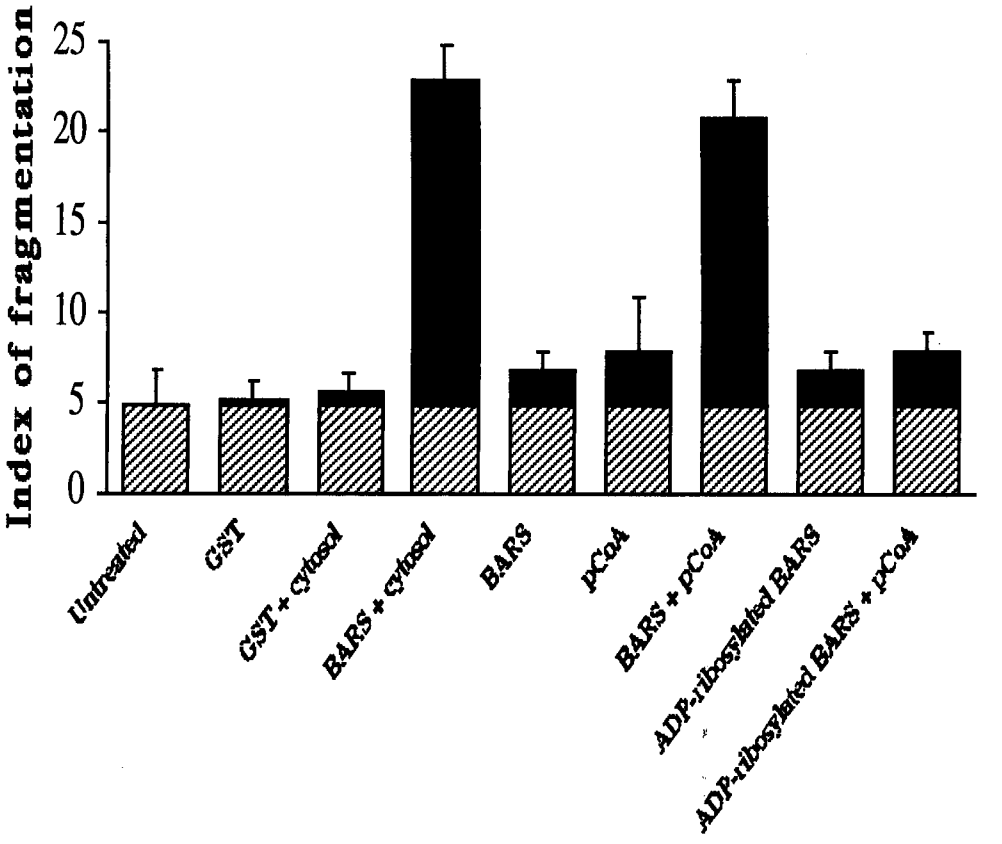

Fig. 5.13 Quantitative analysis of the pCoA and BARS-dependent fragmenting activity

Golgi membranes were left untreated or incubated for 20 minutes with: the incubation buffer (see material and methods), 2 mg/ml cytosol, 2 mg/ml cytosol supplemented with 30 μg/ml of recombinant GST-BARS, 30 μg/ml GST-BARS, 10 μM pCoA, the GST-BARS and the pCoA, 30 μg/ml ADP-ribosylated GST-BARS, ADP-ribosylated GST-BARS and the pCoA. Samples were processed for negative staining and electron microscopy and the index of fragmentation was calculated as described in material and methods The index of fragmentation of untreated membranes (ca. 5, stripes) represents background fragmentation. Values are means ± S.D.s of three independent experiments.

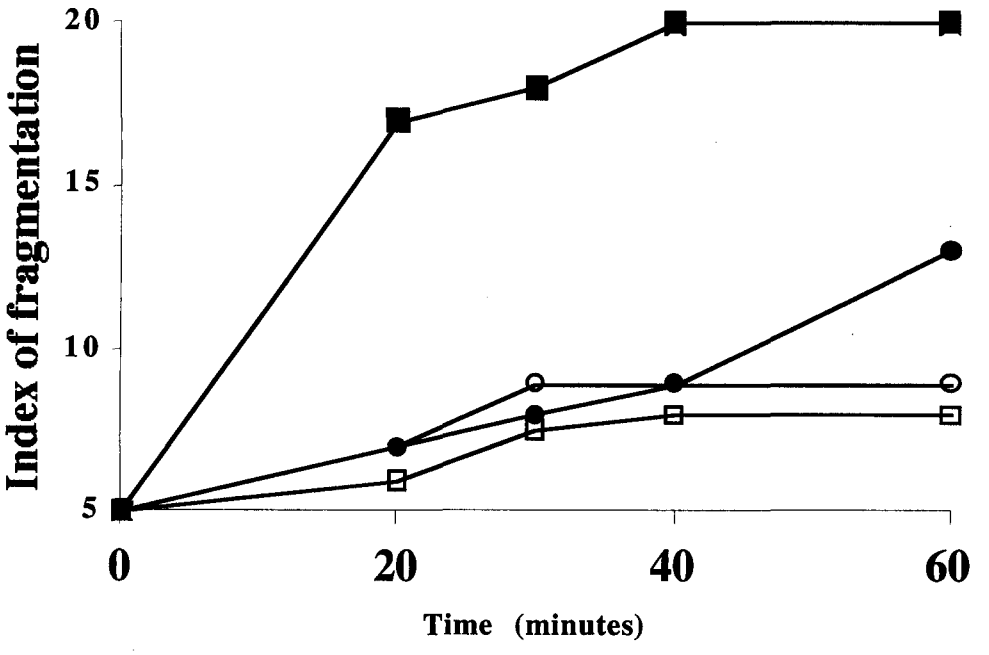

Fig. 5.14 Time course of the acyl-CoA and BARS-dependent fragmenting activity

Golgi membranes were incubated for the time indicated with 30 μg/ml GST in the absence (empty circles) or presence of 10 μM pCoA (filled circles), or with 30 μg/ml GST-BARS in the absence (empty squares) or presence (filled squares) of 10 μM pCoA. Samples were processed for negative staining and electron microscopy. The index of fragmentation was calculated as described in material and methods. The experiment was repeated three times with similar results.

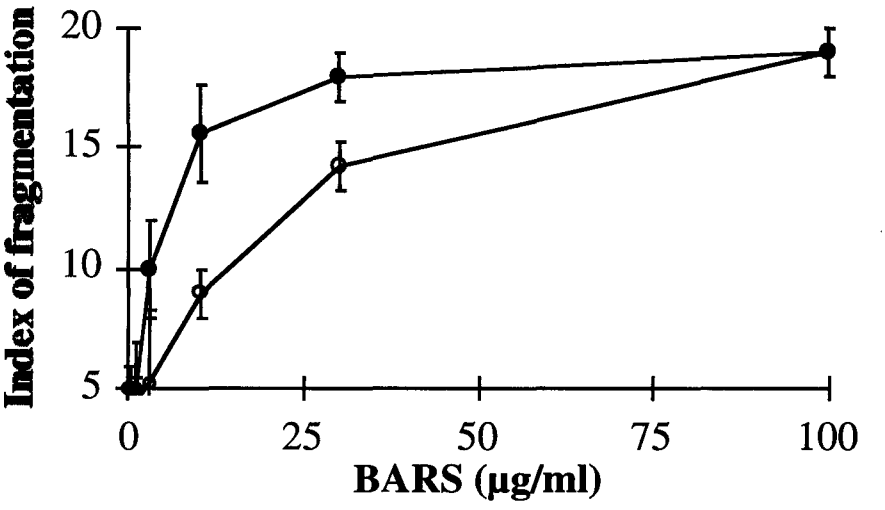

Fig. 5.15 Fragmenting activity of partially purified and recombinant BARS in the presence of pCoA

Golgi membranes were incubated for 15 min in the presence of 10 µM pCoA and increasing concentrations of either partially purified or recombinant GST-BARS. Values are means ± S.D.s of three independent experiments.

and oleoyl-CoA (C18:1) were the most potent (fig. 5.16). Notably, CoA itself was active. As shown in section 4.2.2 CoA activity could be linked to the resynthesis of AcCoAs, due to ATP-dependent ligases utilising the free fatty acids present in the lipid bilayers. For this reason the incubations with CoA and some other long chain AcCoAs (C16:0-, C18:0-, C18:1-CoA) were performed in the absence of ATP and in the presence of an ATP scavenger (20 U/ml Hexokinase and 10 mM glucose). Under these conditions CoA no longer supported the BARS-fragmenting activity, whereas the long-chain AcCoAs were still active (fig. 5.17). This finding indicates that AcCoAs are essential components of the BARS-dependent fragmenting activity of Golgi associated tubules.

5.4.2 BARS is a LPA-specific acyltransferase

Palmitoyl- and myristoyl-CoA are the substrates of two classes of enzymes, the palmitoyl and the N-myristoyl transferases, which are known to covalently transfer the fatty acyl residues from the AcCoAs to a cysteine or a glycine residue of target proteins (Resh, 1996). However even though the longer AcCoAs have not been described to work as cofactors for these enzymes, it was possible that the BARS induced fragmentation was mediated by the palmitoylation of a Golgi protein, or of a cytosolic protein or even of BARS itself.

Recombinant GST-BARS (50 μg/ml), or GST as control, were incubated with 10 μM [^{14}C]-pCoA for 15 or 60 minutes as follows: i) with no other additions (fig. 5.18 lane 1, 2), ii) with 2 mg/ml of non-dialysed cytosol (fig. 5.18 lane 3, 4), iii) with 0.1 mg/ml of isolated Golgi membranes (fig. 5.18 lane 5, 6), iv) with both cytosol and Golgi membranes (2 mg/ml and 0.1 mg/ml respectively) (fig. 5.18 lane 7, 8). Reactions were stopped by the addition of an equal volume of sample buffer 2x and processed for SDS-page. Radiolabelled bands were evaluated by electronic autoradiography (Instant Imager - Canberra Packard). No differences were observed in the pattern of palmitoylation in BARS treated samples, ruling out the involvement of a palmitoylation reaction in the BARS-dependent

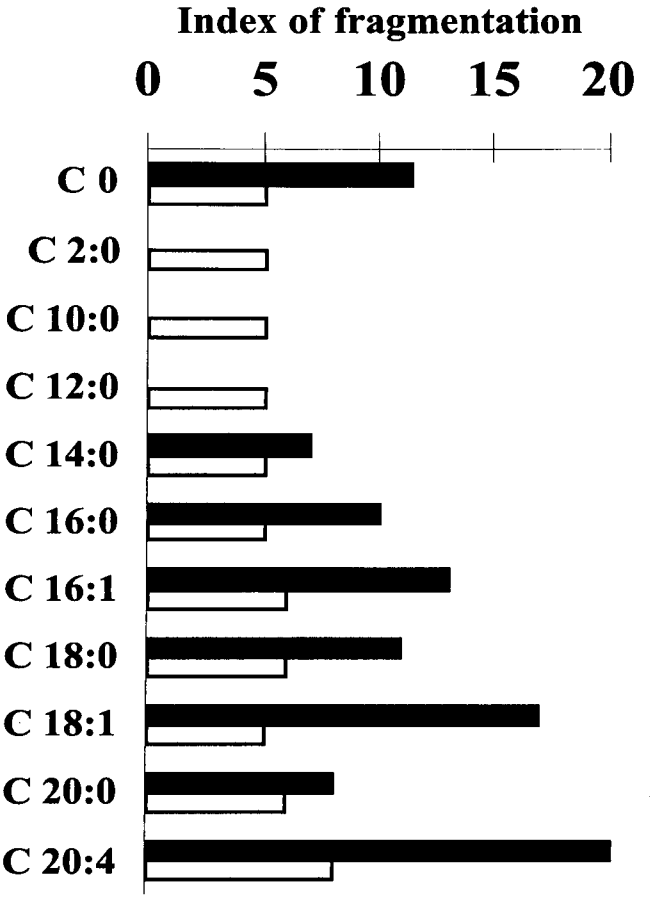

Fig. 5.16 Activity of different acyl-CoAs in supporting the BARS-dependent fragmentation of Golgi tubules

Golgi membranes were incubated with different acyl-CoAs (10 μM) for 5 min in the presence of either 30 μg/ml GST (empty bars) or 30 μg/ml of recombinant GST-BARS (filled bars). This short incubation time, at which the fission reaction is beginning, was chosen to ampliphy the differences in activity among the various acyl-CoAs. Samples were processed for negative staining and eletron microscopy and the index of fragmentation was calculated as described in material and methods. The experiment was repeated three times with similar results.

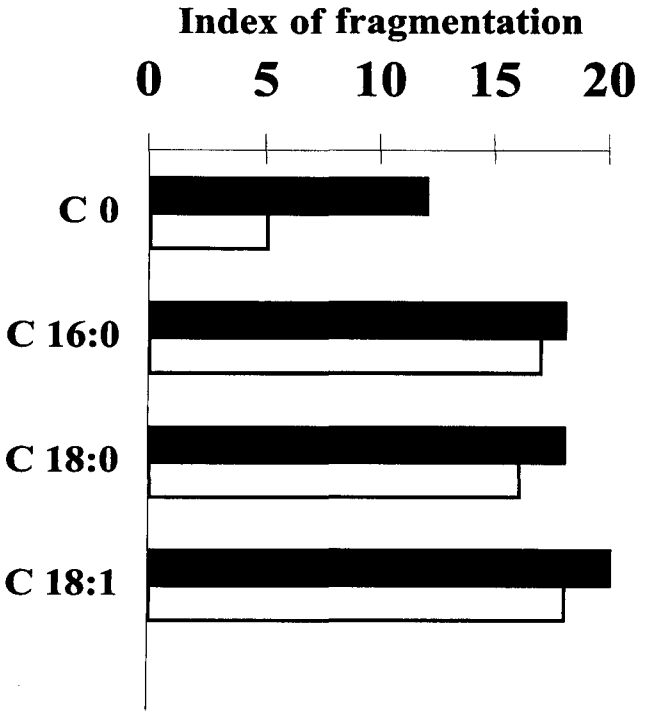

Fig. 5.17 Effect of ATP-depletion on acyl-CoA and BARS fragmenting activity of Golgi associated tubules

Golgi membranes were incubated for 20 minutes with 30 μg/ml of recombinant GST-BARS and with 10 μM of the indicated acyl-CoAs. Incubations were carried out in the presence of 1mM ATP and the ATP regenerating system (filled bars) or without ATP but in the presence of 20 U/ml Hexokinase and 10 mM glucose (filled bars). Samples were processed for negative staining and electron microscopy and the index of fragmentation was calculated as described in material and methods. The experiment was repeated twice with similar results.

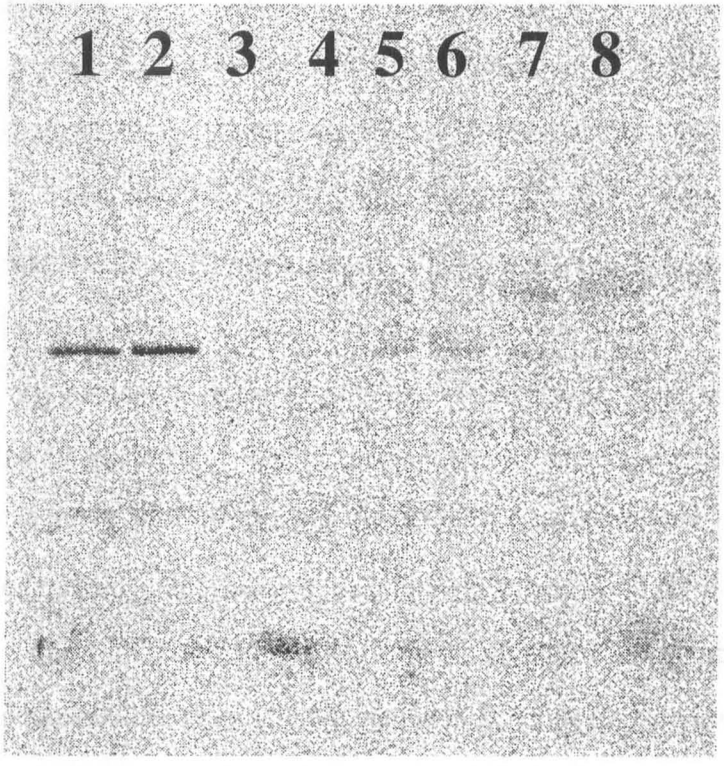

Fig. 5.18 Palmitoylation assay

2 μg of either recombinant GST (lanes 1, 3, 5, 7) or recombinant GST-BARS (lanes 2, 4, 6, 8) were incubated for 60 minutes with 10 μM [^{14}C]-pCoA as follows: with the incubation buffer (lanes 1, 2), with 2 mg/ml of rat brain cytosol (lanes 3, 4), with 0.1 mg/ml of Golgi membranes (lanes 5, 6) or with cytosol and Golgi membranes (lanes 7, 8). Samples were processed for SDS page as described in material and methods. Radiolabelled proteins were visualised by electronic autoradiography (Instant Imager, Canberra Packard). The experiment was repeated twice with similar results.

fission/fragmentation of the Golgi apparatus. Long chain acyl-CoAs are known to play a major role in lipid metabolism as acyl donors for lysolipids and lipid headgroups, or in transacylation reactions (Heath and Rock, 1998, Kent, 1995, Aguado and Campbell, 1998, Hollenback and Glomset, 1998). Thus, BARS might be an enzyme catalysing lipid acylation. To test this hypothesis, a series of commercial lipids, lysolipids and corresponding headgroups were incubated with 50 µg/ml of GST-BARS and 10 µM [^{14}C]-pCoA, and the radioactive acylated products were analysed by thin layer chromatography as described in the material and methods. Reactions were carried out for 10 and 40 minutes, in the presence of the incubation buffer (see section 4.1) in a final volume of 12.5 µl. Lipids were tested at concentrations ranging from 0.1 to 10 µM, lysolipids from 1 to 40 µM, polar headgroups from 1 to 100 µM (fig. 5.17). Of all these compounds sn1 C18:1-lysophosphatidic acid (LPA) was the only one that showed a detectable activity as acyl acceptor from [^{14}C]-pCoA, resulting in incorporation of the label into a new radioactive species. This product was [^{14}C]-phosphatidic acid (PA), as demonstrated by perfect co-migration with pure [^{14}C]-PA standard in different TLC (fig. 5.19) and HPLC chromatographic systems (fig. 5.20). Thus, BARS is an acyl-CoA dependent LPA-acyl-transferases (LPAAT).

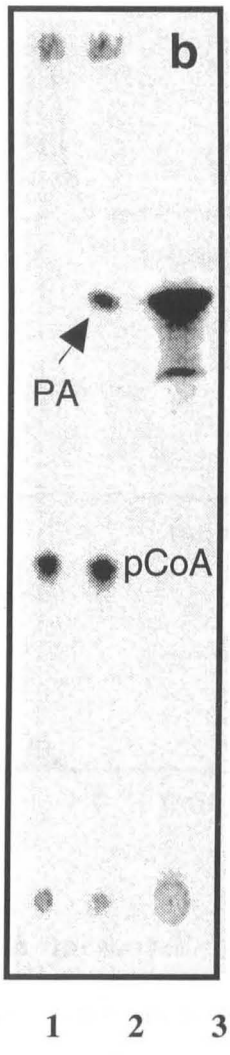

Fig. 5.19 Synthesis of PA measured by TLC

[^{14}C]-pCoA (10 μM) was incubated in the presence of 30 μM LPA (C18:1-LPA) in the absence (lane 1) or in the presence (lane 2) of 50 μg/ml recombinant BARS for 40 min. Lipids were analyzed by TLC. The [^{14}C]-PA standard is in lane 3. Other lysolipids (C14:0, C16:0 and C18:0 LPC, C16:0 and C18:0 LPE, LPI, lysophosphatidylserine (LPS), sphingosine-1phosphate), headgroups (glycerol, 3-glycerophosphate, glycero-PC, glycero-PI, glycero-PE, dihydroxyacetone) or lipids (PC, PE, PS, PI, PA) were used at various concentrations (0.1-100 μM), as potential substrates for the transferase activity of recombinant BARS. They were all inactive at all concentrations tested.

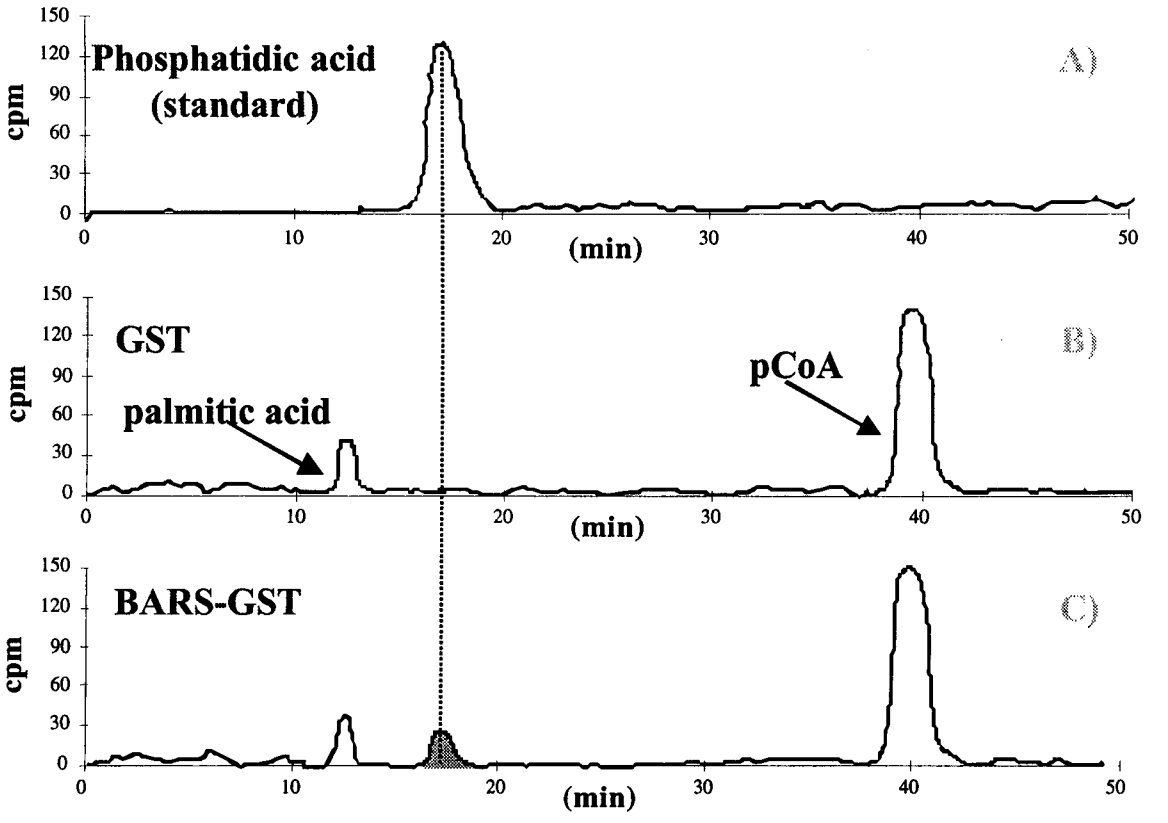

Fig. 5.20 Synthesis of PA measured by HPLC

[^{14}C]-pCoA (10 μM) was incubated in the presence of 30 μM LPA (C18:1-LPA) in the absence (B) or presence (C) of 50 μg/ml recombinant BARS for 40 min. Lipids were analyzed by HPLC in the laboratory of Molecular and Cellular Endocrinology (Department of Cell Biology and Oncology, Consorzio Mario Negri Sud) as described in Falasca et al., 1997. A. The [^{14}C]-PA standard This figure is representative of two experiments.

5.4.3 Enzymatic characterization of BARS-specific LPAAT activity

The BARS-induced LPA acyl-transferase reaction was characterized kinetically. The rate of PA formation was linear for at least 60 min in the presence of 5 μM pCoA, 30 μM LPA and 50 μg/ml of recombinant BARS. These were optimal concentrations of pCoA and LPA (5 and 30 μM, respectively), beyond which the formation of PA became gradually inhibited, making it difficult to estimate the true kinetic reaction parameters (fig. 5.21 B-C). This behaviour has previously been described for other acyl-transferases and is attributed to overcoming the CMC of the lipid substrates that became unavailable during the reaction (Jolly et al., 1998). The optimal concentration for BARS was determined (at 5 μM of pCoA and 30 μM LPA) performing a dose response curve at different time points as shown in fig 5.21 A. The catalytic rate of the reaction (approximately 1 min-1) is extremely low if compared with that of other enzymes. This could be due to the fact that the reacylation of a lysolipid is a reaction which occurs within the lipidic bilayer and the kinetic measurements were performed in an aqueous environment. To improve the presentation of the substrate different concentrations (0.01, 0.1 and 1%) of the detergent Triton X-100 were added to the reaction mixture but the formation of PA was markedly inhibited (fig. 5.21 E). Another approach was to include LPA in liposomes prepared from purified Golgi fractions as described in material and methods. Under these conditions, the PA yield increased 4-fold, suggesting that BARS is more efficient when it acts in a membrane context (fig. 5.21 D). However, the reason for such a low activity could reside in the absence of an essential cofactor or alternatively in the fact that the recombinant protein might lack an essential post-translational modification.

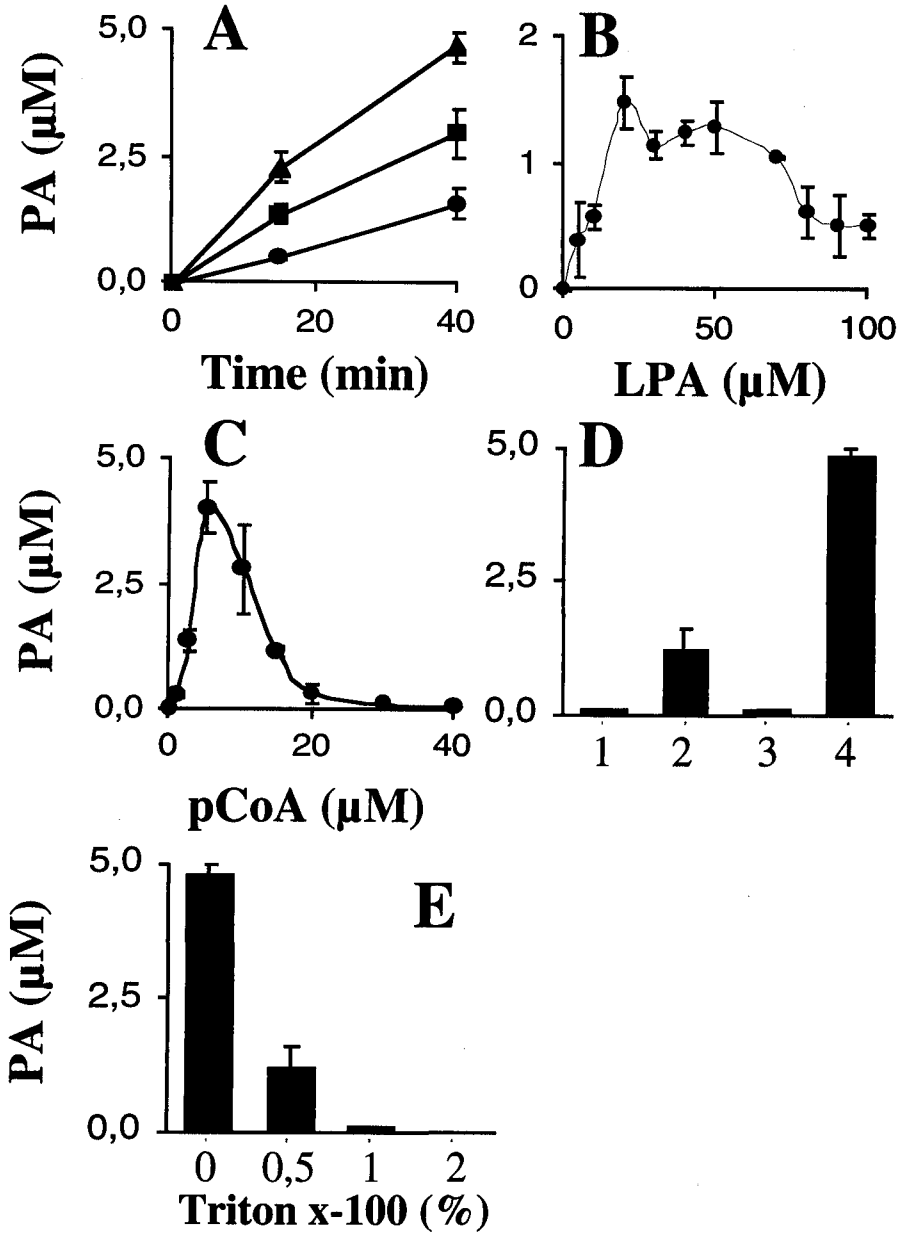

Fig. 5.21 Characterization of the BARS-dependent LPA acyltransferase activity by TLC

A. Relationship between BARS concentration and yield of PA. 25 µg/ml (circles), 50 µg/ml (squares), 100 µg/ml (triangles) of recombinant BARS were incubated for 15 or 40 min with 5 µM pCoA and 30 µM LPA. B, C. Relationship between substrate concentrations and yield of PA. Recombinant BARS (50 µg/ml) was incubated for 40 min with different concentrations of LPA (B) or pCoA (C) D. Effect of the incorporation of LPA into liposomes on the LPAAT activity of BARS. Fifty µg/ml of either recombinant BARS (2, 4) or GST (1, 3) were incubated with 5 µM pCoA for 15 min in the presence of 30 µM LPA resuspended in 25 mM Hepes, pH 7.4 (1, 2) or included in Golgi-derived liposomes (3, 4). E. Effect of Triton X-100 on the LPAAT activity of BARS. 50 µg/ml of recombinant BARS were incubated for 40 min with 5 µM pCoA and 30 µM LPA in the presence of the indicated concentrations of triton X-100. Values are means ± S.D.s of three independent experiments.

5.4.4 Acyl-Coenzymes As cofactors for LPAAT activity

The selectivity of BARS for acyl-CoAs with different acyl chains was tested. [^{3}H]-LPA (30 μM) was incubated with BARS and a series of different acyl-CoAs (10 μM) of increasing acyl chain length and degree of saturation. Short chain acyl-CoAs were inactive (C<12); above C12, the reaction rate increased with the chain length and was maximal with unsaturated long-chain compounds such as palmitoleoyl- (C16:1), oleoyl- (C18:1) and arachidonoyl- (C20:4) CoAs. Arachidonoyl-CoA was 6 times as active as pCoA (fig. 5.22). This was expected since the lysolipid-specific acyltransferases have a specificity for unsaturated AcCoAs (Kent, 1995). Notably the rank order of potency of the acyl-CoAs was the same in the acyltransferase reaction as in the Golgi tubule fission assays (compare with fig. 5.16). This is in agreement with the idea that the enzymatic and fissiogenic activities of BARS are linked.

5.4.5 ADP-ribosylation and α-PEP9 abolish LPAAT activity

To further demonstrate that the acyltransferase activity of BARS was responsible for its fissiogenic activity two different approaches were used. 50 μg/ml of the recombinant GST-BARS were pre-incubated for 1h on ice with 0.14, 0.35, 0.7, 1.4 mg/ml of the a-PEP9 antibody (already known to block the fissioning activity of BARS) corresponding to 1, 2.5, 5 and 10 fold excess of antibody. As controls, pre-incubations were carried out in parallel with the same concentrations of a purified fraction of total IgG from a pre-immune serum. The pre-incubated BARS samples were then used in a standard acyl transferase assay. The BARS acyltransferase activity was inhibited by α-PEP9 pretreatment in a dose dependent manner while the IgG pretreatment had no effect (fig. 5.23 A).

A second approach was to pre-ADP ribosylate BARS. Different concentrations of ADP-ribosylated BARS (50, 100 and 150 μg/ml) were used in the acyltransferase assay using as controls the same concentrations the mock-ribosylated BARS. The activity of the ADP-ribosylated BARS was reduced 5 folds with respect to the controls (fig. 5.23 B).

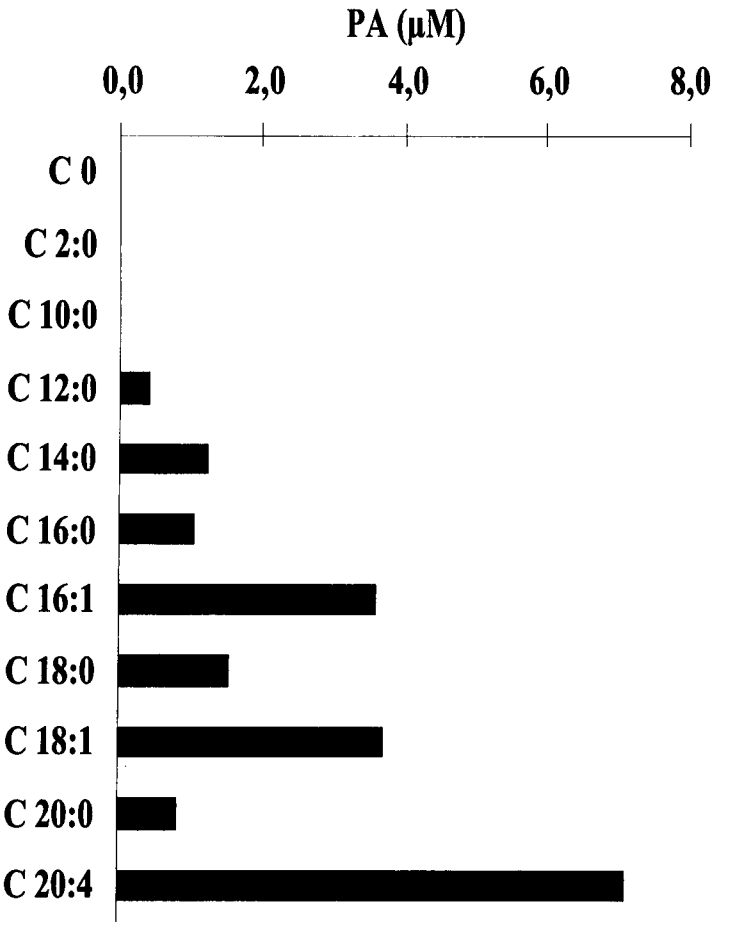

Fig. 5.22 Selectivity of the BARS LPA-acyltransferase activity with respect to type of acyl chain in acyl-CoAs

Recombinant GST-BARS or GST (30 µg/ml) were incubated for 40 minutes with [^{3}H]-C18:1 LPA (30 µM) and different unlabelled acyl-CoAs (10 µM) as substrates. TLC plates were evaluated by gas ionisation scanning using a linear analyser INB 384 (Inotech, Switzerland). Counting efficiency was ~2%. Counts were collected until a counting error <2 % was obtained. Values represent means of triplicates. S.D.s never exceeded 10% of the means. The experiment was repeated three times with similar results.

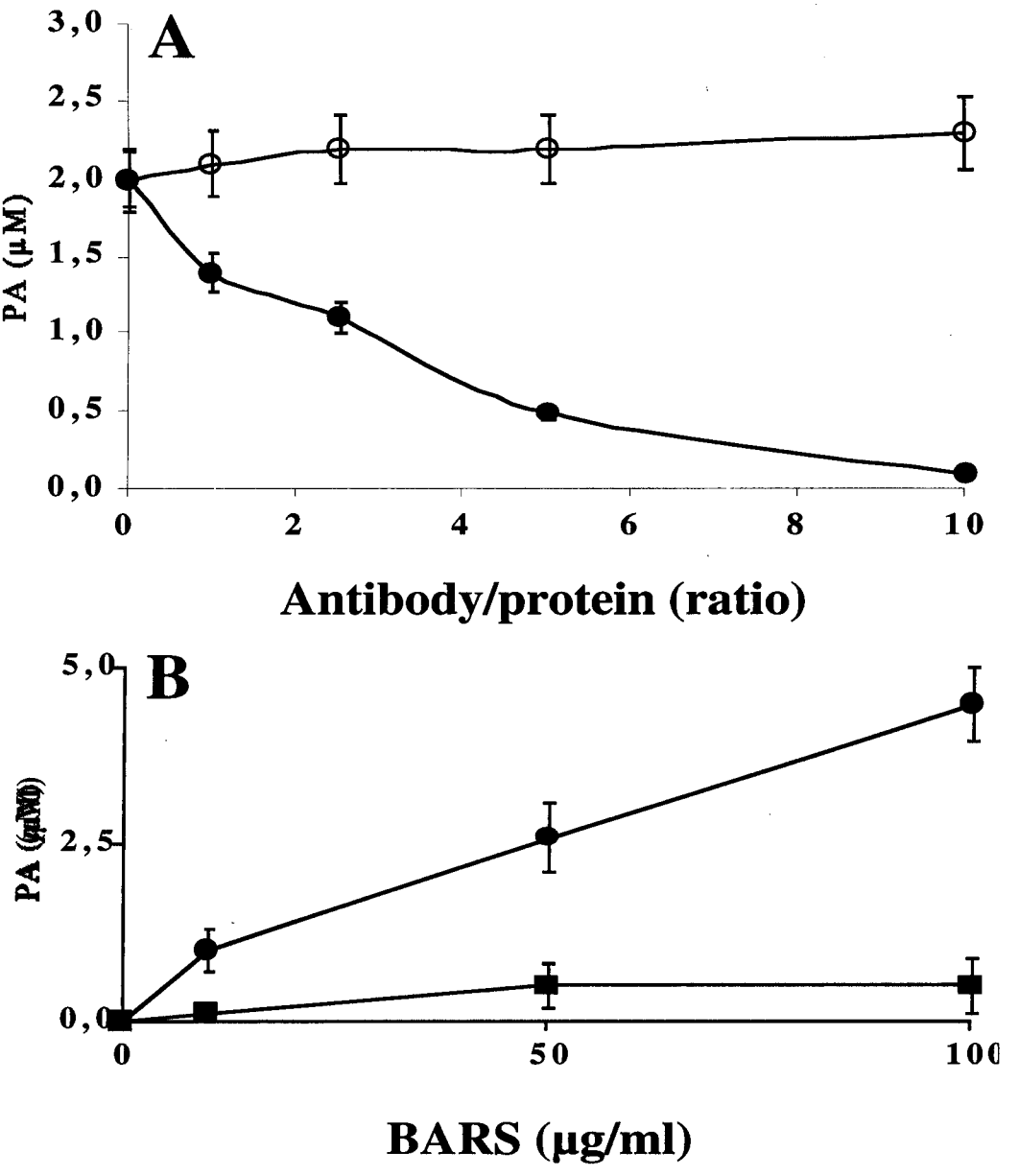

Fig. 5.23 Effect of ADP-ribosylation and the anti-PEP9 antibody on BARS-dependent LPA-acyltransferase activity

A. 50 µg/ml of recombinant GST-BARS were pretreated for 60 minutes on ice with increasing amount of either the α-PEP9 antibody (filled circles) or a purified IgG fraction (empty circles) and then incubated for 40 min with 5 µM pCoA and 30 µM LPA. B. Increasing concentrations of recombinant BARS either in the native (circles) or ADP-ribosylated (squares) forms were incubated for 40 min with 5 µM pCoA and 30 µM LPA. Lipids were analyzed by TLC and the amount of PA formed was measured. Values are means ± S.D.s of three independent experiments.

Both these observations are compatible with a causal link between the LPA acyl-transferase and fissiogenic activities of the protein, though it cannot be excluded that the fissiogenic activity might be prevented by an inhibition of the binding of the protein to the Golgi membranes.

5.4.6 PA formation in Golgi membranes

To be functionally relevant, the LPA-dependent acyl-transferase activity of BARS should result in changes in PA levels in Golgi membranes incubated under the conditions that lead to fissioning of the Golgi associated-tubules. To examine whether this was the case, the metabolic activity of the isolated Golgi membranes was first characterized in the absence of BARS. 0.1 mg/ml of Golgi membranes were incubated under standard conditions with 10 μM [^{14}C]-pCoA for 20 minutes. Golgi membranes rapidly hydrolysed [^{14}C]-pCoA to [^{14}C]-palmitic acid and CoA, and incorporated the fatty acid into several radiolabelled spots some of which were identified by using cold standards (revealed by iodination, see material and methods) or by using radiolabelled standards. PC, PI, DAG/TAG (not resolved by this chromatographic system) were identified (fig. 5.24 A) Radioactive PA was also formed, albeit in very small amounts. This finding indicates that endogenous levels of lysolipids are present in the Golgi membranes and are available for acylation reactions.

The effect of exogenous additions of both lysolipids and polar headgroups was analyzed. The addition of 30 μM of LPA, LPC, LPI was found to lead to an increase in the synthesis of the corresponding lipids (fig. 5.25). The radiolabelled spots that were increased coincided with PA, PC and PI that were previously identified in the absence of the lysolipids. None of the polar headgroups tested was acylated to the corresponding lysolipids. Thus, Golgi membranes have significant lysolipid-specific acyltransferase activity and can use the small amounts of lysolipids existing in membranes at steady state as substrate. When the effect of BARS was tested on this background activity, the formation of PA increased 3-fold (fig. 5.24).

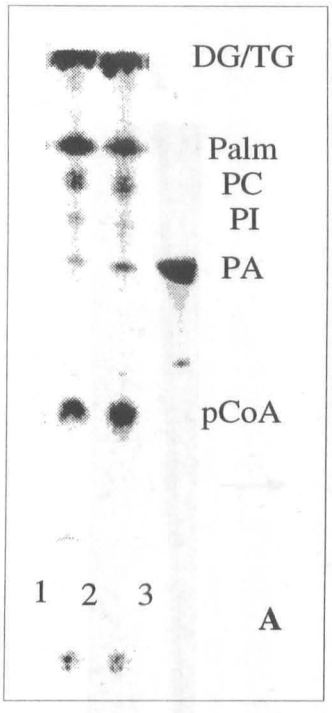

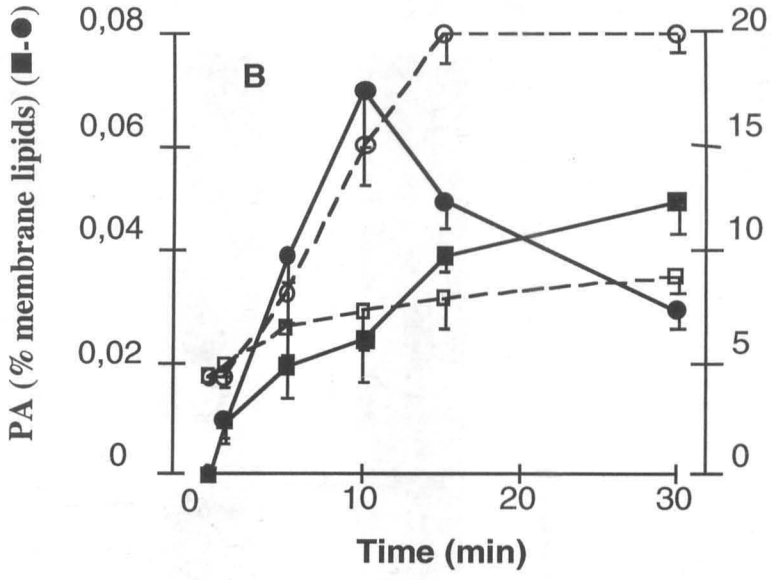

Fig. 5.24 BARS-dependent formation of PA in Golgi membranes

A. Golgi membranes were incubated with 10 μM [^{14}C]-pCoA in the absence (lane 1) or presence (lane 2) of 20 μg/ml recombinant BARS for 10 min. The label was incorporated into the lipids indicated in the figure (identified by co-migration with cold standards. PA was increased in the presence of BARS; B. Time-course of PA formation and tubule fragmentation in Golgi membranes. Membranes were incubated as described in A in the absence (squares) or in the presence (circles) of recombinant BARS and processed for lipid analysis or negative-stain electron microscopy. PA levels, calculated as percentage of total membrane lipids, are shown on the left axis (filled symbols, continuous lines) while the index of fragmentation is shown on the right axis (empty symbols, dashed lines). Values are means ± S.D.s of three independent experiments.

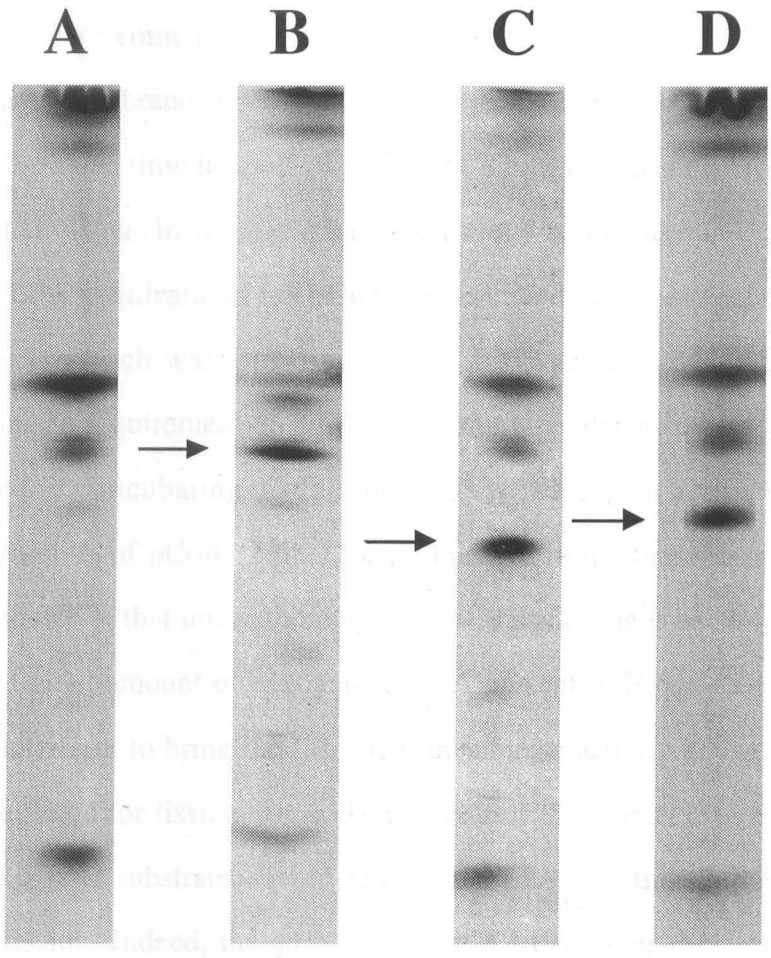

Fig. 5.25 Endogenous acyltransferase activity of Golgi membranes

Golgi membranes were incubated for 15 minutes with 10 μM [^{14}C]-pCoA with the incubation mixture (A), 30 μM LPC (B), 30 μM LPA (C), 30 μM LPI (D). Each lysolipid is acylated to the corresponding lipid. Lipids were analyzed by TLC and radiolabelled spots were revealed by electronic autoradiography (Instant Imager, Canberra Packard).

The increase was relatively rapid and transient, with a peak at 10-15 min, and a return to basal levels within 20-30 min (fig. 5.24 B). The labelling of other lipids was not changed (fig. 5.24 B). When PA levels and fission response were compared under the same conditions (in terms of BARS, pCoA and membrane concentrations), the two processes occurred roughly within the same time interval (fig. 5.24 B). Thus, BARS-induced fission is associated with an increase in PA levels in Golgi membranes.

5.4.7 LPA requirement for pCoA and BARS-dependent fission

Another approach was aimed at establishing whether, under appropriate conditions, a requirement for LPA fission could be demonstrated. This was achieved by incubating Golgi membranes with just above-threshold concentrations of pCoA (2 μM) for 20 minutes in the presence of BARS. The rationale is that under these conditions, fission might be slow because the very small amount of endogenous LPA present in Golgi membranes is barely sufficient to bring the LPA acyl-transferase activity of BARS to the levels required for fission. Thus, the addition of exogenous LPA (2μM), by providing more substrate, should activate the LPA acyl-transferase rate and trigger fission. Indeed, the addition of 2 μM LPA under these conditions induced massive fission/fragmentation of the Golgi tubular networks (fig. 5.26). In the absence of BARS, LPA or pCoA alone were inactive, and when combined only slightly active (fig. 5.26). Other lysolipids had no effect

5.4.8 PA induces fragmentation

To test whether PA was necessary for inducing the fission of the Golgi associated tubules the synthesis of PA from LPA was stimulated even in the absence of BARS. Golgi membranes were incubated for 15 minutes with different concentrations of pCoA (1, 2, 5 and 10 μM) and LPA (1, 2, 5 and 10 μM) in all possible combinations and the fission of Golgi tubules was evaluated by the negative staining technique. In parallel Golgi membranes were incubated under exactly the same conditions but using the [^{3}H]-LPA. The amount of PA was determined as described earlier.

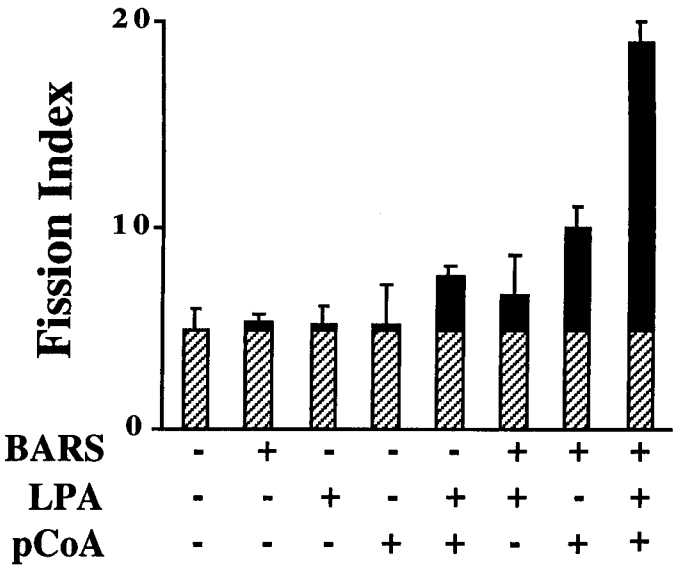

Fig. 5.26 Requirement for LPA in the BARS-induced fragmentation of isolated Golgi membranes

Golgi membranes were incubated for 15 min with 2 μM pCoA, 2 μM C18:1 LPA and 10 μg/ml recombinant BARS either alone or in combination, as indicated in the graph. The index of fragmentation (see material and methods) of untreated membranes (ca. 5, stripes) represents background fragmentation. Values are means ± S.D.s of three independent experiments.

As expected, PA was efficiently synthesised in amounts linearly related to the concentration of LPA and pCoA, and its level correlated with the fission response. At levels of PA above 0.2 % of the total membrane lipids, fission began to occur, and reached a maximum at 0.6 % (fig. 5.27). The morphological features of the resulting fragments were similar to those induced by BARS, and constricted fission intermediates were also observed. A difference from the effects of BARS was that not only tubular networks, but also Golgi cisternae underwent a degree of fragmentation, possibly because PA is synthesised non-specifically in all of the Golgi components under these conditions. Notably, LPA in the absence of pCoA had no fissiogenic activity; it only induced a small degree of tubulation and formation of bud-like structures at concentrations above 10 μM. Other lysolipids (LPC and LPI used at 30 μM) incubated with pCoA under the same conditions gave rise to the corresponding lipids with the same efficiency as LPA, but showed no sign of fissiogenic activity. These results show that the acylation of LPA to PA is sufficient to cause membrane fission. Interestingly, however, if the levels of PA associated with fission in the absence and in the presence of BARS are compared, it appears that less PA (3-6-fold) is needed for fission when BARS is present (fig. 5.27). An interpretation is that BARS acts at specific sites on Golgi tubules, while endogenous transferases probably increase PA non-specifically throughout the surface of the Golgi membranes, as is also suggested by the features of fission in the absence of BARS.

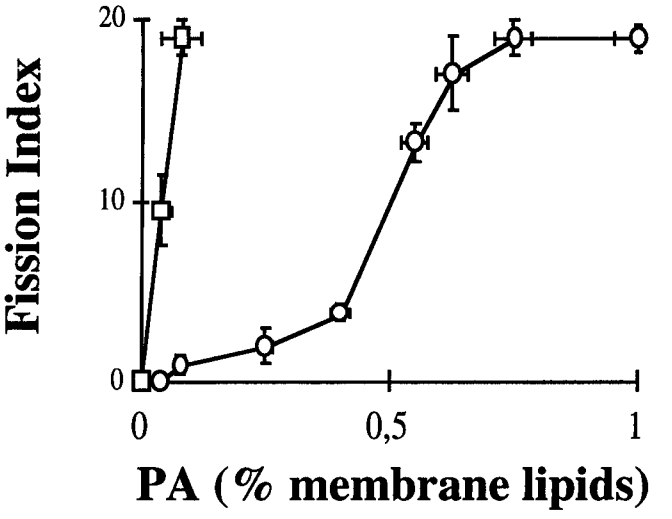

Fig. 5.27 PA synthesis in Golgi membranes is associated with membrane fragmentation

Golgi membranes were incubated for 15 min in the presence of 10 μg/ml recombinant BARS plus 5 or 10 μM [^{14}C]-pCoA (squares), or of increasing concentrations of pCoA (1 to 10 μM) plus [^{3}H]-C18:1 LPA (1 to 10 μM) (circles), and the newly formed PA was measured. Parallel, unlabelled samples were obtained and processed for electron microscopy. The index of fragmentation is reported as a function of the PA levels in Golgi membranes. Values are means ± S.D.s of three independent experiments.

5.6 Discussion

BARS is an essential component of the mechanism which promotes the fission of the Golgi tubular networks into clusters of vesicles of different diameters. This has been shown both by the in vitro morphological assay, developed during this thesis work, and by conventional electron microscopy. Further, the BARS fissioning/fragmenting activity has been reproduced in permeabilized cells. Very interestingly, this effect was preceded by the formation of constrictions on the surface of tubules, that were considered as intermediates in fission. They were found to reach the surprisingly small diameter of 11 nm, that is more compatible with the accumulation of non-bilayer lipids (see section 1.1.4). This observation is in agreement with the enzymatic activity of BARS that was found to be a rather specific acyltransferase which catalyses, in Golgi membranes, the acylation of LPA to PA. Several pieces of evidence suggest that the LPAAT activity of BARS is linked closely with its fission activity. First, conditions that inhibit the LPAAT activity (the blocking antibody α-PEP9 and the ADP-ribosylation) also block fission; second both the fission and the LPAAT activity have a stringent requirement for both the acyl-CoAs and LPA; and finally, the increase in PA levels in Golgi membranes is sufficient to cause fission even in the absence of BARS.

CHAPTER 6
FINAL DISCUSSION

One of the main achievements of this work has been to set up a morphological assay suitable for visualising Golgi-associated tubules and for studying their behaviour under different experimental conditions. This assay was based on the negative staining technique of whole-mount preparations and this was chosen for the following reasons. First, it has the necessary resolution for visualising Golgi tubules whose diameters are in the nanometer range. Second, it allows unambiguous discrimination of tubules and vesicles (not possible with the conventional electron microscopy since this is based on sectioning procedures). Finally, it is appropriate for screening purposes since it is extremely rapid for both the realisation and the analysis of the results.

Although the negative staining technique was originally developed in the fifties (Hall, 1954), it has only recently has been used to study Golgi tubules in vitro (de Figueiredo et al., 1999, Banta et al., 1995, Cluett et al., 1993). However, previous studies were carried out without proper controls and in the absence of any fixation. As shown in this thesis work, the stabilisation of membranes with a chemical fixative is extremely important for the reliability of the results, suggesting that many of the reported findings in the literature need to be carefully re-evaluated. The assay set up in this work has been extensively characterized and has allowed the in vitro reproduction of the well known effects of BFA and GTP-γS. These reagents were chosen for their quite different actions on the Golgi apparatus, the former inducing a strong tubulation effect (Orci et al., 1991), the latter an extensive vesiculation (Melançon et al., 1987). Furthermore, most of the crucial experiments were performed in parallel using negative staining and conventional thin sections and similar results were obtained. This assay was also amenable to a quantitative analysis and this was always performed in

single blind fashion and by using an unbiased systematic random procedure (Lucocq, 1993, Misteli and Warren, 1995, 1994).

The assay has been used to screen for molecules and experimental conditions that could potentially affect the morphology of the Golgi associated tubules. The involvement of specific molecules was investigated and some had interesting effects in stimulating the formation or disruption of Golgi-associated tubules. In particular, the effects of the small GTP-binding protein ARF (Boman and Kahn, 1995), the coatomer complex (Sheckman and Melmann, 1997), the nucleotide NAD^+ (Mironov et al., 1997), some lipidic modifying enzymes as the phospholipases A2, C and D (Kent, 1997), the small lipidic molecules AcCoAs (Kent, 1997), and BARS, the substrate of the BFA-dependent ADP-ribosylation (Spano' et al., 1999) were analyzed. Among these BARS was the most interesting and its effect was extensively characterized.

BARS was found to selectively fragment Golgi associated tubules generating a series of vesicles of different diameters. This activity is a cytosolic activity, it can be inhibited by a specific blocking antibody (α-PEP9) or by mono-ADP ribosylation, it requires a cytosolic cofactor and its activity can also be seen in permeabilised cells. Interestingly the complete fragmentation of Golgi tubules was preceded by the formation of constrictions along the tubules with curvatures varying from slight to extreme. The constrictions delineated vesicular structures with diameters matching those of fully formed vesicles detected at later times. This strongly suggests that these constrictions are intermediates in the fission process.

The physiological role of the BARS-induced fission of the Golgi associated tubules is of interest for several reasons. First, the sites where fission occurs can also be observed in living cells and specifically at the level of the TGN which is thought to contain intermediates in the formation of secretory granules (Ladinski et al., 1997, Rambourg and Clermont, 1990). Further the fragmentation of both the tubules and the cisternae can be observed during mitosis (Misteli and Warren, 1995, 1994). Since BARS belongs to the CtBP

family, a class of proteins involved in the regulation of transcriptional events and that are phosphorylated during the cell cycle (Schaeper et al., 1998, 1995), it is attractive to speculate that BARS may play a role in mitotic fragmentation. Under the experimental conditions used in this work, the tubular elements of the isolated Golgi stacks or those present in permeabilized cells were fragmented regardless of their location (cis or trans side, non compact zone), making it difficult to be sure of the in vivo role of BARS. However, the availability of the BARS cDNA and a antibody reagent should facilitate more detailed analysis of this issue.

The morphological analysis of the fission intermediates has revealed that the BARS-induced constrictions are extremely narrow, reaching the surprising low value of 11 nm. Since the lipid bilayer measures 4 nm in thickness, the lumenal space is reduced to 3 nm. At equilibrium, this level of membrane curvature is almost certainly incompatible with the lipid composition of a normal membrane bilayer. The minimum vesicular diameter that will accommodate "cylindrical" lipids (e.g. PC) is 25 nm (Cullis and de Kruijff, 1979). Thus, the presence of cylindrical lipid species should be energetically unfavourable in constricted fission sites. Instead, an enrichment with "cone-shaped" lipids (e.g. DAG) in the lumenal leaflet, and "inverted cone-shaped" lipids (lysolipids) in the cytosolic leaflet of the membrane might facilitate the formation of such highly curved intermediates, and thereby reduce the energy barrier to fission. The finding that BARS is an acyl-CoA-dependent acyltransferase specific for LPA would be consistent with this proposal. This activity appears to be closely linked with BARS-induced fission for three reasons. First, both activities are inhibited by mono-ADP-ribosylation and by the antibody α-PEP9. Second, both activities show the same requirement for acyl-CoA and LPA. Finally, the BARS-induced formation of PA in Golgi membranes correlates temporally with BARS-induced fission/fragmentation.

What is unique about the LPA/PA system, and what are the mechanisms by which the LPA acyl-transferase reaction triggers fission? PA does have

unique physical properties. This lipid is rare in living cells (around 2% of the total phospholipids; Kent, 1997), but it is a key intermediate in many metabolic pathways. It has a small headgroup with a high charge density, capable of acting both as a hydrogen donor and acceptor. Thus, a reduction in ionisation of PA, e.g. upon binding divalent cations, results in the formation of PA-rich microdomains through intermolecular hydrogen bonding; the same probably holds for LPA (Boggs, 1987). Moreover, the shape of PA can vary depending on the presence of calcium: its normal cylindrical shape becomes conical when mM calcium is present (Verkleij et al., 1982). In contrast, LPA has an inverted-cone shape. Moreover, PA can be rapidly dephosphorylated to diacylglycerol, which is in itself strongly conical. Diacylglycerol can spontaneously flip-flop across the bilayer, and hence affects the composition of the lumenal leaflet even when it is formed at the cytosolic surface. Thus, a lipid microdomain containing LPA, PA and diacylglycerol rapidly interconverting, has the potential to act as a lipid machine driving, or at least facilitating, the formation of highly curved fission intermediates leading to fission.

A more detailed model of lipid-driven fission is premature at this time. The lipid fission machinery might be more complex, and involve phospholipases, PA phosphatases, flippases, as well as lipid-binding proteins, such as the phosphatidylinositol carrier protein, recently implicated in fission in the Golgi (Simon et al., 1998). However, it could not be excluded that the formation of the fission intermediates might be facilitated by a mechanical stress imposed on the membrane, such as that which has been proposed to be induced by dynamin (McNiven, 1998). It is important to point out that the differences in the number of fission intermediates detected in the absence of cytosol (i.e. with BARS and acyl-CoA) suggests that other factors might be implicated at least in the final stage of the fission process and that possibly, the BARS-induced formation of PA is linked specifically to the initial deformation of the membrane. Finally, it has to be mentioned that very recently, while this thesis was under preparation, lipid

modifications have been shown to be important in dynamin-driven fission. A dynamin binding protein, SH3p4 (Ringstadt et al., 1997) has been proposed to be required for the formation of endocytic vesicles and very strikingly like BARS, it has a LPA acyl-transferase enzymatic activity. This would suggest that dynamin, in addition to its proposed mechanochemical activity, requires synergy with a lipid metabolic pathway, similar to the one activated by BARS.

In conclusion, the main goal of this thesis work has been achieved, and the mechanism for regulating the breakdown of Golgi-associated tubules has been elucidated at the molecular level. BARS represents an extremely useful tool that could be used to interfere with tubular homeostasis with the potential to provide a better understanding of the physiological role of the tubules. This assay is already being used to characterize other molecules that might affect Golgi tubules (see chapter 4).

ABBREVIATIONS

AcCoAs	Acyl-coenzyme As
APS	Ammonium per sulphate
ARF	ADP-ribosylation factor
ATP	Adenosine 5' triphosphate
BARS	BFA-dependent ADP-ribosylation substrate
BFA	Brefeldin A
BSA	Bovine serum albumin
CaBP1	Calcium binding protein
CGN	Cis-Golgi network
CHO	Chinese hamster ovary
CM	Ceramide
CMC	Critical micellar concentration
CP	Creatin phosphate
CPK	Creatinphosphokinase
CtBPs	C-terminal binding proteins
DAG	Diacyglycerol
DMEM	Dulbecco's Modified Eagle Medium
DTT	DL-dithiothreitol
EDTA	Ethylendiaminetetraacetic acid
EGTA	Ethylene glycol bis (βaminoethylether) N,N,N',N' - tetracetic acid
ER	Endoplasmic reticulum
ERGIC	ER-Golgi intermediate compartment
FCS	Fetal calf serum
GAPDH	Glyceraldehyde 3-phosphate dehydrogenase
GAP	GTPase activating protein
GEF	Guanosine exchange factor

GFP	Green fluorescent protein
GST	Gluthathione-S-transferase
GTP	Guanosine tri-phosphate
HRP	Horse radish peroxidase
HVEM	High voltage electron microscopy
LPA	Lyso-PA
LPAAT	LPA acyltransferase
LPC	Lyso-PC
LPE	Lyso-PE
LPI	Lyso-PI
LPS	Lyso-PS
MEM	Modified Eagles Medium
MPRS	Mannose 6-phosphate receptors
MVB	Multivesicular bodies
NAD^+	Nicotinamide adenine di-nucleotide
NRK	Normal rat kidney
OsO_4	Osmium tetroxide
PA	Phosphatidic acid
PBS	Phosphate saline buffer
PC	Phospahtidylcholine
pCoA	Palmitoyl-CoA
PE	Phospahtidylethanolamine
PG	Phosphatydilglycerol
PI	Phosphatydilinositol
PI-PLC	PI-specific phospholipase C
PIs	Phosphoinositides
PITP	Phosphatidylinositol transfer protein
PLA_2	Phospholipases A_2
PLD	Phospholipase D
PM	Plasma membrane
PS	Phosphatidylserine

PTA	phosphotungstic acid
RBL	Rat basophilic leukaemia 2H-3
RER	Rough ER
SDS	Sodium dodecyl sulphate
SER	Smooth ER
SLBPA	Semilysobisphospahtidic acid
SLO	Streptolysin O
SM	Sphingomyelin
STI	Soybean trypsin inhibitor
TEM	Transmission electron microscopy
TGN	Trans-Golgi network
TLC	Thin layer chromatography
TMD	Transmembrane domain
TRIS	Trizma-base
UA	Uranyl acetate

ACKNOWLEDGEMENTS

I would like to start by thanking both Alberto Luini and Prof. Alan Hall for their continuous support during the course of this investigation.

Thanks also to a number of colleagues for their precious help and for the useful scientific discussions, and in particular to Roberto Buccione, Daniela Corda, Alexander Mironov, Roman Polishchuk, and Elena Polishchuk.

A special thanks to Chris Berrie for his patience, especially during this last months.

A very special thanks to Gabriele Turacchio for his continuous and extremely important help.

Finally, thanks to my parents who have supported me during the last four years.

REFERENCES

Acharya, U., J.M. Mc Caffery, R. Kacobs, and V. Malothra "Reconstitution of vesiculated Golgi membranes into stacks of cisternae: requirement of NSF in stack formation"(1995) *J. Cell Biol.* 129:577-589

Acharya, U., Mallabiabarrena, A., Acharya, J.K. J.M., and V. Malothra "Signalling via mitogen-activated protein kinase kinase (MEK1) is required for Golgi fragmentation during mitosis" (1998) *Cell* 92: 183-192

Aguado, B., and Campbell, R.D. "Characterization of a human lysophosphatidic acid acyltransferase that is encoded by a gene located in the class III region of the human major histocompatibility complex" (1998) *J. Biol. Chem.* 273: 4096-4105

Ajala, J.S. "Transport and internal organization of membranes: vesicles, membrane networks and GTP-binding proteins" (1994) *J. Cell Sci.* 107: 753-763

Allan, B.B., and Balch, W.E. "Protein sorting by directed maturation of Golgi compartments" (1999) *Science* 285: 63-66

Allan, D. and Kallen, K.J. "Is plasma membrane lipid composition defined in the exocytic or the endocytic pathway ?" (1994) *Trends in Cell Biol.* 4:350-353

Allan, V. and Vale, R. "Cell cycle control of microtubule-based membrane transport and tubule formation in vitro" (1991) *J. Cell Biol.* 113: 347-359

Allan, V. and Vale, R. "Movement of membrane tubules along microtubules in vitro: evidence for specialised sites of motor attachment" (1994) *J. Cell Sci.* 107: 1885-1897

Altschuler, Y., Barbas, S.M., Terlecky, L.J., Tang, K., Hardy, S., Mostov, K.E., Schmid, S.L. "Redundant and distinct functions for dynamin-1 and dynamin-2 isoforms" (1998) *J. Cell Biol.* 143: 1871-1881 .

Balch, W.E., Dunphy, W., Braell, W.A., and Rothman, J.E., "Reconstitution of the transport of protein between successive compartments of the Golgi measured by the coupled incorporation of N-acetylglucosamine" (1984) *Cell* 39: 405-416

Bannykh, S.I., and Balch, W.E. "Membrane dynamics at the endoplasmic reticulum-Golgi interface" (1997) *J.Cell Biol* 138: 1-4

Bannykh, S.I., Nishimura, N., and Balch, W.E. "Getting into the Golgi" (1998) *Trends in Cell Biol.* 8: 21-25

Bannykh, S.I., Rowe,T., and Balch, W.E. "The organization of endoplasmic reticulum export complexes" (1996) *J. Cell Biol.* 135:19-35

Banta, M., Polizotto, R.S., Wood, S.A., de Figuereido, P., and Brown, W.J., "Characterization of a cytosolic activity that induces the formation of Golgi membranes tubules in a cell-free reconstitution system". (1995) *Biochemistry*, 34: 13359-13366

Bar-Tana, J., and Shapiro, B. "Long-chain fatty acyl-CoA synthetase from rat liver microsomes. EC 6.2.1.3 fatty acyl-CoA ligase (ATP)" (1975) *Methods Enzymol.* 35:117-22

Barlowe, C., Orci, L., Yeung, T., Hosobuchi, M., Hamamoto, S., Salama, N., Rexach, M.F., Ravazzola, M., Amherdt, M., and Schekman, R. "COPII: a membrane coat formed by Sec proteins that drive vesicle budding from the endoplasmic reticulum" (1994) *Cell* 77:895-907

Barr F.A., Puype, M., Vandekerckhove, J., and Warren, G. "GRASP65, a protein involved in the stacking of Golgi cisternae" (1997) *Cell* 91: 253-62

Beams, H.W., and Kessel, R.G. "The Golgi apparatus: structure and function" (1968) *Int Rev Cytol* 23:209-76

Bereiter-Hahn, J. "Behavior of mitochondria in the living cell" (1989) *Int. Rev. Cytol* 122: 1-63

Berger, E.G. "The Golgi apparatus: from the discovery to contemporary studies" (1997) in *The Golgi apparatus* eds Berger, E. G. & Roth, J. 1-36

Bergmann, J.E. "Using temperature-sensitive mutants of VSV to study membrane protein biogenesis" (1989) *Methods Cell Biol.* 32: 85-110

Boggs, J.-M. "Lipid intermolecular hydrogen bonding: influence on structural organization and membrane function" (1987) *Biochim Biophys Acta* 906:353-404

Boman, A.L. and Kahn, R.A. "ARF proteins: the membrane police ?" (1995) *Trends in Bioch. Sci.* 20: 147-150

Bonfanti, L., Mironov, A., Jr., Martinez-Menarguez, J.A., Martella, O., Fusella, A., Baldassarre, M., Buccione, R., Geuze, H.J., Mironov, A.A., and Luini, A. "Procollagen traverses the Golgi stack without leaving the lumen of cisternae: evidence for cisternal maturation" (1998) Cell 95: 993-1003

Boyd, J.M., Subramanian, T., Schaepher, U., La Regina, M., Bayley, S., and Chinnaduray, G. "A region in the C-terminus of adenovirus 2/5 E1a protein is required for association with a cellular phosphoprotein and important for the negative modulation of T24-ras mediated tranformation, tumorigenesis and metastasis" (1993) *EMBO J.* 12: 469-478

Bremser, M., Nickel, W., Schweikert, M., Ravazzola, M., Amherdt, M., Hughes, C.A., Sollner, T.H., Rothman. J.E., and Wieland, F.T. "Coupling of coat assembly and vesicle budding to packaging of putative cargo receptors" (1999) *Cell* Feb 19;96(4):495-506

Bretscher, M.S., and Munro, S. "Cholesterol and the Golgi Apparatus". (1993) *Science* Vol. 61: 1280-1281

Buccione, R., Bannykh, S., Santone, I., Baldassarre, M., Facchiano F., Bozzi, Y., Di Tullio, G., Mironov, A., Luini, A. and De Matteis, M.A. "Regulation of constitutive exocytic transport by membrane receptors. A biochemical and morphometric study" (1996) *J. Biol. Chem.* 271: 3523-3533

Campbell, J.L., and Schekman, R. "Selective packaging of cargo molecules into endoplasmic reticulum-derived COPII vesicles" (1997) *Proc. Natl. Acad. Sci.* USA94:837-842

Cao, H., Garcia, F. & McNiven, M. A. "Differential distribution of dynamin isoforms in mammalian cells" (1998) *Mol. Biol. Cell* 9, 2595-2609.

Cavenagh, M.M,Whitney, J.A., Carrol, K., Zhang, C.J., Boman, A.L., Rosenwald, A.G., Mellman, I., and Kahn, R.A. (1996) *J. Biol. Chem.* 271: 21767-21774

Chalfie, M., Tu, Y., Euskirchen, G., Ward, W.W., Prasher, D.C. "Green fluorescent protein as a marker for gene expression" (1994) *Science* 263: 802-5

Chirulovu, S., Warriner, H.E., Naranjo, E., Idziak, S.H.J., Radler, J.O., Plano, R.J., Zasadzinski, J.A., and Safinya, C.R. "A phase of liposomes with entangled tubular vesicles" (1994) *Science* 266: 1222-1225

Clapham, D.E., and Neer, E.J. "G protein βγ subunits" (1997) *Annu. Rev. Pharmacol. Toxicol.* 37: 167-203

Cluett, E.B. and Brown W.J. "Adhesion of Golgi cisternae by proteinaceous interactions: intercisternal bridges as putative adhesive structures" (1992) *J. Cell Sci.* 103: 773-784

Cluett, E.B., and Machamer, C.E. "The envelope of vaccinia virus reveals an unusual phospholipid in Golgi complex membranes" (1996) *J. Cell Sci.* 109: 2121-2131

Cluett, E.B., Kuismanen, E., and Machamer, C.E. "Heterogeneous distribution of the unusual phospholipid semilysophosphatidic acid through the Golgi complex" (1997) *Mol. Biol. Cell* 8: 2233-2240

Cluett, E.B., Wood, S.A., Banta, M., and Brown, W.J. "Tubulation of Golgi membranes in vivo and in vitro in the absence of brefeldin A". (1993), *J. Cell Biol.* 120: 15-24

Cole, N.B., Ellenberg, J., Song, J., DiEuliis, D., Lippincott-Schwartz, J. "Retrograde transport of Golgi-localized proteins to the ER" (1998) *J. Cell Biol.* 140:1-15

Conradt, B., Shaw, J., Vida, T., Emr, S., and Wickner, W. "In vitro reactions of vacuole inheritance in Saccharomyces Cerevisiae" (1992) *J. Cell Biol.* 119: 1469-1479

Cooper, M.S., Cornell-Bell, A.H., Chernjavsky, A., Dani, J.W., and Smith S.J. "Tubulovescicular processes emerge from Trans-Golgi cisternae, extend along microtubules, and interlink adjacent trans-Golgi elements into a reticulum" (1990) *Cell* 61: 135-145

Corsi, A.K. and Sheckman, R. "Mechanism of polypeptide translocation into the endoplasmic reticulum" (1996) *J. Biol. Chem* 271: 30299-30303

Cosson, P., and Letourneur, F. "Coatomer (COPI)-coated vesicles: role in intracellular transport and protein sorting" (1997) *Curr Opin. Cell Biol.* 9: 484-7

Cremona, O., and De Camilli, P. "Synaptic vesicle endocytosis" (1987) *Curr. Opin. Neurobiol.* 3: 323-30

Cullis, P. P., Fenske, D. B. and Hope, M. in *Biochemistry of Lipids, Lipoproteins and Membranes* (eds Vance, D. E. & Vance, J. E.) 1-32 (Elsevier Science, 1996).

Cullis, P.R. and De Kruijff, B. "Lipid polimorphism and the functional roles of lipids in biological membranes" (1979) *Bioch. Biophys. Acta* 559: 399-420

Cunningham, W.P., Morre', J.D., and Mollenhauer, H.H. "Structure of isolated plant Golgi apparatus revealed by negative staining" (1966) *J. Cell Biol* 28: 169-179

Cunningham, W.P., Staehlin, A.L., Rubin, R.W., Wilkins, R., and Bonneville, M. "Effect of phosphotungstate negative staining on the morphology of the isolated Golgi apparatus" (1974) *J. Cell Biol* 62: 491-504

Dabora, S.L. and Sheetz, M.P. "The microtubule-dependent formation of a tubulovescicular clusters network with characteristics of the ER from cultured cells extracts" (1988) *Cell* 54:27-35

Dalton, A.J., and Felix, M.D. (1954) *Am. J. Anat.* 94: 171-187

De Matteis, M.A., Di Girolamo, M., Colanzi, A., Pallas, M., Di Tullio, M., Mc Donald, L.J., Moss, J., Santini, G., Bannykh, S., Corda, D. and Luini A. "Stimulation of endogenous ADP-ribosylation by brefeldin A" (1994) *Proc. Natl. Acad. Sci.* 91:1114-1118.

De Matteis, M.A., Di Tullio, G., Buccione, R., and Luini A. "Characterization of calcium-triggered secretion in permeabilized rat basophilic leukemia cells" (1991) *J. Biol. Chem.* 266: 10452-10460

de Figueiredo, P., Drecktrah, D., Katzenellenbogen, J.A., Strang, M., and Brown, W.J. "Evidence that phospholipase A_2 activity is required for Golgi complex and trans Golgi network membrane tubulation" (1998) *Proc. Natl. Acad. Sci.* USA 95: 8642-7

de Figueiredo, P., Polizotto, R.S., Drecktrah, D., and Brown, W.J. "Membrane Tubule-mediated Reassembly and Maintenance of the Golgi Complex Is Disrupted by Phospholipase A_2 Antagonists" (1999) *Mol.Biol. Cell* 10: 1763-1782 .

de Figuereido, P. and Brown, W.J. "A role for calmodulin in organelle membrane tubulation" (1995) *Mol. Biol. Cell* 6: 871-887

Denker, S.P., McCaffery, J.M., Palade, G.E., Insel, P.A., and Farquhar, M.G. "Differential distribution of alpha subunits and beta gamma subunits of heterotrimeric G proteins on Golgi membranes of the exocrine pancreas" (1996) *J. Cell Biol.* 133:1027-40

Dennis, E.A. "Diversity of group types, regulation, and function of phospholipase A2" (1994) *J. Biol. Chem.* 269: 13057-13060

Di Girolamo, M., Silletta, M.G., De Matteis, M.A., Braca, A., Colanzi, A., Pawlak, D., Rasenik, M.M., Luini, A., and Corda, D. "Evidence that the 50-kDa substrate of brefeldina A-dependent ADP-ribosylation binds GTP and is modulated by the G-protein $\beta\gamma$ subunit complex" (1995) *Proc. Natl. Acad. Sci.* USA 92:7065-7069

Dominguez, M., Fazel, A., Dahan, S., Lovell, J., Hermo, L., Claude, A., Melancon, P., and Bergeron, J.J. "Fusogenic domains of golgi membranes are sequestered into specialized regions of the stack that can be released by mechanical fragmentation" (1999) *J Cell Biol* 145: 673-88

Donaldson, J.G. , and Klausner, R.D. "ARF: a key regulatory switch in membrane traffic and organelle structure" (1994) *Current Opin. in Cell Biol.* 6: 527-532

Donaldson, J.G. , Lippincott-Schwartz, J. and Klausner, R.D. "Guanine nucleotides modulate the effects of brefeldin A in semipermeable cells: regulation of theassociation of a 110-kD peripheral membrane protein with the Golgi apparatus" (1991) *J. Cell. Biol.* 112:579-588

Donaldson, J.G. , Lippincott-Schwartz, J., Bloom, G.S., Kreis, T.E., and Klausner, R.D. "Dissociation of a 110-kD peripheral membrane protein from the Golgi apparatus is an early event in brefeldin A action." (1990) "*J. Cell. Biol.* 111:2295-2306

Donaldson, J.G., Finazzi, D., and Klausner, R.D. "Brefeldin A inhibits Golgi membrane-catalysed exchange of guanine nucleotide onto ARF protein" (1992) *Nature* 360: 350-352

Epand, R.M., ed. Lipid Polymorphism and Membrane Properties, *Current Topics in Membranes*, Vol. 44, Academic Press, San Diego (1988).

Farquhar, M.G., and Hauri, H.P. in *The Golgi apparatus* (eds Berger, E. G. & Roth, J.) 37-60 (Birkhauser Verlag, 1997).

Farquhar, M.G., and Palade, G. "The Golgi apparatus 100 years of progress and controversy" (1998) *Trends in Cell Biol.* 8:2-10

Fuchs, H., Gessner, R., Tauber, R., and Ghosh, R. "Functional reconstitution of the human placental transferrin receptor into phospholipid

bilayer leads to long tubular structures proceeding from the vesicle surface" (1995) *Biochemistry* 34: 6196-6207

Fullekrug, J., Sonnichsen, B., Wunsch, U., Arseven, K., Nguyen, Van P., Soling, H.D., and Mieskes, G. "CaBP1, a calcium binding protein of the thioredoxin family, is a resident KDEL protein of the ER and not of the intermediate compartment" (1995) *J Cell Sci* 107:2719-27

Fullerton, A.T., Bau, M.Y., Conrad, P.A., and Bloom, G. "In vitro reconstitution of microtubule plus end-directed, GTPγS-sensitive motility of Golgi membranes" (1998) *Mol. Biol. Cell* 9: 2699-2714

Ganong, B. R. & Bell, R. M. Transmembrane movement of phosphatidylglycerol and diacylglycerol sulfhydryl analogues. *Biochemistry* 23, 4977-4983 (1984).

Gilman, A.G. "G proteins: transducers of receptor-generated signals" (1987) *Annu. Rev. Biochem.* 56: 615-649

Glick, B. S. and Rothman, J. E. "Possible role for fatty acyl-coenzyme A in intracellular protein transport" (1987) *Nature* 326: 309-312

Gneny, M.E. "Calmodulin in neurotransmitter and hormone action" (1993) *Annu. Rev. Pharmacol. Toxicol.* 32:45-70

Godi, A., Pertile, P., Meyers, R., Marra, P., Di Tullio, G., Iurisci, C., Luini, A., Corda,D. and De Matteis, M.A. "ARF mediates recruitment of PtdIns-4-OH kinase- and stimulates synthesis of PtdIns(4,5)P2 on the Golgi complex" (1999) *Nature Cell Biol.* 1 :280-287

Godi, A., Santone, I., Pertile, P., Devarajan, P., Stabach, P.R., Morrow, J.S., Di Tullio, G., Polishchuk, R., Petrucci, T.C., Luini, A., and De Matteis, M.A. "ADP ribosylation factor regulates spectrin binding to the Golgi complex" (1998) *Proc. Natl. Acad. Sci.* U S A 95 :8607-12

Griffiths, G., Parton, R.G., Lucoq, J., van Deurs, B., Brown, D., Slot, J.W., Geuze, H.J. "The immunofluorescent era of membrane traffic" (1993) *Trends in Cell Biol.* 3: 214-219

Griffiths, G., Pfeiffer, S., Simons, K., and Matlin, K. "Exit of newly synthesized membrane proteins from the trans cisterna of the Golgi complex to the plasma membrane" (1985) *J. Cell Biol* 101: 949-964

Gruenberg, J. and Maxfield, F.R. "Membrane transport in endocytic pathway" (1995) *Curr. Opin in Cell Biol.* 7:552-563

Guo, Q., Vasile, E., and Krieger, M. "Disruption in the Golgi structure and membrane traffic in a conditional lethal mammalian cell mutant are corrected by ε-COP" (1994) *J. Cell Biol.* 125:1213-1224

Hall, C.E. (1954), *J. Biophys. Biochem. Cytol.*, 1:1

Hamilton, R.L., Moorehouse, A. and Havel, R.J. "Isolation and properties of nascent lipoproteins from highly purified rat hepatocytes Golgi fractions" (1991) *Journ. of Lipid research* 32:529-543

Happe, S., and Weidmann, P. "Cell-free transport to distinct Golgi cisternae is compartment specific and ARF independent" (1998) *J.Cell Biol.* 140: 511-523

Harri, E., Loeffer, W., Sigg, H.P., Stahelin, H., and Tamm, H. (1963) *Helv. Chem. Acta* 46:1235-1243

Hauri, H.P., and Schweitzer, A. "The endoplasmic reticulum-Golgi intermediate compartment" (1992) *Curr. Opin. Cell Biol.* 4:600-608

Heath, R.J. and Rock, C.O. "A conserved histidine is essential for glycerolipid acyltransferase catalysis" (1998) *J. Bacteriol.* 180: 1425-1430

Helms, J.B., and Rothman, J.E. "Inhibition by brefeldin A of a Golgi membrane enzyme that catalyses exchange of guanine nucleotide bound to ARF" (1992) *Nature* 360: 352-354

Hemery, I., Durand-Schneider, A., Feldmann, G., Vaerman, J.P. and Maurice, M. "The transcytotic pathway of an apical plasma membrane protein (B10) in hepatocytes is similar to that of IgA and occours via a tubular pericentriolar compartment" (1996) *J. Cell Sci.* 109: 1215-1227

Hermo, L., and Smith, C.E. " The structure of the Golgi apparatus: a sperm's eye view in principal epithelial cells of the rat epididymis" (1998) *Histochem. Cell Biol.* 109: 431-447

Hidalgo, J., Muniz, M. and Velasco, A. "Trimeric G proteins regulate the cytosol-induced redistribution of Golgi enzymes into the endoplasmic reticulum" (1995) *J. Cell Sci.* 108:

Hinshaw, J.E., and Schmid, S.L. "Dynamin self-assembles into rings suggesting a mechanism for coated vesicle budding" (1995) *Nature* 374: 190-192

Hirschberg, K. *et al.* "Kinetic analysis of secretory protein traffic and characterization of Golgi to plasma membrane transport intermediates in living cells" (1998) *J. Cell Biol.* 143: 1485-1503

Hollenback, D. and Glomset, J. A. "On the relation between a stearoyl-specific transacyclase from bovine testis membranes and a copurifyng acyltransferase" (1998) *Biochemistry* 37: 363-376

Hopkins, C.R., Gibson, A., Shipman, M., and Miller, K. "Movement of internalized ligand receptor complexes along a continuous endosomal reticulum" (1990) *Nature* 346: 335-339

Howell, K.E. and Palade, G. "Hepatic Golgi fractions resolved into membrane and content subfractions" (1982) *J. Cell Biol.* 92: 822-832

Inoue', T. "Complementary scanning electron microscopy: technical notes and applications" (1992) *Arch. Histol. Cytol.* 55: 45-51

Inoue', T., and Osatake, H., "Complementary observation on fractured intracellular structures, especially the Golgi apparatus, by scanning electron microscopy" (1988) *J. Electron Microsc.* 37: 333-336

James, P., Vorherr, T., and Carafoli, E. "Calmodulin-binding domains: just two faced or multi-faced ?" (1995) *Trends Biochem. Sci.* 20: 38-42

Jamora, C., Takizawa, P.A., Zaarour, R.F., Denesvre, C., Faulkner, D.J., and Malhotra, V. "Regulation of Golgi structure through heterotrimeric G proteins" (1997) *Cell* 91:617-626

Johnson, L.V., Walsh, M.L., and Chen, L.B. "Localization of mitochondria in living cells with rhodamine 123" (1980) *Proc. Natl. Acad. Sci.* USA 77: 990-994

Jolly, C.A., Murphy, E.J., Schroeder, F. "Differential influence of rat liver fatty acid binding protein isofrom on phospholipid fatty acid composition: phospahtidic acid biosynthesis and phospholipid fatty acid remodelling" (1998) *Biochim. Biophys. Acta* 1390: 258-268

Jones, S.M. and Howell, K.E. "Phosphatidylinositol 3-kinase is required for the formation of constitutive transport vesicles from the TGN" (1997) *J. Cell Biol.* 139: 339-349

Jones, S.M., Howell, K.E., Henley, J.R., Cao, H., McNiven, M.A. "Role of dynamin in the formation of transport vesicles from the trans-Golgi network" (1998) *Science* 279: 573-577

Kahn, R.A., Yucel, J.K., and Malhotra, V. "ARF signalling: a potential role for phospholipase D in membrane traffic" *Curr. Opin Cell Biol.* (1993) 75: 1045-1048

Kastanis, N., and Fisher, E.M. "A novel C-terminal binding protein (CTBP2) is closely related to CTBP1, an Adenovirus E1A-binding protein, and maps to human chromosome 21q21.3" (1998) *Genomics* 47: 294-299

Kelly, R. B. "New twists for dynamin" (1999) *Nature Cell Biol.* 1, E8-E9

Kent, C. "Eukaryotic phospholipid biosynthesis" (1995) *Annu. Rev. Biochem.* 64, 315-343 .

Kim, U.H., Kim, M.K., Kim, J.S., Han, M.K., Park, B.H., and Kim, H.R. "Purification and characterization of NAD glycohydrolase from rabbit erythrocytes" (1993) *Arch Biochem Biophys* 305: 147-52

Kinnunen, P.K.J., Koiv, A., Lehtonen, J.Y.A., Rytomaa, M., and Mustonen, P. "Lipid dynamics and peripheral interactions of proteins with membranes surfaces" (1994) *Chemistry and Physiscs of Lipids* 73:181-207

Klausner, R.D., Donaldson, J.G., and Lippincott Schwartz, J. (1992) *J. Cell Biol.* 116:1071-1080

Kragh-Hansen, U., le Maire, M., and Moller, J.V. "The mechanism of detergent solubilization of liposomes and protein-containing membranes" (1998) *Biophys. J.* 75: 2932-2946

Kreitzer, G., and Rodriguez-Boulan, E. "Role of MT motors in exit of TGN-derived transport intermediates in vivo" (1999) in the abstract book of the ASCB-EMBO joint meeting on "Membrane traffiking and the cytoskeleton: an integrated view S.M. Imbaro June 26-30, 1999

Krijnse-Locker, J., Ericsson, M., Rottier, P.J.M., and Griffiths, G. "Characterization of the budding compartment of mouse hepatitis virus: evidence that transport from RER to the Golgi complex requires only one vesicular step" (1994) *J. Cell Biol.* 124: 55-70

Ladinsky, M.S., Kremer, J.R., Furcinitti, P.S., McIntosh, J.R., and Howell, K.E. "HVEM Tomography of the Trans-Golgi Network: structural insights and identification of a lace-like coat" (1994) *J. Cell Biol.* 127: 29-38

Ladinsky, M.S., Kremer, J.R., Mastronade, D.N., McIntosh, J.R., Howell, K.E. and Staehelin, L.A. "Golgi structure in three dimension: functional insights from the normal rat kidney" (1999) *J. Cell Biol.* 144: 1135-1149

Lavoie, C., Lanoix, J., Kan, F.W.K., and Paiement, J. "Cell-free assembly of rough and smooth endoplasmic reticulum" (1996) *J Cell Sci.* 109:1415-1425

Lawrence, J.B., Moreau, P., Cassagne, C., and Morre' D.J. "Acyl transfer reaction associated with cis-Golgi apparatus of rat liver" (1994) *Bioch. Biophys. Acta* 1210: 146-150

Lee, C. and Chen, L.B. "Dynamic behaviour of Endoplasmic reticulum in living cells" (1988) *Cell* 54: 37-46

Lee, C., Ferguson, M., and Chen, L.B. "Construction of the endoplamic reticulum" (1988) *J. Cell Biol.* 109: 2045-2055

Leelavathi, D.E., Estes, L.W., Feingold, D.S., and Lombardi, B. "Isolation of a Golgi-rich fraction from rat liver" (1970) *Biochim. Biophys. Acta* 211: 124-138

Leslie, C.C. "Properties and regulation of cytosolic phospholipase A2" (1997) *J. Biol. Chem.* 272: 16709-16712

Lewis, M.J., and Pelham, H.R.B. "Ligand-induced redistribution of a Human KDEL receptor from the Golgi complex to the endoplasmic reticulum" (1992) *Cell* 68: 353-364

Lichtenberg, D. "Micelles and Liposomes" (1993) in *Biomembranes. Physical aspects* Ed. by M. Shinitzky - VCH

Lindsey, J.D. and Ellisman, M.H. "The Neuronal Endomembrane system. II. The multiple forms of the Golgi apparatus cis element" (1985) *J.of Neuroscience* 5: 3124-3134

Linstedt, A.D. and Hauri, H.P. "Giantin, a novel conserved Golgi membrane containing a cytoplasmic domain of at least 350 kDa" (1993) *Mol Biol Cell* 4:679-693

Lipowsky, R. "Domain-induced budding of fluid membranes" (1993), *Biophys.J.* 64: 1133-1138

Lippincott-Schwartz, J., Cole, N., and Presley, J. "Unravelling Golgi membrane traffic with green fluorescent protein chimeras" (1998) *Trends in Cell Biol.* 8: 16-20

Lippincott-Schwartz, J., Donaldson, J.G., Schweizer, A., Berger, E.G., Hauri, H.P., Yuan, L.C., and Klausner, R.D. (1990) *Cell* 60: 821-836

Lippincott-Schwartz, J., "Membrane cycling between the ER and Golgi apparatus and its role in biosynthetic transport" (1993) *Subcell Biochem.* 21:95-119.

Lippincott-Schwartz, J., Yuan, L.C., Bonifacino, J.S., and Klausner, R.D. "Rapid redistribution of Golgi proteins into ER in cells treated with brefeldin A: evidence for membrane cycling from Golgi to ER" (1989) *Cell* 56: 801-813

Lippincott-Schwartz,J., L.C. Yuan, J.S. Bonifacino, and R.D. Klausner "Rapid redistribution of Golgi proteins into the ER in cells treated with brefeldin A: evidence formembrane cycling from Golgi to ER" (1989) *Cell* 56: 801-813

Lippincott-Schwartz,J., Yuan, L., Tipper, C., Amherdt, M., Orci, L. and Klausner, R.D. (1991) "Brefeldin A's effects on endosomes, lysosomes, and the TGN suggest a general mechanism for regulating organelle structure and membrane traffic" *Cell* 67: 601-616

Lowe, M., Nakamura, N., and Warren, G. "Golgi division and membrane traffic" (1998) *Trends in Cell Biol.* 8: 40-44

Lucocq, J. "Unbiased 3-D quantitation of ultrastructure in cell biology" (1993)*Trends Cell Biol.* 3: 354-358

Ma, Q., K. Cui, F. Xiao, A.Y.H. Lu, and C.S. Yang (1992) *J.Biol. Chem.* 267:22298-22304

Machamer, C.E. "Golgi retention signals: do membranes hold the key ?" (1991) *Trends in Cell Biol.* 1:141-144

Machamer, C.E. "Targeting and retention of Golgi membrane proteins" (1993) *Curr. Opin. Cell Biol.* 5:606-612

Malhotra, V., T. Serafini, L. Orci, J.C. Sheperd, and Rothman, J.E. "Purification of a novel class of coated vesicles mediating biosynthetic protein transport through the Golgi stack" (1989) *Cell* 58: 329-336.

Marsh, D. "Bilayers, monolayers, multilayers and non-lamellar lipid phases" (1993) in *Biomembranes. Physical aspects* Ed. by M. Shinitzky - VCH

Mayer, R.J., and Marshall, L.A. "New insights on mammalian phospholipase A2(s); comparison of arachidonoyl-selective and -nonselective enzymes" (1993) *FASEB J.* 7:339-348

McGee, T.P., Skinner, H.B., Whitters, E.A., Henry, S.A. and Bankaitis, V.A. "A phosphatidylinositol transfer protein controls the phosphatydilcholine content of yeast Golgi membranes" (1994) *J. Cell Biol.* 124:273-287

McNiven, M. "Dynamin: a molecular motor with pinchase action" (1998) *Cell* 94: 151-154

McPherson, P.S., Garcia, E.P., Slepnev, V.I., David, C., Zhang, X., Grabs, D., Sossin, W.S., Bauerfeind, R., Nemoto, Y., and De Camilli, P. "A presynaptic inositol-5-phosphatase" (1996) *Nature* 379: 353-357

Melançon, P. *et al.* "Involvement of GTP-binding "G" proteins in transport through the Golgi stack" (1987) *Cell* 51: 1053-1062

Mellman, I. and Simons, K. "The Golgi complex: in vitro veritas" (1992) *Cell* 68:829-840

Mironov, A. *et al.* "Role of NAD^+ and ADP-Ribosylation in the mainentance of the Golgi structure" (1997)a*J. Cell Biol.* 139: 1109-1118

Mironov, A. Jr., Luini, A., and Mironov, A. "A synthetic model for intra-Golgi traffic" (1998) *FASEB J.* 12:249-52

Mironov, A.A., Weidman, P. and Luini, A. "Variations on the intracellular transport theme: maturing cisternae and trafficking tubules" (1997)b *J. Cell Biol.* 138, 481-484

Mironov, AA., Luini, A., and Buccione, R. "Constitutive transport between the trans-Golgi network and the plasma membrane according to the maturation model. A hypothesis" (1998) *FEBS Lett* 440:99-102

Misteli, T. and Warren, G. "A role for tubular networks and a COP I-indipendent pathway in the mitotic fragmentation of Golgi stacks in a cell-free system" (1995)*J. Cell Biol.* 130: 1027-1030

Misteli, T. and Warren, G. "COP-coated vesicles are involved in the mitotic fragmentation of Golgi stacks in a cell-free system" (1994) *J. Cell Biol.* 125: 269-282

Misteli, T. "Molecular mechanism in the disassembly and reassembly of the mammalian Golgi apparatus during M-phase" (1996) *FEBS-Letters* 389: 66-69

Mollenhauer, H.H. , Morre', J.D. and Totten, C. "Intercisternal substances of the Golgi apparatus unstacking of plant dictyosomes using chaotropic agents" (1973) *Protoplasma* 78:443-459

Mollenhauer, H.H. and Morre', J.D. "Structural compartmentation of the cytosol: zone of exclusion, zone of adhesion, cytoskeletal and intercisternal elements" (1968) *Subcellular Biochemistry* 5: 327-359

Mollenhauer, H.H., and Morre', J.D. "The tubular network of the Golgi apparatus" (1998) *Histochem .Cell Biol.* 109: 533-543

Moreau, P., and Morre', J.D. "Cell-free transfer of membrane lipids" (1991) *J. Biol. Chem.* 266: 4329-4333

Morre', J.D. "Isolation of a Golgi apparatus-rich fraction from rat liver. I. Method and morphology" (1970) *J Cell Biol.* 44: 484-91

Morre', J.D., Mollenhauer, H.H., and Bracker, C.E. "Origin and continuity of Golgi apparatus" (1971) in: Reinert, J., Urspring, H. (eds) Origin and continuity of cell organelles. Springer, Berlin Heidelberg New York 88-126

Morre', J.D., Morre', D.D., and Heidrich, H.G. "Subfractionation of rat liver Golgi apparatus by free-flow electrophoresis" (1983), *Eur. J. Cell Biol.* 31: 263-274

Morre, J.D. "Isolation of Golgi apparatus" (1971) in *Methods in Enzymol.* Vol XXII: 130-148

Moss, J. and Vaughan, M. (1988) *Adv. Enzym.* 61, 303-379

Mouritsen, O.G., and Bloom, M. "Models of lipid-protein interaction in membranes" (1993) *Annu. Rev. Biophys. Biomol. Struct.* 22:145-171

Mui, B.L.S., Dobereiner, H.G., Madden, T.D., and Cullis, P.R. "Influence of transbilayer area asymmetry on the morphology of large unilamellar vesicles" (1995) *Biophys. J.* 69:930-941

Munro, S. "Localization of proteins to the Golgi apparatus" (1998) *Trends Cell Biol.* 8: 11-15

Nakamura, N., Lowe, M., Levine, T.P., Rabouille, C., and Warren, G. " The vesicle docking protein p115 binds GM130, a cis-Golgi matrix protein in a mitotically regulated manner" (1997) *Cell* 89:445-455

Nakamura, N., Rabouille, C., Watson, R., Nillson, T., Hui, N., Slusarewicz, P., Kreis, T.E., and Warren, G. "Characterization of a cis-Golgi matrix protein, GM130" (1995) *J. Cell Biol.* 131: 1715-1726

Nakata, T., Terada, S. and Hirokawa, N. "Visualization of the dynamics of synaptic vesicle and plasma membrane proteins in living axons" (1998) *J. Cell Biol.* 140: 659-674

Narula, N., Mc Morrow, I., Plopper, G., Doherthy, J., Matlin, K.S., Burke, B. and Stow, J.L. (1992) *J. Cell. Biol.* 117: 27-38

Nillson, T., Hoe, M.H., Slusarewicz, P., Rabouille, C., Watson, R., Hunte, F., Watzele, G., Berger, E.G., and Warren, G. "Kin recognition between medial Golgi enzymes in Hela cells" (1994) *EMBO Journal* 13: 562-574

Orci, L, Perrelet, A., .Ravazzola, M., Amherdt, A., Rothman, J.E. and Schekman, R. "Coatomer-rich endoplasmic reticulum" (1994) *Proc. Natl.Acad.Sci USA* 91:11924-11928

Orci, L, Schekman, R. and Perrelet, A. "Interleaflet clear space is reduced in the membrane of COPI and COPII-coated buds" (1996) *Proc. Natl.Acad.Sci* USA 93:8968-8970

Orci, L., Glick, B.S. and Rothman, J.E. "A new type of coated vesicular carrier that appears not to contain clathrin: its possible role in protein transport within the Golgi stack" (1986) *Cell* 46:171-184

Orci, L., Montesano, R., Meda, P., Malaisse-Lagae, F., Brown, D., Perrelet, A. and Vassalli, P. "Heterogeneous distribution of filipin-cholesterol complexes across the cisternae of the Golgi apparatus" (1981) *Proc. Natl.Acad.Sci* USA 78:293-297

Orci, L., Palmer, D.J., Ravazzola, M., Perrelet, A., Amherdt, A. and Rothman, J.E. "Budding from Golgi membranes requires the coatomer complex of non-clathrin coat proteins" (1993) *Nature* 362: 648-652

Orci, L., Tagaya,M., Amherdt, M., Perrelet, A., Donaldson, J.G., Lippincott-Schwartz, J. Klausner, R.D., and Rothman J.E. "Brefeldin A, a drug that blocks secretion, prevents the assembly of non-clathrin-coated buds on Golgi cisternae" (1991) *Cell* 64:1183-1195

Oster, G.F., Cheng, L.Y., Moore, H.P. and Perelson, A.S. "Vesicle formation in the Golgi apparatus" (1989) *J. Theor. Biol.* 141: 463-504

Ostermann, J., Orci, L., Tani, K., Amherdt, M., Ravazzola, M., Elazar, Z., and Rothman, J.E. "Stepwise assembly of functionally active transport vesicles" (1993) *Cell* 75:1015-1025

Ovtracht, L., Morre', J.D., Cheetham, R.D., and Mollenhauer, H.H. "Subfractionantion of Golgi apparatus from rat liver: method and morphology" (1973) *J. Microsc.* 18: 87-102

Palmer, D.J., Helms, J.B., Beckers, C.J.M., Orci, L. and Rothman, J.E. "Binding of coatomer to Golgi membranes requires ADP-ribosylation factor" (1993) *J. Biol. Chem.* 268: 12083-12089

Papahadjopulos, D., Vail, W.J., Pangborn, W., and Poste, G. "Studies on membrane fusion. II. Induction of fusion in pure phospholipid membranes by calcium ions and other divalent cations" (1976) *Biochim. Biophys. Acta* 448:265-283

Pavelka, M. and Ellinger, A. "Early and late transformations occurring at organelles of the Golgi area under the influence of Brefeldin A: An ultrastructural and lectin cytochemical study" (1993) *J. of Hist. and Cytochem.* 41: 1031-1042

Pearse, B.M., and Robinson, M.S. "Clathrin adaptors, and sorting" (1990) *Ann. Rev. Cell. Biol.* 6:151-171

Peyroche A, Paris S, Jackson C.L. "Nucleotide exchange on ARF mediated by yeast Gea1 protein" (1996) *Nature* 384: 479-81

Pfanner, N., Glick, B.S., Arden, S.R., and Rothman, J.E. "Fatty acylation promotes fusion of transport vesicles with Golgi cisternae" (1990) *J. Cell Biol.* 110: 955-961

Pfanner, N., Orci, L., Glick, B.S., Amherdt, M., Arden, S.R., Malhotra, V., and Rothman, J.E. "Fatty Acyl-Coenzyme A is required for budding of transport vesicles from Golgi cisternae" (1989) *Cell* 59: 95-102

Podos, S.D., Reddy, P., Ashkenas, J. and Krieger, M. (1994) *J. Cell. Biol.* 127: 679-691

Polishchuk, R.S., Polishchuk, E.V., Marra, P., Alberti, S., Buccione, R., Luini, A., and Mironov, A.A. "Novel GFP-based correlative light-electron microscopy reveals the saccular-tubular ultrastructure of carriers in transit from the Golgi apparatus to the plasma membrane" (1999) *J. Cell Biol.* (in press)

Presley, J. F., Smith, C., Hirschberg, K., Miller, C., Cole, N.B., Zaal, K.J.M., and Lippincott-Schwartz, J."Golgi membrane dynamics" (1998) *Mol. Biol. Cell* 9, 1617-1626.

Prezbindowski, K.S., Sun, F.F., and Crane, F.L."Characterization of microsomal membranes by negative staining technique" (1968) Exp Cell Res 50:2 41-56

Pryer, N.K., Wuesthube, L.J., and Schekman, R. "Vesicle-mediated protein sorting" (1992) *Annu. Rev. Biochem.* 61:471-516

Rabouille, C, and Warren, G. "Changes in the architecture of the Golgi apparatus during mitosis" (1997) in *The Golgi apparatus*, E.G. Berger & J. Roth (eds)

Rabouille, C., Hui, N., Hunte, F., Kieckbush, R., Berger, E.G. , Warren, G. , and Nillson, T. "Mapping the distribution of Golgi enzymes involved in the construction of complex oligosaccarides" (1995)a, *J Cell Sci.* 108:1617-1627

Rabouille, C., Misteli, T., Watson, R., and Warren, G. "Reassembly of Golgi stacks from mitotic Golgi fragments in a cell-free system" (1995)b *J. Cell Biol.* 129: 605-18

Rambourg, A. & Clermont, Y. in *The Golgi apparatus* (eds Berger, E. G. & Roth, J.) 37-60 (Birkhauser Verlag, 1997).

Rambourg, A. and Clermont, Y. "Three-dimensional electron microscopy: structure of the Golgi apparatus" (1990) *Eur. J. Cell Biol.* 51: 189-200

Rambourg, A., Clermont, Y, Jackson, C. L. and Kepes, F. "Ultrastructural modifications of vesicular and Golgi elements in the Saccharomyces cerevisiae sec21 mutant at permissive and non-permissive temperatures" (1994) *Anat. Rec.* 240: 32-41

Rambourg, A., Clermont, Y. and Kepes, F. "Modulation of the Golgi apparatus in Saccharomyces cerevisiae sec7 mutants as seen by three-dimensional electron microscopy" (1993) *Anat. Rec.* 237, 441-452

Rambourg, A., Clermont, Y., Ovtracht, L. and Kepes, F. "Three-dimensional structure of tabular networks, presumably Golgi in nature, in varius yeast strains: a comparative study" (1995) *Anat. Rec.* 243, 283-293

Reithmeier, R.A.F. "Assembly of proteins into membranes" (1996) in *Biochemistry of lipids, lipoproteins and membranes* Ed by D.E. Vance and J.E. Vance - Elsevier Science

Requero, M. A., Goni, F. M. and Alonso, A. "The membrane-perturbing properties of palmitoyl-coenzyme A and palmitoylcarnitine. A comparative Study" (1995) *Biochemistry* 34, 10400-10405

Resh, M.D. "Regulation of cellular signalling by fatty acid acylation and prenylation of signal transduction proteins" (1996) *Cell. Signal.* 8: 403-412

Ringstad, N., Nemoto, Y. & De Camilli, P. The SH3p4/Sh3p8/SH3p13 protein family: binding partners for synaptojanin and dynamin via a Grb2-like Src homology 3 domain. *Proc. Natl. Acad. Sci. USA* 94, 8569-8574 (1997).

Robertson, A.M., and Allan, V. "Cell cycle regulation of organelle movement along microtubules" (1998) in the abstract book of The Golgi Complex meeting in Pavia Sep 19-23 1998

Robinson, M.S. and Kreis, T.E. (1992) *Cell.* 69: 129-138

Roos, J. and Kelly, R. B. "Is dynamin really a 'pinchase'?" (1997) *Trends Cell Biol.* 7, 257-259

Rossanese, O.W., Soderholm, J., Bevis, J.B., Sears, I.B., O'Connor, J., Williamson, E.K., and Glick, B.S. "Golgi structure correlates with transitional endoplasmic reticulum organization in Pichia Pastoris and Saccharomyces Cerevisiae" (1999) *J. Cell Biol.* 145: 69-81

Roth, J. and Taatjes, D. J. "Tubules of the trans Golgi apparatus visualized by immunoelectron microscopy" (1998) *Histochem. Cell Biol.* 109: 545-553

Rothman, J.E. and Orci, L. "Molecular dissection of the secretory pathway" (1992) *Nature* 355: 409-415

Rothman, J.E. and Wieland, F.T. "Protein sorting by transport vesicles" (1996) *Science* 272: 227-234

Rothman, J.E. "Mechanisms of intracellular protein transport" (1994) *Nature* 372: 55-62

Rothman, J.E. "The reconstitution of intracellular protein transport in cell-free systems" (1992) *Harvey Lect.* 86: 65-85

Rothman, J.E., and Warren, G. "Implication of the SNARE hypothesis for intracellular membrane topology and dynamics" (1994) *Curr. Biol.* 4: 220-233

Rusinol, A.E., Cui, Z., Chen, M.H., and Vance J.E. (1994). *J. Biol. Chem.* 260: 27494-27502

Sackmann E. "Membrane bending energy concept of vesicle- and cell-shapes and shape transitions" (1994) *FEBS Letters* 346: 3-16

Sanan, D.A., and Anderson, R.G.W. "Simultaneous visualisation of LDL receptor distribution and Clathrin lattices on membranes torn from the upper surface of cultured cells" (1991) *J. Histochem. and Cytochem.* 39: 1017-1024

Saraste, J., and Kuismanen, E. "Pathways of protein sorting and membrane traffic between the rough endoplasmic reticulum and the Golgi complex" (1992) *Semin. Cell Biol.* 3:343-549

Schaeper, U., Boyd, J.M., Verma, S., Uhlmann, E., Subramanian, T., and Chinnadurai, G. "Molecular cloning and characterization of a cellular phosphoprotein that interacts with a conserved C-terminal domain of adenovirus E1A involved in negative modulation of oncogenic transformation" (1995) *Proc. Natl. Acad. Sci.* USA 92: 10467-10471

Schaeper, U., Subramanian, T., Lim, L., Boyd, J.M., and Chinnadurai, G. "Interaction between a cellular protein that binds to the C-terminal region of adenovirus E1A (CtBP) and a novel cellular protein is disrupted by E1A through a conserved PLDLS motif" (1998) *J. Biol. Chem.* 273: 8549-8552

Scheckman, R., and Mellman, I. " Does COPI go both ways" (1997) *Cell* 90: 197-200

Scheckman, R., and Orci, L. "Coat proteins and vesicle budding" (1996) *Science* 271:1526-33 .

Scheiffele, P., Roth, M.G., Simons, K. "Interaction of influenza virus haemagglutinin with sphingolipid-cholesterol membrane domains via its transmembrane domain" (1997) *EMBO J* . 16:5501-8

Schmidt, A., Wolde, M., Thiele, C., Fest, W., Kratzin, H., Podtelejnikov, A.V., Witke, W., Huttner, W.B., Soling, H. "Endophilin I mediates synaptic vesicle formation by transfer of arachidonate to lysophosphatidic acid" (1999) *Nature* 401: 133-141

Schoen, P.E., Price, R.R., Schnurr, J.M., Gulik, A., and Gulik-Krzywicki T. "Formation of lipid tubule microstructures: time-resolved freeze-fracture electron microscopy and X-ray characterization" (1993) *Chemistry and Phys. of Lipids* 65:179-191

Schrader, M., Krieglstein, K., and Fahimi, D.H. "Tubular peroxisomes in HepG2 cells: selective induction by growth factors and arachidonic acid" (1998) *Eur. J. Cell Biol.* 75: 87-96

Sciaky, N., Presley, J., Smith, C., Zaal, K.J.M., Cole, N., Moreira, J.E., Terasaki, M., Siggia, E., and Lippincott-Schwartz, J. "Golgi tubule traffic and the effects of brefeldin A visualized in living cells" (1997) *J. Cell Biol.* 139: 1137-1155 .

Scroeder, F., Jolly, C.A., Cho, T., and Frolov, A. "Fatty acid binding protein isoform: structure and function" (1998) *Chem. Phys. of lipidis* 92: 1-25

Sever, S., Muhlberg, A. B. & Schmid, S. L. Impairment of dynamin's GAP domain stimulates receptor-mediated endocytosis. *Nature* 398, 481-486 (1999).

Shima, D.T., Scales, S.J., Kreis, T.E., Pepperkok, R. "Segregation of COPI-rich and anterograde-cargo-rich domains in endoplasmic-reticulum-to-Golgi transport complexes" (1999) *Curr Biol* 9: 821-824

Simon, J.P. *et al.* "An essential role for the phosphatidylinositol transfer protein in the scission of coatomer-coated vesicles from the trans-Golgi network" (1998) *Proc. Natl. Acad. Sci. USA* 95, 11181-11186

Simon, J.P., Ivanov, I.E., Adesnik, M., and Sabatini, D.D. "The production of post-Golgi vesicles requires a protein kinase C-like molecule but not its phosphorylating activity" (1996)a *J. Cell Biol.* 135: 355-370

Simon, J.P., Ivanov, I.E., Shopsin, B., Hersh, D., Adesnik, M., and Sabatini, D.D. "The in vitro generation of post-Golgi vesicles carrying viral envelope glycoproteins requires an ARF-like GTP-binding protein and a protein kinase C associated with the Golgi apparatus" (1996)b *J. Biol. Chem* . 271: 16952-16961

Sjostrand, F.S., and Hanzon, V. (1954) *Exp. Cell Res.* 7, 415-429

Slusarewicz, P., Nilsson, T., Hui, N., Watson, R., and Warren, G. "Isolation of a matrix that binds medial Golgi enzymes" (1994) *J. Cell Biol.* 124: 404-413

Spanò, S. *et al.* "Molecular cloning and functional characterization of brefeldin A-ADP-ribosylated substrate" (1999) *J. Biol. Chem.* 274, 17705-17710

Stinchcombe, J.C., Nomoto, H., Cutler, D.F., and Hopkins, C.R. "Anterograde and retrograde traffic between the rough endoplasmic reticulum and the Golgi complex" (1995) *J. Cell Biol.* 131: 1387-1401

Stoorvogel, W., Oorschot, V., and Geuze, H.J. "A novel class of clathrin-coated vesicles budding from endosomes" (1996) *J. Cell Biol.* 132: 21-33

Stowell, M. H. B., Marks, B., Wigge, P. & McMahon, H. T. Nucleotide-dependent conformational changes in dynamin: evidence for a mechanochemical molecular spring. *Nature Cell Biol.* 1, 27-32 (1999).

Sugimoto, H., and Satoshi, Y. "Purification, characterization, and inhibition by phosphatidic acid of lysophospholipase transacylase from rat liver" (1994) *J. Biol. Chem.* 269: 6252-6258

Sugiura, T., Masuzawa, Y., and Waku, K. "Coenzyme A-dependent transacylation system in rabbit liver microsomes" (1988) *J. Biol. Chem.* 263: 17490-17498

Swanson, J., Bushnell, A., and Silverstein, S.C. "Tubular lysosome morphology and distribution within macrophages depend on the integrity of cytoplasmic microtubules" (1987) *Proc. Natl. Acad. Sci.* USA 84: 1921-1925

Sweitzer, S.M. and Hinshaw, J.E. "Dynamin undergoes a GTP-dependent conformational change causing vesiculation" (1998) *Cell* 93: 1021-1029

Takei, K. McPherson, P.S., Schmid, S.L., and De Camilli, P. "Tubular membrane invaginations coated by dynamin rings are induced by GTP-gS in nerve terminals" (1995) *Nature* 374:186-190

Takei, K., Haucke, V., Slepnev, V., Farsad, K., Salazar, M., Chen, H., and De Camilli, P. "Generation of coated intermediates of clathrin-mediated endocytosis on protein-free liposomes" (1998) *Cell* 94: 131-141 .

Takei, K., Slepnev, V. I., Haucke, V. and De Camilli, P. "Functional partnership between amphiphysin and dynamin in clathrin-mediated endocytosis" (1999) *Nature Cell Biol.* 1, 33-39

Takizawa, P.A., Yucel, J.K., Veit, B., Faulkner, D.J., Deerinck, T., Soto, G., Ellisman, M., and Malhotra, V. "Complete vesiculation of Golgi membranes and inhibition of protein transport by a novel sea sponge metabolite, ilimaquinone" (1993) *Cell* 73:1079-1090

Tanaka, K., Mitsushima, A., Fukudome, H., and Kashima, Y. "Three-dimensional architecture of the Golgi complex observed by high resolution scanning electron microscopy" (1986) *J. Submicrosc. Cytol.* 18: 1-9

Tanigawa, G., Orci, L., Amherdt, M., Ravazzola, M., Helms, J.B., and Rothman, J.E. "Hydrolisis of bound GTP by ARF protein triggers uncoating of Golgi-derived COP-coated vesicles" (1993) *J. Cell Biol.* 123: 1365-1371

Taylor, C.T., Kanstein, M., Weidman, P. and Melançon, P. "Cytosolic ARFs are required for vesicle formation but not for cell-free intra-Golgi transport: evidence for coated vesicle-independent transport" (1994) *Mol.Biol. Cell* 5:237-252

Taylor, R.S., Jones, S.M., Dahl, R.H., Nordeen, M.H., and Howell, K.E. "Characterization of the Golgi complex cleared of proteins in transit and examination of calcium uptake activities" (1998) *Mol. Biol. Cell* 8: 1911-1931

Thorne-Tjomsland, G., Dumontier, M., and Jamieson, J.C. "3D Topography of noncompact zone Golgi tubules in rat spermatids: a computer-assisted serial section reconstruction study" (1998) *Anat. Rec.* 250:381-396

Toomre, D., Keller, P., White, J., Olivo, J. C. and Simons, K. "Dual-color visualization of trans-Golgi network to plasma membrane traffic along microtubules in living cells" (1999) *J. Cell Sci.* 112: 21-33.

Tooze J. and Hollinshead (1992) *J. Cell. Biol.* 118: 813-830

Ueda, K. (1985) *A. Rev. Biochem.* 54: 73-100

Urrutia, R., Henley, J., Cook, T., and McNiven, M.A. "The dynamins: redundant or distinct functions for an expanding family of related GTPases ?" (1997) *Proc. Natl. Acad. Sci.* USA 94:377-384

Vale, R.D. and Hotani, H. "Formation of membrane networks in vitro by kinesin-driven microtubule movement" (1988) *J. Cell Biol.* 107:2233-2241

van Blitterswijk, W.J. and Hilkmann, H. "Rapid attenuation of receptor-induced diacylglycerol and phospahtidic acid by phospholipase D-mediated transphosphatidylation: formation of bisphosphatidic acid" (1993) *EMBO J.* 12: 2655-2662

van Deurs, B., von Bulow, F., Vihardt, F., Kaae Holm, and Sandvig, K. "Destabilization of plasma membrane structure by prevention of actin polymerization" (1996) *J. Cell Sci.* 109: 1655-1665

van Meer, G. "Lipids of the Golgi membranes" (1998)*Trends in Cell Biol.* 8: 29-33

Varki, A. "Factors controlling the glycosilation potential of the Golgi apparatus" (1998) *Trends in Cell Biol.* 8: 34-40

Veit, B., J.K. Yucel, and V. Malothra (1993) *J. Cell Biol.* 122: 1197-1206

Velasco, A., Hendricks, L., Moremen, K.W., Tulsiani, D.R., Touster, O., and Farquhar, M.G. "Cell type-dependent variations in the subcellular distribution of alpha-mannosidase I and II" (1993) *J. Cell Biol.* 122 :39-51

Verkade, P. and Simons, K. "Lipid microdomains and membrane trafficking in mammalian cells" (1997) *Histochem. Cell Biol.* 108: 211-220

Verkleij, A.J., de Maagd, R., Leunissen-Bijvelt, J. and de Kruijff, B. "Divalent cations and chloropromazine can induce non-bilayer structures in phosphatidic acid containing model membranes" (1982) *Biochim. Biophys. Acta* 684: 255-262

Warren, G. and Malhotra, V. "The organisation of the Golgi apparatus" (1998) *Curr. Opin. Cell. Biol.* 10, 493-498

Warren, G., Levine, T.P., and Misteli, T. "Mitotic disassembly of the mammalian Golgi apparatus" (1995), *Trends Cell Biol.* 5: 413-416

Weidman P. J. "Anterograde transport through the Golgi complex: do Golgi tubules hold the key?" (1995)*Trends Cell Biol.* 5, 302-305

Weidman, P., Roth, R., and Heuser, J. " Golgi membrane dynamics imaged by freeze-etch electron microscopy : views of different membrane coatings involved in tubulation versus vesiculation" (1993), *Cell,* 75:123-133

Weigert, R., et al. "Characterization of chemical inhibitors of brefeldin-A-activated mono-ADP-ribosylation" (1997) *J. Biol. Chem* 272: 14200-14207

Weiss, O., Holden, J., Rulka, C., and Kahn, R.A. "Nucleotide binding and cofactor activities of purified bovine brain and bacterially expressed ADP-ribosylation factor" (1989) *J. Biol. Chem.* 264:21066-21072

Welti, R. and Glaser, M. "Lipid domain in model and biological membranes". (1994), *Chem. Phys. Lipids*, 73: 154-159

Wood, S.A., and W.J. Brown "The morphology but not the function of endosomes and lysosomes is altered by BFA" (1992) *J. Cell. Biol.* 119: 273-285

Wood, S.A., Park, J.E. and Brown, W.J. "Brefeldin A causes a microtubule-mediated fusion of the trans-Golgi network and early endosomes" (1991) *Cell* 67: 591-600

Yamamoto, K., and Fahimi, D.H. "Three dimensional reconstruction of a peroxisomal reticulum in regenerating rat liver: evidence of interconnections between heterogeneous segments" (1987) *J. Cell Biol.* 105: 713-722

Zhao, L., Helms, J.B., Brugger, B., Harter, C., Martoglio, B., Graf, R., Brunner, J., and Wieland, F.T. "Direct and GTP-dependent interaction of ADP-ribosylation factor 1 with coatomer subunit β" (1997) *Proc. Natl. Acad. Sci.* USA 94: 4418-4423